## *Slope instability along the north-west coast in Malta*

Magri, Odette

# Slope instability along the north-west coast in Malta

**Odette Magri**



Thesis submitted for the degree of Master of Science.

University of Durham, Department of Geography.

May 2001

## Abstract

### Slope instability along the north-west coast in Malta

Mass movement processes operating along the coastal zone, north of the Great Fault are examined. Slides fall under three main categories. Rotational slides and translational slides occur in the Upper Coralline Limestone whereas mudslides are found where Blue Clay outcrops. Two other processes are present: rockfall and soil creep. Rockfall can be considered as the most important mass movement process, whereas soil creep is the least significant identified at one locality. In this study particular attention is given to Blue Clay slopes.

A coastal geomorphological survey was undertaken for the northern region. Two geomorphological maps were produced to determine the spatial distribution of coastal features, identify the main mass movement processes and establish a relationship between the geology and geomorphology. Three representative sites were selected based on the mapping exercise to conduct further research.

Detailed geotechnical testing was performed on soil material collected from selected slopes at the three field sites. The physical and mechanical properties of Blue Clay were determined to assess the current state of stability of the slopes and the strength of the material.

A series of stability analyses were performed on the selected clay slopes at each field site. The Simplified Bishop method was used to calculate Factor of Safety values and to establish the transition between stability and instability. Geomorphological and geotechnical investigations performed at previous stages of the research provided the necessary input data to be used in the stability analyses. Variation in the pore pressure ratio allowed the identification of the critical phreatic conditions at which the slopes fail.


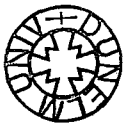

## Contents

## List of Tables

## List of Figures

### Chapter 2



### Chapter 3

**Chapter 4**



**Chapter 5**

## List of Plates

### Chapter 3

## Acknowledgements

Needless to say that without the help of many people during the past three years completion of this work would not have been possible. While I thank everyone who in some way was involved in this research, I would like to express my gratitude and appreciation towards the following people who deserve special thanks and acknowledgement.

Mr. C. Mifsud Borg, Director of the Building Construction Industry Department, Works Division at the Ministry for the Environment, for making it possible to use the laboratory facilities. In this regard I would like to thank all the staff at the Quality Control Lab, especially Mr. A. Kitcher, Mr. M. Darmanin and Mr. V. Zammit who were always willing to help and showed interest in my work. Thanks also go to the staff of the Civil Engineering Laboratory at the University of Malta for the permission to use some of the equipment available, and to Mr. A. Cassar, Department of Building and Civil Engineering, Faculty of Architecture and Civil Engineering, University of Malta for reviewing the laboratory results.

I would like to acknowledge the help of Mr. L. Caruana, Chief of the Land Surveying Section, Building and Engineering Department, Works Division at the Ministry for the Environment, and the technical staff for providing the necessary equipment and assistance with the surveying of slopes, even at places which were not so easily accessible. I am grateful to the staff of the Mapping Unit at the Planning Authority for giving me access to view coastal aerial photographs prior to field surveys.

I wish to show my appreciation and thanks in the help provided by my friends. Kurt Bonnici who assisted me in several field sessions and showed great dexterity with the drawing of maps. Hermann Bonnici who helped with the computation of data and cross-sections of the surveyed slopes and also assisted with the collection of material samples and geotechnical tests. In this regard I would like to acknowledge the permission to collect material samples at Ghajn Tuffieha Bay granted by Dr. R. Ragonesi of the Gaia Foundation. Thanks also go to Deborah Sammut who has produced the plates and Michael Azzopardi for his assistance with the computer, especially when performing the slope stability analyses.

Special thanks go to my research supervisor, Professor R. J. Allison and my family. Bob has helped me in many ways both academically and personally, especially during my visits at Durham. He has offered support and was always available when I needed his help. I appreciate the guidance and constructive criticism which he has given at various stages of this work.

My family, especially my parents have offered endless support, care and confidence in myself and my work. My father has accompanied me in most of the field sessions without ever complaining, even when weather conditions were hot and stifling. For this I am really grateful. Without my family's continuous support, lifting my morale and encouraging me when everything seemed so difficult, I would have never been able to finish this research. The merit of this work is partly theirs.

Last but not least thanks to the University of Malta who has believed in my abilities and granted me the scholarship to read for this postgraduate degree. Without this financial support I would not have been able to study at Durham.

# *Chapter 1*

# *Introduction*

## 1.1 Research aims

This research has been undertaken because there is little knowledge regarding mass movement processes and slope instability along the northern coastline in Malta. Clay slopes are given particular attention since they dominate the coastal cliffs and are significant in influencing the geomorphology.

The study adopts a multidisciplinary approach, including within its framework geological, geomorphological and geotechnical investigations. Each element is combined to produce a comprehensive study, contributing to existing information and providing original knowledge.

The research upon which this thesis is based includes the following.

i. Field investigations have been undertaken to highlight the spatial distribution of coastal features, especially landslides.
ii. The mass movement processes occurring at the northern coast of Malta have been reviewed to identify the triggering mechanisms and establish the relationship between the geology and geomorphology.
iii. Three key sites, representative of the northern coastal region, have been subject to detailed field investigation.
iv. Geotechnical investigation have been completed for slope materials, to determine the physical and mechanical properties and associated behaviour.
v. Slope stability analysis has been performed for the three study sites, simulating different scenarios to determine the critical conditions that will influence the stability of slopes.

Previous geomorphological studies in Malta lack information on material behaviour and do not include studies on soil or rock mechanics. In this regard this dissertation makes an original contribution linking geomorphological processes, landform development and material behaviour.

## 1.2 The Maltese Islands

The Maltese Islands, located in the central Mediterranean region, consist of three main islands, Malta, Gozo and Comino, several uninhabited islets and few other minor rocks. The islands have a total land area of 316 km$^2$ and a coastline about 190 km long (Schembri, 1990).

The geological strata belong to the Oligo-Miocene epoch. Limestone is the predominant geological strata. Blue Clay outcrops mainly on the south-west, north-west, north and north-east coasts. The main geomorphological features are karstic limestone plateaux, clay slopes, *rdum* or undercliff areas, flat-floored basins and Globigerina Limestone hills and plains. The coast has been significantly influenced by tectonics (Paskoff and Sanlaville, 1978) and despite the small size of the islands, there is a large variety of coastal features. The south-west coast features cliffs of a rectilinear aspect, whereas the north-east coast is rocky and shallow, gradually descending under the sea.

The geological structure is heavily faulted. Two main faults prevail. First, NE-SW faults which form part of the Great Fault of the Victoria Lines. These feature a horsts and graben landscape giving north-west Malta a characteristic topography of ridges and valleys. Second, NW-SE faults which form the Maghlaq Fault. The latter determines the south-west littoral of Malta and is responsible for the tilting of the islands towards the north-east.

This study is focussed on the region north of the Great Fault, because the combination of the structural setting and geological formations display a very interesting and varied topography, especially evident at the coastal zone. Other areas on mainland Malta display a more uniform topography and less variation in landforms due to a simpler structural and geological setting. The study area provides an excellent environment to conduct research in terms of geology, geomorphology and soil mechanics in an attempt to elucidate mechanisms of slope processes and mass movements.

## 1.3 Background to the present study

There have been numerous studies on the geology of the Maltese Islands and the subject is well documented. Contributions have been mostly in the form of papers on the geology and paleontology of the Tertiary and Quaternary deposits. The first description of the geology goes back one and a half centuries and was given by Spratt (1843, 1852). Other key studies were those of Adams (1864, 1870, 1879), Murray (1890), Cooke (1893, 1896), Rizzo (1914, 1932), Trechmann (1938), Reed (1949), Hyde (1955), House *et al.* (1961), Wigglesworth (1964), Felix (1973), Pedley (1975, 1976, 1978), Pedley *et al.* (1976, 1978) and Zammit-Maempel (1977).

There seems to have been less interest regarding the geomorphology of the islands. The most significant studies include those of House *et al.* (1961), Vossmerbäumer (1972) and Alexander (1988). The coastal geomorphology has been dealt in the studies of Guilcher and Paskoff (1975), Paskoff and Sanlaville (1978), Ellenberg (1983) and Paskoff (1985). There is a significant lack of more recent information in this regard. Detailed work on mass movement processes is largely absent. This thesis will therefore serve two purposes: provide an update on existing literature sources where information is already available and present original work where the information is inadequate. It may be significant to note that the region north of the Great Fault of the Victoria Lines has never been dealt with as a separate study but always included in research related to mainland Malta.

Information regarding the physical and mechanical properties of the geological strata in the Maltese Islands is insufficient. Some information can be found in Civil Engineering and Architecture undergraduate dissertations (see for example Bonello, 1988; Saliba, 1990; Farrugia, 1993 and Psaila, 1995). However the dissertations focus mainly on limestone and exclude completely clay material. Some data on clay material is found in Bonello (1988) but this is very limited and not applied to geomorphological studies. The information derived from the dissertations reflects an engineering perspective and is of little relevance to this study.

## 1.4 Approach and organisation of the thesis

The following outlines the structure and organisation of this thesis.

Chapter 2 gives a review of the existing literature on the tectonic and structural setting of the Maltese Islands, putting into context the research presented in the proceeding chapters. The chapter starts with a history of the evolution of fault tectonics in the Maltese Islands. The structural geology and the Oligo-Miocene succession are then discussed in detail as important controls on the general topography and hydrogeological structure.

Chapter 3 deals with the geomorphology of the Maltese Islands with particular reference to the coastal geomorphology. A geomorphological mapping programme was undertaken to determine links between geology and geomorphology and highlight the spatial distribution of coastal landforms. The triggering factors leading to mass movement are examined. The mapping exercise has been used to identify three key sites to perform a more detailed investigation on selected slopes.

The physical and geotechnical properties of Blue Clay are examined in chapter 4 in an attempt to determine the behaviour of the material. Data is interpreted and analysed to explain geomorphological processes and landform development as observed in the field. Chapter 5 attempts to provide a quantitative assessment of slope stability for the north-west coast of Malta. Different results were obtained for the three sites where instability was reached at different stages. The data links other elements of the research presenting additional information and complementing the whole study.

Chapter 6 includes a synopsis of the main conclusions and original contributions derived from this study. The issues of mass movement processes and slope instability set as the main investigating problems of this research present a new and challenging research area in the Maltese Islands. Suggestions are made for further research.

# *Chapter 2*

# *The tectonic, structural and geological setting of the Maltese Islands*

## 2.1 Introduction

The Maltese Islands are located in the central Mediterranean region between Italy and North Africa, at a latitude of 35°48'28" to 36°05'00" North and a longitude of 14°11'04" to 14°34'37" East (Schembri, 1993). The archipelago consists of three main islands: Malta, Gozo and Comino and a number of small uninhabited islets which include: Cominotto (Maltese: *Kemmunett*), Filfola (better known by its Maltese name *Filfla*), St.Paul's Islands (Maltese: *Il-Gzejjer ta' San Pawl*, or Selmunett Islands), Fungus Rock (Maltese: *Il-Hagra* / *Il-Gebla tal-General* or General's Rock) and a few other minor rocks (Figure 2.1).

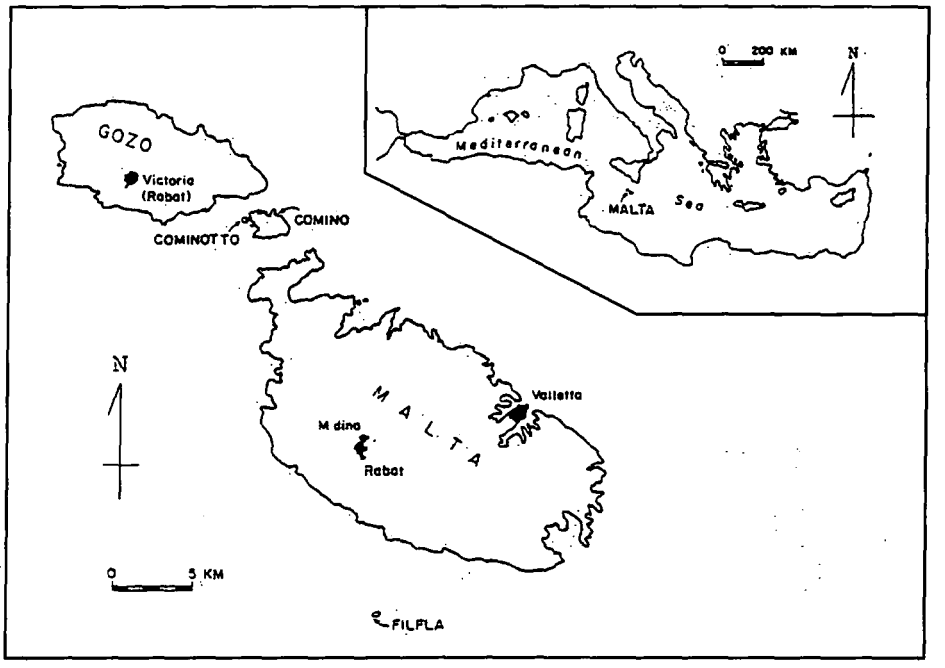


**Figure 2.1: Location of the Maltese Islands**
Source: Alexander, 1988

The islands have a total land area of 316 km² (Malta: 245.7 km², Gozo: 67.1 km², Comino: 2.8 km²) and a coastline about 190 km long, with a submerged area (up to 100 m) of 1,940 km² (Schembri, 1990). The length of the whole archipelago is 45 km; Malta being 27 km long, Gozo 14.5 km long and Comino 2.5 km. The North Comino Channel, which separates Gozo from Comino, is 1 km wide. The South Comino Channel, separating Comino from Malta, is 2 km wide (Figure 2.2).

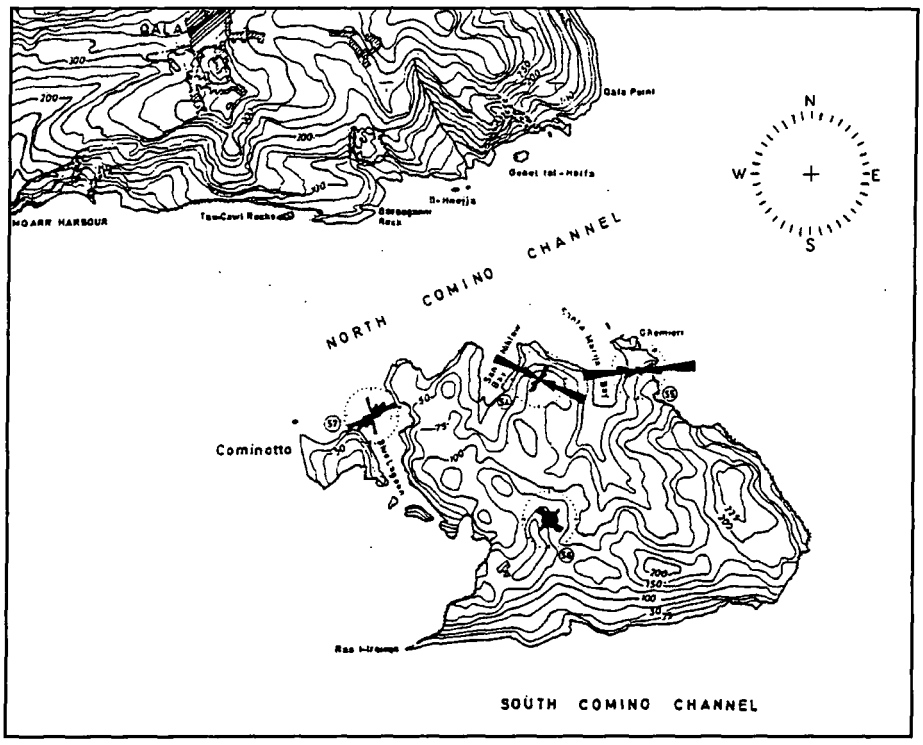


**Figure 2.2: The North and South Comino Channels**
Source: Vossmerbäumer, 1972

The islands lie approximately 96 km from Sicily to the north, 290 km from North Africa to the south, 1,836 km from Gibraltar to the west and 1,519 km from Alexandria, Egypt to the east. They are situated on a shallow shelf, the Malta-Ragusa Rise, part of the submarine ridge which extends from the Ragusa peninsula of Sicily southwards to the North African coasts of Tripoli and Libya. Geophysically the Maltese Islands and the Ragusa peninsula of Sicily are regarded as forming part of the African continental plate. The archipelago is linked to the Ragusa peninsula in the Sicilian Channel by a submarine ridge, which reaches a maximum depth of 200 m below present sea-level and is mostly less than 90 m deep. The sea depth between the islands and North Africa is much deeper, sometimes reaching more than 1000 m (Morelli *et al.*, 1975 *in* Schembri, 1993). According to Spratt (1867) the submarine ridge was an epicontinental land bridge during the Pleistocene and facilitated the migration both northwards and southwards of exotic fauna.

The first description of the geology of Malta was given by Spratt (1843, 1852) and later by Adams (1864, 1870, 1879). An account given by John Murray (1890) has stimulated others, especially Cooke (1893, 1896), to examine the rocks in more detail. During this century Rizzo (1914, 1932), Trechmann (1938), Reed (1949), Hyde (1955), House *et al.* (1961), Wigglesworth (1964), Felix (1973), Pedley (1975, 1976, 1978), Pedley *et al.* (1976, 1978) and Zammit-Maempel (1977) have all made significant contributions. The stratigraphy of the Maltese Islands is summarised in Table 2.1

**Table 2.1: Stratigraphy of the Maltese Islands**

| *Epoch* | *Stage Years BP* | *Formation* | *Maximum thickness (m)* |
|---|---|---|---|
| U. Miocene | Tortonian (12-7.5 Ma) | Upper Coralline Limestone | 104-175 |
| | | Greensand | 0-16 |
| M.Miocene | Serravallian (13-12 Ma) | Blue Clay | 0-75 |
| M.Miocene | Langhian (15-13 Ma) | Upper Globigerina Limestone | 5-20 |
| | | Upper Main Conglomerate (C2) | |
| L.Miocene | Burdigalian (20-15 Ma) | Middle Globigerina Limestone | 0-110 |
| | | Lower Main Conglomerate (C1) | |
| L.Miocene | Aquitanian | Lower Globigerina Limestone | 5-110 |
| U.Oligocene | Chattian | Lower Coralline Limestone | 140 |

Lithostratigraphy mainly after Murray (1890); chronostratigraphy after Felix (1973)

Sources: Pedley *et al.*, 1978; Alexander, 1988

The islands were settled continuously from the middle Neolithic onwards. Important stone temples were constructed in the period 2600-1700 BC (Evans, 1971 *in* Alexander, 1988). Since then the islands have been occupied by Phoenicians, Greeks, Carthaginians, Romans, Arabs, Normans, Angevins, Aragonese, the Knights of St.John, French, and finally the British. Malta became an independent country in 1964. The islands presently have a population of around 378,132 (Census, 1995). This figure results in a population density of 1,200 persons per $km^2$, one of the highest in the world.

This chapter will review existing literature on tectonics, stratigraphy, structural geology and hydrogeology of the Maltese archipelago, in order to assess their influence on the evolution of the present geomorphological features with special reference to coastal landslides.

## 2.2 Evolution of Maltese fault tectonics

The structural setting of the Maltese Islands is dominated by two rift systems of different ages and trends (Figure 2.3). Accompanying faults are exposed at many places along cliffs and are associated with rift faulting (Illies, 1981). The older rift generation traversing the islands strikes about 50° to 70° to create a basin-and-range or horst and graben structure on western Malta, Comino and eastern Gozo. The second-generation rift, associated with the Pantelleria Rift, strikes Malta at about 120° and Gozo between 80° and 90° (Figure 2.4). Rifting mainly originated during the Late Miocene / Early Pliocene, to continue in parts up to the present (Illies, 1981). A set of transform faults runs through the straits on both sides of Comino to form a complicated *en echelon* or Riedel shear structure on eastern Gozo and western Malta. Shoulder up-warping related to the Pantelleria rift has considerably tilted the block of Malta towards the NNE and caused the inundated river valleys of the natural harbour of Valletta. The superimposition of the two rift structures of different trends has been caused principally by a rotation of the controlling stress regime about 10 Ma years ago. As the trends of both rift systems are different, the related structural patterns are crossing each other to form a biaxial system.

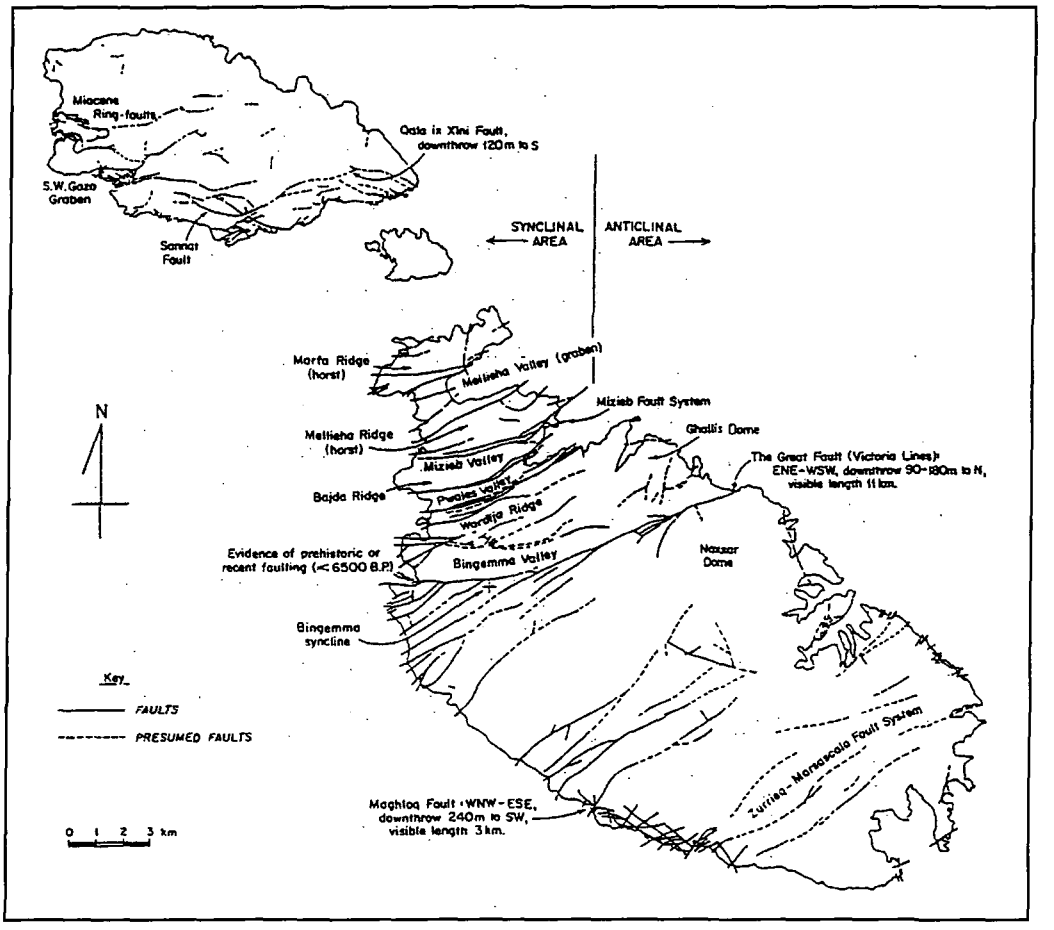


**Figure 2.3: The tectonic structure of the Maltese Islands**
Source: Alexander, 1988

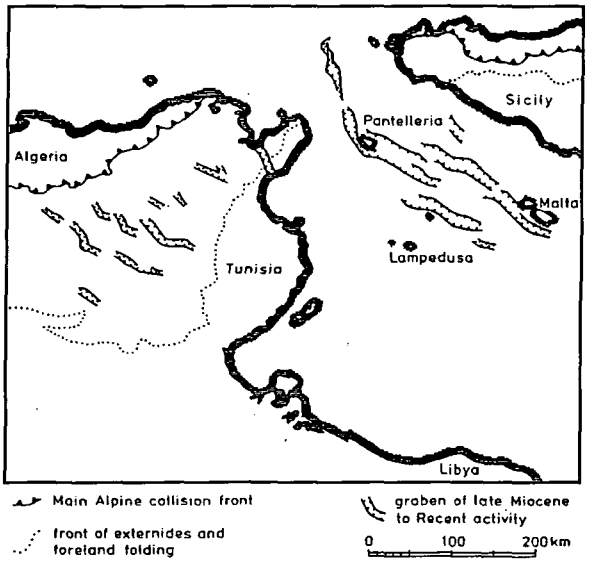


**Figure 2.4: The system of the Pantelleria Rift traverses the shelf between Sicily and Northern Africa. Parallel grabens are observed in Tunisia. The general trend of foreland rifting is about normal to the northward adjacent segment of the Alpine collision front.**

Source: Illies, 1981

The Maltese Islands form an elevation on a submarine ridge that extends southwards from Sicily. On Malta and Gozo, the bedding is generally sub-horizontal, with a maximum dip of about 5°. The fracture pattern is dominated by two intersecting fault systems which alternate in tectonic activity. A NE-SW to ENE-WSW trending fault, the Grand Fault, traverses the islands and is crossed by a NW-SE trending fault, the Maghlaq Fault (Figure 2.3), parallel to the Malta trough, which is the easternmost graben of the Pantelleria Rift System. In general the faults, all vertical or subvertical, are part of a horst and graben system of relatively small vertical displacement. Folding is restricted to slump, drag folding and one larger anticlinal structure.

Reuther (1984) has summarised the structural evolution of the Maltese Islands as follows.

1. **Lower Miocene:** synsedimentary NE-SW (50° to 70°) trending extension fractures developed.
2. **Upper Tortonian:** synsedimentary normal faults, trending 150°, reflect the first tectonic impulse in the formation of the Pantelleria Rift (south-west Malta) which interrupts, in a NW-SE direction, the shelf bridge that connects northern Africa with southern Sicily.
3. **Post Tortonian – Lower Messinian** and **pre-Quaternary:** NE-SW to ENE-WSW (60° to 80°) trending horsts and grabens were formed. At the same time the Pantelleria Rift evolved with its climax in the Pliocene. The contemporaneousness of both events might be due to a mantle updoming which hit pre-existent crossing weakness zones in the overlying crust.
4. **Quaternary – Recent:** normal faulting orientated 120° and associated with the Pantelleria Rift. Continuous rifting leads to ongoing shoulder unwarping, with the Maltese Islands tilting towards the north-east.

### 2.2.1 An extinct basin-and-range structure

Western Malta, Comino, and easternmost Gozo are characterized by a basin-and-range physiography. Subsided basins, often filled with Quaternary gravel fans, are between cuesta-like asymmetric ridges of Miocene hard rocks. The coastlines

accentuate the 50° to 70° striking features by bay-to-bay and point-to-point configurations, respectively (Figure 2.5). A series of tilt blocks is observed along the cliffs (House *et al.*, 1961). They are separated by normal faults dipping mostly between 55° and 75°. The fault planes are often split into two or more separate sheets, formed by down-dragged lenses of Blue Clay. Due to antithetic tilt block rotations, the individual blocks exhibit inclinations between 2° and 30°.

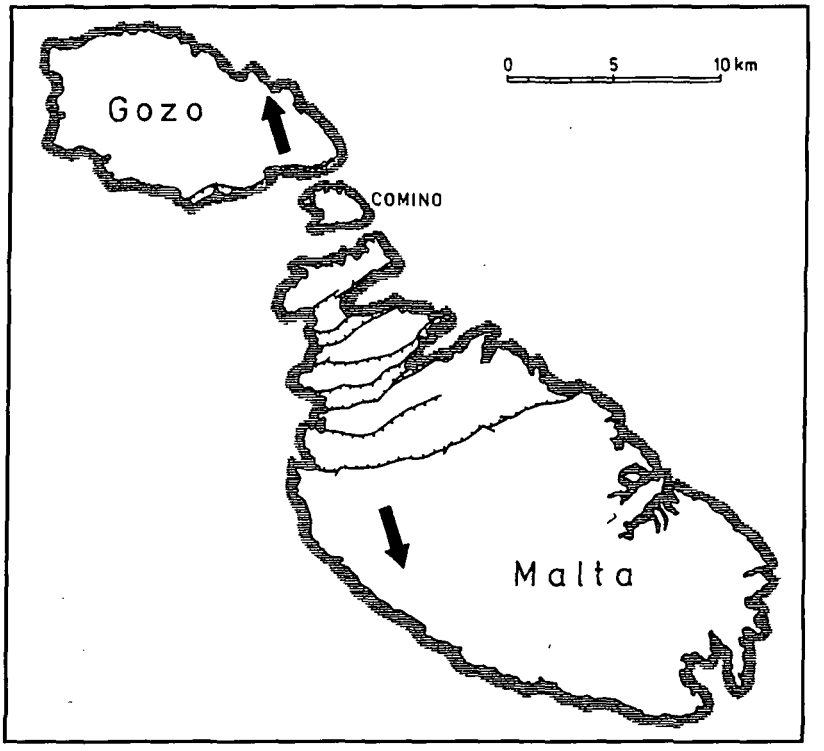


**Figure 2.5: Basin-and-range features, physiographically as well as tectonically, characterize the segment between central Malta and southern Gozo. A crustal spreading of intra- to end-Miocene age has brought about an approximately 15 per cent extension normal to the rift belt (arrows).**

Source: Illies, 1981

The vertical throw of the internal faults ranges from some decimeters to about 120 m. As a whole, the basin-and-range pattern is framed by two parallel master faults, forming a 13 km to 14 km wide wedge-block of a graben-like configuration. The maximum throw of the master faults is about 200 m.

The basin-and-range feature is framed on both flanks by upwarped shoulders, stratigraphically, and in part physiographically, forming the hills of the Victoria Lines

in Malta and of Nadur in Gozo. Independent tectonic movements and events, parallel to the future basin-and-range structure, were first indicated during the deposition of the Globigerina Limestone.

The main basin-and-range faults separate the whole Oligo-Miocene succession. Consequently, physiographic rifting has evolved after the deposition of the Upper Coralline Limestone. No post-Tertiary vertical displacements are known from this fault generation. The deformational cycle forming the basin-and-range physiography became extinct before an extensive denudation set in during Early Pleistocene or perhaps Pliocene times.

The extinct basin-and-range structure constitutes the oldest tectonic movements observable on the Maltese Islands. The movements have produced synsedimentary NE-SW trending extension features, which were formed during the deposition of the Globigerina Limestone Formation. The structures were first interpreted by Illies (1980) who described growth faulting with a trend of 55° south of Xlendi Bay on Gozo. The synsedimentary movements took place before the deposition of the first main phosphorite layer, which marks the top of the Lower Globigerina Limestone Formation and corresponds to the Aquitanian / Burdigalian boundary (Felix, 1973). The main dip-slip events forming the NE-SW trending horsts and grabens, which are also topographically very well pronounced, took place after the deposition of the Upper Coralline Limestone Formation. The throw along the northward dipping Victoria Lines Fault reaches 183 m on the west coast of Malta and decreases towards the east coast to about 90 m (House *et al.*, 1961). The vertical displacement of the South Gozo Fault, dipping southwards, is about 100 m. This graben generation, traceable to the Aquitanian, became extinct before the Quaternary (Illies, 1980, 1981). No vertical displacements of Quaternary deposits at this fault generation are known on the islands; rather the fault scarps are unconformably capped by Pleistocene sediments.

### 2.2.2 Pantelleria rift system

The Maltese Islands rise up to 253 m above sea-level, from an emerged part on the southern upwarped north-east shoulder of the Pantelleria Rift (Figure 2.4). The latter is a graben system active in Late Miocene to Recent time, which interrupts the shallow shelf platform connecting Europe and Africa (Illies, 1981). The fracture pattern of the islands has been created by tectonic processes governed by the relative motions between the European and African plates. The plate boundary runs about 200 km to 400 km to the north of Malta from Tunisia to Sicily.

Faults on the Maltese Islands associated with the Pantelleria Rift are represented by the NW-SE trend. The NW-SE trending normal faulting occurred before the Tortonian sedimentation of the Upper Coralline Limestone. This is interpreted to be connected with the initial movements of the Pantelleria Rift System. The main subsidence lasted through the Pliocene (Finetti and Morelli, 1973 *in* Reuther, 1984). Some faults of the Pantelleria Rift are considered to be active up to present times.

The most prominent young tectonic feature is the system of the Maghlaq Fault (Pedley and Waugh, 1976 *in* Reuther, 1984) (Figure 2.6) south-east of Ix-Xaqqa, along the southern coast of Malta, with a vertical displacement of at least 240 m to the SW (House *et al.*, 1961). The 120° trending fault shows neotectonic activity. An interstratification of red soil, breccia and caliche at Ras il-Bajjada 3 km south-east of Ix-Xaqqa is cut by the fault and slickensided. At Ix-Xaqqa young sediments of probably Quaternary age are smeared in the fault plane. Quaternary and post-Quaternary tectonics along the Maghlaq fault have also been mentioned by Trechmann (1938) and Illies (1980, 1981). The NW-SE trending faults cross-cut and displace the previous structures (Illies, 1980, 1981; Reuther, 1983b *in* Reuther, 1984). This is to be observed in central Malta and along the southern and northern coast of south-east Malta. A very expressive exposure showing the displacement of a 70° striking normal fault along two 135° trending normal faults, is to be seen in the Globigerina Limestone at Il-Gzira on the eastern coast of Malta.

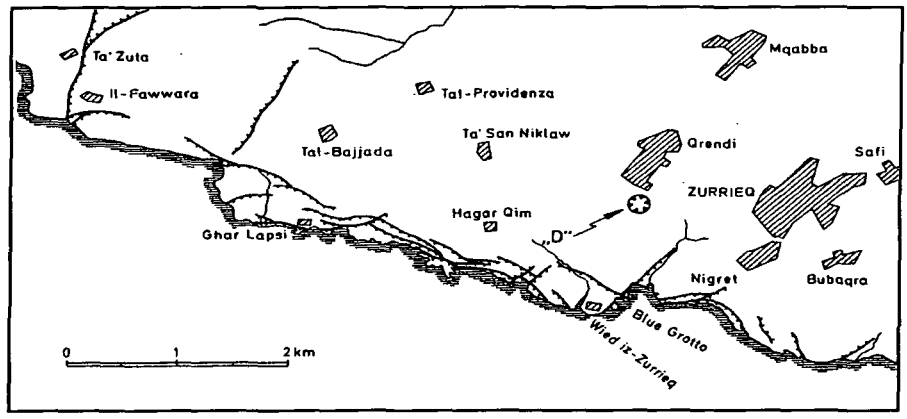


**Figure 2.6: The main features of the Maghlaq fault system strike parallel to the southern coastline of Malta. This fault pattern represents the outer master fault of the Pantelleria rift. D refers to Il-Maqluba doline.**

Source: Illies, 1981

Besides normal faulting, the Maltese Islands have been affected by horizontal movements. This is indicated at many sites by the formation of second order tension-and-shear fractures. The features specify the relative sense of strike-slip movements. The second order shear structures visible in the Globigerina Limestone at the northern coast of Malta in the Sliema region are related to sinistral strike-slip movements trending between 140° and 160°. Small scale shear structures are very well developed in the Lower Globigerina Limestone on the northern coast of Gozo. In general the NE-SW shear direction is of dextral polarity while the NW-SE direction is of sinistral polarity.

On Malta, fault systems belonging to the two generations of rifting are cross-cutting each other in many places. This may be observed particularly well in the Valletta area (Illies, 1980), where 120° striking minor dip-slip faults dislocate to about 50° trending faults of the first generation (Figure 2.7). The magnificent natural harbour system of Valletta with cross-cutting basins and ridges of both directions has been formed by inundated river valleys that erosionally followed the traces of the two rupture systems.

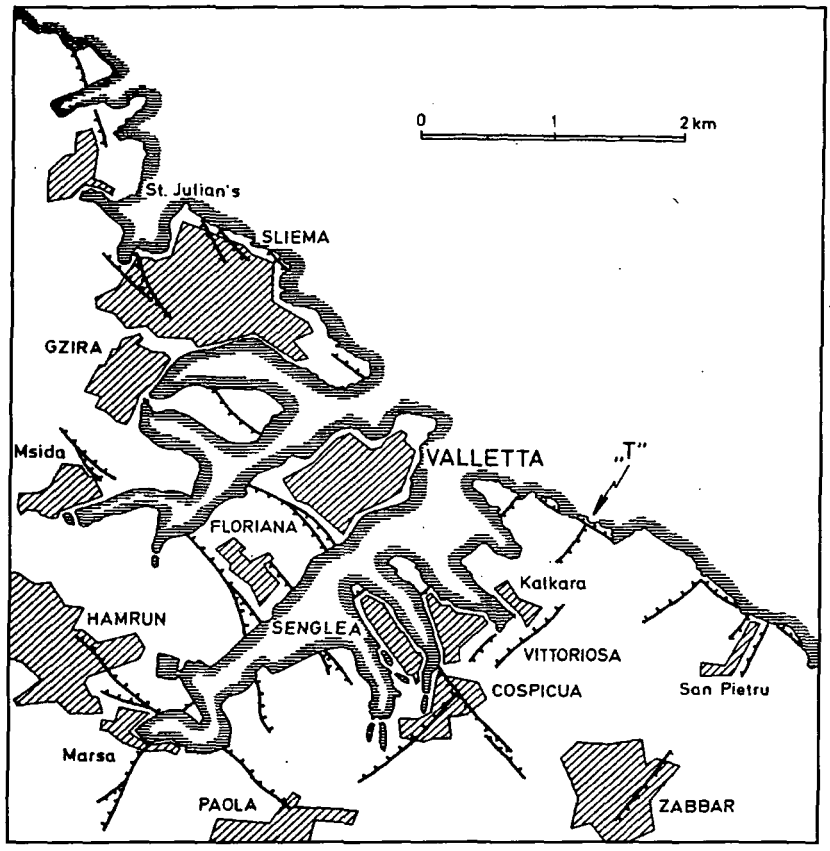


**Figure 2.7: The Valletta area is characterized by the cross-cutting of minor faults associated with the two stages of rifting. The basins and ridges of the natural harbour are conditioned by an inundated drainage pattern which followed the traces of the two rift generations. T refers to well exposed cross-cutting of faults.**

Source: Illies, 1981

### 2.2.3 Age of the tectonic features

The major faults all incise the entire Oligo-Miocene succession and there is considerable evidence that movement has been continuous since Miocene times. Many of the faults exhibit fresh fault-scarp faces, with mullion-style slickensiding and negligible scarp recession, suggesting that the faulting must partly be quite recent. Trechmann (1938) believed that the Maghlaq Fault had moved during the Quaternary. Pedley (1974 *in* Pedley *et al.*, 1976) has demonstrated that the solution subsidence structures of the islands have been activated at a number of periods since their initiation during the Miocene. More general regional movements in post-Quaternary times have resulted in the development of localised raised beaches, the submergence of Neolithic cart-tracks at St.George's Bay and St.Paul's Bay (Hyde, 1955), and the

presence of stalagmites below the breakwater foundations of the Grand Harbour (Rizzo, 1932). There is evidence that the structural movements are still in progress. Earthquakes were recorded in 1659, 1693, 1740, 1811, 1856, and 1972. Minor tremors have been recorded during recent years.

## 2.3 Geology of the Maltese Islands

### 2.3.1 Stratigraphy

The Maltese Islands are entirely composed of Tertiary limestones with subsidiary marls and clays. Quaternary deposits, mostly Pleistocene in age, are limited to few localities and take the form of cliff breccias, cave and valley loams, sands and gravels. Deposition occurred in the following simple succession.

i. Upper Coralline Limestone: youngest formation and last deposited
ii. Greensand
iii. Blue Clay
iv. Globigerina Limestone
v. Lower Coralline Limestone: oldest formation and first deposited.

Table 2.1 presents in detail the litho- and chronostratigraphy of the Maltese Islands.

This succession represents a varied cross-section of Oligo-Miocene lithologies and facies, but consist almost entirely of carbonates. The geological formations of the islands are very distinctive lithologically and this is reflected in characteristic topography and vegetation (House *et al.*, 1961). The Lower Coralline Limestone is reponsible for forming spectacular cliffs, some reaching 140 m in height, which bound the islands especially in the west. Inland the Lower Coralline Limestone forms barren grey limestone-pavement topography. The succeeding Globigerina Limestone, which is the most extensive formation on the islands, forms a broad, rolling landscape. The soil is thin but intensively cultivated and hillslopes on it are densely terraced. The Blue Clay produces slopes that tend to slide over the underlying Globigerina Limestone Formation. It forms the most fertile bedrock on the islands,

especially where springs seep from the overlying Upper Coralline Limestone. The latter, which also includes Greensand, forms massive cliffs and limestone pavements with karstic topography similar to Lower Coralline Limestone. It caps tabular hills and mesas reaching a maximum height of 253 m at Ta' Zuta, near Dingli in south-west Malta (Pedley *et al.*, 1978). Figure 2.8 illustrates the spatial distribution of the different geological formations of the Maltese Islands.

The lithostratigraphy of the Maltese Islands has been well known since the time of Spratt (1843) due to its simple structure and the gentle regional dips. The current terminology applied to the individual formations originated from the detailed work of Murray (1890). Although Murray's lithostratigraphy is still generally accurate, work by Pedley (1975) has substantially improved the detailed understanding of both lithostratigraphy and palaeoecology, especially within the two Coralline Limestone formations. Spratt (1867) was the earliest worker to publish on the Quaternary geology. A more detailed study was carried out by Trechmann (1938).

The biostratigraphy and chronostratigraphy have remained subject to debate since the earliest times, despite the acceptance of the lithostratigraphic subdivision of the sequence. This is primarily due to the isolated position of the archipelago. Fuchs (1874 *in* Pedley *et al.*, 1976) first appreciated the mid-Tertiary age of the Maltese strata. However this was followed by other comparisons put forward by Gregory (1891 *in* Pedley *et al.*, 1976) using echinoids. Bather (date not available) (*in* Trechmann, 1938) established the occurrence of both Oligocene and Miocene strata.

House *et al.* (1961) following Eames and Cox (1956 *in* Pedley *et al.*, 1976), assigned the Lower Coralline Limestone and Lower Globigerina Limestone to the Aquitanian, the remaining Globigerina Limestone and Blue Clay to the Burdigalian, and the Greensand and Upper Coralline Limestone to the Helvetian and Tortonian. A more restricted range was envisaged by Eames *et al.* (1962 *in* Pedley *et al.*, 1978) on the evidence of foraminiferal studies. They considered all the strata to be of Lower Miocene age, the Lower Coralline Limestone being Aquitanian and overlying formations Burdigalian. A later correlation, also based on foraminifera, is that of Felix (1973) (Table 2.1).

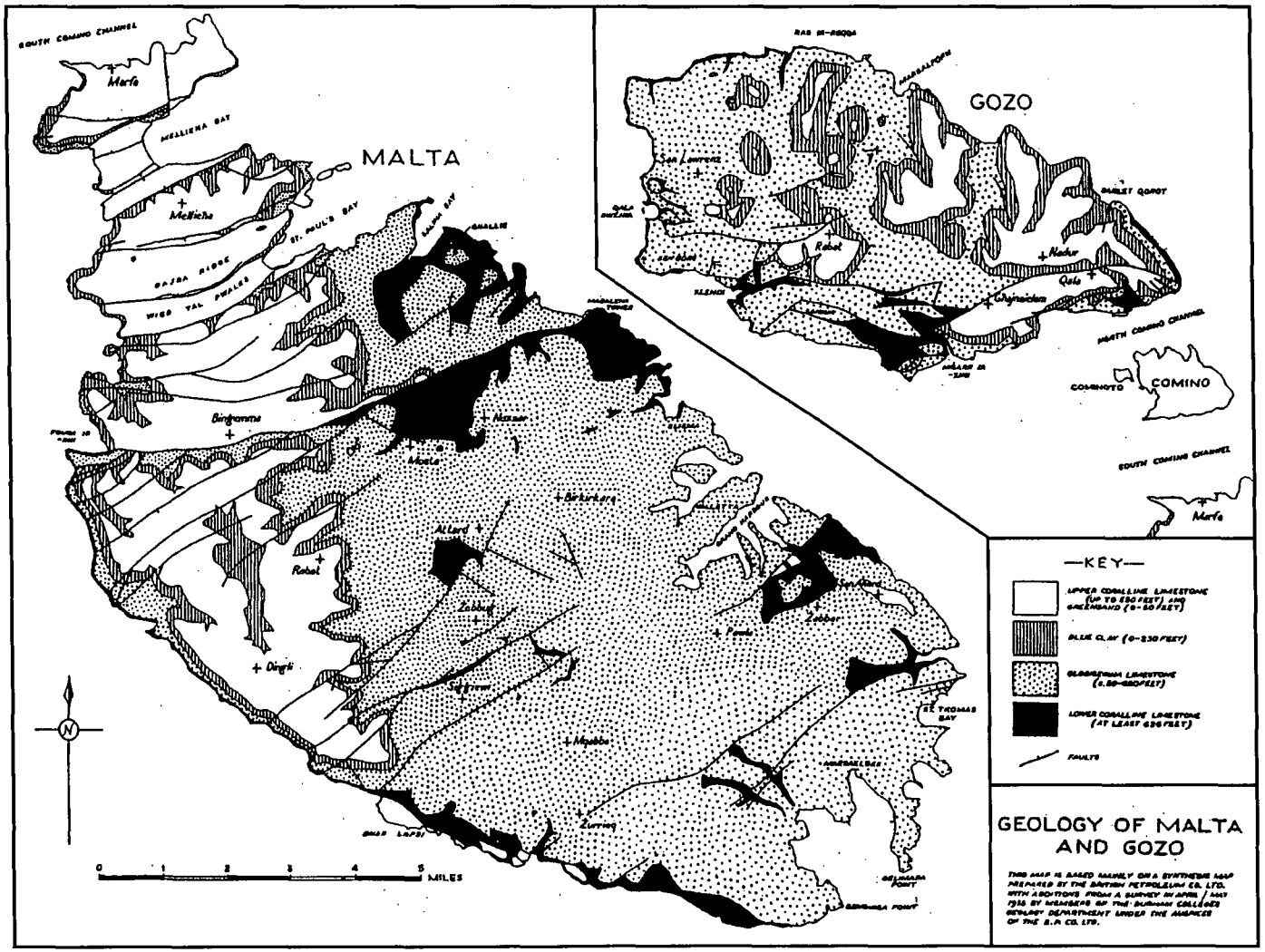


**Figure 2.8: The geology of the Maltese archipelago**
Source: House *et al.*, 1961

### 2.3.2 The Oligo-Miocene succession

The sequence of rock units of limestones and associated marls represents a succession of sediments deposited within a variety of shallow water marine environments (Pedley *et al.*, 1978). In many respects these resemble the mid-Tertiary limestones occurring in the Ragusa region of Sicily and North Africa. Paleomagnetic and volcanological evidence from Sicily (Barberi *et al.*, 1974 *in* Pedley *et al.*, 1978) demonstrates that the Africa-Europe plate boundary passes through northern Sicily. Consequently, it would appear that Malta was part of a mid-Tertiary Tethyan carbonate platform, extending from southern Sicily to North Africa, with Malta situated toward the leading edge of the African plate. Geophysical data from Cooper, Harrison and Willmore (1952 *in* Pedley *et al.*, 1976) further indicate that the islands are situated above a region of high gravity anomaly values, which are coincidental with the Ragusa-Malta Rise.

A deep borehole dug by the British Petroleum Co.Ltd. at Naxxar indicates that Malta has been a region of continued carbonate sedimentation for a considerable period prior to the Miocene (Pedley *et al.*, 1978). Commencing at the top of the Lower Coralline Limestone, the hole terminated at a depth of 3000 m in dolomites which carry spores of Lower Cretaceous association. Higher Cretaceous and Eocene rocks were also dolomitized limestones. The uppermost 650 m of shelly limestones and subordinate shales was referred to the Oligocene by Felix (1973) (Table 2.1).

The succession gives the impression that the depositional area first subsided and then there was a gradual shallowing (Felix, 1973). The sequence starts with the Lower Coralline Limestone, deposited in a shallow gulf-type area followed by a sea with shoals. The Globigerina Limestone and Blue Clay show a deepening in an open marine environment, to a maximum depth of 150 m to 200 m, as suggested by the foraminiferal faunas. The upper two formations, the Greensand and the Upper Coralline Limestone and their foraminiferal associations, indicate a gradual shallowing to an area with shoals but still in an open marine environment.

### 2.3.2.1 Lower Coralline Limestone

The Lower Coralline Limestone is the oldest formation visible on the islands. Outcrops are mainly restricted to coastal sections along the western sides of Malta and Gozo (Pedley *et al.*, 1976). Vertical cliffs show up to 140 m in south-west Gozo and about 100 m in the sections between Fomm ir-Rih and Benghisa Point in western and southern Malta. Inland exposures are mostly associated either with valley-gorge sections, as in southern Malta, or with faulted inliers such as at Naxxar. The upper part of the Lower Coralline Limestone Formation is exploited in quarries (Pedley *et al.*, 1978). The lowest horizons of the formation are exposed in cliff-sections around Maghlaq, south-west Malta (Pedley *et al.*, 1976). Local terminology for this formation is *Zonqor*.

Pedley (1978) has subdivided the Lower Coralline Limestone Formation into four members: the Maghlaq Member (oldest); the Attard Member; the Xlendi Member; and the Il-Mara Member (youngest). The name attributed to each member indicates the site where the member is best exposed.

With the exception of the highly variable *Scutella* Bed, the Lower Coralline Limestone Formation lacks macrofossils that might be useful for correlation except at a local scale (Pedley, 1978). Deposition of the Lower Coralline Limestone appears to have initially been in a shallow gulf-type area (Felix, 1973). Succeeding beds provide evidence of increasingly open marine conditions during which algal rhodolites developed. Finally a shallow marine shoal environment succeeded as the dominant environment in all areas except south-eastern Malta. In this area calmer conditions prevailed in a protected deeper water environment (Pedley *et al.*, 1976).

### 2.3.2.2 Globigerina Limestone

The Globigerina Limestone Formation is given this name due to the high percentage of planktonic foraminifera present in the rock (Pedley *et al.*, 1976, 1978). The formation covers large areas of central and southern Malta and Gozo. The outcrops are frequently obscured by housing and agricultural development. The most accessible sections in Malta are along the Qammieh coastline, northern Malta. In

Gozo the formation is well exposed in the *wied* gorges around San Lawrenz. The formation shows marked thickness variations ranging from 23 m near Fort Chambrey, southern Gozo, to about 207 m around Marsaxlokk, southern Malta. A thick succession is also developed in the Valletta Basin, where only the Lower Globigerina Limestone is now preserved. The usual colour of the formation is pale-yellow. A pale-grey subdivision, bounded both above and below by phosphorite conglomerate horizons, occurs in the middle of the sequence. The Globigerina Limestone provides most of the building stone in Malta and in local terminology is referred to as *Franka* (Pedley *et al.*, 1976). This formation is further subdivided into Lower, Middle and Upper Globigerina Limestone separated by two phosphorite conglomerate horizons.

#### 2.3.2.3 Blue Clay

The Blue Clay Formation comprises a sequence of alternating pale grey and dark grey banded marls, with lighter bands containing the highest proportion of carbonate (Pedley *et al.*, 1978). The formation never contains more than 30 per cent carbonate material (Murray, 1890). This lithology is found throughout the islands and possibly also at the base of the cliffs on the island of Filfla, off the western coast of Malta (Pedley *et al.*, 1976). Towards the Comino Straits the upper part of the succession contains clays which are uniformly dark grey in colour, lacking banding, and yielding abundant limonite and goethite concretions (Pedley *et al.*, 1978).

The maximum thickness of the Blue Clay Formation is approximately 75 m recorded at Xaghra, northern Gozo, and on the western coast of Malta north of Fomm ir-Rih Bay (Pedley *et al.*, 1976, 1978). Marked thinning occurs towards the south and east, where the formation has been mostly removed by erosion, and at San Leonardo in Malta where the Blue Clay is absent as a result of pre-Upper Coralline Limestone erosion. In Gozo the formation increases in thickness from 10 m along the southern coast to over 60 m in the north. A depositional high in the region of the Comino Straits is again apparent.

Although common, most fossils are restricted to microfauna or crushed specimens of macrofauna, except in the upper horizons of the Blue Clay around northern Malta and southern Gozo (Pedley *et al.*, 1976). In this region goethite impregnated specimens of

the corals *Balanophyllia*, *Flabellum* and *Stephanophyllia* are common, as are the molluscs *Aturia aturi*, *Sepia*, *Flabellipecten*, *Chlamys* and indeterminate gastropods. The echinoid *Schizaster* and the pteropod *Vaginella* also occur. Foraminifera are abundant throughout, with species of *Globigerina* and *Orbulina* being the most common (Pedley *et al.*, 1978). Marine vertebrate remains are invariably disarticulated and consist of fragments and centrae of *Phoca*, *Cetacea*, many fish and dugongs.

An open muddy marine environment is envisaged with water depths up to 150 m for the lowest part of the formation. Shallowing probably occurred in the upper parts of the unit to depths less than 100 m (Pedley *et al.*, 1978).

#### 2.3.2.4 Greensand

The Greensand Formation is composed of thickly bedded, coarse, glauconitic, bioclastic limestones (Pedley *et al.*, 1978). In unweathered sections the green and black glauconite grains are readily discernible. Usually due to the release of limonite upon weathering and oxidation of the glauconite, the rock possesses a characteristic orange-brown colour. The transitional change upwards from the Blue Clay is frequently sharp, particularly in the western areas of the islands. In eastern parts assimilation of the top of the Greensand into the base of the overlying Upper Coralline Limestone, as a result of bioturbation, has produced the effect of a gradual change in sedimentation (Pedley *et al.*, 1976).

The maximum development of the Greensand Formation is at Il-Gelmus in Gozo, where 16 m can be measured. In a second structure to the north of Il-Gelmus a 7 m thickness is recorded (Pedley *et al.*, 1976). Throughout the rest of Malta and Gozo the formation, if restricted to the main glauconitic beds, is usually less than 1 m thick and shows extensive reworking and assimilation into the overlying strata (Pedley *et al.*, 1978).

The formation largely consists of transported material which also includes most of the glauconite grains and derived fossil casts such as *Conus*. Other areas of Greensand outcrop yield vertebrate fragments of sharks, *Cetacea* and smaller marine mammals. The foraminifer *Heterostegina* is common in western areas. The intense bioturbation

suggests deposition under shallow water marine conditions. Much of the sediment was transported into the region from areas of erosion outside the present confines of the islands (Pedley *et al.*, 1976).

### 2.3.2.5 Upper Coralline Limestone

The Upper Coralline Limestone is the youngest Tertiary formation of the Maltese Islands and is similar in many aspects to the Lower Coralline Limestone Formation, especially in colour and coralline algal content (Pedley *et al.*, 1976). It is a durable sequence, frequently weathering into steep cliffs and featuring a well-developed karst topography. Outcrops occur on all islands of the Maltese archipelago and the formation is extensively developed especially in western Malta, Comino and east-central Gozo, where it displays a wide range of lateral and vertical facies variations. A maximum thickness of approximately 100 m of strata is present in a lithological sequence, which can be divided into three divisions (Pedley *et al.*, 1978). The Maltese terminology used for this formation is *Tal-Qawwi.*

Pedley (1978) divides the Upper Coralline Limestone Formation into four members, each member consisting of several beds: Ghajn Melel Member; Mtarfa Member; Tal-Pitkal Member; and the Gebel Imbark Member.

The Ghajn Melel Member overlies the basal Upper Coralline Limestone erosion surface and is included within the formation. This member includes the Ghajn Znuber Beds in the east and the Zebbug Beds in the west (Pedley, 1978).

The Mtarfa Member has been subdivided into three units: Coralline Algal Bioherm (oldest), Gebel Mtarfa Beds, and Rdum il-Hmar Beds (youngest). A brachiopod bed (*Terebratula–Aphelesia* Bed) occurs in the Coralline Algal Bioherm and basal sections of Gebel Mtarfa Beds. The Rdum il-Hmar Beds developed as a result of a later reduction in the volume of iron oxides entering the eastern area, together with a slight regional subsidence of the sea floor (Pedley, 1978).

Tal-Pitkal Member consists of the following beds: Rabat Plateau Beds (oldest), Depiru Beds, Ghadira Beds and Ghar Lapsi Beds. Increasing turbulence within the

Maltese area and probable shallowing of the region to the west of the area gave rise to the coarse, bioclastic, Rabat Plateau Beds. Along the shallowest western margins of the area, patch reefs developed the Depiru Beds. The Ghadira Beds formed as a result of the eastwards influence of the reefs. The thin-bedded Ghar Lapsi Beds were deposited in a sheltered intertidal embayment adjacent to a low coastline (Pedley, 1978).

Outcrops of the Gebel Imbark Member are restricted to outliers preserved on hilltops, as at Gebel Imbark, or in the cores of synclines, as at Bingemma, both on Malta. A local erosion surface is developed at the base of the succession in western localities. This member is further subdivided into Tat-Tomna Beds, Qammieh Beds and San Leonardo Beds (Pedley, 1978).

#### 2.3.2.6 Quaternary deposits

Trechmann (1938) carried out a detailed study of the quaternary deposits of the Maltese Islands and has classified them into valley loams and breccias; coastal conglomerates and breccias; and ossiferous deposits in caves and fissures. The earliest of the deposits are the Pleistocene ossiferous deposits of various cave systems in Malta, which have yielded numerous interesting animal remains (Pedley *et al.*, 1978). The Ghar Dalam cave is the most well-known. Others are found at Qrendi, Zebbug, and Mellieha. The oldest faunas include Pleistocene dwarf hippopotami, pygmy elephants, dormice and swans. A later deposit features horse and deer (House *et al.*, 1961). The presence of so many land quadrupedal animals is taken as evidence that there was land communication between Sicily and Malta at this period (Pedley *et al.*, 1978).

Later deposits, which invariably possess a distinct red colour, include alluvial fans, caliche soil profiles and calcreted breccias and conglomerates. All are stained red by iron oxidation. The first two developments are well seen at Wied Maghlaq, Malta, at the foot of the Maghlaq fault-scarp. Over 8 m of fanglomerate and caliche soil horizons, sometimes containing root casts, occur here. Similar fan deposits occur in Pwales Valley and near St.Paul's Bay (Pedley *et al.*, 1976). Conglomerates and coastal breccias, often with Pleistocene mollusca, occur in small patches around the

Marfa Ridge, St.Paul's Bay, Mellieha Bay, Ghar Lapsi, Benghisa Point and St.Thomas Bay. They usually form a moderately cemented rock composed of local material (Trechmann, 1938). A caliche soil profile, capped by a red carbonate horizon at Marfa Point, northern Malta, yields terrestrial gastropods (Cooke, 1896c *in* Pedley *et al.*, 1978).

## 2.4 Structural geology

The geological structure of the Maltese Islands is usually divided into three main regions (House *et al.*, 1961; Pedley *et al.*, 1976, 1978).

i. Malta, north of the Victoria Lines Fault.
ii. Malta, south of the Victoria Lines Fault.
iii. Gozo.

### 2.4.1 Malta, north of the Victoria Lines Fault

The Victoria Lines Fault crosses the island from Fomm ir-Rih on the western coast to the proximity of Madliena Tower on the eastern coast (Figures 2.3, 2.9 and 3.3). The fault forms a fault scarp, which is the most significant topographic feature of the island. The maximum effect of the fault can be seen in central areas where the Upper Coralline Limestone on the northern, downthrown side of the fault, is brought into juxtaposition with the Lower Coralline Limestone. Throws along the fault vary from about 200 m near the Bingemma Syncline (Morris, 1952) in the west, to about 100 m in the east near Madliena Tower.

North of the Victoria Lines Fault the structure is dominated by the development of horst and graben blocks, bounded by ENE trending normal faults (Figure 3.3). Such structures are indicated by prominent ridges and valleys, the main units from north to south being Marfa Ridge, Mellieha Valley, Mellieha Ridge, Mizieb Valley, Bajda Ridge, Pwales Valley, Wardija Ridge and Bingemma Valley (Figures 2.3 and 3.3). Comino probably represents the exposed part of an otherwise submerged graben to the north of the Marfa ridge.

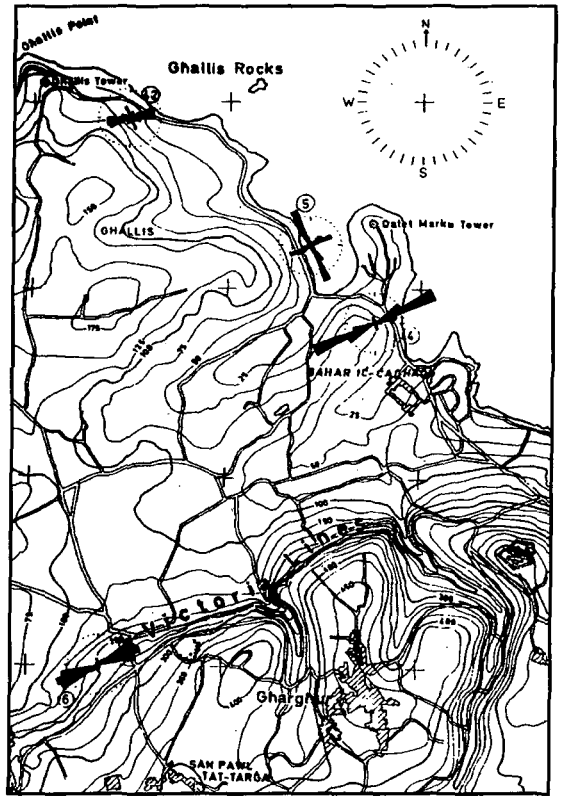


**Figure 2.9: The Victoria Lines Fault cutting through the eastern coast in Malta**
Source: Vossmerbäumer, 1972

The structures are not simple. The fault fractures are often compound, and sharp stratal flexures in both valleys and ridges occur. Approximate figures varying from 10 m to over 100 m with values diminishing eastwards were given by House *et al.* (1961). These have also been discussed by Vossmerbäumer (1972). The fault of greatest throw would appear to be that forming the southern margin of the Marfa Ridge where the Upper Coralline Limestone has a displacement of over 100 m. The throws serve to depress the top of the Lower Coralline Limestone below sea-level for much of this region. In the Ghallis area, to the east of the major dislocations, the Lower Coralline Limestone lies up to 50 m above sea-level and is associated with a broad culmination, the Ghallis Dome (Figure 2.9). Minor north-south faults are also associated with this structure.

The largest syncline structure occurring on the downthrown side of the Victoria Lines Fault is the Bingemma Syncline, associated with the former fault, in which the top of the Lower Coralline Limestone is depressed to an estimated 120 m below sea-level.

### 2.4.2 Malta, south of the Victoria Lines Fault

South of the Victoria Lines Fault a different structural pattern is apparent. The horst and graben structures are absent. Although normal faults are numerous, the dominant fault trend is north-easterly with throws invariably less than 20 m, rapidly diminishing eastwards (Figure 2.3).

In the north-western area of the Rabat Plateau, the faulting is closely associated with the Victoria Lines Fault and all fractures ultimately merge in an easterly direction. Further south at Rdum Dikkiena a second group of normal faults extends north-eastwards into central Malta, whilst faults associated with the Zurrieq-Marsascala system (Figure 2.3) cross the entire width of southern Malta.

Although it is usually considered that the fault pattern of the Maltese Islands constitutes a conjugate system, it is only in southern Malta where the second, north-westerly trending set is evident. This is provided by the Maghlaq Fault (Figure 2.6), which with its smooth, slickensided, seaward facing fault-plane running parallel to the coast, downthrows the Upper Coralline Limestone to the south by at least 230 m. The downfaulted strata are inclined at a high angle. The Maghlaq Fault is not a single fracture but consists, in part, of two closely spaced parallel faults. This results in slivers of Globigerina Limestone and Blue Clay caught up between the two fault walls, at several localities along the fault complex, particularly where the Lower and Upper Coralline Limestone Formations are in juxtaposition. A similar situation is evident at Fomm ir-Rih, at the western end of the Victoria Lines Fault, and in the Qammieh Fault of northern Malta. To the east of the spectacular cliffs formed by the Maghlaq Fault, a series of parallel subsidiary fractures occur which increase in effect towards the south-east. The only other north-westerly trending fault is the minor development along the San Leonardo coastline of eastern Malta. It is possible that the north-west trending coastlines of Malta are bounded by faults of this set.

Apart from faulting, large-scale gentle folding is an important structural feature of central and southern Malta. House *et al.* (1961) confirmed that a major structural high passes southwards from the Victoria Lines Fault to Ghar Lapsi. There are several culminations, the largest of which is the Naxxar Dome in eastern Malta. Here the top

of the Lower Coralline Limestone is 120 m above sea-level. Smaller culminations bring the Lower Coralline Limestone to 80 m and 120 m above sea-level near Zebbug and east of Ghar Lapsi respectively. In other regions folding is very gentle and is usually affected by faulting. This is the case north of Zabbar, where a culmination, abruptly truncated by the Cospicua Fault, brings the top of the Lower Coralline Limestone up to 50 m above sea-level.

At Marsa Creek, around the Grand Harbour, a major basinal depression results in the Lower Coralline Limestone being 40 m below sea-level. In a second depression, centred on Delimara Peninsula, the limestone shelves 130 m below sea-level to the south-east, and extends seawards to unknown depths.

### 2.4.3 Gozo

Gozo is characterised by a gentle regional dip to the north-east. As a result, the Lower Coralline Limestone, which forms vertical cliffs over 120 m high along the south-western coast between Dwejra and Sannat, is depressed to over 20 m below sea-level on the northern coast between Marsalforn and San Blas Bay. The northern parts of Gozo are characterised by this rather simple structural pattern. The structure complicates itself south from San Lawrenz to Qala Point. To the west, at Qawra, Dwejra and Xlendi, three solution subsidence structures with their characteristic circular faults (Murray, 1890; Trechmann, 1938; Hyde, 1955 and Pedley, 1976, 1978) are associated with east-west trending normal faults, extending eastwards as far as the Victoria-Xewkija region in central Gozo. The two largest faults in Gozo, the Sannat and Qala Faults are centred on Mgarr ix-Xini in southern Gozo. The Sannat Fault extending WNW from Mgarr ix-Xini, brings the Lower Coralline Limestone into juxtaposition with the Globigerina Limestone on the northern downthrown side of the fault. The Ix-Xini-Qala Fault has a north-easterly trend with a maximum throw to the south of approximately 120 m just to the south of Nadur. It tectonically separates south-eastern Gozo from the rest of the island. South of the Sannat-Qala Fault system numerous small faults cut the southern coast, and local flexuring depresses the top of the Lower Coralline Limestone below sea-level at Mgarr and Qala Point.

## 2.5 Hydrogeology

The work carried out by Chadwick (1884), Zammit (1931), Morris (1952), Newbery (1963, 1968) and Zezza (1971) includes the main studies on the hydrology and water resources of the Maltese Islands.

The natural water resources depend entirely on rainwater percolating through the porous limestone rock and accumulating in aquifers, from where it either seeps out or is pumped. It has been estimated that between 16 per cent and 25 per cent of the annual rainfall infiltrates to recharge the aquifers (Morris, 1952; Newbery, 1968; Chetcuti, 1988 and Chetcuti *et al.*, 1992). The largest aquifer is the Main Aquifer, also known as the Mean Sea-Level Aquifer, which consists of a lens of freshwater floating on denser saline water in limestone at sea-level (Figure 2.10). The other aquifers of importance are the Perched Aquifers, which consist of rainwater trapped in the permeable Upper Coralline Limestone due to the underlying layer of impermeable Blue Clay (Figure 2.10). Water seepage from the Perched Aquifers, wherever the Upper Coralline Limestone / Blue Clay interface is exposed, gives rise to so-called High Level springs which drain into watercourses. Many of the springs used to flow all year round. Most of them are now tapped by farmers for irrigation. Over the years there have been a number of programmes of small dam construction across the drainage channel watercourses. Construction is aimed at reducing flow and retaining water in the drainage channels for longer periods, to allow increased infiltration and to supply water for irrigation.

In the Lower Coralline Limestone aquifer, where the water-table is controlled by sea-level, the downward percolating fresh water from rainfall rests on a layer of denser sea water, the Ghyben-Herzberg fresh water lens (Figure 2.10). The difference in salinity (D = 0.028 at 20°C) is sufficient to keep the fresh water uncontaminated if left undisturbed. The aquifer is replenished by seepage from a perched aquifer in the Upper Coralline Limestone and by rainfall, which averages 500 mm per year. The parts of the Upper Coralline Limestone that are downfaulted to sea-level also contribute to the lower aquifer. There are few fresh water bodies on the islands and most streams are ephemeral or dry, as the flow of water tends to be karstic. In the Upper Coralline Limestone aquifer the percolating water settles on the underlying

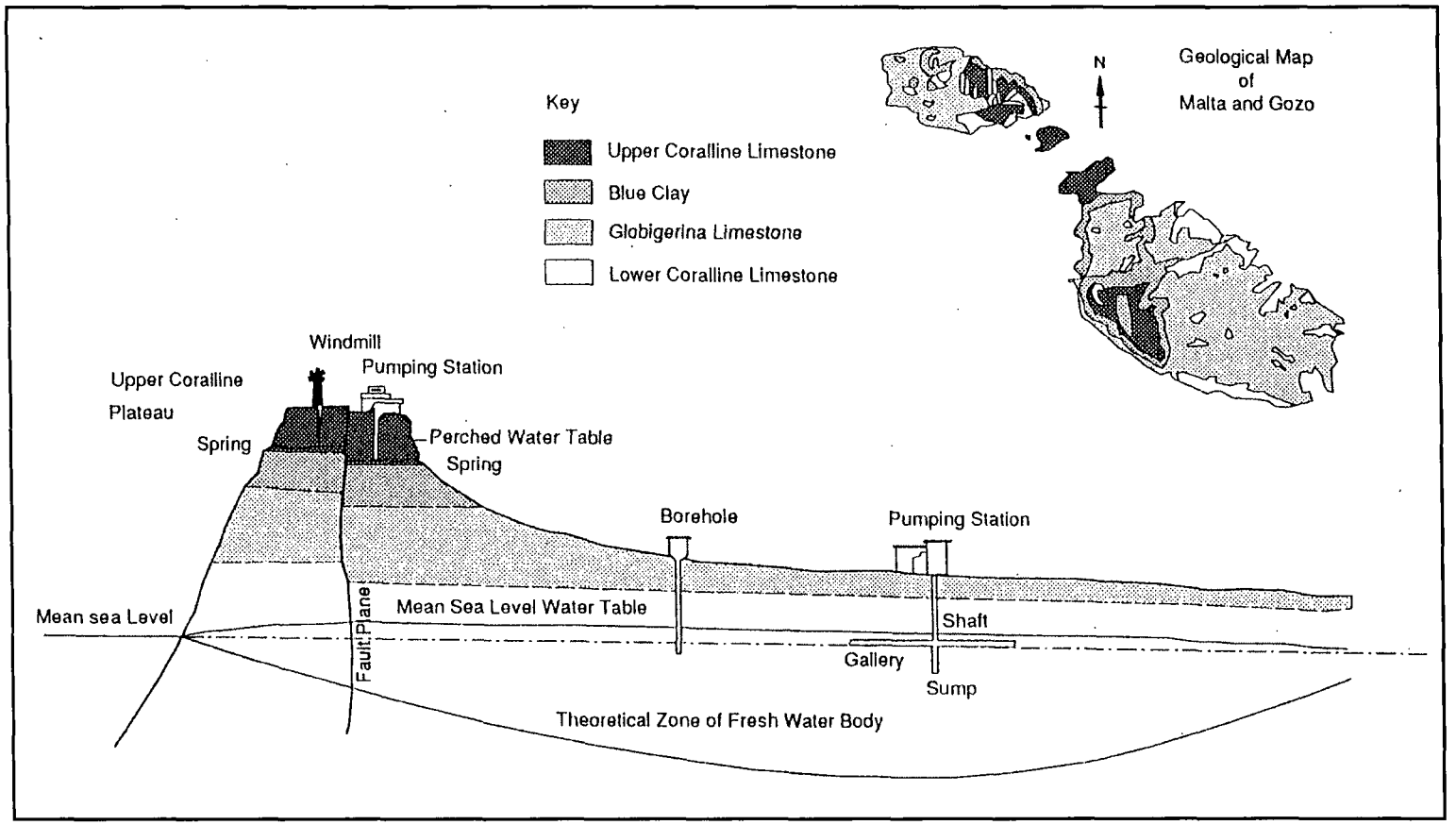


**Figure 2.10: The hydrogeological structure of the Maltese Islands**
Source: Gauci, 1993

impermeable Blue Clay Formation aquiclude, forming a perched water-table which gives rise to springs around the periphery of the limestone.

Newbery (1968) points out that the rich history of Malta can be attributed largely to the favourable hydrogeological conditions that have supported an underground supply of water. This fact can be contrasted to the relative historical insignificance of the neighbouring volcanic islands of Malta. In the Lower Coralline Limestone the water-table is controlled by sea-level. In the Upper Coralline Limestone the aquifer is perched. Over-pumping of the sea-level water-table took place as demand increased, resulting in an increase in salinity of the water supply. Attention then turned to the upper aquifer. Hydrogeological investigations and the construction of new development schemes started in 1956 and were completed in 1963. Presently 55.06% of the water produced in the Maltese Islands is supplied from five Reverse Osmosis Plants, the rest (44.94%) is groundwater (Water Services Corporation, 1997/98).

## 2.6 Conclusion

In Malta there are very clear relations between tectonics and landforms. The morphological response to superimposed phases of strike-slip faulting and rifting, with associated up-arching and down-warping can be observed. Stream channel formation and incision, coastal morphology, erosion surface formation and scarp morphology have all responded sensitively to the tectonic events of the last 15 Ma (Alexander,1988).

The structural setting of the Maltese Islands is dominated by two rift systems of different ages and trends (Illies, 1981). The older rift generation, the Great Fault, trends in a NE-SW to ENE-WSW direction. This creates a horst and graben structure on western Malta, Comino and eastern Gozo. The second rift generation – the Maghlaq Fault, is associated with the Pantelleria Rift and trends in a NW-SE direction. This fault determines the south-west littoral of Malta and is responsible for the north-east tilt of the islands.

The geological succession represents a varied cross-section of Oligo-Miocene lithologies and facies but consists almost entirely of carbonates. The geological formations of the islands are very distinctive lithologically, reflected in characteristic topography and vegetation (House *et al.*, 1961). The NE-SW trending horsts and graben cut through the entire Tertiary rock succession.

The background information presented in this chapter can be used as the basis for reviewing the geomorphology of the Maltese Islands with particular attention to coastal landslide sequences. The geomorphology of the Maltese Islands with particular reference to coastal landforms is dealt with in chapter 3. Paskoff and Sanlaville (1978) claim that the general outline of the Maltese littoral zone has been determined by tectonics. Bays in northern Malta correspond to down-thrown blocks that were partially submerged. High cliffs on the south-west coast are associated with a major fault. Some cliffs are associated with wave-cut platforms. Others plunge directly into the sea or are skirted by landslides. Landslides and slope instability are especially evident on the western coast north of the Victoria Lines. Landslides occur both in Upper Coralline Limestone and Blue Clay Formations. The former feature translational and rotational slides whereas the latter displays mudslides.

This research focusses on slope instability in Blue Clay. Three sites on the north-west coast have been chosen: Gnejna Bay, Ghajn Tuffieha Bay and Rdum id-Delli. These sites were chosen as they are representative sites of the northern coastal region, where outcrops of the Blue Clay Formation are significant. Detailed investigation on the mechanisms which trigger instability was carried out on selected slopes at each field site. The surveyed slopes have defined lateral shears and extend from the base of the Upper Coralline Limestone plateau to sea-level. The research is presented in the proceeding chapters.

# *Chapter 3*

# *The coastal geomorphology of the Maltese Islands, north of the Great Fault*

## 3.1 Introduction

Landforms on the Earth surface are influenced by the geology, an important determinant of the shape, size and type of the feature. The relationship between geology and geomorphology has to be considered when carrying out this research, so as to understand better the processes and mechanisms involved. In the case of Malta, different geological units have produced different landforms. This is especially evident along the coast, where the landscape is varied, due to outcrops of all the geological strata which compose the Maltese Islands. Upper Coralline Limestone and Lower Coralline Limestone feature sheer cliffs of a rectilinear aspect. Upper Coralline Limestone is also responsible for the presence of plateaus, rockfall, rotational and translational slides. Lower Coralline Limestone displays itself as a low rocky shoreline on the north-east coast. Blue Clay is exposed as clay slopes in several parts along the north, north-west and north-east coasts, whereas the occurrence of Globigerina Limestone at the littoral zone is marked by the presence of shore platforms and cliffs, especially evident in eastern and southern Malta.

A number of exercises were undertaken to identify the relationship between the geology and geomorphology for the northern coast of Malta. Aerial photographs were reviewed to get a first impression of the coastal features present and to map those areas which presented problems of accessibility. Queries were then spot checked during a boat survey. Detailed geomorphological mapping was carried out to provide the basis for more detailed work at three specific coastal sites. At each of the sites, further mapping at a larger scale, surveying and the collection of samples for laboratory testing were performed, to assess slope instability within a local context.

## 3.2 Geomorphology of the Maltese Islands

The geomorphology of the Maltese Islands has been discussed by House *et al.* (1961), Vossmerbäumer (1972) and Alexander (1988). Coastal geomorphology is dealt with in the studies of Guilcher and Paskoff (1975), Paskoff and Sanlaville (1978), Ellenberg (1983) and Paskoff (1985). There is a significant lack of more recent sources.

The predominant control on landforms in Malta is undoubtedly that of tectonic activity including faulting, up-arching and subsidence (Alexander, 1988). The highest land, around south-west Malta and western Gozo, occurs at the intersection of the rift system shoulders (Illies, 1980). Isopachyte maps published by Pedley *et al.* (1976) indicate that the extinct NE-SW trending rift system left eminences of the Lower and Middle Globigerina Limestone at the south-east and north-west ends of the archipelago. The latter was removed by erosion on south-east Malta. The present relief of the islands corresponds most closely with the isopachytes of the Lower Coralline Limestone, which reflects all stages of subsidence and upwarping that the various land areas have gone through. Both main islands are tilted towards the north-east. The highest point in Malta is 253 m above sea-level located at Ta'Zuta on Dingli Cliffs, south-west Malta, whereas in Gozo the highest point is 191 m found at Dbiegi. Figure 3.1 features the general topography of the Maltese Islands whereas Figure 3.2 shows the location of all the places referred to in this chapter.

House *et al.* (1961) classify the physical landscape of the Maltese Islands into five categories.

1. Coralline Limestone plateaus, which form the highest areas and are bounded by well-marked escarpments. These uplands range in size from the massive triangular plateau of western Malta to the small mesas of north-west Gozo. In western Malta, the Coralline Limestone plateaus range in heights from 180 m to 245 m. Eastwards the plateaus change into undulating areas developed on Globigerina Limestone, mostly having a height of 120 m. The western plateaus are flanked by deeply incised valleys which have cut back into the upland. The south-west edge has been least affected by such action and the regular line of cliffs are broken only in one place, where the valley complex of Imtahleb forms a deep embayment.

2. Blue Clay slopes, which occur at coastal areas, in valleys and which separate the plateau uplands from the surrounding areas. Blue Clay slopes in Malta occur mostly at the coast at the foot of the Upper Coralline Limestone. On the north-west coast, clay

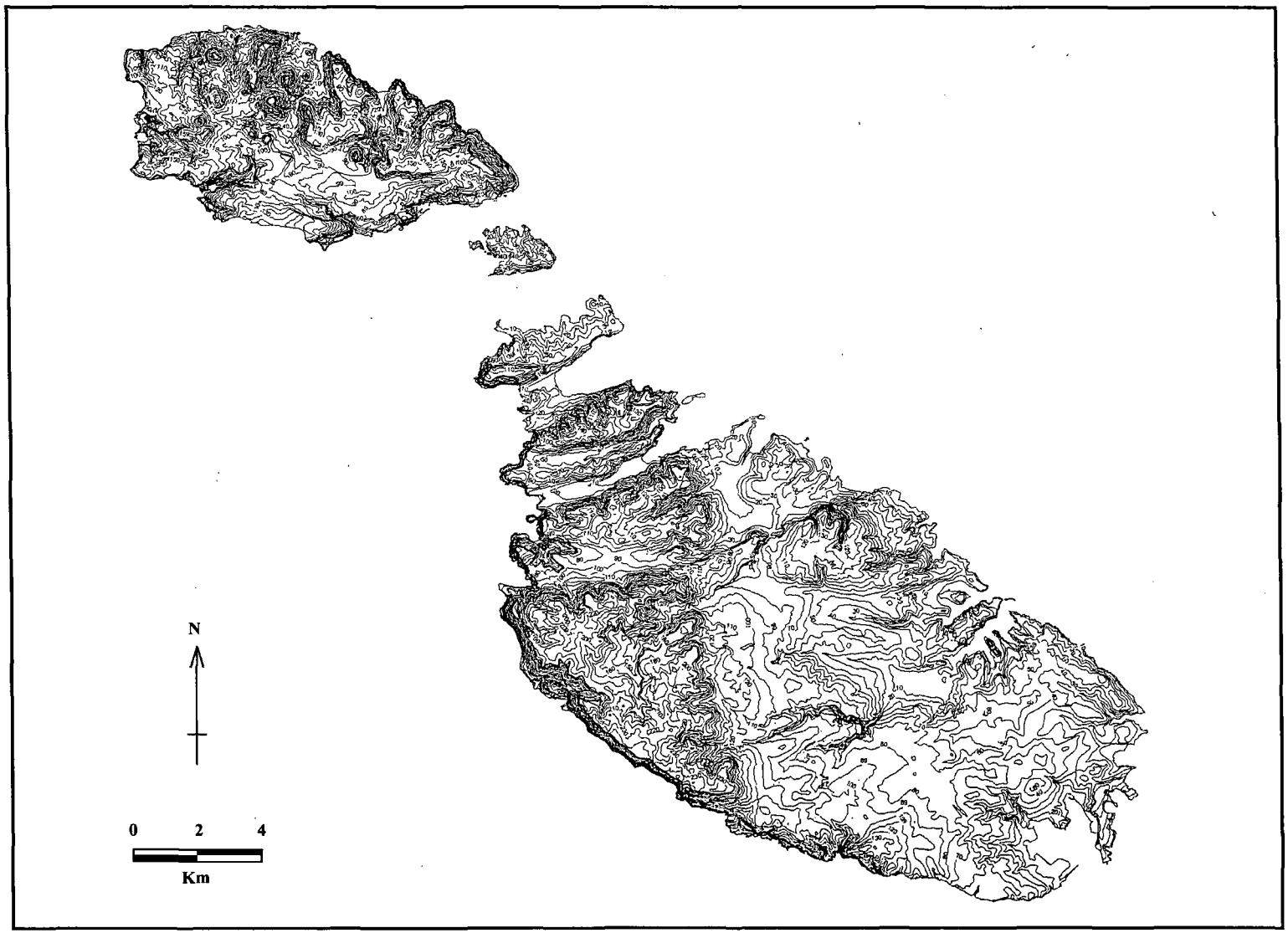


**Figure 3.1: Topography of the Maltese Islands**

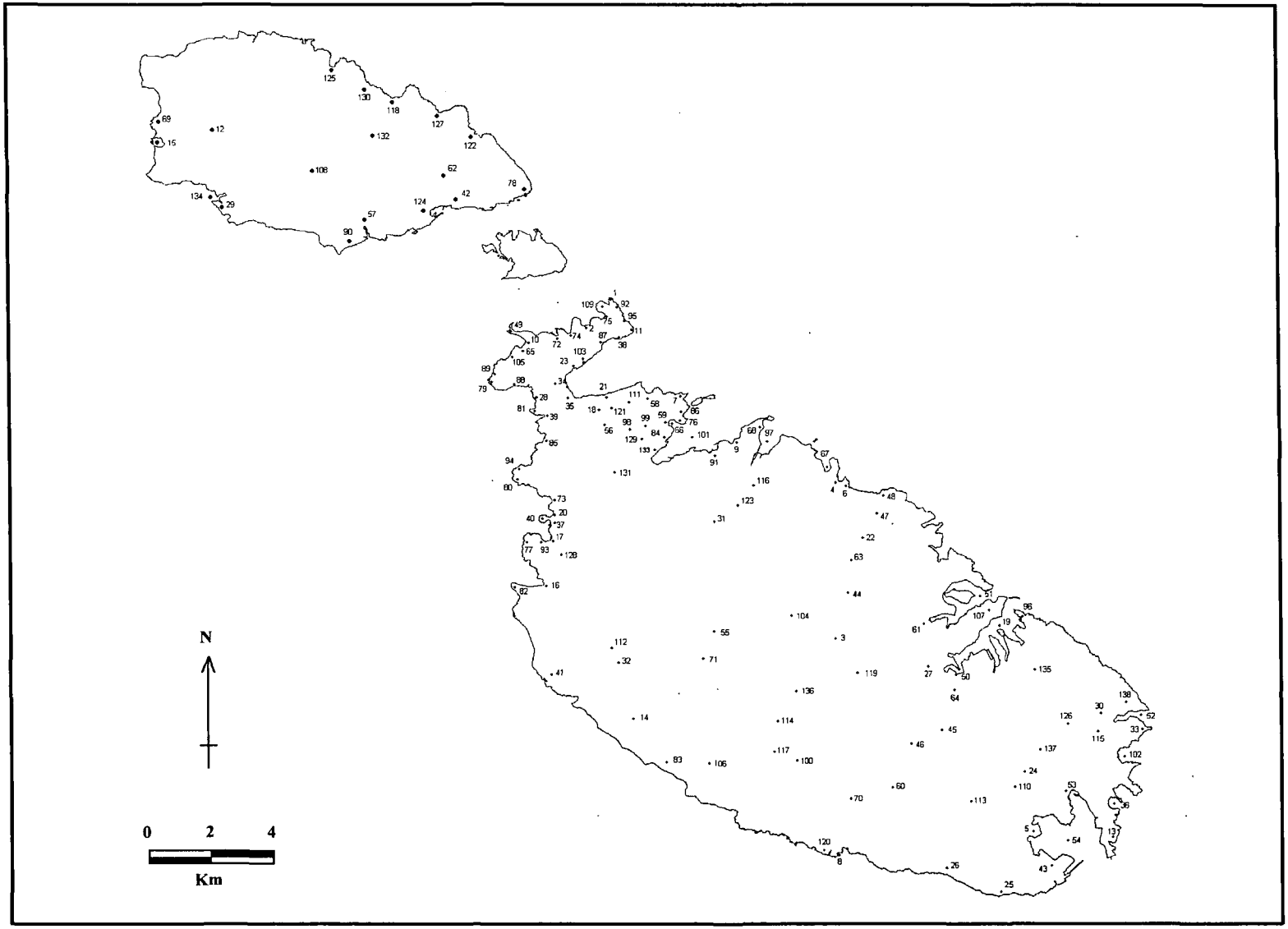


**Figure 3.2: Localities in Malta and Gozo**

## Key to Figure 3.2

1 - Ahrax Point
2 - Armier Bay
3 - Attard
4 - Bahar ic-Caghaq
5 - Birzebbuga
6 - Blata l-Bajda (near Bahar ic-Caghaq)
7 - Blata l-Bajda (near St.Paul's Islands)
8 - Blue Grotto
9 - Bugibba
10 - Cirkewwa
11 - Dahlet ix-Xilep
12 - Dbiegi (Gozo)
13 - Delimara
14 - Dingli
15 - Dwejra (Gozo)
16 - Fomm ir-Rih Bay
17 - Gnejna Bay
18 - Gnien Ingraw
19 - Grand Harbour
20 - Ghajn Tuffieha Bay
21 - Ghajn Zejtuna
22 - Gharghur
23 - Ghar Baqrat
24 - Ghar Dalam
25 - Ghar Hasan
26 - Hal-Far
27 - Hamrun
28 - Ic-Cumnija
29 - Il-Bajda (Gozo)
30 - Il-Bidni
31 - Il-Bidnija
32 - Il-Fiddien
33 - Il-Gzira
34 - Il-Ghadira
35 - Il-Hofra
36 - Il-Hofra z-Zghira
37 - Il-Hotba l-Bajda
38 - Il-Marbat
39 - Il-Prajjet
40 - Il-Qarraba
41 - Imtahleb
42 - Iz-Zewwieqa (Gozo)
43 - Kalafrana
44 - Lija
45 - Luqa
46 - Luqa Airfield
47 - Madliena
48 - Madliena Tower
49 - Marfa Point
50 - Marsa Creek
51 - Marsamxett Harbour
52 - Marsascala Bay
53 - Marsaxlokk
54 - Marsaxlokk Bay
55 - Mdina
56 - Mellieha
57 - Mgarr ix-Xini (Gozo)
58 - Mgiebah
59 - Mistra Bay
60 - Mqabba
61 - Msida
62 - Nadur (Gozo)
63 - Naxxar
64 - Paola
65 - Paradise Bay
66 - Qala tal-Mistra
67 - Qalet Marku
68 - Qawra (Malta)
69 - Qawra (Gozo)
70 - Qrendi

71 - Rabat
72 - Ramla tal-Bir
73 - Ramla tal-Mixquqa
74 - Ramla tal-Qortin
75 - Ramla tat-Torri
76 - Ras il-Mignuna
77 - Ras il-Pellegrin
78 - Ras il-Qala (Gozo)
79 - Ras il-Qammieh
80 - Ras il-Wahx
81 - Ras in-Niexfa
82 - Ras ir-Raheb
83 - Rdum Dikkiena
84 - Rdum Irxaw
85 - Rdum id-Delli
86 - Rdum il-Bies
87 - Rdum il-Hmar
88 - Rdum il-Qammieh
89 - Rdum il-Qawwi
90 - Rdum it-Tafal (Gozo)
91 - Rdum l-Abjad
92 - Rdum l-Ahmar
93 - Rdum l-Imdawwar
94 - Rdum Majesa
95 - Rdum tal-Madonna
96 - Ricasoli
97 - Salina Bay
98 - Santa Maria Estate
99 - Selmun
100 - Siggiewi
101 - St.Paul's Bay
102 - St.Thomas Bay
103 - Ta' l-Imgharrqa
104 - Ta' Qali
105 - Ta' Qassisu
106 - Ta' Zuta
107 - Valletta
108 - Victoria (Gozo)
109 - White Tower
110 - Wied Dalam
111 - Wied Ghajn Zejtuna
112 - Wied Ghemieri
113 - Wied Has-Sabtan
114 - Wied il-Baqqija
115 - Wied il-Ghajn
116 - Wied il-Ghasel
117 - Wied il-Hesri
118 - Wied ir-Ramla (Gozo)
119 - Wied is-Sewda
120 - Wied iz-Zurrieq
121 - Wied Mellieha
122 - Wied ta' Dahlet Qorrot (Gozo)
123 - Wied ta' Ghajn Rihana
124 - Wied ta' l-Imgarr (Gozo)
125 - Wied ta' Marsalforn (Gozo)
126 - Wied ta' Mazza
127 - Wied ta' San Blas (Gozo)
128 - Wied tal-Gnejna
129 - Wied tal-Mistra
130 - Wied tal-Pergla (Gozo)
131 - Wied tal-Pwales
132 - Xaghra (Gozo)
133 - Xemxija
134 - Xlendi Bay (Gozo)
135 - Zabbar
136 - Zebbug
137 - Zejtun
138 - Zonqor

slopes are found at Fomm ir-Rih Bay, Ras il-Pellegrin, Gnejna Bay, Ghajn Tuffieha Bay, Rdum id-Delli, Rdum il-Qammieh and Rdum il-Qawwi. On the north-east coast, clay slopes are found at Mgiebah. Inland, Blue Clay corresponds with the location of dry valleys which have watercourses during the wet season only, although some have perennial springs which flow throughout the year (Schembri, 1993). This is due to the impermeability of Blue Clay. Examples of the valleys include Wied tal-Mistra, Wied tal-Gnejna and Wied Ghemieri. Other places where Blue Clay outcrops such as Il-Bidnija and Il-Fiddien are used for agriculture.

In the northern half of the island of Gozo, erosion has broken the Coralline plateaus into a series of disconnected blocks which diminish in size but increase from east to west. The largest of these, the Nadur and Xaghra uplands, each cover an area of little more than 5 $km^2$ and are between 120 m to 137 m high, occupying most of the north-east part of the island. The uplands are penetrated by numerous sharply-incised valleys whose slopes and floors are developed on the Blue Clay. They include the valleys of Dahlet Qorrot and San Blas and the eastern tributaries of Wied ir-Ramla in the case of the Nadur plateau, while the Xaghra plateau is cut into by the Wied tal-Pergla and the eastern tributaries of Wied ta' Marsalforn.

The north-west part of Gozo is essentially an undulating plain of Globigerina Limestone into which the valleys are for the most part not sharply cut and above which clay slopes lead to numerous mesas. East of Mgarr ix-Xini, inland faulting has preserved a large area of Upper Coralline Limestone, beneath which Blue Clay outcrops to form the seaward slopes. Rdum it-Tafal, Wied ta' l-Imgarr and Iz-Zewwieqa are similar in character to the north-east coastline.

Victoria, in Gozo, is situated on a low elevation of Upper Coralline Limestone, flanked on its eastern side by a minor escarpment beneath which unusually gentle clay slopes occur. This is also the case of Mdina, Rabat and Mellieha on mainland Malta. These localities are situated on Upper Coralline Limestone plateaus and flanked by clay slopes.

3. *Rdum* or undercliff areas, occurring where the Upper Coralline Limestone plateaus meet the sea. In Malta these features are located mainly on the western coast between Rdum Dikkiena up to Paradise Bay at Cirkewwa, broken intermittently at Ras ir-Raheb, Ras in-Niexfa, Gnejna Bay, Ghajn Tuffieha Bay and Fomm ir-Rih Bay. Some *rdum* areas are also found at the north-east coast of Malta between Xemxija and Mistra Bay, extending up to Mgiebah.

In Gozo *rdum* areas occur where the Nadur and Xaghra uplands reach the coast. Blue Clay slopes descend steeply to the sea from beneath the cliffs, which mark the edge of the limestone outcrop. In the north-east, between Dahlet Qorrot and Ras il-Qala, the slope gradient is less steep and a rocky platform occurs where the Lower Coralline Limestone appears in a narrow strip along the coast. West of Wied ta' Marsalforn, the Upper Coralline Limestone plateau has been eroded into small and scattered fragments.

4. Flat-floored basins, which in most cases are the result of faulting, such as Wied tal-Pwales, or down-warping, such as Bingemma Basin. Sometimes flat-floored basins occur due to erosion and subsequent alluvial deposition, such as Wied il-Ghasel, limits of Mosta, central Malta. The region of Wied il-Ghasel and its tributary, Wied ta' Ghajn Rihana, stretches for slightly more than 3 km inland from Salina Bay and lies for the most part at heights below 15 m, being abruptly terminated at its southern end by the escarpment of the Victoria Lines Fault.

The remainder of northern Malta consists of a series of ridges and valleys. From north to south, the major divisions are: Marfa Ridge, Mellieha Valley, Mellieha Ridge, Mizieb Depression, Bajda Ridge, Pwales Valley, Wardija Ridge and Bingemma Basin (Figure 3.3).

Marfa Peninsula (Figure 3.3) reaches a maximum height of 122 m in the west. It is steepest on the southern side where it overlooks the Mellieha Isthmus and Mellieha Bay in an abrupt fault-line scarp. The slope on the northern side is gentle and diversified with several small valleys. Mellieha Ridge (Figure 3.3) is an Upper Coralline Limestone

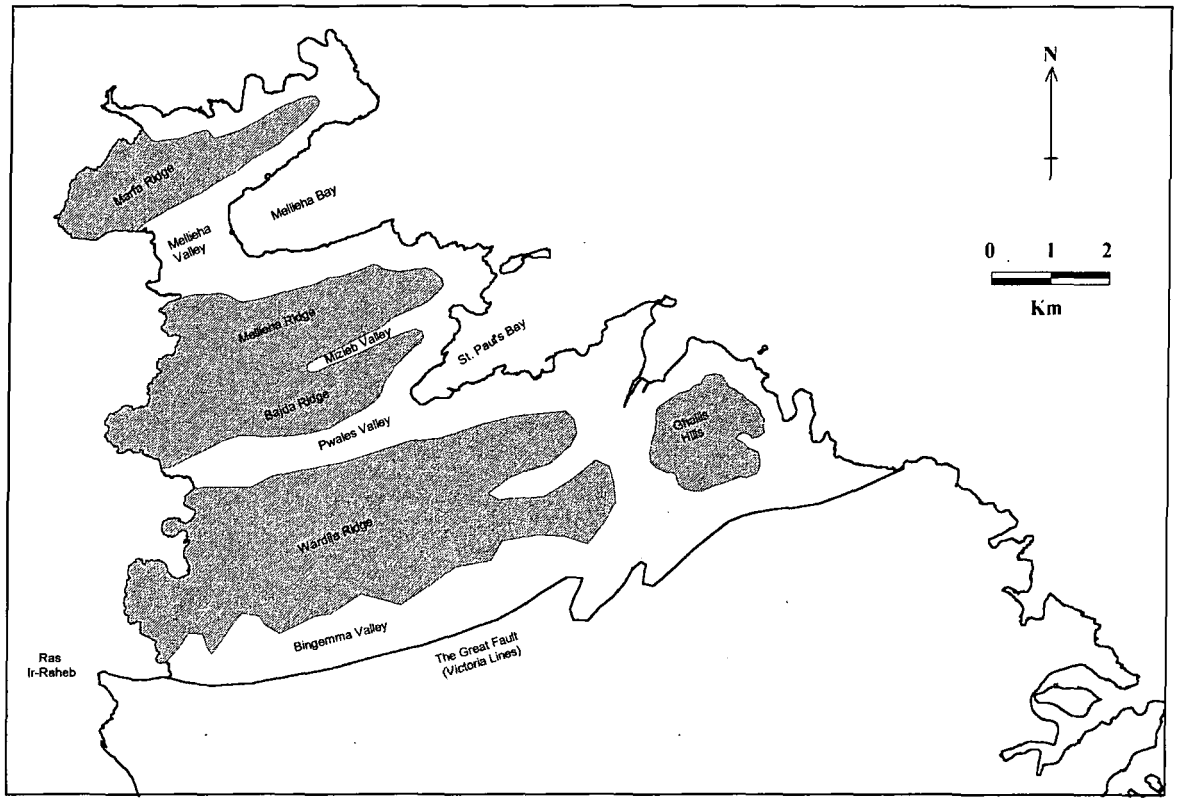


**Figure 3.3: Ridge and valley topography north of the Great Fault**
Source: Ransley and Azzopardi, 1988

plateau (122 m to 137 m) declining to the east (around 90 m) near Selmun. It has been tilted from north to south. Its major escarpment, where Blue Clay outcrops, faces north over the isthmus and is interrupted by a series of narrow steep-sided valleys, such as Gnien Ingraw, Wied Mellieha, and Wied Ghajn Zejtuna which form deep embayments in the scarp face. The northern and southern alluvial depressions of the Mellieha Isthmus (Figure 3.3) – Il-Ghadira and Il-Hofra respectively – are separated by a low slope of Coralline Limestone which reaches a summit of about 61 m near Ras in-Niexfa. The Mizieb Depression (Figure 3.3) is a narrow plain about 550 m across and 3.6 km long with its lowest point about 30.5 m above sea-level. To the east it leads to Wied tal-Mistra, where erosion from Qala tal-Mistra has exposed the Globigerina Limestone and Blue Clay and produced a valley whose floor lies less than 15 m above sea-level over a distance of about 2.4 km. The Mizieb Depression is synclinal in structure. Its southern side forms the gentler northern side of Bajda Ridge (Figure 3.3). A minor escarpment about 15 m to 30 m high separates Bajda Ridge from Pwales Valley (Figure 3.3), a flat-

floored depression about 0.8 km wide which runs right across the island from Ghajn Tuffieha Bay to St.Paul's Bay. The highest point in this area is about 23 m above sea-level and most of the region is below 15 m. The dip slope of the Wardija Uplands leads south to the Bingemma Basin (Figure 3.3), a flat-floored depression at heights of about 75 m to 85 m. This region leads to the Wied ta' Ghajn Rihana which is incised into the basin floor. The southern side of the basin is made up of slopes, developed on Globigerina Limestone and Blue Clay, which lead up, through a vertical distance of about 150 m, to the Victoria Lines Fault.

5. Globigerina hills and plains – large areas of gently sloping land which, in Malta, take the form of a series of low ridges and shallow valleys and in Gozo, have a more varied topography. The central, southern and eastern regions are mostly areas of gentle relief, although steep slopes occur in a number of places. West of the Paola-Luqa-Mqabba-Qrendi area, a series of ridges and valleys converge towards Marsamxett and Grand Harbour. The Naxxar-Gharghur Hills are succeeded southwards by the Lija-Msida Valley which is followed by the Attard-Hamrun Ridge. An open valley, Wied is-Sewda, follows, bounded on the south by Zebbug Ridge. Beyond the Zebbug Ridge, there are the valleys of Il-Baqqija and Il-Hesri, followed by Siggiewi Ridge. The southern edge of this region is made up of sea cliffs. The cliffs are backed by steep slopes rising to a crest line which runs parallel to the coast for about 1.5 km. The height of this crest line declines eastwards from a maximum of about 138 m to about 45 m south of Kalafrana.

East of the Paola-Qrendi area, the general relief trend is from east to west. Ridges running from Ricasoli to Zonqor, from Zabbar to Il-Bidni and from Zejtun to Il-Gzira are separated by Wied il-Ghajn and Wied ta' Mazza. These features all converge towards Marsascala Bay. Further south, the convergence of ridges and valleys is towards Marsaxlokk. This setting gives an undulating character to the area, and steep slopes are confined to the coasts of Zonqor and Delimara and the valleys of Has-Sabtan and Dalam, both the latter being incised in the Lower Coralline Limestone. The landscape of Globigerina Limestone areas features low ridges and valleys. Flat land is very limited, occurring around the head of Marsa Creek, Ta' Qali and Luqa airfield.

## 3.3 Coastal geomorphology of the Maltese Islands

Two studies by Paskoff and Sanlaville (1978) and Ellenberg (1983) have made a significant contribution to understanding the coastal geomorphology of the Maltese Islands.

Paskoff and Sanlaville (1978) claim that the general outline of the Maltese littoral zone has been determined by tectonics. Lithology and advanced karstification have to be considered when studying the coast in detail. In spite of the small size, the Maltese Islands display a large variety of coastal features. Bays in northern Malta correspond to downthrown blocks that were partially submerged. High cliffs which characterize the south-west coast are associated with a major fault (Plate 3.1). Beaches are rare and constitute only 2.4 % of the coastline (Schembri, 1990) (Plates 3.2 and 3.3). Low limestone coasts display interesting examples of both mechanical and chemical processes such as hydraulic pressure and corrosion (Plate 3.4). Most of the coasts have a high relief and show different types of cliffs. Some are associated with wave-cut platforms (Plate 3.5). Others plunge directly into the sea (Plates 3.1 and 3.6) or are skirted by landslides (Plate 3.7).

Since its definitive emersion after the Tortonian, the Maltese archipelago has been affected by karstification, now found at an advanced stage of development, which is evident at the south of Malta, Comino and western Gozo. In Malta, for example, one finds important circular depressions such as the doline structure of Il-Maqluba, near Qrendi, which is 60 m wide and 40 m deep. Long caves, such as Ghar Hasan (Plate 3.8), south of Hal-Far and especially Ghar Dalam, close to Birzebbuga, explored to about 100 m and famous for its palaeontological richness in bone fossils, are also found (Paskoff and Sanlaville, 1978). The karstification, remarkable in underground structures, is principally cut in Coralline Limestone, which is very sensible to actions of solution because of its purity in calcium carbonate and its dense fractures and thickness (Paskoff and Sanlaville, 1978). In subterranean cavernous areas of karstic origin, revealed by cliff retreat, wave action during storms may provoke roof collapse, which forms roughly semi-

circular coves. Blue Grotto (Figure 3.4), in southern Malta, is an example of such a landform (Paskoff, 1985).

There is evidence of past processes involved in the subsidence of Malta during the Quaternary period accompanied by a tilting movement. The following support this idea:

i. general topography and stratigraphic sequence inclined towards the north-east;
ii. sinking of the bays on the north-east coast;
iii. traces of Neolithic cart ruts passing below sea-level in Marsaxlokk Bay;
iv. stalactites hanging at the ceiling of caves which today are found below sea-level at the entrance of Grand Harbour in Valletta (Hyde, 1955);
v. the presence of immersed levels about 9-11 m, 17-21 m, 25-30 m and 33 – 40 m at the foot of high cliffs on the south-west coast (Martineau, 1965 *in* Paskoff and Sanlaville, 1978).

Faults resulting from tectonic activity determine the outline of the Maltese coasts. Some faults are perpendicular to the littoral zone. Horsts at the north of the island (Wardija, Bajda, Mellieha and Marfa Ridges and the island of Comino) are separated by sunk blocks which the sea has partially (at St.Paul's and Mellieha Bays) or totally overrun (North Comino and South Comino Channels) (Figures 2.2 and 3.3). Ras ir-Raheb at the end of the projection in Fomm ir-Rih Bay, western Malta coincides with the western extremity of the Great Fault of the Victoria Lines (Figure 3.3 and Plate 3.9).

The south-west littoral zone of Malta is determined by the Maghlaq Fault (Figure 2.6 and Plate 3.10), oriented WNW-ESE, and starting from where the island has been tilted towards the north-east (Paskoff and Sanlaville, 1978). The result is a striking contrast between a south-west coast featuring sheer cliffs of a rectilinear aspect (Plate 3.1), more than 200 m high near Dingli, and a rocky but shallow north-east coast (Plate 3.4), gradually descending under the sea (Figure 3.4). Other evidence of the tilting is the water drainage division which runs near the south-west coast and the location of the highest point of the island, at 253 m on the south-west coast at Ta' Zuta, near Dingli (Figure 3.2).

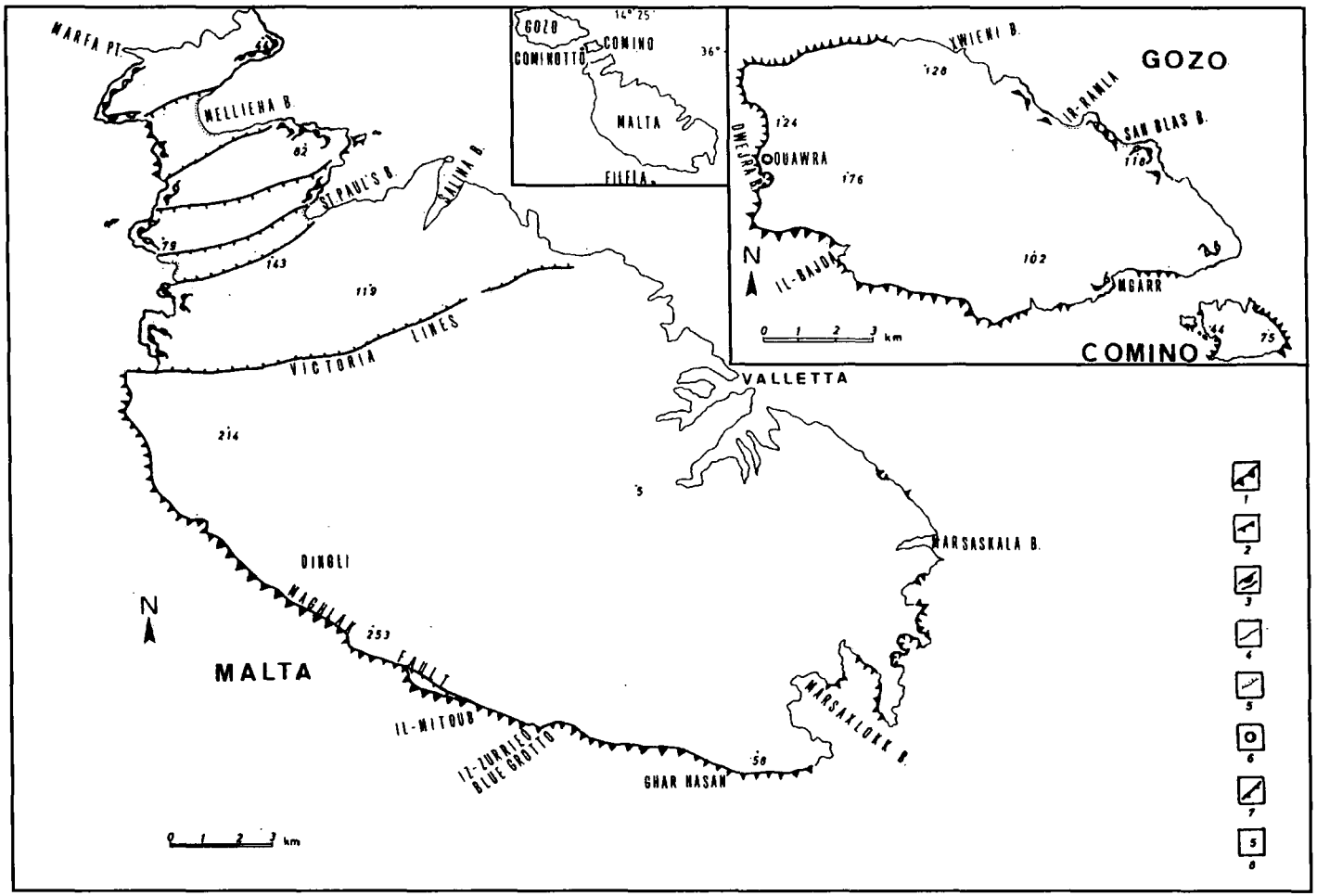


**Figure 3.4: Predominant coastal landforms in the Maltese archipelago**
Source: Paskoff, 1985

**Key**

| | | | | | | | |
|---|---|---|---|---|---|---|---|
| 1 | high cliff (more than 100 m high) | 3 | *rdum* type cliff | 5 | sandy beach | 7 | major fault |
| 2 | cliff (less than 100 m high) | 4 | low rocky coast | 6 | sinkhole structure | 8 | height in metres from datum line |

The role of tectonics is not as important in Gozo. However numerous faults are located on the southern coast of the island and very likely determine its outline (Paskoff and Sanlaville, 1978).

Semi-circular coves, such as Qawra, near Dwejra Point and Dwejra Bay in western Gozo (Figure 3.4), the two creeks on the western coast of Comino, Blue Grotto on the southern coast of Malta, Paradise Bay on the north-western coast, Rdum il-Hmar (Plate 3.11), Ghar Baqrat and Ta' l-Imgharrqa on the north shore of Mellieha Bay, Il-Qala tal-Mistra on the north shore of St.Paul's Bay and Il-Hofra z-Zghira (Plate 3.12) on the south-east coast of Malta, represent a conspicuous feature of the Maltese coastline. They originate from widely distributed typical karstic landforms inundated by the sea (Paskoff, 1985). Post-Miocene solution of carbonates has reached an advanced stage, producing well-developed sinkholes and extensive subterranean cavern and gallery systems in all formations, especially in the Coralline Limestones.

In Qawra, western Gozo (Figure 3.4), there is a large (400 m in diameter and 70 m deep) elliptical sinkhole structure of complex origin (Pedley, 1974 *in* Paskoff, 1985), bounded by vertical walls and developed in the Lower Coralline Limestone. Its bottom has been partially inundated because a karstic gallery connects the depression with the open sea and allows small boats to pass. Dwejra Bay (Figure 3.4), close to Qawra is another former closed depression, measuring approximately 340 m in diameter. It has largely been invaded by the sea and only its eastern half has been preserved. An islet, Fungus Rock, is the last remnant of its western wall, destroyed by marine erosion.

Malta and Gozo display inlets that are partially drowned valleys of subaerial erosion. Typical *calanques* are found: Wied iz-Zurrieq in southern Malta and Il-Bajda in south-west Gozo are narrow, shore inundated valleys with steep sides cut in Lower Coralline Limestone. Wider and more developed inlets, such as Salina Bay and Marsascala Bay in Malta, correspond to finger-shaped, broad and more open valleys, subaerially eroded in the soft Globigerina Limestone and subsequently submerged (Figure 3.4). Changes in sea-level have also submerged the mouth of some drainage channels on the coast, giving rise to headlands, creeks and bays, especially evident on the north-east coasts, since the seaward tilt of the island is in that direction.

Especially important is the system of drowned valleys which form the creeks of the two main harbours of Malta, Marsamxett Harbour and Grand Harbour, separated by the Valletta headland (Figure 2.7). Important examples of inundated river valleys in Gozo include Mgarr ix-Xini and Xlendi Bays.

Steep cliffs, more than 50 m high and in some places more than 200 m (Plate 3.1), represent half the length of the Maltese coastline (Guilcher and Paskoff, 1975; Paskoff and Sanlaville, 1978). They characterize southern and south-west Malta, eastern Comino, and most of the coast of Gozo (Ellenberg, 1983). Vertical plunging cliffs are generally cut in the Lower Coralline Limestone and lack shore platforms at their feet, such as at Ghar Hasan, southern Malta. These cliffs are vertical, rectilinear and probably of tectonic origin (Paskoff and Sanlaville, 1978). Marine erosion appears to be biochemical and inefficient. At sea-level, an undercut notch is formed (Plate 3.13). It is quite regular and measures between 0.80 m to 1.50 m in depth and width (average 0.60 m). The immersed lower part features an irregular sloping pavement with a cavity formed by waves.

Where cliffs are cut in the Globigerina Limestone they are fronted, in most cases, by shore platforms produced by mechanical action of waves, mainly through hydraulic pressure that dislodge and remove blocks from stratified and jointed rocks (Plate 3.5). Between Marsaxlokk Bay and St.Thomas Bay, the Globigerina Limestone features a perfectly vertical cliff which reaches a height of more than 50 m (Plate 3.6). At sea-level a structural platform, above which there is a notch (Plate 3.14), is the result of mechanical erosion. The rock here is quite uniform which helps to maintain the steepness of the cliff, and rather soft allowing marine erosion to work efficiently (Paskoff and Sanlaville, 1978).

The *rdum* areas constitute a very original and spectacular element of the Maltese coasts and correspond to a type of marine cliff related to a specific geological structure that is prone to mass movements. The *rdum* areas occur where Blue Clay crops out at sea-level and is overlaid with the massive strata of Upper Coralline Limestone (Plates 3.7, 3.11 and 3.15). The clay is easily eroded by wave action. In addition, rain water percolates through fissures of the limestone into the underlying clay. This causes the Blue Clay to become plastic and unstable. Jointing and faulting

in the Upper Coralline Limestone causes the latter to dislodge and eventually break up, falling on the clay. The landforms are characterised by a boulder scree at sea-level and larger landslides at the foot of the scarp face. As a result cliff retreat is probably slow, since a certain time is necessary for the removal of the boulders. The huge limestone blocks are too large to be displaced by the sea and form a strong protective buttressing to the clayey part of the cliff. This type of cliff probably retreats much less quickly than Globigerina Limestone cliffs (Paskoff and Sanlaville, 1978). *Rdum* areas are especially found north of the Victoria Lines Fault (Figure 3.4) and in eastern Gozo.

In north-east Malta and northern Gozo, cliffs are largely absent. Long tracts of low, rocky coastlines of corrosion (Paskoff, 1985) are found (Plate 3.4). Pools and lapiés give an extremely irregular topography to shore platforms, particularly when they are cut in Coralline Limestone (Plate 3.4). Chemical and biological weathering are the prevailing processes of evolution. Evidence of abrasion is absent. Structural controls account for the simultaneous development of several platforms at different levels up to more than 10 m above the sea. This is evident in northern Gozo, where the Globigerina Limestone crops out. On exposed coasts large boulders dislodged by storm waves lie scattered on the shore platform, and corrosion microforms are less developed.

No trace of former shorelines higher than the present one has been found in spite of careful investigations (Paskoff and Sanlaville, 1978). Emerged wave-cut terraces or notches as well as marine deposits seem to be entirely lacking. Formerly reported raised beaches (Hyde, 1955) are in fact pediment features. The situation suggests evidence of recent crustal subsidence, which is probably still in progress. At St.Paul's Bay, cart tracks of Neolithic age enter the sea at one side and emerge on the opposite side of the inlet (Hyde, 1955). Moreover, as far as Malta is concerned, there has been tilting of its lengthwise axis towards the north-east in addition to the general subsidence of the archipelago.

In order to provide more detail on the coastal landforms of Malta, a geomorphological mapping exercise was performed, to supply information about geology, landforms and mass movement processes operating on the coast in the northern region.

**Plate 3.1: Plunging cliffs developed in Lower Coralline Limestone characterize the south and south-west coasts from Benghisa to Fomm ir-Rih. These cliffs are associated with the Maghlaq Fault and reach a height of 200 m in some parts.**

**Plate 3.2: Sandy beach backed by clay slopes at Ghajn Tuffieha Bay. This Bay which is popular and frequented both by locals and tourists has been designated by the Planning Authority as an area of ecological importance and is a protected site.**

**Plate 3.3: Sandy beach at Gnejna Bay. Gnejna Bay is surrounded by scree and clay slopes. The beach is backed by Gnejna Valley. In the background Rdum l-Imdawwar features terraced fields.**

**Plate 3.4: Low rocky shore cut in Lower Coralline Limestone on the north-east coast. Pools and lapiés which produce a very irregular surface are the result of corrosion.**

**Plate 3.5: Low cliff and shore platform formed in Globigerina Limestone, characteristic of the southern coast. Globigerina Limestone being a softer material than Coralline Limestone displays a smoother surface. This is mainly the result of the mechanical action of waves, especially hydraulic pressure.**

**Plate 3.6: Globigerina Limestone cliff, about 45 m high. Featured here is a spur extending into the inlet adjacent to Xrobb il-Ghagin peninsula on the southern coast. Only the upper part of the cliff is vertical. The lower part is sloping probably as a result of different rates of erosion and cliff retreat.**

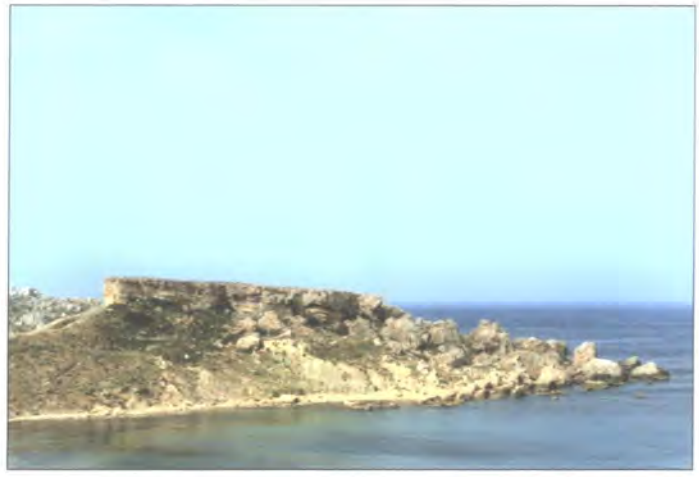

**Plate 3.7: Il-Qarraba is a peninsula separating Gnejna Bay from Ghajn Tuffieha Bay on the north-west coast. It features an *rdum* landform and its shape is unique in the Maltese Islands. Il-Qarraba is linked to the mainland by clay slopes and has been assigned the highest level of conservation and protection by the Planning Authority.**

**Plate 3.8: Ghar Hasan, found on the southern coast. This cave has formed as a result of karstification. The latter prevails in Coralline Limestone where water charged with carbon dioxide dissolves the calcium carbonate in the porous limestone.**

**Plate 3.9: The western extremity of the Great Fault featuring Lower Coralline Limestone plunging cliffs. The Great Fault runs along the whole width of the island from Fomm ir-Rih on the west coast to Madliena on the east coast. The terraced fields are the result of human activity.**

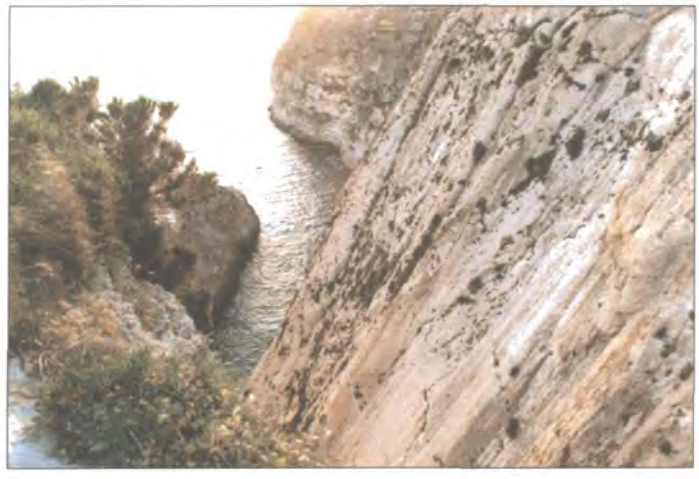

**Plate 3.10: Slickenside at Ix-Xaqqa on the south-west coast. This is a result of the Maghlaq Fault which has produced here a vertical displacement of at least 240 m to the south-west. Lower Coralline Limestone (right side) and Upper Coralline Limestone (left side) are found in juxtaposition.**

**Plate 3.11: Rdum il-Hmar is an example of a semi-circular cove found on the northern shore of Mellieha Bay. Semi-circular coves represent a distinct feature of the Maltese coastline and originate from karstic landforms inundated by the sea.**

**Plate 3.12: Il-Hofra z-Zghira features a semi-circular cove on the south-east coast of Malta. In this case the cove has developed in Globigerina Limestone and is surrounded by cliffs.**

**Plate 3.13: Undercut notch formed by the action of waves at the lower part of plunging cliffs on the south-west coast. The notch measures around 0.80 m deep and 1.50 m wide.**

**Plate 3.14: Globigerina Limestone cliff fronted with a structural platform at Delimara on the southern coast. A notch is formed above the shore platform as a result of mechanical erosion.**

**Plate 3.15: Fomm ir-Rih Bay located on the western coast, adjacent to the western extremity of the Great Fault. It featues an *rdum* area, a characteristic landform of the Maltese coasts. This type of marine cliff is prone to mass movements both in clay and limestone.**

**Plate 3.16: An example of a translational slide found at Rdum Majesa on the north-west coast. In the Maltese Islands this type of landslide occurs in the Upper Coralline Limestone. Usually these slides involve a displacement from the *in situ* material to several metres downslope and in some cases extending to the shoreline.**

**Plate 3.17: An example of a rotational slide found at Ras il-Pellegrin on the north-west coast. Rotational slides, similar to translational slides, develop in the Upper Coralline Limestone. These slides are usually found below the *in situ* material from where they have been detached and involve a rotational movement on the slip surface resulting in a tilted upper surface.**

**Plate 3.18: Complex of rotational slides at Ras il-Wahx on the north-west coast. Ras il-Wahx offers the best example of multiple rotational slides most commonly found at headlands along the Maltese coasts. Here rotational slides occur in multiple succession covering an area of about 400 m².**

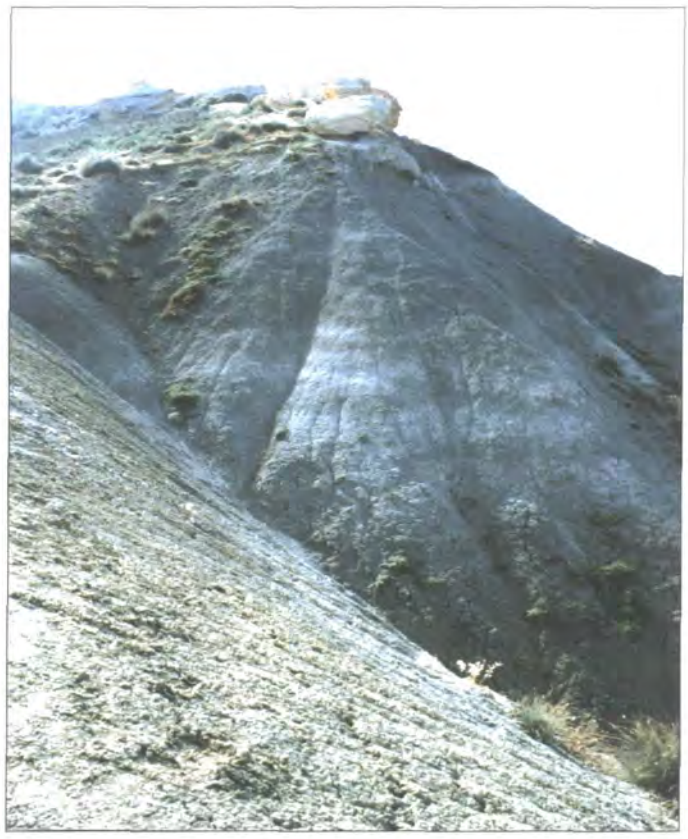

**Plate 3.19: Where Blue Clay is exposed it features slopes. At the coast these slopes usually extend from the Upper Coralline Limestone plateau to sea-level. The clay slopes featured here are situated at the southern end of Ghajn Tuffieha Bay, overlooking Gnejna Bay and connecting Il-Qarraba with the mainland.**

**Plate 3.20: A closer view of the clay slopes overlooking Gnejna Bay. The slopes are quite steep and stable allowing some steppic vegetation to grow on them. In the background Globigerina Limestone shore platforms are evident. These are situated at sea-level and are backed by the clay slopes.**

**Plate 3.21: Rockfall at Il-Prajjet situated on the north-west coast. Rockfall is the most important mass movement process along the Maltese coasts. This process occurs in the Upper Coralline Limestone where blocks are detached from the plateau and fall on the underlying strata.**

## 3.4 Geomorphological mapping

The aim of geomorphological mapping is to record information on landforms by mapping surface form, surface materials and surface processes. It provides a basis for terrain assessment which is useful in the context of many environmental problems (Cooke and Doornkamp, 1990). In geomorphological mapping, landform genesis is considered (Gardiner and Dackombe, 1983). Landform genesis usually involves attributing a form to a process, past or continuing (Goudie *et al.*, 1990). Mapping of present-day processes is mostly limited to hazards such as landslides, avalanches and gullying. Slower processes such as wash, creep and solution are usually deduced from form because measurements of their rates are too localised to allow mapping (Goudie *et al.*, 1990). The relevance of mapping surface materials depends on the purpose of the map (Cooke and Doornkamp, 1990) such as recording information on bedrock lithology or assessing slope instability which requires a knowledge of shear strength.

When only surface form is taken into consideration, the technique used is known as morphological mapping (Savigear, 1965; Cooke and Doornkamp, 1990). The latter includes information on the slope gradient, direction and form of slope (convex or concave), the break of slope and change of slope. Slope gradient is the most important morphometric variable for many processes and applications (Goudie *et al.*, 1990). A map of slope steepness, for example, can be of value to both planners and engineers. When a morphological map includes a genetic interpretation it is considered to be a geomorphological map (Tricart, 1965, 1970 *in* Goudie *et al.*, 1990).

Geomorphological mapping has various applications which include the following (adapted from Demek, 1972 *in* Cooke and Doornkamp, 1990).

i. Land-use: regional area planning; conservation of the natural and cultural landscape.
ii. Agriculture and forestry: soil erosion control; drainage and irrigation; reclamation of destroyed or new areas.
iii. Underground and civil engineering: construction of communication lines; design of dams, reservoirs, canals, and harbours; shore protection.

iv. Prospecting and exploitation of mineral resources: geological survey; mining and exploitation; areas of landsliding and subsidence.

At the reconnaissance stage, geomorphological mapping provides a rapid and cheap source of information which can save enormous resources. A considerable amount of land information can be obtained rapidly by air photo interpretation, preferably before and after fieldwork. Presently the trend is to produce simpler maps for both scientific and applied purposes. Nowadays the use of GIS permits flexibility of map content and the production of more maps which last over a shorter period of time (Goudie *et al.*,1990).

## *3.5 The geomorphology of the northern coast of Malta*

### 3.5.1 Geomorphological mapping of the northern coast of Malta

Geomorphological mapping is an essential tool when studying landforms as it provides a basic knowledge of the features present in an area, together with their spatial distribution and relationship. This technique is ideal to determine the relationship between geological formations and landform types and processes (Enriquez-Reyes *et al.*, 1990) and provides additional information to published topographic maps.

A geomorphological survey was carried out for the northern shoreline of Malta, north of the Victoria Lines Fault from Fomm ir-Rih Bay on the western coast to Madliena on the eastern coast, covering a distance of about 56.5 km. The aims of this survey are several:

i. to determine the association between geology and geomorphology;
ii. to highlight the spatial distribution of coastal features, especially landslides;
iii. to assess coastal slope instability and mass movement processes for the northern coast of Malta.

The Victoria Lines Fault crosses the island from Fomm ir-Rih Bay to Madliena and forms a fault scarp which is the most significant topographic feature of the island. North of this fault, the geological structure is dominated by the development of horst and graben blocks, bounded by ENE trending normal faults. Such structures are indicated by prominent ridges and valleys, the main units being from north to south: Marfa Ridge, Mellieha Valley, Mellieha Ridge, Mizieb Valley, Bajda Ridge, Pwales Valley, Wardija Ridge and Bingemma Valley (Figure 3.3). The survey was performed in this region because the structural setting and geological formations combined together present a very interesting and varied topography which is especially evident at the coastal zone. Elsewhere on mainland Malta, the topography and coastal features are presented in a less complex structural and geological setting and geomorphologically is not as interesting as the northern region.

The initial part of the survey was a desk study using air photographs. This was mainly carried out because some of the terrain was difficult to access and imposed limitations on the geomorphological mapping. Besides such an exercise provided a more clear idea of the landforms present along the coast. The features were marked on topographic maps at a scale of 1: 10000. The exercise proved to be useful to get a first impression of the landscape for further research but left several queries which had to be spot checked during a boat survey. The latter followed the route from Qawra in Salina Bay (north-east coast) along the northern coast and finally the north-west coast to Fomm ir-Rih Bay. Queries were checked and these were marked on the 1: 10000 topographic sheets. A final geomorphological survey was undertaken, using standard geomorphological mapping symbols (Gardiner and Dackombe, 1983; Cooke and Doornkamp, 1990) for different landforms along the coast. A large part of the mapping was done from the top of the Upper Coralline Limestone plateau to get a general view of the landforms and because most of the coastal zone below the plateau is inaccessible due to the presence of landslides and rockfall. The Upper Coralline Limestone plateau was also used to demarcate the inland distance up to where the coastal features were mapped. Where this was absent on the north-east coast, the coastal road or buildings were utilised as the inland boundaries to geomorphological mapping.

Two maps, scale 1: 10000 (Figures 3.5 and 3.6) were produced featuring the coastal landforms in Malta, north of the Victoria Lines Fault. Figure 3.5 covers a coastal stretch from Fomm ir-Rih Bay (marking the start of the Great Fault) to the northern littoral of Mellieha Bay. Figure 3.6 features the coast from the sandy beach of Mellieha Bay (the isthmus) to Madliena Tower where the Great Fault cuts on the north-east coast. Figure 3.7 shows the location of the coastal stretch covered in Figures 3.5 and 3.6. Eleven different types of landforms were identified along the northern coast and mapped in Figures 3.5 and 3.6. These include:

Cliff face 

Translational slide 

Rotational slide 

Mudslide / Clay slope 

Rockfall 

Soil creep 

Rocky shoreline 

Rock shore platform 

Sand / Shingle 

Agriculture in use A

Abandoned agriculture 

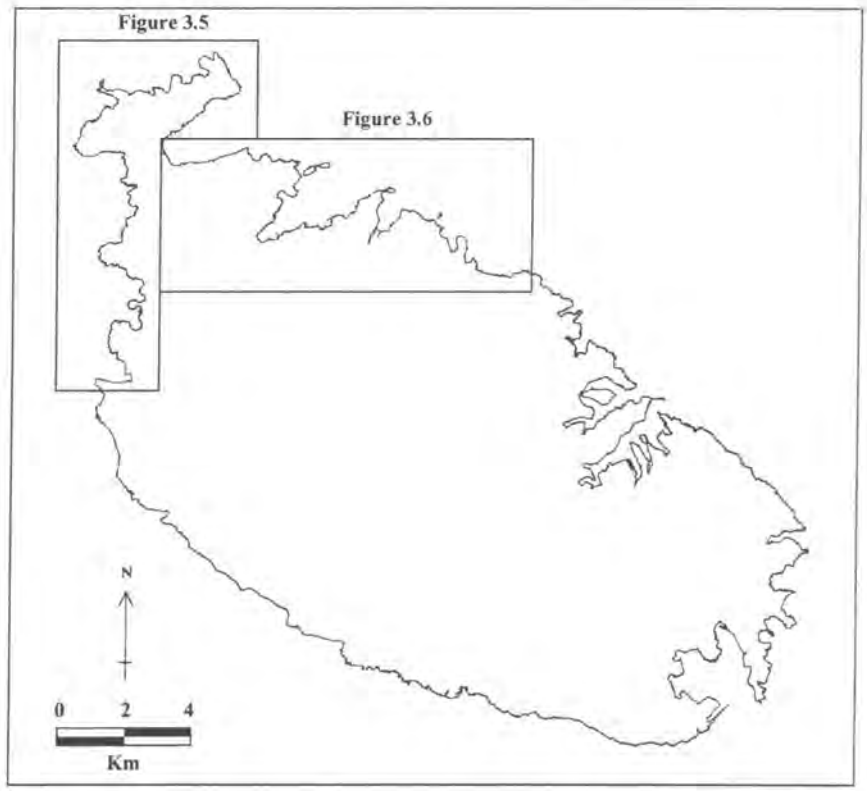


**Figure 3.7 Location of the coastal stretch covered in Figures 3.5 and 3.6**

All the formations of the geological succession of the Maltese Islands are present along the northern coast (Figure 3.8). Upper Coralline Limestone typically features plateaus, scarp faces, cliffs and rotational and translational landslides. These landforms are especially evident all along the north-west coast from Fomm ir-Rih Bay to Rdum il-Qawwi and Ta' Qassisu near Paradise Bay (Figure 3.5). Globigerina Limestone, being a softer formation, is easily eroded and produces characteristic smooth shore platforms with a gentle gradient (Figure 3.5). In some instances, such as at Blata l-Bajda near St.Paul's Islands, in the proximity of Rdum l-Abjad and close to Bahar ic-Caghaq, salt pans have been incised in the shore platforms for salt extraction (Figure 3.6). Lower Coralline Limestone features mainly a low rocky karstic shoreline (Figure 3.6). However at Qammieh where all the geological formations are present, and at Fomm ir-Rih Bay, Lower Coralline Limestone displays cliffs which plunge directly into the sea (Figure 3.5). Blue Clay differs from the other formations in that it is an unconsolidated material and exhibits itself as slopes, such as at Il-Pellegrin, Gnejna Bay, Ghajn Tuffieha Bay, Rdum id-Delli, Rdum il-Qammieh, Rdum il-Qawwi and Ta' Qassisu near Paradise Bay (Figure 3.5). Mass movements

characterising the coasts of northern Malta include landslides and rockfall. The former occurs in Upper Coralline Limestone and Blue Clay formations, whereas the latter takes place in the Upper Coralline Limestone Formation only.

Figure 3.8 shows the relationship between geology and geomorphology at the coast, north of the Great Fault. Areas of mass movement or slope instability are evident where there are outcrops of Upper Coralline Limestone and Blue Clay. Faulting in the Upper Coralline Limestone plateau and basal undermining by Blue Clay cause blocks of rock to dislodge and fall producing rockfall and landslides. When heavy rainfall occurs, Blue Clay slopes can become unstable and mudslides develop. Instability is more widespread on the north-west coast where outcrops of Upper Coralline Limestone and Blue Clay are extensive. The north-east coast is more stable as the geological structure is mainly composed of Globigerina Limestone and Lower Coralline Limestone. The colours used in Figure 3.8 for the different geological layers are the same as those featured in the geological map of the Maltese Islands.

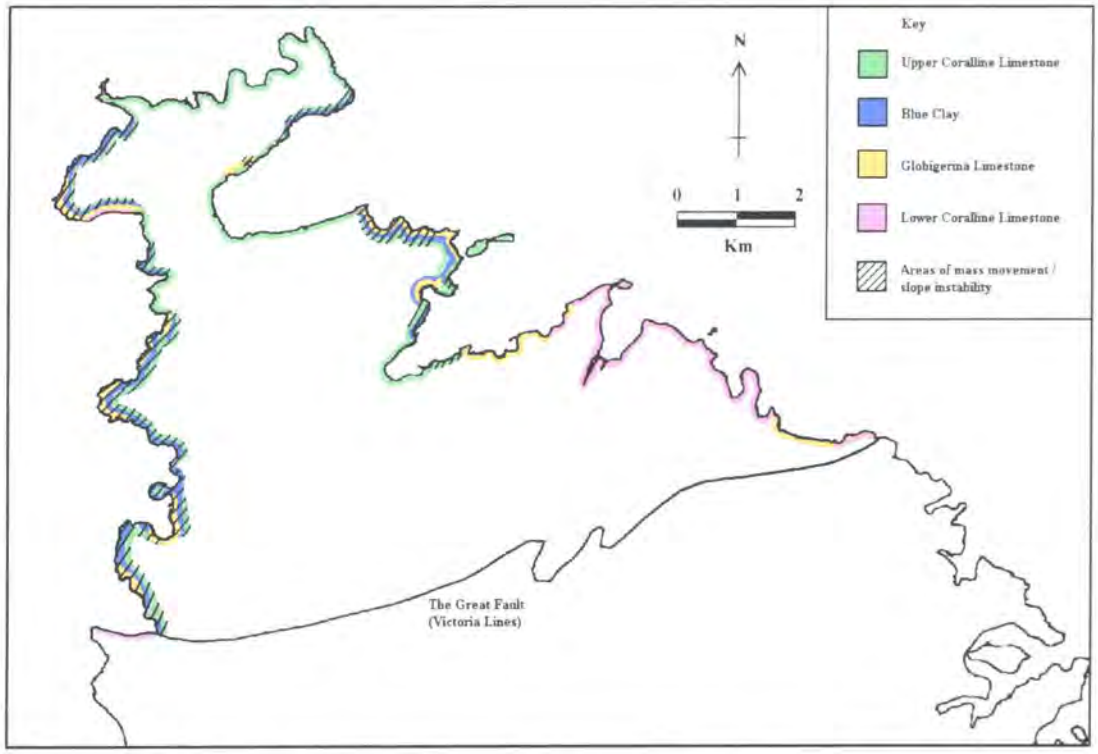


**Figure 3.8: Relationship between geology and geomorphology north of the Great Fault**

Agriculture, both in use and abandoned is evident in some areas along the coast where large blocks have been dislodged from the scarp face on the underlying Blue Clay. This is characterised by small patches of soil surrounded by rubble walls and is sometimes terraced. Such a practice is typical of a semi-arid climate and characteristic of Mediterranean countries. Abandoned agriculture can be identified where rubble walls are not well maintained. Rubble walls help prevent soil erosion and delimit field boundaries. Large limestone blocks dislodged from the scarp face provide shelter from wind and an ideal location for agriculture. The clay being impermeable provides water for the crops. Abandoned agriculture can be identified at Mgiebah (north-east coast) (Figure 3.6) and at Fomm ir-Rih Bay, Rdum l-Imdawwar, Rdum il-Qawwi and at the foot of plateau at Rdum il-Qammieh (north-west coast) (Figure 3.5). Agriculture still in use is found in small patches at Rdum l-Imdawwar (overlooking Gnejna Bay), Ras il-Wahx where trees (probably citrus fruits) are cultivated in patches of soil among landslides, at Rdum il-Qammieh close to shore platform, Rdum il-Qawwi, Ta' Qassisu and at Paradise Bay (Figure 3.5). Agricultural practice is very intensive in these areas and most of the work is performed manually due to the inaccessibility and complex conditions presented by the geomorphological setting.

The resulting geomorphological maps (Figures 3.5 and 3.6) were used as the framework for additional fieldwork. Three coastal locations - Gnejna Bay, Ghajn Tuffieha Bay and Rdum id-Delli, were identified and selected on the basis of information presented on the maps. At these sites further geomorphological mapping at a larger scale (1:1000) (Figures 3.16, 3.18, 3.20), surveying and sample collection provided the necessary information for a more detailed investigation programme to be performed in terms of material testing and slope stability analysis.

### 3.5.2 Coastal landforms north of the Victoria Lines Fault

A range of coastal landforms, situated north of the Victoria Lines Fault, were identified and their spatial distribution determined during the geomorphological survey. Features evident along the northern coast include cliffs, rocky shoreline, rock shore platform and beaches. Other features, namely rotational and translational slides,

mudslides, rockfall, and soil creep were also identified. These landforms which have been formed as a result of mass movement processes are discussed in section 3.5.3.

The north-west coast is bordered almost uninterrupted by an Upper Coralline Limestone plateau scarp face. This extends from Fomm ir-Rih Bay to Paradise Bay and is only broken at Gnejna Bay, Ghajn Tuffieha Bay and Ir-Ramla tal-Mixquqa (Figure 3.5). The height of cliffs ranges from 23 m at Il-Prajjet and reaches a maximum height of 129 m at Il-Qammieh. The plateau appears again at Rdum l-Ahmar on the eastern part of the northern coast, Rdum tal-Madonna and Rdum il-Hmar facing the north-east coast. On the eastern coast the plateau is present only in three localities; Mgiebah, Rdum il-Bies and Rdum Irxaw (Figure 3.6). The Upper Coralline Limestone plateau is skirted by rotational and translational landslides, mudslides and rockfall all along the coast. In some places, such as Ras il-Pellegrin, Rdum Majesa, Ras in-Niexfa, Ras il-Qammieh and Ta' Qassisu (north-west coast), Rdum tal-Madonna, Dahlet ix-Xilep, Il-Marbat and Rdum il-Hmar (northern coast) and Mgiebah (north-east coast) the plateau is heavily faulted. Widening of the faults results in blocks being dislodged from the scarp face and the plateau retreating inland, although this is a slow process.

Cliffs which plunge directly into the sea, where mass movement processes are all but absent, occur both in Lower Coralline Limestone and Upper Coralline Limestone formations. These include Fomm ir-Rih Bay (1.2 km), Il-Prajjet (1.1 km), Ic-Cumnija and Rdum il-Qammieh (1.3 km), Rdum l-Ahmar (1.15 km) (Figure 3.5), Rdum il-Bies (0.33 km) and St.Paul's Islands (1.38 km) (Figure 3.6). The figures indicate the length of the coastal stretch covered by cliffs. Height of cliffs ranges from 15 m at Ic-Cumnija to 61 m at Fomm ir-Rih Bay.

A low rocky shoreline characterises the northern and north-east coasts and occurs in both types of Coralline Limestone formations. The Upper Coralline Limestone stretches from Marfa Point near Cirkewwa to Ahrax Point (6.5 km) (Figure 3.5), part of the northern and the southern littoral of Mellieha Bay (3.25 km), Ras il-Mignuna (close to Rdum il-Bies - 0.63 km) and Xemxija (0.70 km) (Figure 3.6). The Lower Coralline Limestone stretches from Bugibba to Il-Blata l-Bajda (near Bahar ic-Caghaq Bay) and resumes at Madliena Tower (11.45 km) at the junction of the Great Fault of

the Victoria Lines on the north-east coast. Figures indicate the length of the rocky shoreline. The gradient of this type of shoreline varies from 4° (near White Tower in the north) to 18° near Ghajn Zejtuna at Mellieha Bay. Paskoff (1985) attributes chemical (corrosion) and biological weathering as the main processes operating on such coasts. Solution of the limestone by water has led to the formation of pools and lapiés which result in a very irregular topography. This type of coast can also be considered as shore platform. However for the purposes of this study a distinction was made on the basis of the geological formation and the term shore platform was utilised in the case of Globigerina Limestone.

Where Globigerina Limestone outcrops on the coast it displays itself as a smooth shore platform with a gentle gradient (2° to 3°). This is due to the fact that Globigerina Limestone is soft and erodes at a quicker rate than the Coralline Limestone. This type of shore platform is found at Gnejna Bay (0.55 km), Rdum il-Qammieh (1.1 km), Qammieh Point (0.35 km) (Figure 3.5), Mgiebah (1.18 km), where part of the shore platform is submerged below sea-level and at the foot of the cliff on St.Paul's Islands (0.14 km) (Figure 3.6). The figures indicate the length of the Globigerina Limestone shore platform in different locations. Mechanical action of waves, mainly through hydraulic pressure, results in the formation of the shore platforms (Paskoff and Sanlaville, 1978).

Beaches are uncommon in the Maltese Islands. They constitute only 2.4% of the coastline (Schembri, 1990) and consist of small sandy pockets. The longest stretch is found at Mellieha Bay on the north-east coast, which covers a distance of 0.8 km (Figure 3.6). Most of the sandy beaches are found in northern Malta. They include Paradise Bay, Cirkewwa, Ramla tal-Bir, Ramla tal-Qortin, Armier Bay, and Ramla tat-Torri (Figure 3.5). The coast is characterised by headlands which protrude adjacent to each other. Consequently the geomorphological setting might imply that the formation of sandy pockets is the result of erosional processes at headlands and transport and deposition of sediment by longshore drift at the bays. This assertion might be further strengthened by the fact that there exists no other source of sediment such as the location of valleys behind the bays. Sandy beaches found on the north-west coast include Gnejna Bay, Ghajn Tuffieha Bay and Ramla tal-Mixquqa. Shingle pockets on the north-west coast are found at Fomm ir-Rih Bay and Il-Prajjet (Figure

3.5). On the north-east coasts, beaches and sandy pockets are present at Mellieha Bay, Mgiebah, Mistra Bay, Xemxija, Salina Bay, Bahar ic-Caghaq and Qalet Marku. Shingle pockets on the north-east coast are found at Irdum Irxaw, Mistra Bay and Bahar ic-Caghaq (Figure 3.6).

The contrast of a high north-west coast and a shallow north-east coast can be explained by the presence of the Maghlaq Fault, oriented WNW-ESE on the south-west littoral. This became active during the Upper Tortonian, and was responsible for the tilting of the island towards the north-east during the Quaternary to Recent period.

### 3.5.3 Mass movement processes along the northern coast of Malta

Mass movement is the downslope movement of soil or rock material under the influence of gravity without the assistance of moving water, ice or air (Selby, 1993). Over the years several classifications have been proposed to try and classify mass movement processes and landforms (for example Sharpe, 1938; Varnes, 1958, 1978; Carson and Kirkby, 1972 and Hutchinson, 1988) on the basis of different criteria such as velocity and mechanism of movement, type of material and water content available in the material. Given the great diversity in terms of form, origin, movement and magnitude, no single classification is universally satisfactory, although one has to appreciate these attempts as they provide a valuable contribution to hillslope geomorphology.

Mass movement processes along the coast of Malta, north of the Victoria Lines Fault, occur mostly on the north-west shoreline (Figure 3.8) and fall under three main categories: slides, falls and creep (Figures 3.5 and 3.6). Creep is the least significant process as it can be located only at one site. Slides and falls predominate the north-west coast and occur at specific localities on the northern and north-east coasts. Three types of slides can be identified: translational slides, rotational slides and mudslides. The first two types occur in the Upper Coralline Limestone Formation, whereas mudslides develop in Blue Clay. Rockfall is also generated in the Upper Coralline Limestone Formation and varies in magnitude from debris to boulder scree and large blocks.

Landslides occur mainly as a result of shear failure at the boundaries of the moving mass (Brunsden, 1971 *in* Gardiner and Dackombe, 1983) and include both sliding and flowing motions. Landslides are characterised by movement above a sharply defined shear plane, which follows a structural plane such as a plane of foliation or bedding (Selby, 1993). Both translational and rotational slides are triggered by a temporary excess of shear stress over shear strength within the slope. There are many factors which cause such events. These include alternate wetting and drying, clay mineral swelling, deep weathering, after snowmelt or prolonged and intense rainfall (Trenhaile, 1997). Deep-seated events such as rotational slides can be triggered by groundwater build-up and basal undercutting.

### 3.5.3.1 Translational slides

Translational slides move downslope along a more or less planar surface on shallow shear planes which are roughly parallel to the ground surface (Cooke and Doornkamp, 1990) (Figure 3.9). Translational slides include rock slides, block slides and debris slides and can be used as a universal term to cover lateral spreads as well (Hutchinson, 1968 *in* Cooke and Doornkamp, 1990). The upper surface of a translational slide does not tilt during displacement. This type of landslide can develop in both lithified rock such as limestones, as is the case in Malta, and more clayey materials (Allison, 1992). In limestone, jointing is the main cause which dislodges blocks of material, causing them to slide on discontinuity surfaces such as bedding planes. In poorly lithified material, translational slides are usually associated with weathering. Trenhaile (1997) mentions several factors which can cause translational sliding. They include seaward-dipping rocks, alterations of permeable and impermeable strata, massive rocks overlying incompetent materials, or argillaceous and other easily sheared rocks with low bearing strength. Translational landslides can move across low gradients when the slide is joint bounded at the sides and displacements involve linear motion.

Along the Maltese littoral translational slides have developed in several localities (Plate 3.16). The landslides are usually shallow and in most cases there is a displacement from the *in situ* material to several metres downslope and even extending to the shoreline. The landslides vary in length from 4 m (Ta' Qassisu and

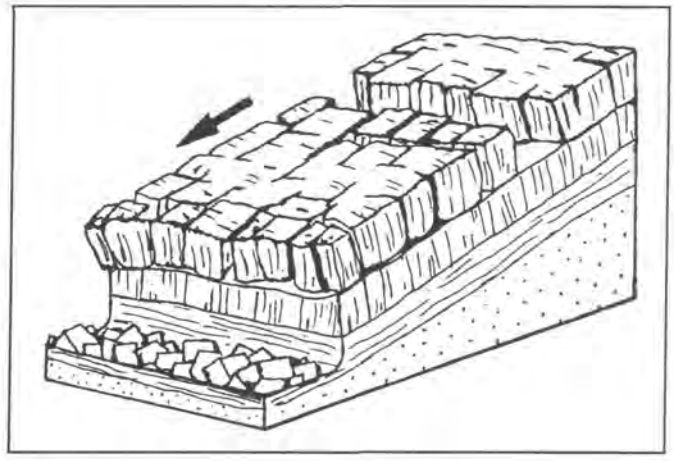

**Figure 3.9: Characteristics of translational slides**
Source: Allison, 1992

Ras il-Wahx) to 40 m (Il-Marbat), with an average length between 10 m to 15 m, and are located in close proximity to rotational slides or else surrounded by rockfall. Translational slides can be found at Fomm ir-Rih Bay, Ras il-Pellegrin, Ras il-Wahx, Rdum Majesa (Plate 3.16), Rdum id-Delli, Ras in-Niexfa, Rdum il-Qawwi, Ta' Qassisu (north-west coast), Il-Marbat (northern coast) and Mgiebah (north-east coast) (Figures 3.5 and 3.6). Sometimes during movement the translational slide can break up and become incorporated in other types of slides such as mudslides and mudflows or rockfall. This is evident along the coast in Malta where the slide is fragmented and is incorporated within the rockfall at Rdum il-Qawwi and Il-Marbat.

### 3.5.3.2 Rotational slides

Rotational slides involve a rotational movement on the slip surface parallel to the slope that often leaves an upper surface, on the failed mass, tilted back into the hillside (Cooke and Doornkamp, 1990) (Figure 3.10). They occur with a concave-upwards curved shear plane - the rupture surface - and are common where slopes consist of thick homogeneous materials such as clay or shale, although they also develop in more competent rock such as limestone. Rotational slides are more deep-seated than translational slides. Very often the shape of the slip surface is influenced by faults, joints and bedding. When a rotational slide is detached it supports the ground behind it. As movement increases, the ground will become unsupported and a

new failure might occur (Richards and Lorriman, 1987 *in* Allison, 1992). This results in rotational slides developing in multiple succession one behind the other. Rotational slides are often found in active eroding cliffs.

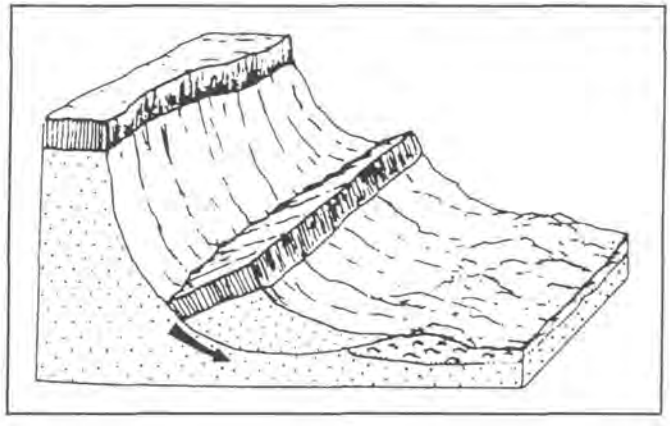

**Figure 3.10: Characteristics of rotational slides**
Source: Selby, 1993

In Malta, rotational slides occur in the Upper Coralline Limestone Formation and are situated just below the *in situ* material from where they have been detached (Plate 3.17). Only in the case of multiple *en echelon* failures, do the slides extend from the base of the Upper Coralline Limestone plateau to sea-level. Rotational slides (like translational slides) are more common on the north-west coast, where they are found at Fomm ir-Rih Bay, Ras il-Pellegrin, Il-Qarraba, Ras il-Wahx, Rdum id-Delli, Ras in-Niexfa, Rdum il-Qawwi and Ta' Qassisu (Figure 3.5). On the north-east coast, this type of landslide occurs only at Mgiebah (Figure 3.6). The size of rotational slides varies in length from 4 m to 6 m at Ras il-Wahx and Rdum id-Delli to 25 m at Ta' Qassisu and Rdum il-Qawwi. Multiple rotational slides invariably occur at headlands namely Il-Qarraba, Ras il-Wahx, Ras in-Niexfa and Ta' Qassisu. Ras il-Wahx (Plate 3.18) provides definitely the best example of this type of event, as it features a complex structure of rotational slides occurring in multiple succession covering an area of about 400 $m^2$.

### 3.5.3.3 Mudslides

The other type of sliding movement present along the northern coast in Malta is mudslides, evident where clay slopes are located. Mudslides can be defined as a form of mass movement in which softened clay, silt or very fine sand debris advances chiefly by sliding on discrete boundary shear surfaces in relatively slow moving, lobate or elongate forms (Hutchinson and Bhandari, 1971 *in* Allison, 1992). A mudslide consists of three morphological zones: the headward feeder, main track and toe lobe (Allison and Brunsden, 1990) (Figure 3.11).

The headward feeder or bowl (Figure 3.11) forms the main area of supply and is found at the rear of the slope. It marks the interface between stable and unstable ground and is usually backed by a cliff. In the case of Malta this is the Upper Coralline Limestone plateau. Material is supplied by a combination of falls, weathering and erosional processes. Instability causes the debris to spread from the headward feeder to the lower parts of the system. Soil moisture and pore water pressure are very irregularly distributed (Allison, 1992).

The main track is generally steep and straight and forms the central part of the mudslide (Figure 3.11). It functions as a zone of transport for material moving from the crest to the toe of the slope. The slip surface at the base of the track is parallel to the ground surface. In the track the debris is fragmented and soft. Short tracks result in lobate mudslides (less than 20 m wide and 1 m to 5 m deep). These are a common feature along coastal cliffs in Malta. Longer tracks produce more sinuous forms and are less common in coastal areas. The main track is defined by lateral shears. Pressure ridges, tension cracks and curved Riedel shears frequently develop at the edges of the moving mass (Allison, 1992).

The toe lobe or accumulation zone (Figure 3.11) consists of two components: the upper flatter area with a slope gradient between 1° and 5° and a convex downslope end with angles between 15° and 25°. This zone is characterised by a sharp basal shear surface (Brunsden, 1984 *in* Allison, 1992). At the coast the toe lobe can be cut by the sea. The leading edge is often surrounded by boulder arcs, which mark

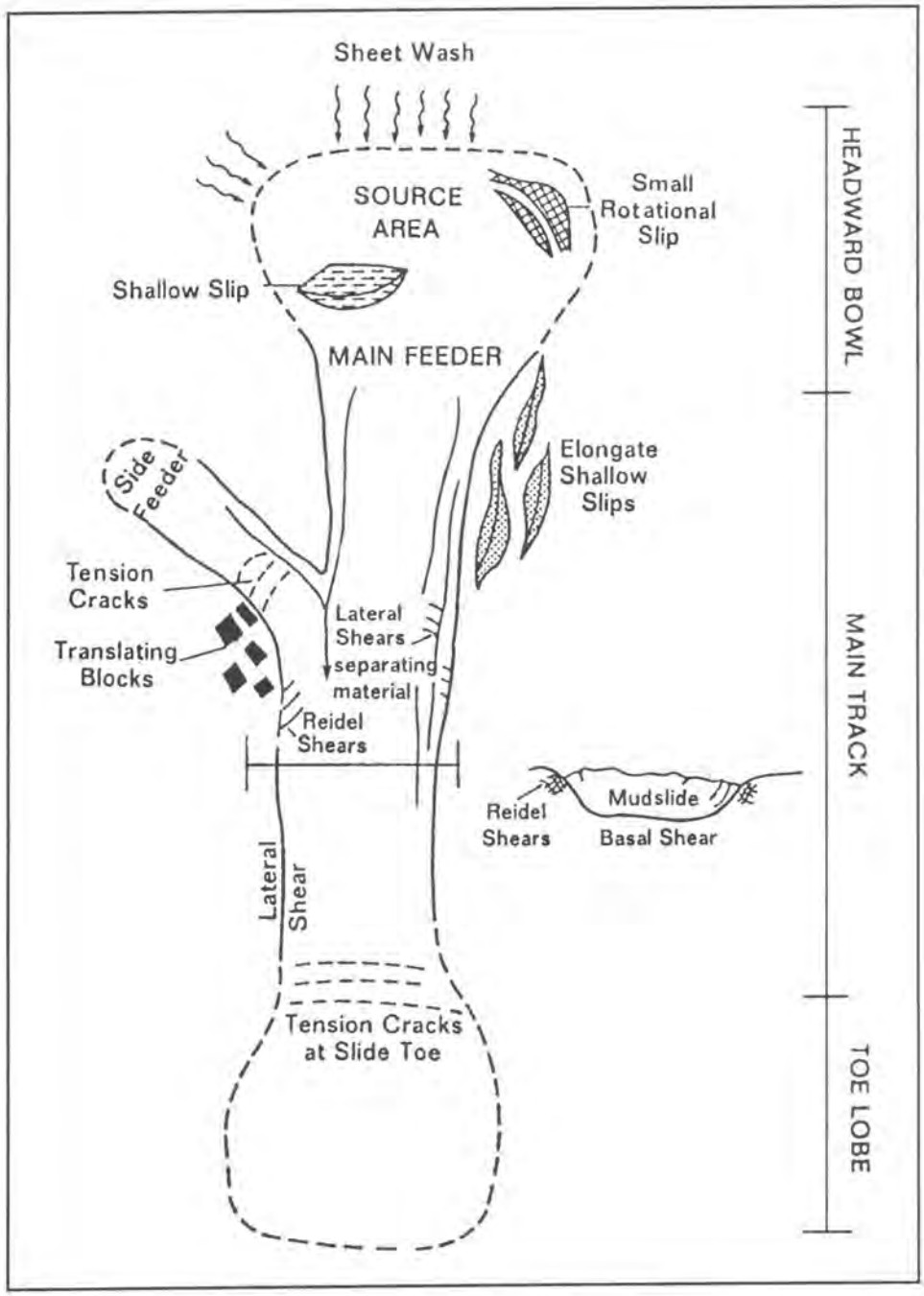


**Figure 3.11: Characteristics of mudslides**
Source: Allison, 1986

previous extents of the mudslide. The accumulation zone usually supports the debris in the track.

Clays being more cohesive tend to move in less distorted units than cohesionless material. The trigger mechanism for movement in unconsolidated materials is usually rainfall creating high pore water pressures. When distortion takes place, movement may include flow as well as sliding. Distinction between slide and flow is not always clear and many slope failures involve both movements. Generally mudslides move in the form of plug flow (Johnson, 1970 *in* Allison, 1992). In this type of movement an edge or bottom layer of variable thickness is deformed by internal changes. A central plug is enclosed and acts as a rigid sliding body. Movement can also be parabolic and is associated with flow caused by continuous internal deformation. In very wet conditions, when the Liquid Limit is exceeded, debris and unconsolidated material will move as flow. Mudflows are rapid failures common in arid and semi-arid regions where infrequent rainfall events trigger the high runoff typical of these dry, poorly vegetated regions and the material becomes saturated. Increased moisture results in decreased shear strength and the wet mass flows rapidly down the channel (West, 1995).

Mudslides in Malta occur where Blue Clay outcrops. At the coastal zone this geological formation features slopes which usually extend from the base of the Upper Coralline Limestone plateau to sea-level. The best examples of clay slopes are found at Gnejna Bay (Plates 3.19 and 3.20) and Il-Qarraba. Blue Clay is exposed in most of the localities on the north-west coast, such as Fomm ir-Rih Bay, Ras il-Pellegrin, Ghajn Tuffieha Bay, Ras il-Wahx, Rdum Majesa, Rdum id-Delli, Ras in-Niexfa, Rdum il-Qammieh, Rdum il-Qawwi and Paradise Bay (Figure 3.5). On the northern and north-east coasts Blue Clay is found in only four localities: Rdum il-Hmar and Ta' l-Imgharrqa (northern coast) (Figure 3.5), Mgiebah and Rdum Irxaw (north-east coast) (Figure 3.6).

Mudslides become active when clay contains a high water content. This type of mass movement is triggered after heavy and prolonged rainfall events, which frequently occur during the period October/November until February/March in Malta. After the summer drought, which lasts from May up till October, Blue Clay loses most of its

moisture and will become very dry. The first rains saturate the clay and fill tension and desiccation cracks with water. The latter develop during the summer months as a result of drying and the associated reduction in volume of the clay. At this stage the Blue Clay would be in a position to absorb water quickly. After prolonged rainfall, the clay becomes fully saturated and starts moving as mudslides or mudflows if the water content is very high. Since most of the mudslides on mainland Malta are found at the coast, damage is limited to the destruction of some boathouses which are used to provide shelter for boats especially during the winter months.

### 3.5.3.4 Rockfall

Rockfall is the downward motion of rock through air due to gravity. This process occurs where a steeply sloping rock-face consists of well-jointed rock (Figure 3.12). Material is detached along lines of structural weakness such as bedding planes and joints. This type of mass movement tends to be generated in three stages (Cooke and Doornkamp, 1990).

i. Creation of cracks.
ii. Enlargement of cracks as a result of pressures related to water freezing, growth of plant roots or as a result of gravity.
iii. Fall takes place because support has been removed from the base of the rock by several agents such as erosion by glaciers, the sea or rivers, as a consequence of differential weathering or human interference.

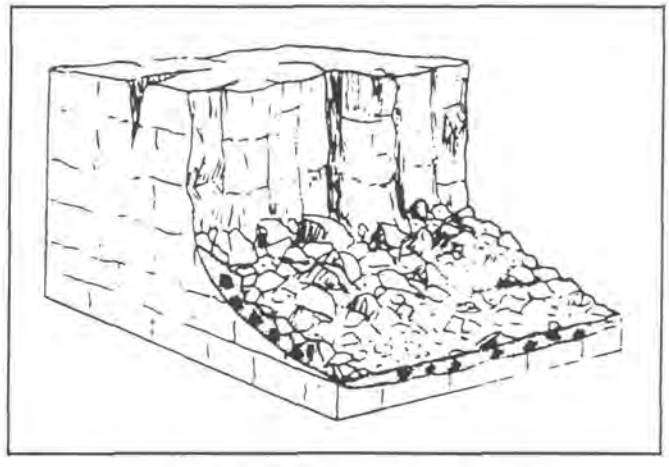

**Figure 3.12: The process of rockfall**
Source: Selby, 1993

Rock detachment can also be caused from a change in the stress distribution within the rock mass, which results from weathering or changes in the pore water pressure within the fissures (Allison, 1992). At first the falling debris moves by sliding but afterwards it becomes detached from the *in situ* material. Usually blocks break up upon impact with the ground and sometimes during movement. Rockfall includes blocks of different sizes which come to rest below the place where they were detached, usually as scree at the base of the cliff. They can later move downslope especially along coastal areas. Sometimes debris becomes incorporated within a moving mass such as a mudslide or mudflow.

In Malta, rockfall can be considered as the most important mass movement process along the northern coast. The process is found extensively on the north-west coast and at specific localities on the north and north-east coasts (Figures 3.5 and 3.6). Rockfall bounds all the north-west littoral and is interrupted only where beaches, shore platforms, plunging cliffs and rocky shores are located. Blocks of rock are detached from the Upper Coralline Limestone plateau and either rest below or move away from the *in situ* material (Plate 3.21). The process can be attributed to several factors.

i. A response to gravity stresses.
ii. Basal undermining caused by Blue Clay.
iii. Widening of joints or other lines of weakness as a result of erosional and weathering processes.
iv. Tectonic activity.

Whalley (1984 *in* Allison, 1992) has proposed a classification based on the volume of material, rather than the type of process involved. Three categories were put forward: debris falls where movement is less than 10 $m^3$, boulder falls involve a displacement between 10 $m^3$ to 100 $m^3$ and blockfalls where the process covers more than 100 $m^3$ of material. Applying this classification within a local context, rockfall in Malta can be classified under two categories: debris falls and boulder falls. Boulder falls involve blocks varying in size between 10 m to 30 m in length. These are characteristic features of several localities such as Rdum Majesa, Rdum il-Qawwi, Ta' Qassisu and Rdum Irxaw (Figures 3.5 and 3.6). Debris falls can result from the fragmentation of

boulders as a result of weathering and are very often found close to the larger blocks (for example at Ras in-Niexfa, Rdum tal-Madonna, Rdum il-Hmar and Mgiebah) or else incorporated in mudslides (Ras il-Pellegrin and Rdum id-Delli).

Slab failures occur at the top of cliffs where tension joints may be seen extending parallel to the cliff face (Figure 3.13). With time the cracks will extend vertically and sideways extending the slab and widening it, until the tensile strength of the rock is exceeded and a fall occurs. Extension of the cracks occurs with the aid of water seepage, debris falling into the crack and ice. This type of failure frequently leaves overhanging 'roofs' of rock above the scar from which they have fallen and further slab failure may develop. Along the Maltese littoral, at several places, the Upper Coralline Limestone plateau exhibits faults or cracks which are parallel to the scarp face resulting in slab failure. The failure can be identified by a large block which has been detached from the plateau and rests parallel to the scarp face. The latter can be identified at Ras il-Pellegrin, Rdum Majesa, Ta' Qassisu, Rdum tal-Madonna, Dahlet ix-Xilep and Rdum il-Hmar (Figure 3.5). Wedge and toppling failures are absent along the northern littoral in Malta, as failure tends to occur along a set of discontinuities trending in the same direction. Besides there is no indication of a forward rotational movement as the rock falls. This causes overturning of columns and occurs where joints are vertically extensive in relation to their width.

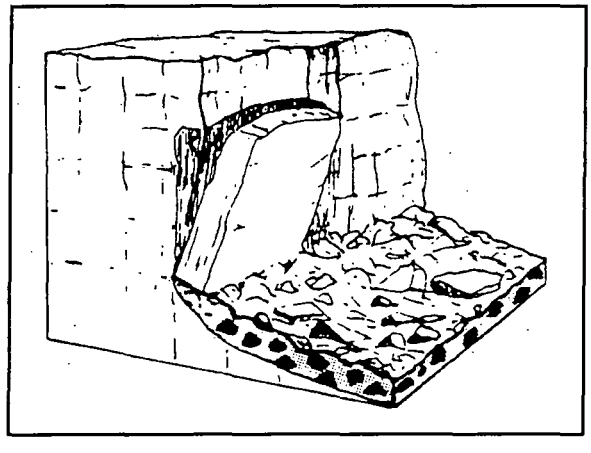

**Figure 3.13: Slab failure**
Source: Selby, 1993

### 3.5.3.5 Soil creep

Soil creep is the least significant mass movement process observed in northern Malta. The process can be defined as the slow downslope movement of superficial soil or rock debris which is usually imperceptible except to observations of long duration (Selby, 1993) (Figure 3.14). Four main mechanisms are responsible for generating this movement: pure shear, viscous laminar flow, expansion and contraction and particulate diffusion (Donohue, 1986 *in* Selby, 1993). Movement is by quasi-viscous flow, occurring under shear stresses sufficient to produce permanent deformation, but too small to result in a discrete failure surface such as landslide (Rahn, 1996). Creep occurs at very slow rates - 1 mm to 10 m per year (Summerfield, 1991) and is especially active where weakly competent materials (such as clay) are overlain by more competent beds. Movement is irregular in both direction and rate and this process is often a precursor of landslides. However other causes can be observed which include cambering, downslope curvature of strata near the surface, bending of the lower parts of tree trunks, cracks in the soil and tilting of structures (Summerfield, 1991; Selby, 1993). Terracettes are perhaps the main surface features attributed to soil creep.

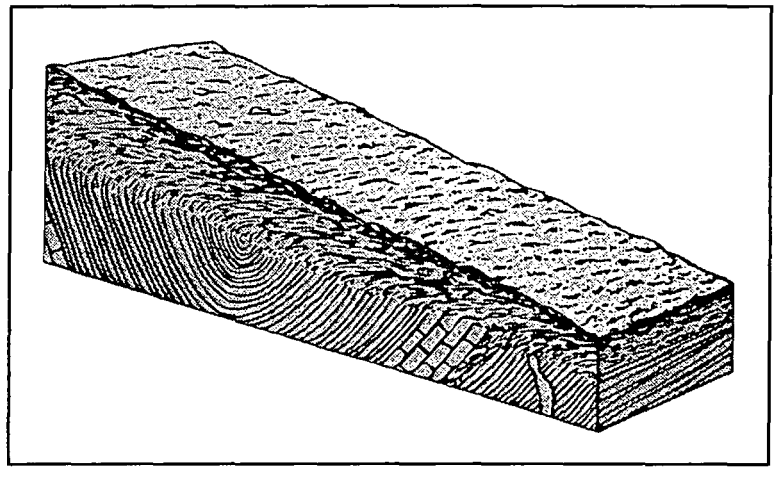

**Figure 3.14: Characteristics of soil creep**
Source: West, 1995

Along the northern coast of Malta, soil creep can only be identified at Rdum id-Delli (Figure 3.5) where it is the main process operating within a Quaternary solution subsidence structure. The latter features a karstic landform of a concave aspect, characterised by bare patches of soil and some steppic vegetation. Soil creep can develop in response to stress generated by the weight of Upper Coralline Limestone overlying the soil underneath. Elsewhere this mass movement can be present occurring in very localised areas and at very slow rates.

## 3.6 Field investigation of three coastal sites

The geomorphological maps (Figures 3.5 and 3.6) provided a good basis to locate three 'type sites' where detailed field investigation could be undertaken. This was possible as the maps featured the spatial distribution of different coastal landforms in northern Malta. In addition to the above, the geomorphological maps formed the basis of three supplementary elements of this study.

i. Detailed site specific geomorphological mapping of the 'type sites' at a scale 1: 2000.
ii. Field sample collection for laboratory testing to determine the physical and geotechnical properties of Blue Clay.
iii. Selecting slope profiles for detailed survey as the basis for slope stability modelling.

The three selected sites are Gnejna Bay, Ghajn Tuffieha Bay and Rdum id-Delli, all located on the north-west coast (Figure 3.15 and Plates 3.22, 3.23, 3.24 and 3.25). These coastal sites were chosen as they provide the best examples of Blue Clay outcrop at the coast which displays itself as slopes extending from the Upper Coralline Limestone plateau to sea-level. The sites were also chosen on the basis of their accessibility where fieldwork could be carried out without particular difficulties.

The first task was to map the landforms and processes present at each locality. The exercise for each site extended on several days as the geomorphological mapping was

carried out at a large scale 1: 1000. The scale was chosen as it allows the production of a detailed map. The geomorphological map produced for each site (Figures 3.16, 3.18 and 3.20) are presented at a smaller scale 1: 2000 for practical reasons.

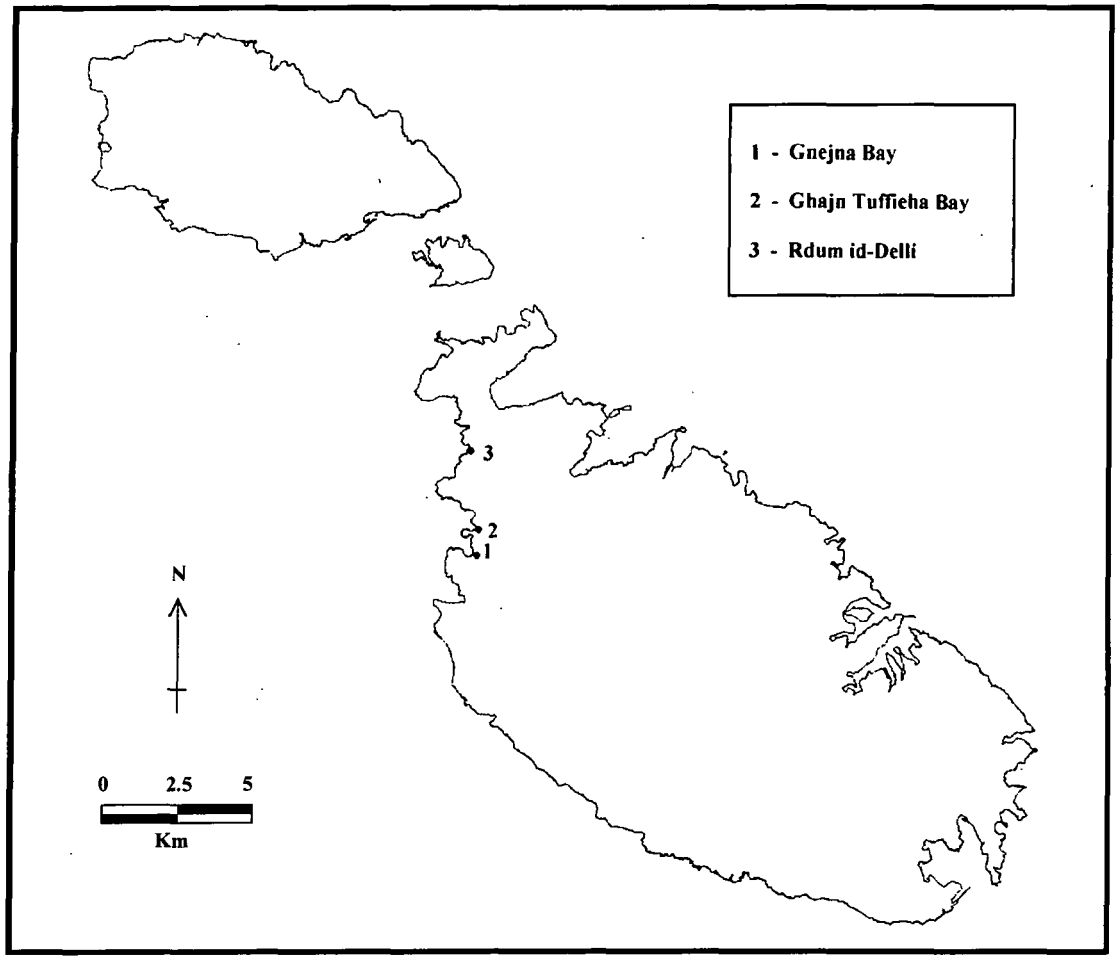


**Figure 3.15: Location of the three field sites**

The following is a list of the symbols utilised for geomorphological mapping, based on standard typology (see for example Gardiner and Dackombe, 1983; Cooke and Doornkamp, 1990).

Plateau scarp face 

Cliff face 

Translational slide 

Rotational slide 

Mudslide / Clay slope 

Rockfall 

Soil creep 

Rock shore platform 

Sand / Shingle 

Angle of slope 


Convex slope unit 

Concave slope unit 

Smooth change of convex slope 

Smooth change of concave slope 

Angular convex break of slope 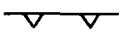

Stable gully 

| | |
|---|---|
| Active gully |  |
| Seepage line |  |
| Rubble wall | RW |
| Vegetation |  |
| Quaternary solution subsidence structure | Q |
| Surveyed slope transect |  |

Following large scale geomorphological mapping, a slope profile was identified at each site to conduct a more detailed study first by surveying and then by collecting samples for laboratory analysis. Each transect was chosen on the basis that it extended over a long distance from the base of the Upper Coralline Limestone plateau to sea-level. Another criterion taken into consideration when choosing the slope was that the lateral shears could be identified, thus the feature could be clearly defined and its boundaries distinguished. At each of the three sites the selected transect was surveyed using a Leica TC600 total station laser level and a cross-section plan (scale 1: 750 for Gnejna Bay, scale 1: 1000 for Ghajn Tuffieha Bay and scale 1: 500 for Rdum id-Delli) was drawn. The chosen transects are marked on the geomorphological maps (Figures 3.16, 3.18 and 3.20) and in the insets of the cross-section plans (Figures 3.17, 3.19 and 3.21). Measurements were recorded where there was a change in the topography along the transect. Data collected included height above sea-level and horizontal distance from sea-level. Slope gradients were calculated from the readings using the tangent computation. During the recording of data on the field a datum level was given for each site (30 m for Gnejna Bay, 110 m for Ghajn Tuffieha Bay and 160 m for Rdum id-Delli). The data regarding the height above sea-level was then reduced from the datum to obtain the actual field measurements. This exercise was undertaken so that the data of the three transects can be used to run a computer modelling software (XSTABL) to assess slope stability at each of the three sites.

### 3.6.1 Gnejna Bay

Gnejna Bay is situated on the north-west coast of Malta between Rdum l-Imdawwar and Il-Qarraba (Figure 3.15 and Plates 3.22 and 3.23). Three geological formations are present in the area under study.

i. Upper Coralline Limestone: this constitutes the plateau and is made up of two members. The top layer belongs to Tal-Pitkal Member, whereas the basal layer consists of the Mtarfa Member.
ii. Blue Clay: this formation is found extensively and is featured as slopes which extend from the base of the Upper Coralline Limestone plateau to sea-level.
iii. Globigerina Limestone: Upper Globigerina Limestone outcrops at the shoreline below the clay slopes as a shore platform and cliff.

Gnejna Bay is characterised by scree slopes on both sides of the Bay. Scree slopes occur when Upper Coralline Limestone boulders which have been dislodged from the plateau, fall on the underlying Blue Clay slopes. The feature results either from erosion by wind and water acting along lines of structural weakness or by tectonic movements (Schembri, 1993). The steepest slopes, close to Il-Qarraba, are completely bare or have little vegetation cover (0 to 10 per cent). The rest of the slopes are covered by steppic vegetation such as Esparto Grass (*Lygeum spartum*). A distinct patch of the Great Reed (*Arundo donax*) covering an area of about 217.5 m² is found below the landslides. This species reaches a height of over 4 m and grows along watercourses and in areas where there is underground water (Lanfranco, 1996).

The area under study (Figure 3.16) is situated close to Il-Qarraba and stretches over a coastal length of 0.56 km. It is delimited by Il-Qarraba on the northern side and a distinct patch of reeds on the southern side. The area is characterised by an Upper Coralline Limestone plateau, beneath which clay slopes are found extending from the base of the plateau to sea-level. The plateau ranges in height from about 3 m close to Il-Qarraba, to 11 m close to the patch of reeds. Globigerina Limestone is exposed at sea-level below the slopes featuring a shore platform and a small cliff. The width of the area from the base of the plateau to sea-level varies from about 125 m to 200 m, widening at the area close to the reeds.

**Plate 3.22: Clay slopes examined at Gnejna Bay, close to Il-Qarraba. In this section the clay slopes are almost completely bare of vegetation cover due to a steep gradient. Above the clay slopes the Upper Coralline Limestone plateau is evident. The vegetated clay slopes featured in the background on the left, are found at Ghajn Tuffieha Bay, whereas in the foreground part of Il-Qarraba is visible. A small sandy pocket and Globigerina Limestone shore platform are seen at the foot of the clay slopes. The shore platform closest to the sandy pocket marks the northern limit of the area under study.**

**Plate 3.23: Clay slopes examined at Gnejna Bay, close to the reeds. Slopes in this section are vegetated since the gradient is not so steep. The Upper Coralline Limestone plateau and scarp face are visible in the background, whereas the Globigerina Limestone cliff and shore platform are seen in the foreground. The reeds at the lower right side mark the southern limit of the area under study.**

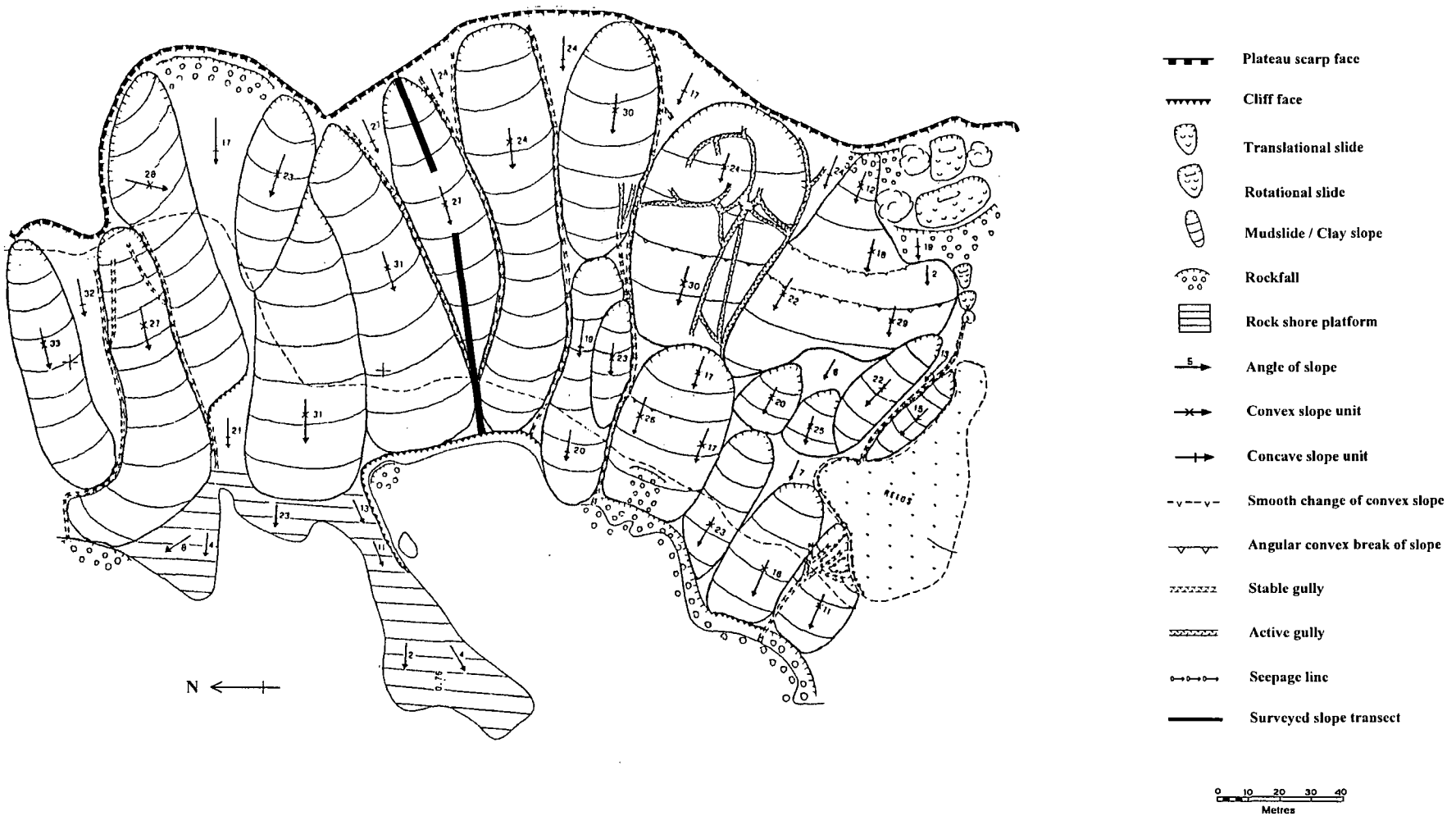


**Figure 3.16: Geomorphological map of Gnejna Bay**

The area can be divided into two parts. The first part close to Il-Qarraba is characterised by well-defined clay slopes extending from the foot of the plateau to the Globigerina Limestone shore platform or cliff below (Plate 3.22), covering a distance between 60 m to 95 m. These have a convex aspect and a steep slope gradient varying from 23° to 33°. The latter are separated by other slopes of a concave aspect ranging from 17° to 32° in gradient (Figure 3.16). A Globigerina Limestone shore platform, 0.34 km long and a cliff, 0.11 km long are found at the base of the clay slopes. The platform is very irregular in shape. At its narrowest point it measures 10 m in width, whereas its maximum width is about 47 m. Overall the platform has a gentle gradient ranging between 2° to 13° but this steepens in one part to 23°. The Globigerina Limestone cliff (5 m to 10 m high) extends from one end of the shore platform along the shore beneath the clay slopes (Figure 3.16).

The second part, closer to the patch of reeds, is characterised by a series of smaller slopes extending from the base of the plateau to about 80 m downslope (Plate 3.23). A second set of slopes extend from this point towards sea-level, stretching over a distance between 60 m to 80 m. Generally the slopes have a convex aspect with a gradient ranging from 11° to 30° (Figure 3.16). The latter are separated by concave slopes at the base of the plateau, having a gradient which ranges from 17° to 24°. Another concave slope is also found at one point extending from about 79 m from the base of the Upper Coralline Limestone plateau to sea-level with a gradient varying between 19° and 20° (Figure 3.16). In some cases the change in topography of the slopes is angular and abrupt getting steeper towards the lower end whereas in the other cases the change is smoother and gentler. The convex slope situated near to the rotational landslides changes its gradient from 12° to 18° at the top part and 22° to 29° at the lower part. The change in slope is generally smooth, although at one side close to the landslides the change is angular above which a flat area of 2° is found. Close to the patch of reeds three levels of slopes are found separated by gentle slopes (6° to 7°) of a rectilinear aspect. Globigerina Limestone is exposed at sea-level featuring a cliff about 17 m long and a small shore platform covered by boulders.

The main geomorphological processes present in the area under study include mudslides, rotational and translational slides and rockfall (Figure 3.16). During mapping there was no indication of mudslides taking place but heavy rainfall can

trigger the clay to become plastic when wet, initiating a sliding process. Mudslides in the area can be common during the winter months when heavy rainfall occurs and the clay becomes softer, causing instability of the Blue Clay slopes.

Landslides are found at the foot of the plateau above the reeds (Figure 3.16). They are of two types: rotational and translational. Rotational slides are more common and seem to have occurred in multiple succession. The blocks are about 4 m to 5 m high and between 17.5 m to 40 m wide. They have been cut off from the scarp face and slided down, rotating and tilting inwards during the process. The translational landslide at Gnejna Bay measures about 12.5 m wide and 4 m high and is found below the rotational slides.

Rockfall is another process which is present at Gnejna Bay. This is mainly found at the foot of the Upper Coralline Limestone scarp face, close to Il-Qarraba around the landslides where the concave gradient is 19° and along the coast (Figure 3.16). The boulders are smaller in size than the landslides. Their dimensions are about 2 m to 3 m in width and height. Rockfall involves detachment of the rock from the scarp face but the movement involves falling under gravity rather than sliding. Some boulders move for a long distance and are found along the shoreline, protecting the coast from erosion.

Desiccation cracks are present in several locations on the edges and sides of clay slopes at Gnejna Bay. They develop as a result of clay losing moisture and changing in volume. Their dimensions vary both in width and depth. Close to Il-Qarraba they are about 10 cm wide and vary from 27 cm to 40 cm in depth. Above the shore platform they are about 10 cm wide and 30 cm deep. At the central part the dimensions vary from 7 cm to 20 cm in width and 26 cm to 46 cm in depth. Near the reeds, desiccation cracks are about 12 cm wide and 23 cm deep.

The hydrological pattern at Gnejna Bay is indicated by a system of gullies, generally situated at the lateral limits of the clay slopes (Figure 3.16). The area is well drained and gullies are distributed extensively. Two types of gullies have been distinguished: active and stable. Active gullies refer to gullies which have started to form and are still being eroded by the action of water. This type of gullies have shallow water

channels which change their direction according to the movement of water. Stable gullies are well developed gullies with permanently established water channels. They are deeper than the active gullies due to erosion caused by water running along the same channel over a long period of time. Gullies are mainly of the stable type and extend all along the lateral limit of the clay slopes from the base of the plateau towards the shore at sea-level. A complex pattern of active gullies is present on one particular clay slope at the base of the plateau, extending to about 80 m downslope. At Gnejna Bay, gullies range in size. Close to Il-Qarraba, the dimensions are about 55 cm in width and 30 cm in depth. On the clay slopes, above the shore platform, gullies range between 90 cm to 94 cm in width and 30 cm to 50 cm in depth. Towards the reeds, gullies are between 55 cm to 60 cm wide and 30 cm to 45 cm deep. Along the area covered by the reeds, water is present all year round. This is indicated by a water seepage line on Figure 3.16. Reeds in fact are a good indicator of the presence of water, made available by the impermeable property of Blue Clay.

A slope transect was selected for surveying after the geomorphological mapping was performed. The selected slope at Gnejna Bay is situated above the Globigerina Limestone cliff, as marked in Figure 3.16. This was chosen as it extends over a long distance and it can be easily recognised from the mapping as an individual landform. Data collected for the slope transect at Gnejna Bay is given in Table 3.1. Figure 3.17 is a cross-section plan (scale 1: 750) of the surveyed slope. The overall horizontal distance from sea-level to the scarp base extends to 132.77 m and the vertical height above sea-level at the highest point is 71.68 m. The slope gradients for different segments varied from 12.15° close to sea-level to 38.35° at the top part of the slope.

**Table 3.1: Surveying data for the selected slope transect at Gnejna Bay**

| *Point* | *Horizontal distance (metres)* | *Vertical height above sea-level (metres)* | *Slope gradient of segment between points (°)* |
|---|---|---|---|
| A | 0.00 | 9.28 | 19.97 |
| B | 7.87 | 12.14 | 30.42 |
| C | 15.21 | 16.45 | 12.15 |
| D | 29.33 | 19.49 | 22.82 |
| E | 37.91 | 23.10 | 17.43 |
| F | 47.91 | 26.24 | 25.76 |
| G | 56.80 | 30.53 | 17.75 |
| H | 71.23 | 35.15 | 35.98 |
| I | 79.73 | 41.32 | 22.12 |
| J | 92.72 | 46.60 | 32.21 |
| K | 100.88 | 51.74 | 25.27 |
| L | 112.91 | 57.42 | 37.04 |
| M | 119.47 | 62.37 | 38.35 |
| N | 126.32 | 67.79 | 31.09 |
| O | 132.77 | 71.68 | - |

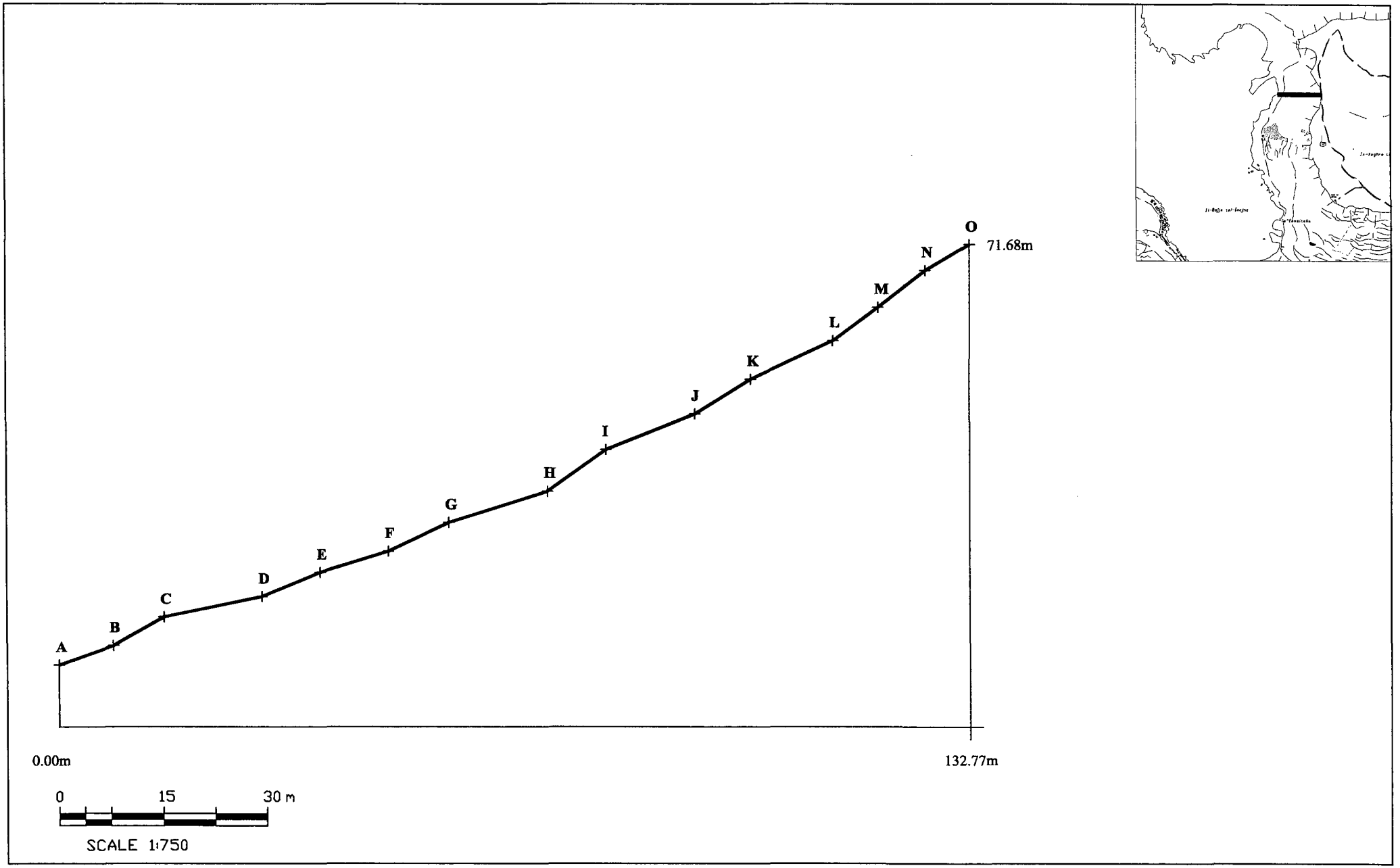


**Figure 3.17: Cross-section of slope profile at Gnejna Bay**

### 3.6.2 Ghajn Tuffieha Bay

Ghajn Tuffieha Bay is located on the north-west coast of Malta between Gnejna Bay and Ir-Ramla tal-Mixquqa (Figure 3.15 and Plate 3.24). The geology is made up of the following formations.

i. Upper Coralline Limestone: two members of the Upper Coralline Limestone Formation constitute a small ridge - Il-Hotba l-Bajda. These include the Mtarfa Member and Ghajn Melel Member. Another Upper Coralline Limestone plateau extending into Gnejna Bay is made up of Mtarfa Member (basal layer) and Tal-Pitkal Member (top layer).
ii. Blue Clay: Il-Hotba l-Bajda is completely surrounded by Blue Clay, which is widely exposed as slopes.

Ghajn Tuffieha Bay is delimited by scree slopes on both sides of the Bay: Il-Qarraba on the southern side which features clay slopes, rockfall and landslides and the northern side which is composed of rockfall backed by an Upper Coralline Limestone plateau.

The Bay is a popular locality both with tourists and locals. In February 1995, the Planning Authority designated Ghajn Tuffieha Bay as an area of ecological importance and a protected site in terms of Section 46 of the Development Planning Act, 1992. It was proposed to turn Ghajn Tuffieha Bay and its surroundings into an "environmental park" managed by a Non-Governmental Organisation. The whole Bay including the clay slopes, the two peninsulas at either side and the beach, were designated as "Areas of Ecological Importance" by the Planning Authority in line with the policies of the Structure Plan on rural conservation.

Four levels of protection and conservation priorities have been assigned to the Bay: Level 1 being the highest level of conservation and protection. Il-Qarraba is given the highest level of protection. No physical development is allowed and human influences are to be kept to the barest minimum. The Blue Clay slopes backing the beach and part of the scree slopes at the northern part of the Bay were assigned Level 2. Human influence is here strictly controlled. The beach and the cliff face of the Upper

**Plate 3.24: An aerial view of Ghajn Tuffieha Bay. The clay slopes extend from the back of the sandy beach to the base of the Upper Coralline Limestone plateau. The sandy beach stretches along the whole length of the Bay. Ghajn Tuffieha Bay has been designated as an area of ecological importance by the Planning Authority in 1995 and is a protected site by law. The Bay is at present managed by the GAIA Foundation, a Non-Governmental Organisation which was responsible for a recent afforestation project.**

Coralline Limestone plateau have been marked Level 3 of protection hindering any residential, industrial, commercial and touristic development. Level 4 has been assigned to the area below a demolished hotel which consists of rubble, boulder scree and clay slopes. Today this Bay is managed by the Gaia Foundation which is an Non-Governmental Organisation dedicated to the protection and understanding of the environment.

Vegetation covers the whole bay and includes various species of maquis and steppe communities. About 40 per cent of Ghajn Tuffieha Bay is covered by maquis vegetation, mainly tamarisk (*Tamarix africana*) and acacia trees (*Acacia cyanophylla*). Steppic vegetation is dominated by Esparto Grass (*Lygeum spartum*). A small patch of the Great Reed (*Arundo donax*) is present at the foot of the plateau at the southern end of the Bay overlooking Gnejna Bay. The area covered by vegetation has increased due to a recent afforestation project undertaken by the Gaia Foundation.

The area under study, excluding the two headlands on either side of the Bay (Figure 3.18) is about 0.52 km long, along the central footpath and varies from 170 m to 220 m in width. The Bay is widest at its central part and narrows towards both ends. Ghajn Tuffieha Bay is mainly composed of Blue Clay slopes both of a convex and concave aspect with a gradient which varies widely. The slopes are backed by two Upper Coralline Limestone plateaux: Il-Hotba l-Bajda which is a small ridge (3 m to 5 m high) and the other plateau extending to Gnejna Bay which is also 3 m to 5 m high. A sandy beach runs along the whole length of the Bay for about 0.32 km having a slight gradient (3°) which steepens towards the centre of the Bay and Il-Qarraba (6° to 8°) where the beach also becomes narrower. The width of the beach varies between 25 m at the northern side to 6 m close to Il-Qarraba. A central footpath stretches the whole length of the Bay, separating the upper clay slopes which extend up to the scarp face from the lower slopes at the back of the beach.

It is convenient to divide the Bay into two distinct parts, so that the landforms can be described in a more logical manner. The southern part of the Bay extends from the slopes joining Il-Qarraba to the mainland up to approximately the central part of the Bay characterised by maquis vegetation. The northern part extends from the maquis vegetation to the clay slopes under the demolished hotel close to the stairway leading to the beach (Figure 3.18).

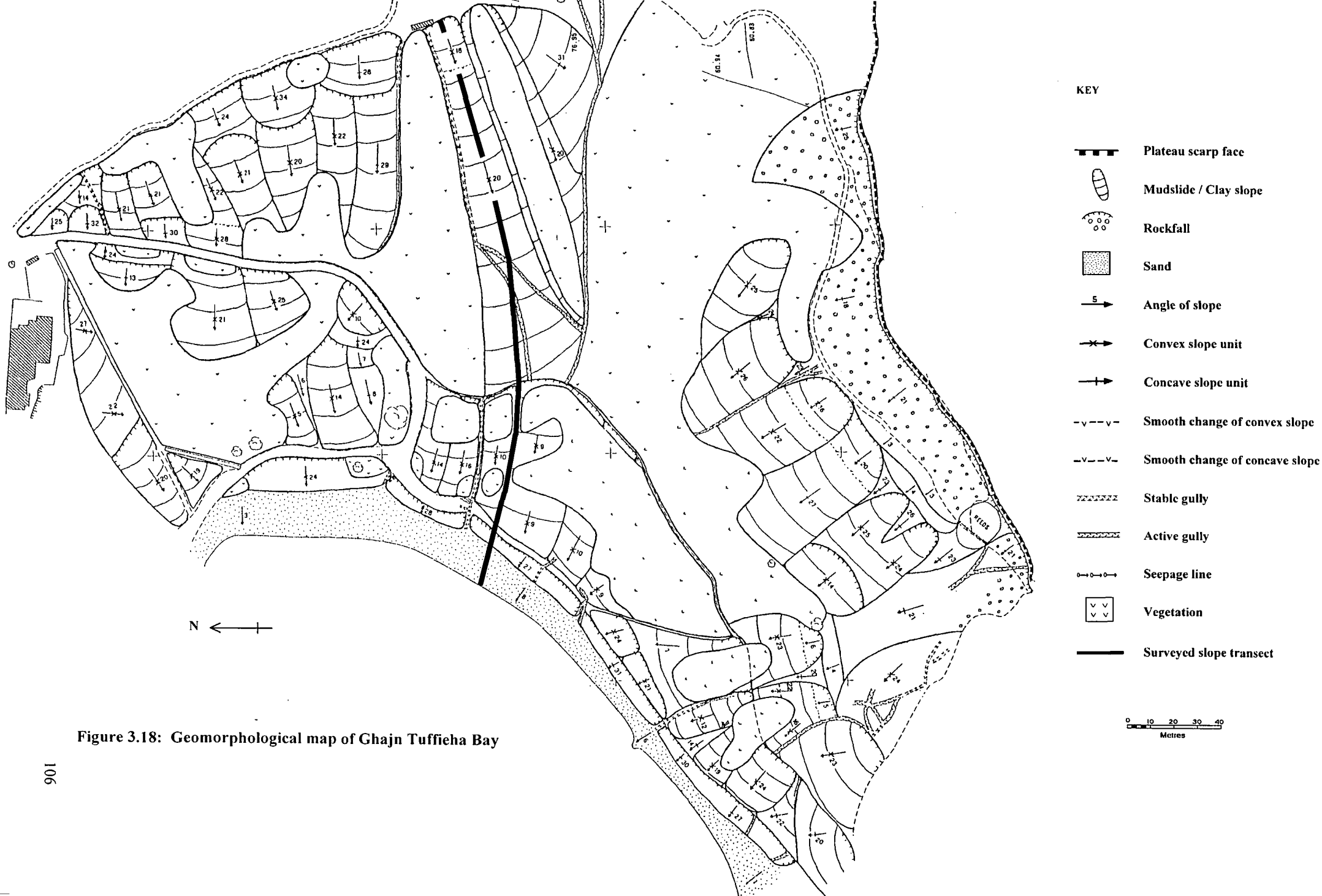


**Figure 3.18: Geomorphological map of Ghajn Tuffieha Bay**

The southern part of Ghajn Tuffieha Bay presents several features. Most of it, especially the central part and the slopes close to the central footpath are covered with maquis vegetation. The upper slopes above the footpath are mainly of a convex aspect with a gradient varying between 14° to 26°. The convex slopes have a smooth gradient change and are separated by concave slopes between 20° to 27° steep. Beneath the boulder scree, an area having a slight gradient of 3° to 4° is found in two levels. Close to the central footpath where the area is not covered by vegetation two slopes of a convex aspect (16° to 23°) are exposed. The slopes are characterised by a flat upper part (5° to 6°) and a smooth change of gradient. Towards the edge of the clay slopes overlooking Gnejna Bay and linking Il-Qarraba to the mainland, the topography is dominated by convex slopes (23° to 24°) and a concave slope (21°) at the foot of which is a flat area with a gentle gradient of 4° (Figure 3.18).

At the southern part of Ghajn Tuffieha Bay, the beach is backed by clay slopes which extend to the central footpath. Two levels of slopes can be distinguished. Those stretching from the central footpath to the lower footpath and those extending from the lower footpath to the beach. The former are mainly convex in morphology (9° to 10°) which steepen towards Il-Qarraba (12° to 24°). Two concave slopes (20° to 22°) are situated at the southernmost edge of the Bay, overlooking Gnejna Bay. A large area is covered by maquis vegetation. This is bordered at its southern side by an area having a gentle gradient of 7° with a rectilinear aspect. The second level of slopes is characterised by steep concave slopes (27° to 31°) which descend directly on to the sandy beach. The change in slope gradient between the two levels is angular (Figure 3.18).

The northern part of Ghajn Tuffieha Bay is also covered to a significant extent by vegetation. Slopes are mainly convex with a gradient ranging from 14° to 34° below Il-Hotba l-Bajda. Concave slopes are found adjacent to convex slopes and close to the central footpath. Their gradient varies from 24° to 32°. A concave slope (31°) below Il-Hotba l-Bajda extends to the maquis vegetation in the central part of the Bay. The two adjacent slopes are covered with maquis vegetation which extends along their whole length to the footpath (Figure 3.18).

Below the footpath, a large area is covered with maquis vegetation. The rest is mainly made up of convex slopes (5° to 25°). Concave slopes are found in different

parts close to the vegetated areas. Their gradient varies from 6° to 24°. A flat area with a gentle gradient of 7° separates two concave slopes close to a vegetated area where the footpath bends towards the beach. The lower slopes at the back of the beach are convex (as opposed to those on the southern side) with a gradient varying between 24° to 28°. Below the demolished hotel clay slopes extend along the stairway leading to the beach. They have a convex aspect with a gradient between 19° to 27°. The steepest gradient is found below the demolished hotel (Figure 3.18).

In terms of mass movement processes, Ghajn Tuffieha Bay is influenced by mudslides and rockfall. As in the case of Gnejna Bay no mudslides were observed during the mapping exercise, although heavy rainfall may trigger this type of movement. Mudslides do occur in the Bay during the wet season, especially where the clay slopes are poorly vegetated. Where present, the maquis and steppe vegetation aid in stabilising the slopes, holding and binding the clay by the roots and preventing erosion or sliding. Mudflows can also take place especially after heavy rainfall events, characteristic of a semi-arid climate.

The other mass movement process present at Ghajn Tuffieha Bay is rockfall. It occurs at the base of the Upper Coralline Limestone plateau which extends into Gnejna Bay, covering a distance of 0.23 km (Figure 3.18). Boulders skirt the base of the plateau, extending to the top part of the clay slopes for a width ranging between 10 m (concave gradient of 21°) at the narrowest part close to the slopes facing Gnejna Bay to about 50 m (concave gradient of 25°) at its widest stretch where the rockfall extends to the limit of the maquis vegetation. Some boulders are also found at the extreme southern end of the Bay overlooking Gnejna Bay (Figure 3.18). On average the larger boulders are around 3 m to 4 m wide and 1.5 m to 3 m high. Smaller rock in the form of debris is also found as a result of the larger boulders being further broken down. There are several processes involved in the detachment of boulders from the Upper Coralline Limestone plateau. One of them is rainfall which penetrates lines of weakness such as joints or faults, widening the gaps, and breaking the rock which falls under its own weight due to gravity.

Desiccation cracks are evident on the slopes close to Gnejna Bay and close to the beach in the central part of Ghajn Tuffieha Bay. In the former case, the dimensions vary from 17 cm to 56 cm in depth and 8 cm to 9 cm in width. In the latter case they

are about 35 cm deep and 5 cm wide. Opening of desiccation cracks occurs during dry periods as a result of volume change in clay soils. During wet periods deep cracks become filled with water. Besides developing high water pressures, water acts as an additional force to soil movement downslope, triggering landslides (Selby, 1993).

A system of active and stable gullies controls the hydrological system of Ghajn Tuffieha Bay (Figure 3.18). Gullies are mainly found at the lateral sides of the clay slopes and are especially concentrated on the lower slopes backing the beach. Through the established gullies water is channelled and drains onto the sandy beach. The central part of the Bay and the area close to Il-Qarraba seem to be the sections where most of the drainage system flows as there is a concentration of active and stable gullies. In several instances the water channels change in their morphology. Usually at their upper part they are stable but change to active channels lower down the slope. The inverse situation can also be the case and is present at Ghajn Tuffieha Bay. The whole area, especially the central part of the Bay, seems to be well drained to support all the vegetation. Close to the patch of reeds, water is present and is indicated by a seepage line on Figure 3.18.

The size and dimensions of the gullies vary across the Bay. On the slopes overlooking Gnejna Bay the width of the gullies varies between 45 cm to 65 cm, whereas the depth is around 30 cm. Close to the central footpath the dimensions range from 20 cm to 40 cm in width and 20 cm to 55 cm in depth. The gullies at the back of the beach are of various sizes: 25 cm to 80 cm wide and 15 cm to 40 cm deep. At the northern side, above the central footpath, gullies are between 55 cm to 110 cm wide and 40 cm to 76 cm deep.

A transect was selected for further study after the mapping exercise was carried out. The transect extends from the base of Il-Hotba l-Bajda to the sandy beach at sea-level. The chosen slope is situated in the central part of Ghajn Tuffieha Bay below Il-Hotba l-Bajda above the central footpath (Figure 3.18). The particular slope was selected as it is located in the central part of the Bay and is a very distinct landform bounded on both sides by maquis vegetation. The horizontal distance from sea-level to Il-Hotba l-Bajda is 226.77 m and the vertical height above sea-level at the highest point (close to Il-Hotba l-Bajda) is 74.31 m. The data is given in Table 3.2 and Figure 3.19 is a

cross-section plan (scale 1: 1000) of the slope transect which was surveyed. Slope gradients varied from 3.90° for the sandy beach to 31.20° for the clay slopes at the back of the beach.

**Table 3.2: Surveying data for the selected slope transect at Ghajn Tuffieha Bay**

| *Point* | *Horizontal distance (metres)* | *Vertical height above sea-level (metres)* | *Slope gradient of segment between points (°)* |
|---|---|---|---|
| A | 0.00 | 1.51 | 3.90 |
| B | 8.94 | 2.12 | 5.29 |
| C | 16.28 | 2.80 | 31.20 |
| D | 23.76 | 7.33 | 6.33 |
| E | 33.32 | 8.39 | 15.48 |
| F | 45.85 | 11.86 | 10.85 |
| G | 56.28 | 13.86 | 6.34 |
| H | 74.82 | 15.92 | 13.01 |
| I | 81.70 | 17.51 | 15.84 |
| J | 90.69 | 20.06 | 16.64 |
| K | 102.23 | 23.51 | 24.24 |
| L | 111.38 | 27.63 | 26.51 |
| M | 119.62 | 31.74 | 20.41 |
| N | 130.69 | 35.86 | 18.53 |
| O | 141.97 | 39.64 | 16.10 |
| P | 152.19 | 42.59 | 23.27 |
| Q | 164.14 | 47.73 | 28.85 |
| R | 172.89 | 52.55 | 22.74 |
| S | 182.22 | 56.46 | 18.91 |
| T | 192.73 | 60.06 | 23.37 |
| U | 204.44 | 65.12 | 16.53 |
| V | 217.01 | 68.85 | 29.22 |
| W | 226.77 | 74.31 | - |

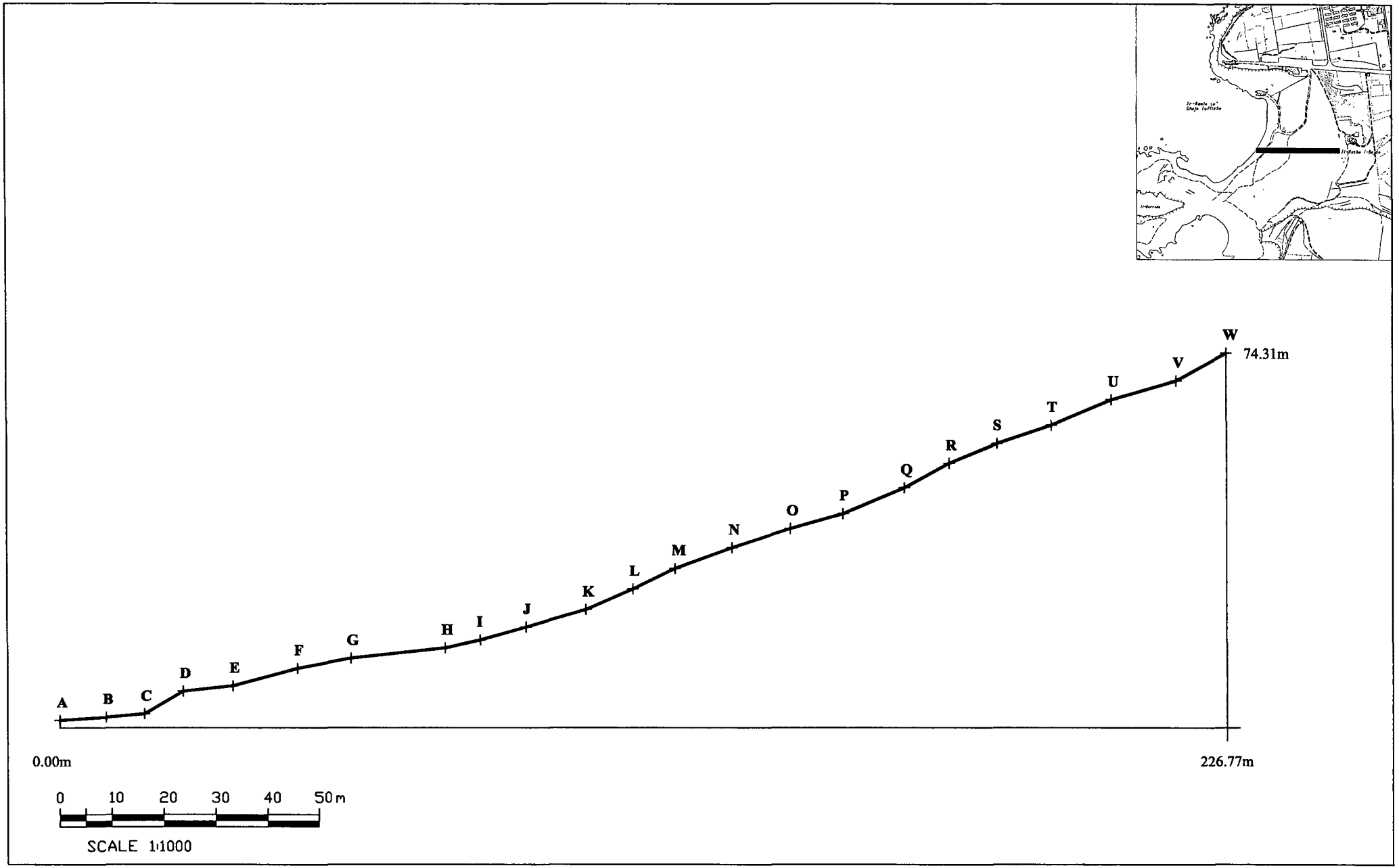




**Figure 3.19: Cross-section of slope profile at Ghajn Tuffieha Bay**

### 3.6.3 Rdum id-Delli

Rdum id-Delli is located on the north-west coast between Rdum Majesa and Il-Prajjet (Figure 3.15 and Plate 3.25). The geological formations present at Rdum id-Delli include the following.

i. Upper Coralline Limestone: this constitutes the plateau and is found in three members. Tal-Pitkal Member and Mtarfa Member compose the top layer and Ghajn Melel Member the basal layer. Greensand which is incorporated within the Ghajn Melel Member on the geological map of the Maltese Islands (scale 1: 25000) is exposed below the plateau and is mainly featured as boulders.
ii. Blue Clay: found extensively all over the area and displays slopes.
iii. Globigerina Limestone: Upper Globigerina Limestone skirts the littoral below the Blue Clay slopes and consists of a low cliff along the shore.

The area under study is delimited by a Quaternary solution subsidence structure on the southern side and an Upper Coralline Limestone plunging cliff (consisting of Tal-Pitkal Member) on the northern side. The etymology of Rdum id-Delli is probably derived from the term *dell* which in the Maltese language means shade. This is due to the fact that the area is sheltered and shaded. Steppic vegetation covers about 90 per cent of Rdum id-Delli. Esparto Grass (*Lygeum spartum*) is the dominant species on the clay slopes, whereas Golden Samphire (*Inula crithmoides*) and Mediterranean Thyme (*Coridothymus capitatus*) are found closer to sea-level. A small area (marked on Figure 3.20) is covered with tamarisk trees (*Tamarix africana*). Only the steep slopes close to the plunging cliff on the northern side are bare of vegetation.

The area under study (Figure 3.20) is about 0.54 km long and between 100 m to 200 m wide, reaching a maximum width of 220 m towards the central part. An Upper Coralline Limestone plateau stretches over a distance of 0.71 km at the top of Rdum id-Delli and is around 5 m high (close to the northern side) to about 10 m near the Quaternary solution subsidence structure. A small cliff below the Upper Coralline Limestone plateau at the northern side extends for 110 m and is about 2 m to 3 m high. Its top is flat with a slight angle of 2°. At the northern side the plateau changes into a plunging cliff which continues for a distance of about 1 km until it reaches Il-

**Plate 3.25: A side view of Rdum id-Delli. The steepest clay slopes are located close to the Upper Coralline Limestone plunging cliff on the left side. Mudslides are active in this section. Rockfall is found extensively throughout the entire area. The Upper Coralline Limestone plateau forms part of Mellieha Ridge. In the background Mellieha Bay is visible.**

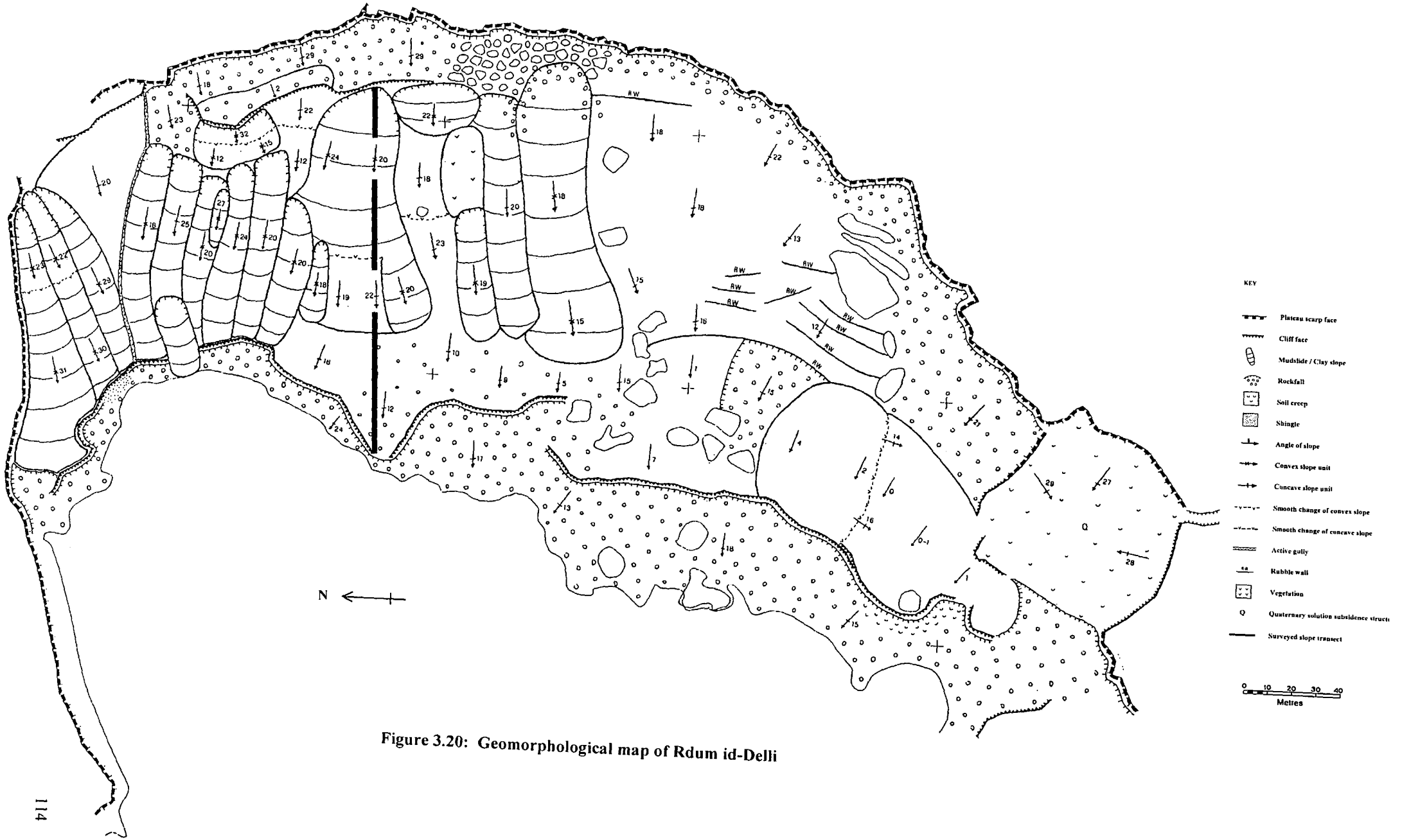


**Figure 3.20: Geomorphological map of Rdum id-Delli**

Prajjet. The height of this cliff line ranges from 23 m (Il-Prajjet) to 46 m (Rdum id-Delli). The plateau located above the steep clay slopes at the northern side of Rdum id-Delli has a notch between 2.2 m to 3.5 m high and 0.5 m to 1.7 m deep. A second cliff line skirted by boulder scree is found along the littoral and consists of the Upper Globigerina Limestone Member. This extends for 0.5 km and is about 5 m high at the northern side beneath the clay slopes and 2 m to 3 m high for the rest of the area. A small patch of shingle is found at the base of the Globigerina Limestone cliff, close to the plunging cliff. At the southern side, a Quaternary solution subsidence structure is found. This is marked by the letter Q on Figure 3.20. This is a very distinct feature and at its widest area it is about 950 m. The structure has a concave aspect with a gradient varying between 27° to 29°. It is flanked on two sides by boulder scree and at the base a flat area with a slight gradient of 0° to 1° is found. The other features which characterise Rdum id-Delli include Blue Clay slopes and boulder scree.

Rdum id-Delli can be divided into two distinct parts. The southern part extends from the Quaternary solution subsidence structure to the central part of the area. This is characterised by boulder scree and rockfall. The northern part extends from the plunging cliff to the central part of Rdum id-Delli and is characterised by clay slopes, although some scree is present (Figure 3.20).

At the northern side clay slopes are mainly of a convex aspect extending over a distance between 90 m to 120 m from the foot of the small cliff below the main plateau to the Globigerina Limestone cliff. The steepest slopes are situated close to the plunging cliff. Three main slopes can be identified, all having a convex aspect with a gradient varying between 22° to 23° at the top part changing smoothly (29° to 31°) at the lower part (Figure 3.20). The slopes are bare or have little vegetation cover (5 to 10 per cent). An area having a concave gradient of 20° separates the three slopes from a series of other slopes (60 m to 90 m long), all having a convex aspect and with a gentler gradient varying from 18° to 27°. The slopes are bare of vegetation cover at the sides and their lower part. Only one of the slopes has a concave aspect and a gradient of 25°. Small pieces of rock are found within the clay matrix. Above these slopes, a convex bulge below the cliff line has a gradient of 32° at the top part, which changes smoothly to 12° to 15° lower down. At its southern side a concave area is found. This has a gradient of 22° which changes smoothly to 12° (Figure 3.20).

The rest of the clay slopes are located in the central part of Rdum id-Delli and extend over a distance between 95 m to 120 m. These extend from the base of the cliff line or scree below the Upper Coralline Limestone plateau and do not reach the edge of the Globigerina Limestone cliff (Figure 3.20). At one particular slope both convex and concave aspects can be identified. The top part is convex with an angle between 20° to 24°. The lateral limits of the bottom part have a convex gradient between 18° and 20°, whereas the middle part is concave (19° to 22°). The slope extends from the cliff face to about 100 m downslope. A concave area with a gradient of 18° changes smoothly to 23°. At the top part of this concave area a convex slope of 22° is found. Three other slopes and an area of about 54 $m^2$ covered with maquis vegetation (mainly *Tamarix africana*) follow. Two slopes are convex (15° to 19°) separated by a concave slope with a gradient of 20°. The slopes at the central part of Rdum id-Delli are bordered by boulder scree, which extends to the Globigerina Limestone cliff. The topography in this area is concave and the gradient is gentle (5° to 10°) which steepens (12° to 16°) towards the clay slopes (Figure 3.20).

The southern part of Rdum id-Delli does not feature any clay slopes. An extensive area of a concave aspect is situated next to the central clay slopes (Figure 3.20). Its gradient is irregular and varies between 12° close to the rubble walls to 22° at its top part beneath the scree. The area is made up of Blue Clay but boulder scree is also present. A series of abandoned rubble walls are found at different levels. They usually indicate that agriculture used to be practised at Rdum id-Delli as their function is to delimit land and minimise erosion and sliding of clay or soil.

Below the concave area, the topography is generally flat with a gradient varying between 1° to 7° (Figure 3.20). The area is covered by large boulders between 3 m to 6 m high and 10 m to 15 m wide. Three very large blocks, 23 m to 30 m wide and 3 m to 6 m high, are located close to the abandoned rubble walls. A second flat area is found in two levels next to the former flat area. At the top level the gradient varies between 2° to 4° whereas the lower part has a slight gradient between 0° to 1° (Figure 3.20). The two levels are separated by a concave slope with a smooth change between 14° to 16°. Boulders and scree are not present in this part. The rest of the southern part is mainly composed of rockfall in the form of individual boulders or scree. This is especially evident at the foot of the plateau, stretching to the northern

side of the subsidence structure (concave gradient of 21°) and below the rubble walls between the two flat areas (concave gradient of 15°).

The main geomorphological processes present at Rdum id-Delli include mudslides, rockfall and soil creep (Figure 3.20). Mudslides are active during the winter season when clay becomes wet and the pore water pressure increases causing the clay to fail. At Rdum id-Delli sliding is evident at the northern part, where it has caused clay to move downslope at one particular area. The clay has moved down onto the Globigerina Limestone cliff beneath, extending to the shoreline below (Figure 3.20). The mudslide has resulted in an upper concave slope where the sliding occurred, having a gradient of 25°. The slope which has moved is inaccessible and its gradient could not be recorded. Sliding is active in other areas as well, incorporating rockfall and other debris. Where steppic vegetation is present, the slopes appear to be more stable and sliding is less evident.

The other process which is widespread all over Rdum id-Delli is rockfall. Apart from rainfall penetrating lines of weakness, rockfall can result from instability caused by basal undermining of Blue Clay and from tectonic activity. Boulder scree is present along the base of the Upper Coralline Limestone plateau, the Globigerina Limestone cliff at the shoreline and at the central part of Rdum id-Delli (Figure 3.20).

At the northern side of Rdum id-Delli, Greensand is exposed below the Upper Coralline Limestone at the base of the plateau. Blocks of Greensand have been detached and form a scree leading towards the clay slopes below. The gradient of the concave slope formed by the scree is 23° (Figure 3.20). It is important to note that the Greensand scree, which consists of boulders less than 1 m to 2 m wide and high, are incorporated within the clay matrix. The base of the plateau is skirted by boulders, mainly belonging to Upper Coralline Limestone (Tal-Pitkal Member) which vary in dimensions between 1 m to 2 m in width and height. The gradient varies between 18° and 29° and the aspect is concave.

The southern part is also characterised by rockfall and scree. The concave area comprises scree integrated within the clay matrix. At the base and sides of this area, large blocks have been detached from the plateau. They vary in dimensions - 10 m to

15 m wide and 3 m to 6 m high. Three very large blocks, 23 m to 30 m wide and 3 m to 6 m high, are found above the abandoned rubble walls close to the scarp face (Figure 3.20). Boulder scree stretches up to the Quaternary solution subsidence structure and at the area below the rubble walls where the gradient is 15° and 21° respectively and the aspect is concave in both parts. The dimensions of the scree blocks situated below the plateau are about 2 m in width and height. The debris found at the foot of the subsidence structure is of 1 m or less both in width and height. Part of the boulder scree is made up of Greensand and extends from the northern side of the subsidence structure to sea-level.

Boulders border the shoreline covering in some parts the Globigerina Limestone cliff (Figure 3.20). This is especially evident at the southern part. Blocks do not vary much in size and are about 2 m to 5 m wide and high. Some larger blocks 10 m to 18 m wide and 3 m to 5 m high are found at the southern part. The gradient all along the coast is concave and varies from 13° (central part) to 15° (southern part) and 24° (northern part) close to where the Globigerina Limestone cliff is exposed as a vertical wall. All along the shore boulders are composed of Upper Coralline Limestone, except close to the cliff, where they consist of Globigerina Limestone.

Soil creep is the third process observed at Rdum id-Delli. It occurs at very slow rates and is especially active where weakly competent materials such as clays are overlain by more competent beds such as limestone. This is the case in the Maltese Islands where Blue Clay is overlain by Upper Coralline Limestone. Soil creep is especially evident within the Quaternary solution subsidence structure. The structure features a karstic hollow depression characterised by bare patches of soil and steppic vegetation. At its northern side it is bounded by a small Upper Coralline Limestone cliff (about 2 m to 3 m high) which is a continuation of the plateau. The process is also evident among the scree bordering the shoreline at the southern side of Rdum id-Delli (Figure 3.20).

Desiccation cracks being the result of volume change in the clay are present at various parts at Rdum id-Delli. At the lateral sides of the clay slopes close to the plunging cliff the dimensions vary from 3 cm to 6 cm in width and 11 cm to 25 cm in depth. Close to the Greensand scree at the northern side, desiccation cracks vary from 5 cm

to 11 cm in width and 9 cm to 45 cm in depth. On the slopes located near to the tamarisk trees, desiccation cracks range from 6 cm to 7 cm wide and 20 cm to 36 cm deep. At the central part of Rdum id-Delli, the sizes vary from 6 cm to 12 cm in width and 18 cm to 58 cm in depth. On the flat area, where the large blocks are situated, desiccation cracks are about 4 cm wide and 22 cm to 28 cm deep.

The hydrological system at Rdum id-Delli does not seem to be well established. Gullies are largely absent and only one active gully extending from the Greensand scree downslope to the Globigerina Limestone cliff can be identified (Figure 3.20). This gully is about 41 cm wide and 20 cm deep. One reason for the absence of gullies can be related to the physical properties of Blue Clay. From laboratory testing (refer to chapter 4) it resulted that Blue Clay at Rdum id-Delli has a high percentage of clay content (61%). Clay being an impermeable material can absorb a significant amount of water allowing for small quantities to flow as surface water and preventing channels or gullies from developing.

Surveying of a slope transect was performed at Rdum id-Delli. The selected transect is situated at the northern side, extending from the cliff line below the main plateau to the edge of the Globigerina Limestone cliff (Figure 3.20). The transect was chosen as it is easily identifiable. The overall horizontal distance from the base of the Upper Coralline Limestone cliff to the edge of the Globigerina Limestone cliff is 118.35 m and the highest point above sea-level at the foot of the Upper Coralline Limestone cliff is 44.81 m. Data is presented in Table 3.3 and Figure 3.21 features a cross-section plan (scale 1: 500) of the selected transect. Slope gradients vary from 13.79° above the Globigerina Limestone cliff to 33.57° further up the slope close to the Upper Coralline Limestone cliff.

**Table 3.3: Surveying data for the selected slope transect at Rdum id-Delli**

| *Point* | *Horizontal distance (metres)* | *Vertical height above sea-level (metres)* | *Slope gradient of segment between points (°)* |
|---|---|---|---|
| A | 0.00 | 0.53 | 13.79 |
| B | 17.27 | 4.77 | 14.40 |
| C | 34.13 | 9.10 | 20.94 |
| D | 49.81 | 15.10 | 26.70 |
| E | 61.92 | 21.19 | 22.57 |
| F | 66.01 | 22.89 | 16.93 |
| G | 77.77 | 26.47 | 25.98 |
| H | 86.08 | 30.52 | 23.61 |
| I | 96.17 | 34.93 | 18.13 |
| J | 102.86 | 37.12 | 33.57 |
| K | 107.26 | 40.04 | 21.29 |
| L | 115.42 | 43.22 | 28.48 |
| M | 118.35 | 44.81 | - |

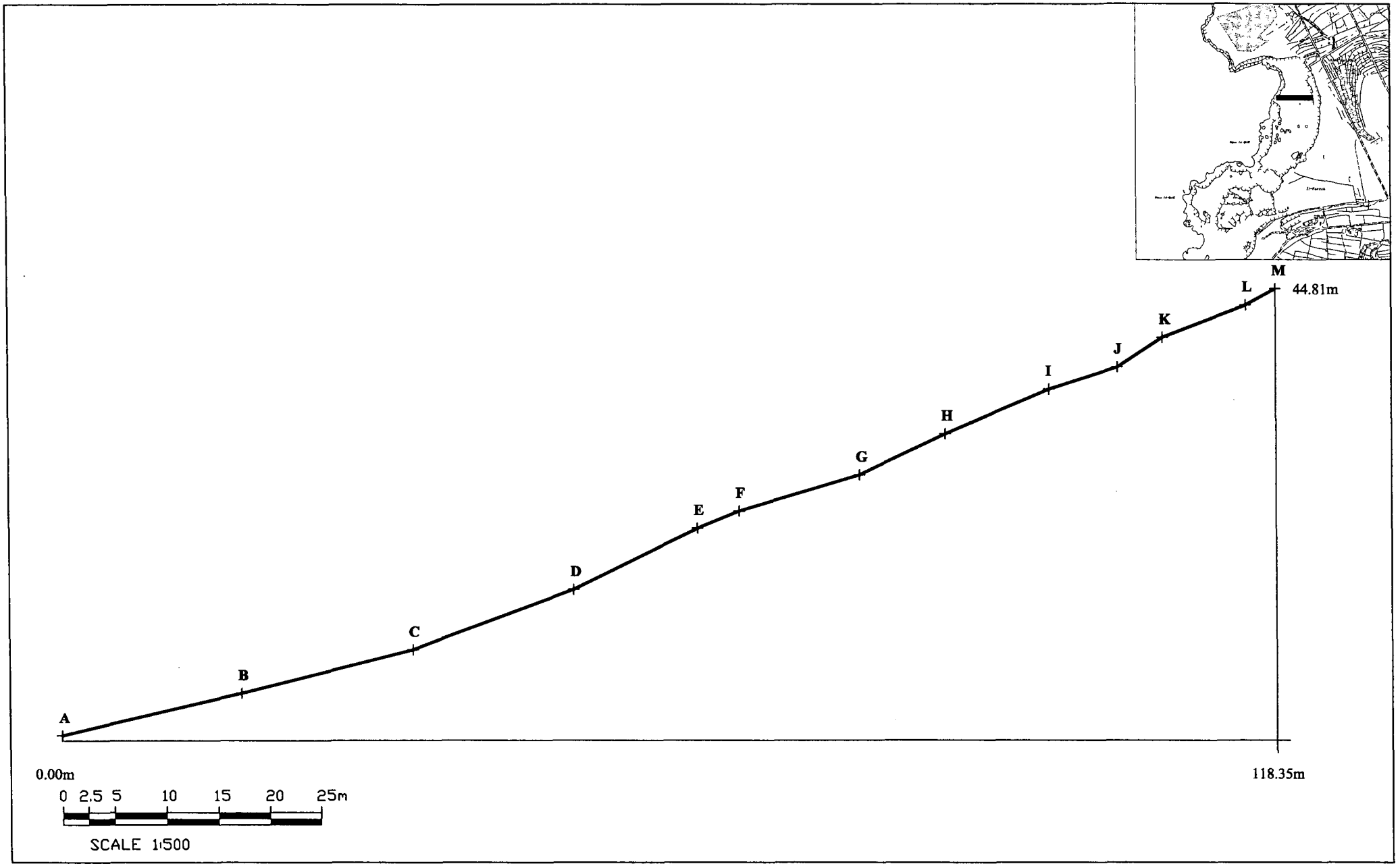


**Figure 3.21: Cross-section of slope profile at Rdum id- Delli**

## 3.7 Conclusion

This chapter discussed the geomorphology of the Maltese Islands with special reference to the coastal geomorphology. The geomorphological mapping carried out at different scales for the coast of Malta, north of the Great Fault, provides the necessary background information in relation to coastal landforms and mass movement processes occurring within this region. This is essential in order to proceed with the other two main objectives of the study, that is examine the behaviour of Blue Clay, in terms of its physical and geotechnical properties, and determine the factors which lead to coastal cliff instability within a local context. These two elements are addressed in chapters 4 and 5 which deal with laboratory testing of clay samples and computer modelling of slope instability respectively. An attempt is thus made to assess mass movement processes and the associated triggering factors within the Blue Clay Formation for the coastal zone, which ultimately can be applied to other areas where the formation is present.

# *Chapter 4*

# *Investigation of the physical and geotechnical properties of Blue Clay*

## 4.1 Introduction

During the last three decades (for example Yatsu, 1966; Whalley, 1976; Selby, 1982 *in* Hart, 1986) a new approach was introduced in the study of geomorphology. A need was felt to understand the mechanics and behaviour of soils and rocks in order to explain geomorphological processes and landform development. The study of materials and their properties was incorporated within the scope of geomorphology as it links together process and form. This is also confirmed by Goudie *et al.* (1990: 111) who claim that:

> *"Geomorphological explanations are incomplete unless they involve some understanding of the way in which the materials that cover the face of the Earth behave and have behaved."*

A description of the basic properties of geomorphological materials is frequently the most important starting point for an explanation of a geomorphological process. Knowledge of the properties can suggest productive lines of experimentation in field or laboratory and may be required in computer simulations or more intensive enquiries, such as in soil mechanical testing (Goudie *et al.*, 1990).

The physical properties of soils are strongly influenced by their mineralogy, texture, and fabric (Selby, 1993). The properties are not constant over time, with water-content and void space capable of changing very quickly and other properties changing more slowly. Nor are properties constant in space with major variations in structure, fabric, and mineralogy being identifiable over distances of a few metres (Beckett and Webster, 1971; Culling, 1986 *in* Selby, 1993). A knowledge of soil physical properties is an important foundation for the classification of soils and a major component of any capacity to predict the behaviour of soils in response to applied stresses and variations in water content. Soil mechanical properties are an expression of the materials which make up the soil and of the water and air temperature changes within them (Pitty, 1979).

Soils, in the geotechnical sense, can be regarded as engineering materials (Head, 1980). Their physical characteristics can be determined either in the field or in the

laboratory and the application of methods of analysis enables the properties to be used to predict likely material behaviour. Many of the procedures used for determining soil characteristics consist of empirical methods derived from practical experience.

The physical properties of soils are usually determined by carrying out tests on samples in a laboratory. The tests can be divided into two main categories (Head, 1980).

i. Classification tests, which indicate the general type of soil and the engineering category to which it belongs.
ii. Tests for the assessment of engineering properties, such as shear strength, compressibility and permeability.

Most present-day laboratory tests employed in soil mechanics are highly developed and perfected. It is necessary to recognise the relation between samples and subsequent testing. Much skill, experience and time may have been used by the site investigation team in obtaining the samples from the site under construction. It is therefore important that the method of sampling, exact location with respect to plan and elevation, date of sampling and all other relevant information are correctly recorded. As far as the samples are concerned, the main requirement is that they are representative of the mass of the strata from which they have been taken. This involves decisions about the size of sample, the method of sampling and the location of sampling (Vickers, 1978).

Undisturbed samples can be obtained either by employing some type of sampler, usually incorporating the use of a sample tube, or by taking the sample from the face of an excavation such as a trial pit and immediately covering it with a protective, impervious layer of wax (Vickers, 1978). Ideally, samples should be tested within a short time of arrival at the laboratory. This is because it has become evident that satisfactory storage of soil samples, maintaining natural moisture content and other properties, is difficult (Vickers, 1978). In addition, early results obtained from testing the initial samples received from a site may well indicate that more samples or larger samples need to be taken, so that a revised programme and procedure for the sampling becomes necessary. Inevitably some storage is needed and may even be essential if

further studies are to be undertaken. Consequently facilities for storage should be adequate in terms of space and of temperature and humidity control (Vickers, 1978).

## 4.2 Research design

### 4.2.1 Choice of sites

Geomorphological mapping (scale 1: 10000) for the northern coast of Malta (Figures 3.5 and 3.6) was used to identify three sites to be representative of the whole region where Blue Clay samples could be collected to conduct detailed laboratory investigations. The three selected sites are Gnejna Bay, Ghajn Tuffieha Bay and Rdum id-Delli, all situated on the north-west coast of Malta (Figure 3.15). At each of the three sites, the geology consists of Blue Clay slopes backed by an Upper Coralline Limestone plateau. The sites were chosen as Blue Clay is widely exposed displaying itself as coastal slopes marked with numerous landslides, that have the dominant control on cliff development at these locations.

Further geomorphological mapping at a larger scale (1: 2000) was performed at each of the selected coastal site, to identify a specific clay slope for surveying and sample collection. Each slope was chosen as it extends over a long distance at each locality. Another criterion taken into consideration when choosing the slope was that the lateral shears could be identified, this clearly defining the feature. Cross-section plans of the three transects are represented in Figures 3.17, 3.19 and 3.21. The surveyed slope transects are marked on Figures 3.16, 3.18 and 3.20 and in the insets of Figures 3.17, 3.19 and 3.21.

The selected clay slopes at each of the three sites were surveyed using a Leica TC600 total station laser level. Data collected includes height above sea-level and horizontal distance. Slope gradients were calculated using the tangent computation. The data is used to perform a stability analysis described in chapter 5. Sections 3.5 and 3.6 in chapter 3 explain in more detail the geomorphological mapping carried out for the northern coast and investigation of the three coastal field sites including the mapping and surveying exercises.

### 4.2.2 Collection of samples

Undisturbed samples were collected about two-thirds of the way up the slope from sea-level at Gnejna Bay and Rdum id-Delli and about 30 metres downslope from the plateau base at Ghajn Tuffieha Bay. The locations were chosen on the basis of little vegetation cover and minimum disturbance. An attempt was made to ensure that at each site the samples collected were representative of the Blue Clay material. Since Blue Clay is largely a uniform material, problems were minimised and the material which was collected and tested possessed characteristic physical and geotechnical properties.

Samples were collected by digging into the clay slope to a depth of about 50 cm. Blocks of clay were cut and care was taken to keep the blocks intact. The samples were covered with plastic film and aluminium foil to avoid loss of moisture during transportation, storage and preparation. The samples were then put in plastic boxes (20.5 cm long, 11.0 cm wide and 15.0 cm high) and taken to the laboratory for physical and geotechnical testing. The use of paraffin wax was not necessary as tests were carried out immediately after the samples were collected, to eliminate the problem of loss of moisture.

The trial pit method was first utilised to collect samples. A rectangular block of material (approximately 1 $m^3$) was left in the middle of the pit and five samples (25 cm x 25 cm) were cut with a saw in a vertical profile from the block. The samples were covered with plastic film, put in tin boxes and taken to the laboratory where tests were conducted afterwards. Some of the results proved to be unsatisfactory and clay samples had to be collected and tested for the second time. The reason for this is that the properties of Blue Clay change with depth - the upper horizons are drier as moisture is lost more easily than at the lower horizons. Using the trial pit technique samples were collected in a vertical profile at different depths and tests were undertaken on clay with properties which were not homogeneous. Thus a comparative analysis of the results could not be performed.

### 4.2.3 Laboratory testing and analysis

An important aspect of this study is the testing and analysis of the physical and geotechnical behaviour of Blue Clay utilising samples collected at Gnejna Bay, Ghajn Tuffieha Bay and Rdum id-Delli. To date no recorded information on the physical and geotechnical properties of Blue Clay in Malta exists. The tests conducted in the laboratory examine both the physical and geotechnical aspects of Blue Clay at each of the three investigation sites. The field moisture content, bulk density and bulk unit weight, particle size distribution and Atterberg Limits were calculated to determine the physical properties of Blue Clay. Direct shear tests on undrained samples were carried out to examine the geotechnical properties of stress, strain and shear so that ultimately material strength could be determined. During laboratory testing established techniques and procedures (BS 1377, 1990; Head, 1980) were followed. The tests were chosen as they are appropriate for soft rocks or soils. Clays are classified as soils and the above include the standard tests carried out on such material. Tests for each of the three sites were performed more than once and the average calculated to obtain accurate results. At each locality physical tests and geotechnical tests were performed from samples collected at the same depth, time and date so that both sets of tests could be correlated. The results provide an indication of coastal slope stability for north-west Malta. The physical properties tests are first considered in section 4.3, followed by an analysis of the geotechnical tests in section 4.4.

## *4.3 Physical properties tests of Blue Clay*

The moisture content, soil density, particle size distribution and Atterberg Limits were performed from samples collected at Gnejna Bay, Ghajn Tuffieha Bay and Rdum id-Delli. Each of the tests will be dealt separately and the laboratory data incorporated and analysed within the relevant technique. Analysis of data is related to the issue of coastal slope instability for northern Malta, using the sample collection sites as key investigation sites representative of the northern region.

### 4.3.1 Moisture Content

Apart from soils in dry desert areas, the voids within all natural soils contain water (Barnes, 1995). Some soils may be fully saturated with the voids full of water, some only partially saturated with a proportion of the voids containing air as well as water. Moisture content or water content is simply the ratio of the mass of water to the mass of solid particles and is an invaluable indicator of the state of the soil and its behaviour.

The moisture content of a soil applies to all types of soil and is the most frequently determined characteristic (Head, 1980). In clay soils an increase in the water content is accompanied by swelling resulting in a change in volume (Rosenak, 1963). The parameter has a fundamental influence on the geotechnical characteristics of the material. Measurement of the moisture content can provide an extremely useful method of classifying cohesive soils and of assessing their engineering properties (Head, 1980) such as strength and the state of the material varying from liquid, plastic, semi-solid or solid states (Vickers, 1978). An inverse relationship exists between the strength of a soil and its water content. An increase in the water content will reduce the shear strength and hence its bearing capacity (Rosenak, 1963). This also applies in the opposite way. A decrease in water content contributes to an increase in shear strength. Even a small change in the water content can affect soil strength (Rahn, 1996). This is indicated by mechanical tests performed on Blue Clay samples. Ghajn Tuffieha Bay, which has the highest moisture content, has the lowest cohesion value, indicating a low shear strength. Gnejna Bay and Rdum id-Delli have a lower moisture content and higher cohesion values, implying an increase in the material strength at these two sites.

The moisture content was determined for Blue Clay samples and the results are presented in Table 4.1. Three tests were performed for each of the sample collection sites and the average result calculated. The weight of the samples was determined before and after the samples were put in the oven. The difference in weight was calculated as the percentage of the moisture content present within the whole sample. The results for Gnejna Bay and Rdum id-Delli are very similar. Samples from Gnejna Bay have an average moisture content value of 24.17% whereas for Rdum id-Delli

this is 26.80%. The moisture content at Ghajn Tuffieha Bay is higher, reaching an average value of 41.45% indicating a factor increase of 1.7 for Gnejna Bay and 1.5 for Rdum id-Delli.

**Table 4.1: Results for Moisture Content tests**

| | *Gnejna Bay* | *Ghajn Tuffieha Bay* | *Rdum id-Delli* |
|---|---|---|---|
| Test 1 | 24.14% | 42.00% | 26.35% |
| Test 2 | 23.47% | 40.65% | 27.45% |
| Test 3 | 24.91% | 41.69% | 26.61% |
| **Average** | **24.17%** | **41.45%** | **26.80%** |

The moisture content is often compared with the Liquid Limit and Plastic Limit test results (Barnes, 1995). Changes in the moisture content influence the index properties and give an indication of how the clay will behave in the field. This is due to the fact that the Atterberg Limits can also be considered as moisture content tests. Comparison of the results derived from moisture content and Atterberg Limits tests on Blue Clay is presented in section 4.3.4.

### 4.3.2 Bulk Density

Soil has three phases: solid, water, and air and is used to relate mass to volume (West, 1995). The total volume of the soil material is expressed as the sum of the volume of these components. The total mass is the sum of the mass of solid particles and mass of water (Selby, 1993).

Density is the mass of a material (mass of solid particles and water) in a unit volume. *In situ* density of soil at depth depends to a large degree on the weight of the overlying soil (Rahn, 1996). Bulk density is the total mass of soil (solid particles, water and air) in a given volume. Dry density is the mass of just the solid particles in a given volume (Barnes, 1995) after the soil is dried at 105°C. The bulk unit weight is

the weight of the soil in a unit volume. Unit weight of a soil and its natural moisture content are the simplest and most commonly used indicators of the state of the material and of its characteristic strength and other properties.

Bulk density is one of the main characteristics which describe the relative proportions of solid and void in a soil. Its expression in any one soil is related to texture. There is a tendency for bulk density to increase as texture becomes coarser (Pitty, 1979). This is indicated in Table 4.2, which presents typical values for bulk density and bulk unit weight for different soil types. Sand and gravel which have a coarse texture, obtain higher bulk densities than silt and clay which contain finer particles. Bulk density increases with compaction occurring primarily at the expense of the largest pores when the soil is compressed by an external load, as this is the zone in which the soil has the least mechanical stability (Pitty, 1979). This is the case of stiff clay and hard rock which have higher bulk densities than soft clay and weak rock due to a more compact structure (Table 4.2).

**Table 4.2: Typical bulk densities for different soil types**

| *Soil type* | *Bulk density* $g/cm^3$ | *Unit weight* $KN/m^3$ |
|---|---|---|
| Peat | 1.0 - 1.4 | 10 - 14 |
| Sand and gravel | 1.6 - 2.2 | 16 - 22 |
| Silt | 1.6 - 2.0 | 16 - 20 |
| Soft clay | 1.7 - 2.0 | 17 - 20 |
| Stiff clay | 1.9 - 2.3 | 19 - 23 |
| Weak rock (mudstone, shale) | 2.0 - 2.3 | 20 - 23 |
| Hard rock (Granite, Limestone) | 2.4 - 2.7 | 24 - 27 |

Source: Modified from Barnes, 1995

To determine the density of soil it is necessary to measure the volume and mass of the sample being tested. The simplest procedure is to use volumes of regular shapes. This approach is only suitable for soils of a cohesive nature and which are little affected by sample collection and preparation. Where it is difficult to trim a sample to a regular shape, determination of the volume by simple linear measurement is not practicable.

In this case two methods can be employed: water displacement and weighing in water. The latter technique makes use of the principle of Archimedes for the measurement of volume and is more accurate than the water displacement method. The weighing in water method was utilised to determine the volume of Blue Clay samples since it was difficult to cut the samples in regular shapes. The bulk density was then calculated for each sample tested.

The bulk density and bulk unit weight were determined for Gnejna Bay, Ghajn Tuffieha Bay and Rdum id-Delli. Three tests were performed for each site and the average value calculated for both the bulk density and bulk unit weight. Results are presented in Table 4.3. As in the case of the moisture content results, Gnejna Bay and Rdum id-Delli have very similar values. The average bulk density is 1.79 g/cm$^3$ for both sites and the average bulk unit weight is 17.59 KN/m$^3$ for Gnejna Bay and 17.53 KN/m$^3$ for Rdum id-Delli. Ghajn Tuffieha Bay has lower values for the average bulk density (1.70 g/cm$^3$) and the average bulk unit weight (16.71 KN/m$^3$) due to a high proportion of silt found within the Blue Clay material (Table 4.4). These slight differences are sufficient to change the performance of the material. By referring to the data presented in Table 4.2, Blue Clay can be classified as a soft clay with typical bulk density values between 1.7 g/cm$^3$ and 2.0 g/cm$^3$ and bulk unit weight between 17 KN/m$^3$ and 20 KN/m$^3$.

Bulk density declines at increased moisture contents. This results from the expansion of mineral particles when colloids swell and from the vertical movement of the soil if the moisture freezes (Pitty, 1979). As a soil dries out, the bulk density increases and even the loss of small amount of water may increase significantly the strength or cohesion of soils (Pitty, 1979). This is relevant for Ghajn Tuffieha Bay where a lower bulk density exhibits a higher moisture content, indicating that there is greater percolation and higher water retention capacities. At this site there is the chance of an increased mudslide activity when compared with the other two sites. Development of desiccation cracks especially at Gnejna Bay and Rdum id-Delli indicate drier conditions, slower rates of movement and higher bulk densities.

## Table 4.3: Results for Bulk Density and Bulk Unit Weight

| | *Gnejna Bay* | | *Ghajn Tuffieha Bay* | | *Rdum id-Delli* | |
|---|---|---|---|---|---|---|
| | ***Bulk Density*** $g/cm^3$ | ***Bulk Unit Weight*** $KN/m^3$ | ***Bulk Density*** $g/cm^3$ | ***Bulk Unit Weight*** $KN/m^3$ | ***Bulk Density*** $g/cm^3$ | ***Bulk Unit Weight*** $KN/m^3$ |
| Test 1 | 1.77 | 17.36 | 1.72 | 16.87 | 1.80 | 17.66 |
| Test 2 | 1.80 | 17.66 | 1.68 | 16.48 | 1.76 | 17.27 |
| Test 3 | 1.81 | 17.76 | 1.71 | 16.78 | 1.80 | 17.66 |
| **Average** | **1.79** | **17.59** | **1.70** | **16.71** | **1.79** | **17.53** |

Bulk density also gives an indication of the load bearing capacity of the material which is relevant to slope stability. A decrease in bulk density may be associated with an increase in movement which might be the case at Ghajn Tuffieha Bay. However mudslides are evident at Rdum id-Delli, although the bulk density is higher than that of Ghajn Tuffieha Bay. From field investigation both Gnejna Bay and Ghajn Tuffieha Bay seem to be quite stable, with no apparent sliding taking place.

### 4.3.3 Particle Size Distribution

Particle sizes vary considerably, from those measured in microns (clays) to those measured in metres (boulders). Most natural soils are composite soils, mixtures of particles of different sizes which together with minerals influence properties of soil such as strength, behaviour under stress, void space, permeability, capacity to retain water, and chemical reactivity. The relative proportions of gravel, sand, silt, and clay define the texture of the soil, whereas the fabric or structure of the soil is determined by the patterns in which the particles are arranged (Selby, 1993). The distribution of the particle sizes gives very useful information about the engineering behaviour of the soil and is determined by separating the particles using two processes – sieving and sedimentation (Barnes, 1995). Sedimentation is based on Stokes' Law, which states that a smooth spherical particle suspended in a fluid (water and dispersant solution) will settle under gravity at a velocity.

Particle size distribution, together with Atterberg Limits can be considered as classification tests. The aim of soil classification is to divide soils into groups with similar characteristics by which they can be identified and which exhibit similar behaviour in engineering situations (Craig, 1978). Several classifications of particle size are in use (Figure 4.1); most use the same boundary between clay and silt (2 μm = 0.002 mm) and between sand and gravel (2000 μm = 2 mm). The chosen boundaries between silt and sand, and within silt and sand, are varied. It is therefore necessary to specify the system being used (Selby, 1993).

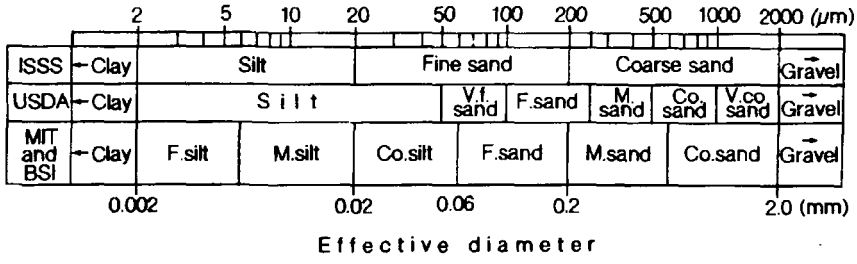


**Figure 4.1 The most commonly used classifications of soil particle sizes**
**ISSS - International Society of Soil Science**
**USDA – United States Department of Agriculture**
**MIT - Massachusetts Institute of Technology**
**BSI - British Standards Institute**
**F. – fine, M. – medium, Co. – coarse, V. - very**

Source: Selby, 1993

Particle size distribution analysis is an important index test for soils as it presents the relative proportions of different sizes of particles and the amount of clay present (Head, 1980). This test helps to identify the type of soil and to a limited extent which particle size ranges are likely to control the engineering properties. The clay fraction, which refers to the proportion of material consisting of particles smaller than 0.002 mm, is often used as an index for correlating with other engineering properties, such as activity. Particle size distribution has a considerable influence on the mechanical and engineering properties of soils (Rosenak, 1963; Vickers, 1978), such as permeability and material strength, hence overall slope instability. A high sand content indicates an increase in friction, whereas a large clay proportion leads to greater cohesion within the soil.

The particle size distribution of soil particles is expressed by a plot of percentage passing, that is the percentage of mass smaller than the equivalent diameter, against particle size. The flatter the distribution curve the larger the range of particle sizes in the soil. The steeper the curve the smaller the range of particle sizes within the sample being tested (Craig, 1978). A well-graded soil is represented by a smooth, concave distribution curve. It is characterised by similar proportions of particles in any size range. A poorly-graded soil is characterised with a high proportion of particles having sizes within narrow limits. Also particles of both large and small sizes are present but with a relatively low proportion of intermediate size particles.

Particle size distribution was determined for Blue Clay samples collected at Gnejna Bay, Ghajn Tuffieha Bay and Rdum id-Delli. Both sieving and sedimentation techniques were used. Blue Clay samples were oven dried and broken to leave a disaggregated sample which passes the 2 mm sieve. Sieving was performed for particles larger than 63 μm, that is sand particles. Particles smaller than 63 μm were classified by sedimentation using the Hydrometer Analysis technique following the guidelines proposed by BS 1377 (1990) and Head (1980). Results are presented as semi-logarithmic particle size distribution curves for each of the three sites (Figures 4.2, 4.3 and 4.4). Table 4.4 presents the results as a percentage for each particle size category. These are reported to the nearest 1%.

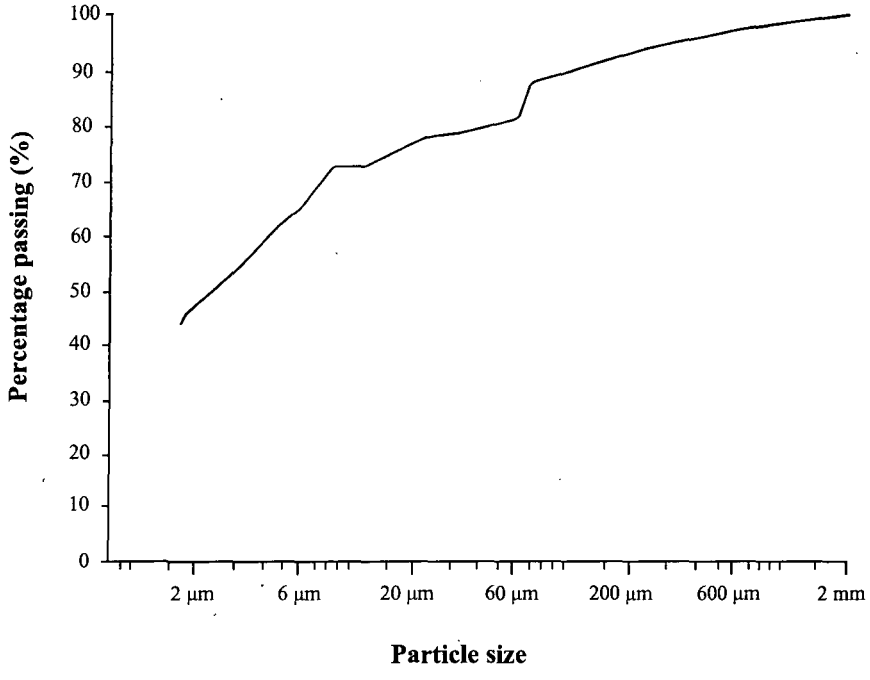


**Figure 4.2: Particle size distribution curve for Gnejna Bay**

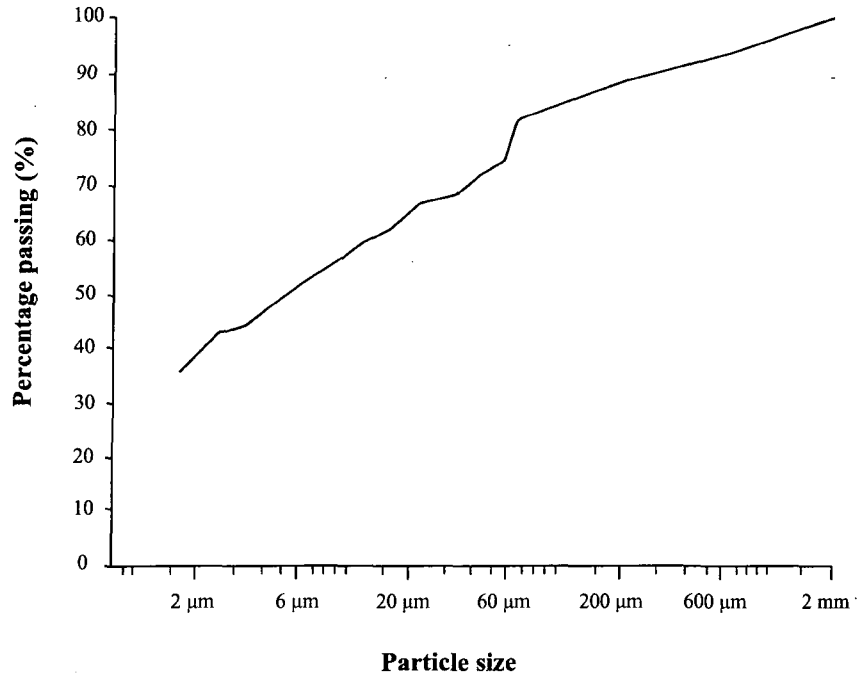


**Figure 4.3: Particle size distribution curve for Ghajn Tuffieha Bay**

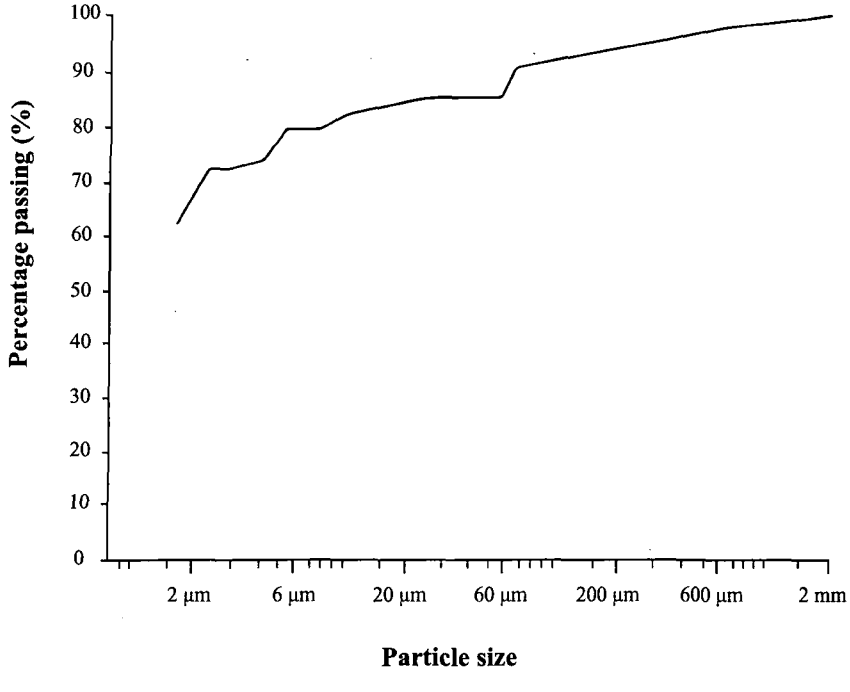


**Figure 4.4: Particle size distribution curve for Rdum id-Delli**

**Table 4.4: Results for Particle Size Distribution**

| *Particle size* | *Gnejna Bay* | *Ghajn Tuffieha Bay* | *Rdum id-Delli* |
|---|---|---|---|
| Clay (< 2 μm) | 44% | 35% | 61% |
| Silt (2 μm - 63 μm) | 44% | 46% | 29% |
| Sand (63 μm - 2 mm) | 12% | 19% | 10% |

The particle size distribution curves indicate clearly that Blue Clay is a cohesive soil due to the high clay content found within the material. The sand proportion is low and does not characterise the soil, whereas silt is found in significant proportions, especially at Ghajn Tuffieha Bay where it predominates. This fact needs further consideration as silt exhibits dilatancy (Head, 1980), which is an increase in volume during deformation leading to unstable conditions. Besides silt has little plasticity indicating that even a small change in moisture content will change the soil from a semi-solid to liquid condition. This is also confirmed by a low Plasticity Index for Ghajn Tuffieha Bay. Clay dries at a slower rate than silt. On drying clay shrinks and exhibits cracks which are more pronounced the higher the plasticity of the clay (Head, 1980). Desiccation cracks are more widespread at Gnejna Bay and Rdum id-Delli where Blue Clay has a higher clay content and higher Plasticity Index than at Ghajn Tuffieha Bay.

Particle size distribution tests also give an indication of the permeability of the soil and its material strength. Silt is more permeable than clay, whereas clay retains most of the water. However when the particle size distribution proportions are compared with the moisture content results, it is observed that the Blue Clay at Ghajn Tuffieha Bay has the highest moisture content although the soil is predominantly composed of silt particles. This can provide an indication that the clay minerals have a high swell capacity and are able to retain a significant amount of water content. Rdum id-Delli which has the highest clay content has also the highest values for the Liquid Limit and Plasticity Index but the lowest values for the Plastic Limit and Activity Index. These results imply a stable situation at Rdum id-Delli. The silt and clay proportions are of equal value for Blue Clay at Gnejna Bay. The values for the Plastic Limit, Plasticity Index and Activity Index lie between those of the other two sites. Moisture content is

lowest for this site indicating that conditions are stable but trending towards instability. From the index property results and particle size distribution curves it can be concluded that a higher silt content in the soil leads to higher moisture content and more unstable conditions. From geotechnical testing it has been observed that a low clay content contributes to a decrease in material strength. Ghajn Tuffieha Bay exhibits the lowest cohesion since the silt fraction predominates, increasing the rate of instability. Rdum id-Delli has the highest cohesion value and a high clay content, resulting in a more competent material and stable conditions.

### 4.3.4 Atterberg Limits

The Atterberg Limits and related indices have become very useful to determine different characteristics of soil material. The limits are based on the concept that a fine-grained soil can exist in any of four states depending on its water content. Thus a soil is solid when dry, and upon the addition of water proceeds through the semi-solid, plastic, and finally liquid states (Figure 4.5). The water contents at the boundaries between adjacent states are termed the Shrinkage Limit (SL), Plastic Limit (PL), and Liquid Limit (LL) (Lambe and Whitman, 1979).

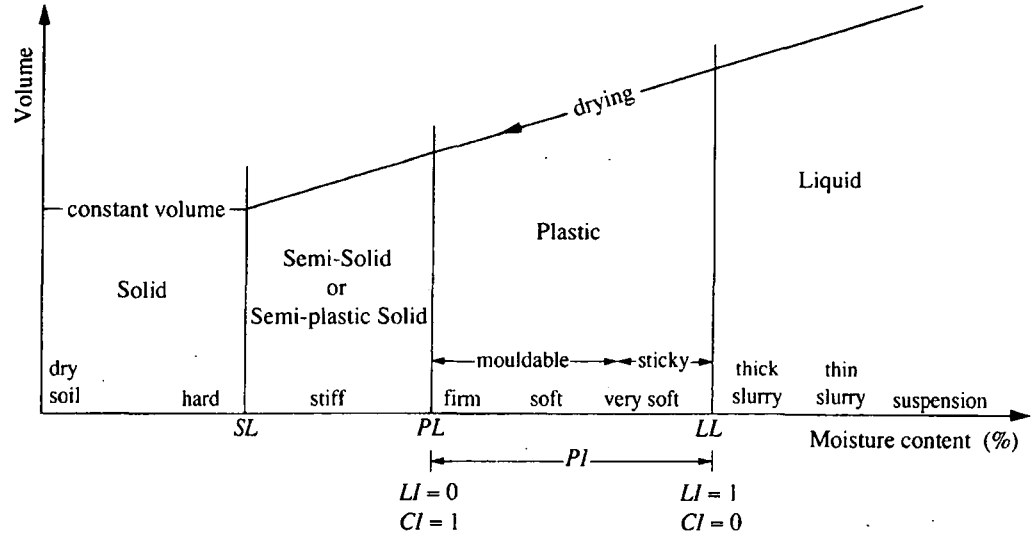


**Figure 4.5: Atterberg Limits**
Source: Barnes, 1995

The Liquid Limit is determined by measuring the water content and the number of blows required to close a specific width groove for a specified length in a standard Liquid Limit device – the Casagrande apparatus (Lambe and Whitman, 1979). The Casagrande method is dependent upon the skill of the operator (Sherwood and Ryley, 1970 *in* Selby, 1993). A drop-cone penetrometer has since been adopted as a standard instrument in many laboratories. The Plastic Limit is determined by measuring the water content when threads of the soil 3 mm in diameter begin to crumble (Lambe and Whitman, 1979). Threads of high-plasticity clay are quite tough whereas those of low-plasticity clay are softer and more crumbly (Head, 1980). The Shrinkage Limit is determined as the water content after just enough water is added to fill all the voids of a dry pat of soil (Lambe and Whitman, 1979).

Atterberg Limits or index property tests have been determined for the Blue Clay. The Casagrande method was used to determine the Liquid Limit for Gnejna Bay, Ghajn Tuffieha Bay and Rdum id-Delli. The Liquid Limit was determined when the groove in the clay closed along 25 mm of its length after 25 blows. For the Plastic Limit two tests were carried out for each site and the average calculated. The results do not differ by more than ±0.5% moisture content, thus there was no need to repeat the tests. The Liquid Limit and the Plastic Limit provide the most useful way of identifying and classifying fine-grained cohesive soils. Both limits are controlled by the clay minerals of the soil and water content. Table 4.5 presents the results of the property index tests. The Liquid Limit values for Gnejna Bay and Ghajn Tuffieha Bay are very similar, 76 and 76.42 respectively. For Rdum id-Delli this value is 79.78. The average values for the Plastic Limit are 37.79 for Gnejna Bay, 41.66 for Ghajn Tuffieha Bay and 36.75 for Rdum id-Delli.

A very useful comparison can be made between Atterberg Limits and moisture content which may provide some indication of the degree of landslip activity (Lambe and Whitman, 1979). When the moisture content is below the Plastic Limit, the clay behaves as a solid material. When the moisture content lies between the Plastic Limit and Liquid Limit, the clay is a plastic material. When the moisture content is above the Liquid Limit, clay behaves like a liquid (Enriquez-Reyes *et al.*, 1990). In the case of Blue Clay, the soil behaves as a solid material as samples tested for the three sites

## Table 4.5: Results for Atterberg Limits and related parameters

| *Site* | *Liquid Limit (%)* | *Plastic Limit (%)* | *Plasticity Index* | *Liquidity Index* | *Consistency Index* | *Activity Index* |
|---|---|---|---|---|---|---|
| **Gnejna Bay** | 76.00 | 37.79 | 38.21 | -0.36 | 1.36 | 0.74 |
| **Ghajn Tuffieha Bay** | 76.42 | 41.66 | 34.76 | -0.006 | 1.006 | 0.82 |
| **Rdum id-Delli** | 79.78 | 36.75 | 43.03 | -0.23 | 1.23 | 0.60 |

have a lower moisture content than the Plastic Limit indicating that mudslide activity is absent. If the moisture content is near the Liquid Limit soil will be more compressible and probably less permeable. This is an indication that the soil is of fairly low strength and subject to significant strength reduction on remoulding. If the moisture content is near the Plastic Limit, as in the case of Blue Clay, soil is stronger, will be relatively firm and less compressible (West, 1995) leading to more stable conditions.

The index property tests have been devised to determine the material behaviour from the moisture content and provide information on the physical behaviour of a clay soil. Atterberg Limits are related to the combined effects of two essential properties of clay, namely particle size and mineral composition (Head, 1980). However the most significant properties of clay are its cohesion and plasticity (Head, 1980; West, 1995). Cohesion refers to the ability of particles to stick together without dependence on interparticle friction (Allaby and Allaby, 1990). Plasticity is the ability of soil to undergo unrecoverable deformation at constant volume without cracking or crumbling (Craig, 1978). Unlike silt, clay does not exhibit dilatancy (Head, 1980). On drying clay shrinks considerably and displays cracks which are more pronounced the higher the plasticity of clay. At Rdum id-Delli, where Blue Clay shows the highest Plasticity Index when compared to Gnejna Bay and Ghajn Tuffieha Bay desiccation cracks are widespread and a common feature throughout the whole site.

Atterberg Limits indicate the water-holding capacity of different types of soils. Soils having high Plastic Limit contain silt and clay and the moisture content of these soils has a direct bearing on their load-carrying capacity (Rahn, 1996). Soils with high Liquid Limit such as the Blue Clay indicate a high clay content and a low load-carrying capacity because soil changes from a solid to a plastic when moisture content is increased. The particle size distribution curves (Figures 4.2, 4.3 and 4.4) confirm the high percentage of clay content found within the Blue Clay Formation at each of the three selected sites. This results in a rapid decrease in the load-carrying capacity above the Plastic Limit. The inverse situation takes place when the moisture content is decreased below the Plastic Limit and the load-carrying capacity increases very rapidly.

Other parameters which include the Plasticity Index, Liquidity Index, Consistency Index and Activity Index, derived from the Atterberg Limits have been determined for Blue Clay (Table 4.5).

The Plasticity Index gives the range in moisture content at which a soil is in a plastic condition (Rahn, 1996). A small Plasticity Index such as 5 per cent indicates that a small change in moisture content will change the soil from a semi-solid to liquid condition. This type of soil is thus very sensitive to moisture. A higher Plasticity Index such as 20 per cent shows that a considerable amount of water can be added before soil becomes liquid. Soils with very high Plasticity Index (more than 35 per cent) such as the Blue Clay may have a high swell capacity (Rahn, 1996), lower permeability, be more compressible and consolidate over a longer period of time under load than clays of low plasticity (Head, 1980). Blue Clay therefore experiences an increase in density under pressure and a decrease in specific volume.

The Plasticity Index has been calculated for the three sample collection sites (Table 4.5). Ghajn Tuffieha Bay has the lowest Plasticity Index (34.76) of the three sites indicating that when compared with the other two sites less water is needed for clay to change into a liquid state. It can be proposed that this site is more prone to landslide activity than Gnejna Bay and Rdum id-Delli. This is also confirmed by the moisture content and bulk density values. Gnejna Bay has a Plasticity Index of 38.21, a little higher than Ghajn Tuffieha Bay but lower than the Plasticity Index of Rdum id-Delli (43.03). The latter value indicates that Blue Clay at Rdum id-Delli has the capacity to retain a high amount of moisture content and is less permeable than at the other two sites. One can conclude that Rdum id-Delli is less prone to sliding movements although mudslides were observed and are evident. The high Plasticity Index value is also attributed to a high clay content in Blue Clay at Rdum id-Delli (61%) which makes the soil less permeable and able to hold a high amount of water. Ghajn Tuffieha Bay has a much lower percentage of clay content (35%) followed by Gnejna Bay (44%) contributing to a type of soil which is more permeable and capable of retaining a lower amount of water.

The Atterberg Limits enable clay soils to be classified physically, and are useful in identifying the type of clay mineral present. Classification is usually achieved by

means of the plasticity chart, known as Casagrande's plasticity chart. This is a graphical plot of the Liquid Limit against the Plasticity Index and provides information about strength, compressibility, plasticity and type of soil (Vickers, 1978). The plasticity chart distinguishes fine-grained soils on the basis of predominantly clays (C) or silts (M) lying above or below the A-line. The chart presents varying degrees of plasticity from low (Liquid Limit < 35%) to extremely high (Liquid Limit > 90%) with symbols for each type of soil. Organic soils usually lie below the A-line and are given the symbol O or Pt for peat. Most soils are found below the B-line (Barnes, 1995).

Using this chart to classify the Blue Clay samples collected at Gnejna Bay, Ghajn Tuffieha Bay and Rdum id-Delli, values of the Liquid Limit were plotted against values of the Plasticity Index on the plasticity chart (Figure 4.6). Clay samples from Gnejna Bay and Ghajn Tuffieha Bay lie below but close to the A-line, whereas for Rdum id-Delli the sample lies on the A-line. The chart indicates that all three samples have a very high degree of plasticity and contain significant amounts of organic matter since they are found below the A-line. Soils with a high Plastic Limit and Plasticity Index are said to be highly plastic or 'fat' clays, whereas those with low values are considered as slightly plastic or 'lean' (Rahn, 1996). According to the location of clay minerals on the plasticity chart (Figure 4.7), the position of Blue Clay samples plotted on Figure 4.6 correspond best to kaolinite.

Another important index is the Liquidity Index which is a measure of the natural soil moisture as related to the Plasticity Index (Blythe and De Freitas, 1984 *in* Rahn, 1996) and provides a good indication of soil sensitivity (West, 1995). If the Liquidity Index is 1, the soil is at the Liquid Limit, has little strength and is highly sensitive. Values greater than 1 indicate ultrasensitive or quick clays. When soils have a Liquidity Index which is larger than 1, these can flow like a viscous liquid if disturbed in any way. If Liquidity Index is 0, soil is at Plastic Limit and is probably not sensitive. When Liquidity Index is less than 0 with negative values, the water content is less than the Plastic Limit, the soil acts like a solid (Rahn, 1996) and will fail as brittle material when sheared (West, 1995). Moving landslides usually have a Liquidity Index smaller than 1 whereas more fluid-like debris flows have a Liquidity Index larger than 1 (Costa and Baker, 1981 *in* Rahn, 1996). The Liquidity Index for Blue

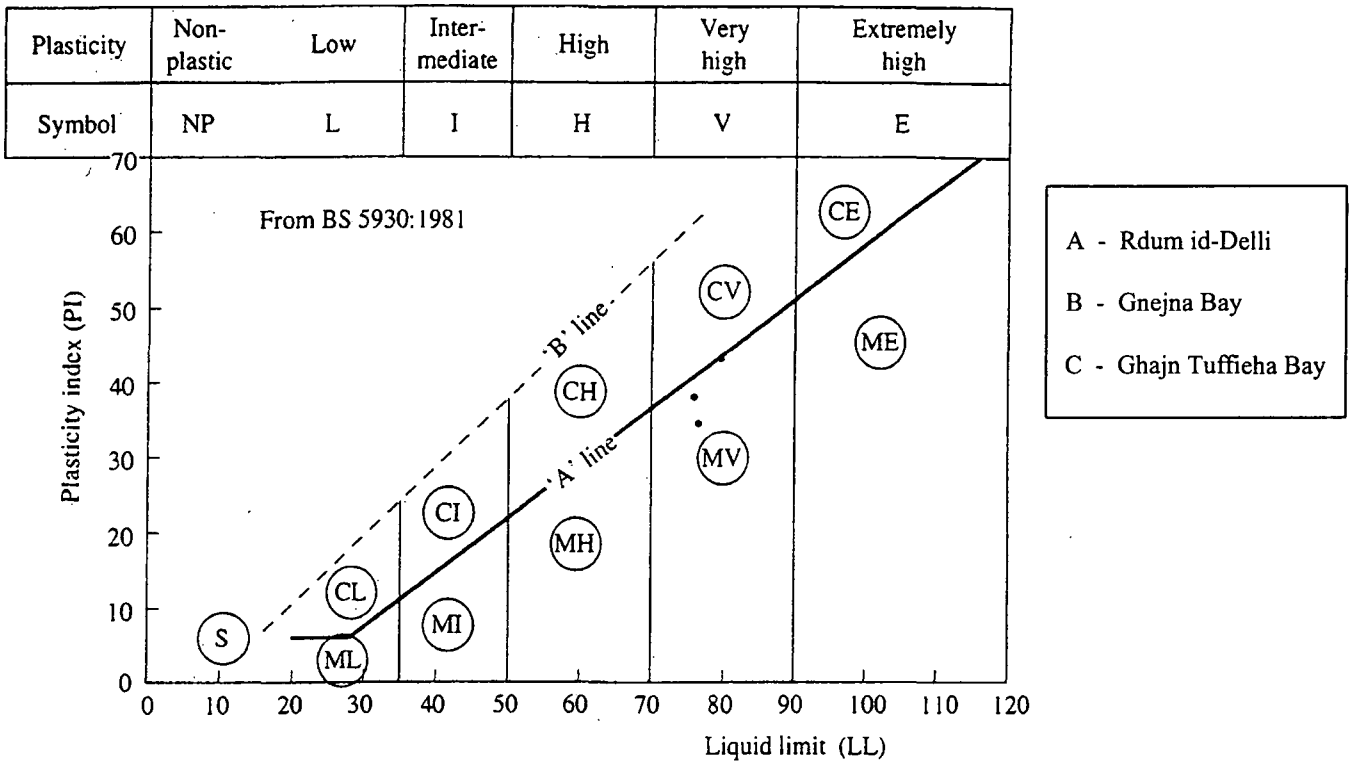


**Figure 4.6 Classification of Blue Clay based on plasticity chart**
Source: Barnes, 1995

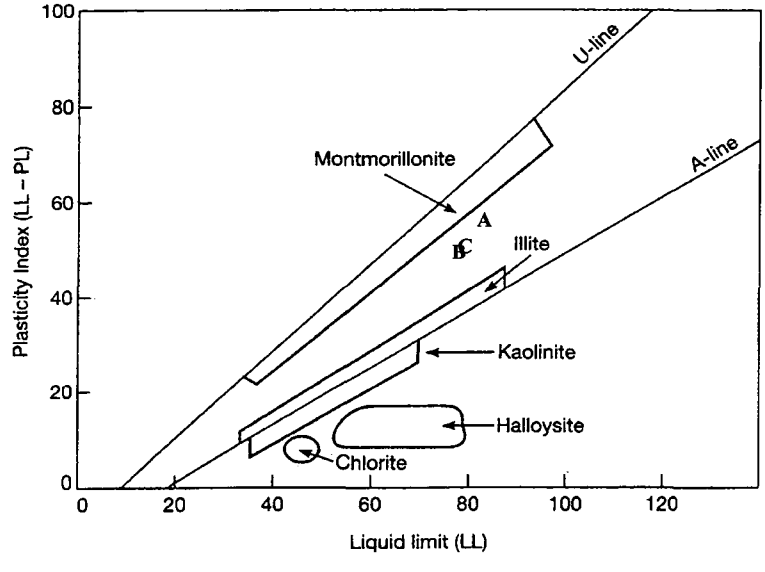


**Figure 4.7: Location of clay minerals on plasticity chart**
Source: West, 1995

Clay at Gnejna Bay, Ghajn Tuffieha Bay and Rdum id-Delli has negative values ranging from -0.36 at Gnejna Bay, -0.006 at Ghajn Tuffieha Bay and -0.23 at Rdum id-Delli (Table 4.5). This indicates that at all three sites the water content is less than the Plastic Limit and that the soil is in a solid state. The soil is dry and there is no indication of mudslide activity. The largest value close to 0 corresponds to Ghajn Tuffieha Bay which has the largest value for moisture content and where the soil is very close to its Plastic Limit.

Consistency is the relative ease with which a soil can be deformed. This is described as soft, firm or hard (West, 1995) and is measured by a Consistency Index which is used less often than the Liquidity Index. Consistency depends on the nature of soil minerals present and the water content and is especially significant for fine-grained soils. The latter are soils whose deformability is most subject to change without changing water content (West, 1995). A change in consistency will alter engineering properties such as shear strength, compressibility and bearing capacity. When the Consistency Index is 1, the Liquidity Index is 0 and the soil is at its Plastic Limit in a firm state. When the Consistency Index is 0, the Liquidity Index is 1 and the soil is at its Liquid Limit in a very soft state. The Consistency Index was calculated for Blue Clay samples collected at Gnejna Bay, Ghajn Tuffieha Bay and Rdum id-Delli (Table 4.5). The values increased with a factor of 1 on the Liquidity Index values. This indicates that Blue Clay is a dry soil, resulting in stable conditions and absence of landsliding. This corresponds to the same interpretation provided by the Liquidity Index results.

The moisture content of a clay soil is affected not only by its particle size and mineral composition but also by the amount of clay present. Silt and sand particles although present in a clay soil will influence the moisture content value but will have little effect on the plasticity properties of the soil since the clay particles dominate (Barnes, 1995). An Activity Index exists which is the ratio of the Plasticity Index to the percentage of clay-size particles within a sample. This index is controlled by the dominant clay mineral species in the soil and is a useful indicator of the presence of those species (Skempton, 1953a *in* Selby, 1993). The higher the activity the more clay-like the soil must be. A correlation exists between activity and clay mineral types. Montmorillonite generally has the highest Activity Index and a high Plasticity

Index since this expansive clay is able to disperse into very fine particles with large water-absorbing volume (Rahn, 1996). Non-expansive clay minerals such as kaolinite and illite have lower Plasticity Index and Activity Index values. Halloysite also has a low Activity Index (West, 1995).

Activity represents the Plasticity Index of the clay minerals alone. Four groups of activity have been defined by Skempton (1953 *in* Barnes, 1995) (Table 4.6).

**Table 4.6: Categories of Activity Index (after Skempton, 1953)**

| *Description* | *Activity Index* |
|---|---|
| Inactive | < 0.75 |
| Normal | 0.75 – 1.25 |
| Active | 1.25 – 2.0 |
| Highly Active | > 2.0 |

Source: Modified from Barnes, 1995

The Activity Index is determined for Blue Clay samples (Table 4.5). It was found that utilising the categories devised by Skempton (1953 *in* Barnes, 1995) in Table 4.6, Blue Clay at Gnejna Bay and Rdum id-Delli can be classified as inactive since the Activity Index is 0.74 and 0.60 respectively. These values reflect other parameters such as low moisture content, high bulk densities and higher plasticity. The Activity Index for Gnejna Bay is very close to the normal category probably because Blue Clay at this site has a lower Plasticity Index than at Rdum id-Delli. At Ghajn Tuffieha Bay the Activity Index is 0.82 and falls under the normal category. It is interesting to note that Blue Clay at Ghajn Tuffieha Bay has the lowest percentage of clay content. This is compensated by a high moisture content, low bulk density and low Plasticity Index for the same site. This indicates that the range between the Liquid Limit and Plastic Limit is lowest for Ghajn Tuffieha Bay, thus less water content is needed to change the soil from a plastic state to a liquid state contributing to an increased rate of mass movement processes when compared with the other two sites.

### 4.3.5 Summary of results

Three proposals can be made when interpreting and comparing the results derived from the physical properties tests. Rdum id-Delli is the most stable site. Gnejna Bay shows stability with a trend towards instability. Ghajn Tuffieha Bay is the site most prone to instability. Field observations at all three sites give no indication of active mass movement processes taking place and clay slopes seem to be in a stable condition. However the most reliable indication of slope instability will only be provided by a synthesis of results obtained from both the physical and geotechnical properties tests.

## *4.4 Geotechnical properties tests of Blue Clay*

There are four main tests which study the stress-strain behaviour of soil (Lambe and Whitman, 1979): isotropic compression, confined compression, triaxial compression and direct shear. The mechanical properties of a material are the response of the material subject to change in stress. Shear strength is one of the most important mechanical properties responsible to maintain the stability of a slope (Pitty, 1979). It is dependent on physical properties such as particle size distribution, particle arrangement, mineralogy and degree of saturation (Ebuk *et al.*, 1990; El-Sohby *et al.*, 1990 *in* Fan *et al.*, 1994). The purpose of shear strength testing of soils is twofold (Vickers, 1978).

i. To allow displacement under working loads to be predicted.
ii. To evaluate the external forces required to cause shear failure of a soil.

In the case of Blue Clay, shear tests using the shear box technique were performed on the samples to study the mechanical behaviour of the material. Shear tests determine the shear strength parameters of soils in terms of total stresses. Therefore measurement of pore water pressure is not required. The shear box test is a simple test to measure the strength of soil where the peak and residual shear strength parameters of cohesive soils are determined. This technique was chosen as both

cohesion and angle of internal friction can be determined. The parameters provide an indication of material strength and stability conditions. The shear box test is often referred to as direct shear test because an attempt is made to relate shear stress at failure directly to normal stress, thus directly defining the Mohr-Coulomb failure envelope (Vickers, 1978).

The shear box consists of a square box split horizontally in two halves (Figure 4.8). The sample is held between metal grilles and porous stones. A horizontal shearing force is applied to the lower part of the box at a constant rate until the sample fails. Shear strength is determined by measuring the shearing force causing failure. To determine the shearing resistance under a normal stress a vertical load is applied to the sample by means of a dead weight (Selby, 1993). Rates of horizontal displacement and vertical deformation are shown on two different dial gauges which measure strain and shear stress. Failure of the sample is indicated by a sudden drop or levelling off, of the proving-ring dial reading which records the reaction to shear stress. When the sample shears, its resistance to shear stress may drop rapidly. Strain is plotted against shear stress for tests with different vertical loads. Values for the normal stress are then plotted against the maximum values from the stress-strain plots which correspond to peak strength. The value of the angle of internal friction is determined from the slope of the line through the plotted points, and the value of cohesion is the displacement of the line above the zero point (Selby, 1993).

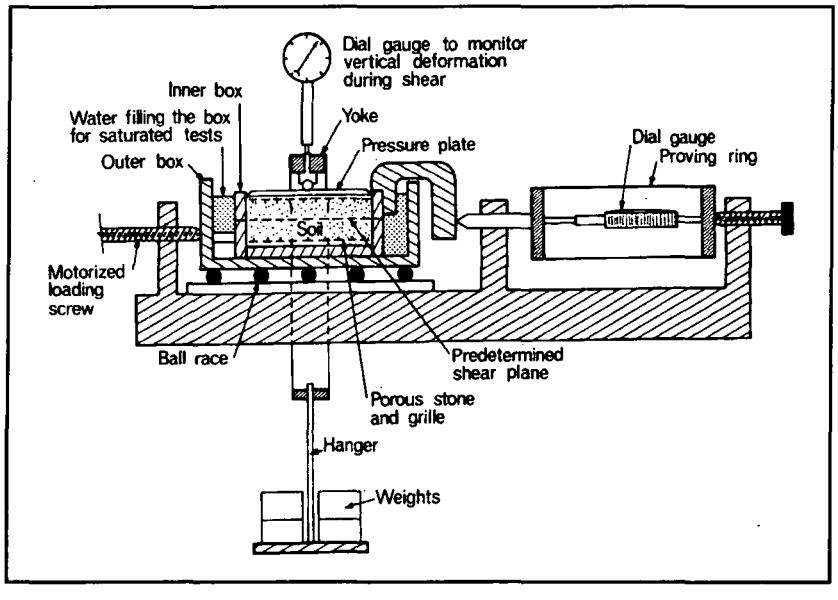


**Figure 4.8: The Shear Box apparatus**
Source: Selby, 1993

The technique explained in section 4.2.2 was used to collect Blue Clay samples for geotechnical tests. To maintain homogeneous properties, samples were collected from the same depth, at the same date and time as the samples which were used to determine the physical properties tests. This allows for a correlation of results between the physical properties and geotechnical properties of Blue Clay. Care was taken to cut the samples in blocks and keep them intact. This facilitates the preparation of samples in the laboratory when the shear box tests are carried out.

Undrained shear box tests were performed for Gnejna Bay, Ghajn Tuffieha Bay and Rdum id-Delli. There are two reasons for adopting this procedure. During undrained tests no drainage is permitted at any stage during shear, therefore the volume and moisture content of the samples remain constant. Blue Clay is an impermeable material, making undrained tests an acceptable procedure. Five tests with different vertical loads ranging from 5 kg to 25 kg were carried out for each site. The horizontal shear force applied on the box was at a constant rate of strain of 1.27 mm/minute. Samples were cut carefully to fit the shear box - 60 mm wide, 60 mm long and 25 mm high, in the form of an intact square block. Readings for both the horizontal displacement, that is the strain and vertical deformation were recorded every 15 seconds. Each test was terminated when the specimen failed. Examination of the samples after testing showed that in most cases a shear plane had developed.

Table 4.7 displays data for the geotechnical properties of Blue Clay at Gnejna Bay, Ghajn Tuffieha Bay and Rdum id-Delli. The angle of internal friction and values for cohesion were calculated using the procedure described previously. Figures 4.9, 4.11 and 4.13 are stress-strain plots whereas Figures 4.10, 4.12 and 4.14 are shear stress - normal stress plots for the three investigation sites.

**Table 4.7: Results for geotechnical tests**

| *Strength parameters* | *Gnejna Bay* | *Ghajn Tuffieha Bay* | *Rdum id-Delli* |
|---|---|---|---|
| Cohesion (KPa) | 0.239 | 0.024 | 0.658 |
| Angle of internal friction (°) | 30 | 25 | 22.5 |

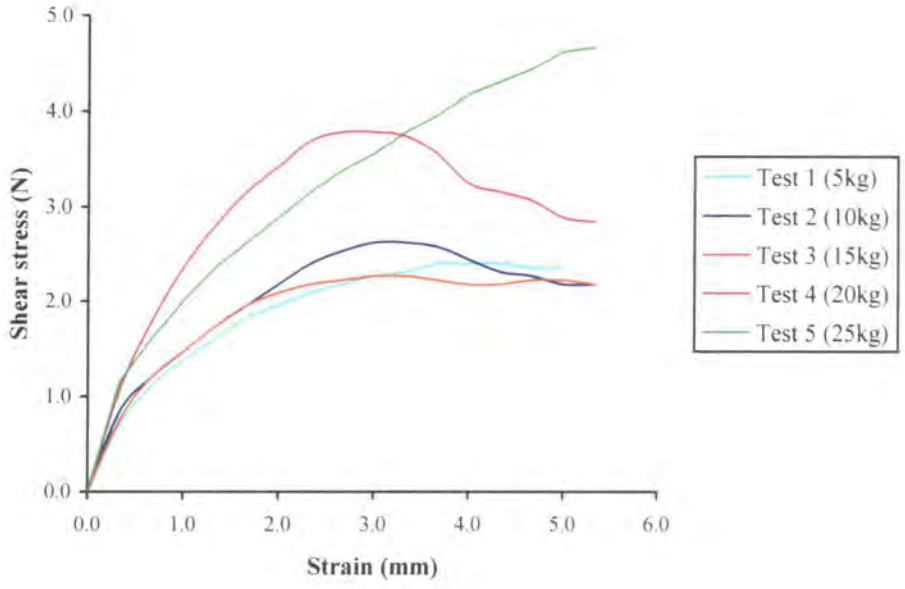


**Figure 4.9: Stress - strain plots for Gnejna Bay**

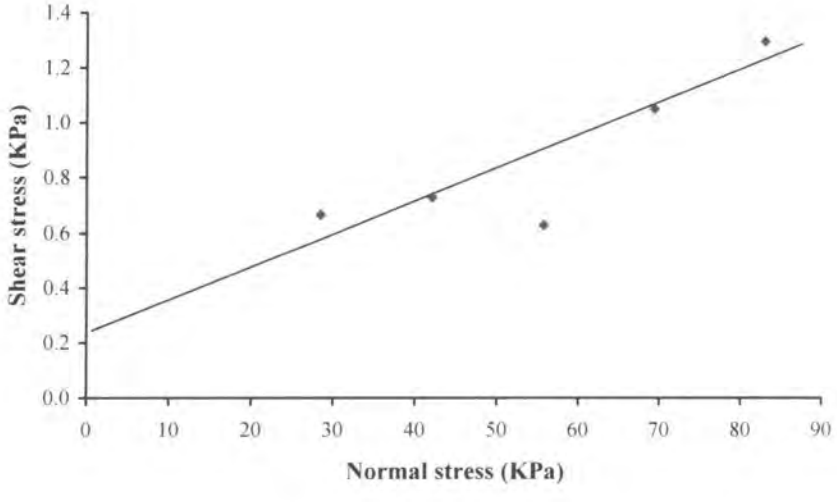


**Figure 4.10: Shear stress - normal stress plot for Gnejna Bay**

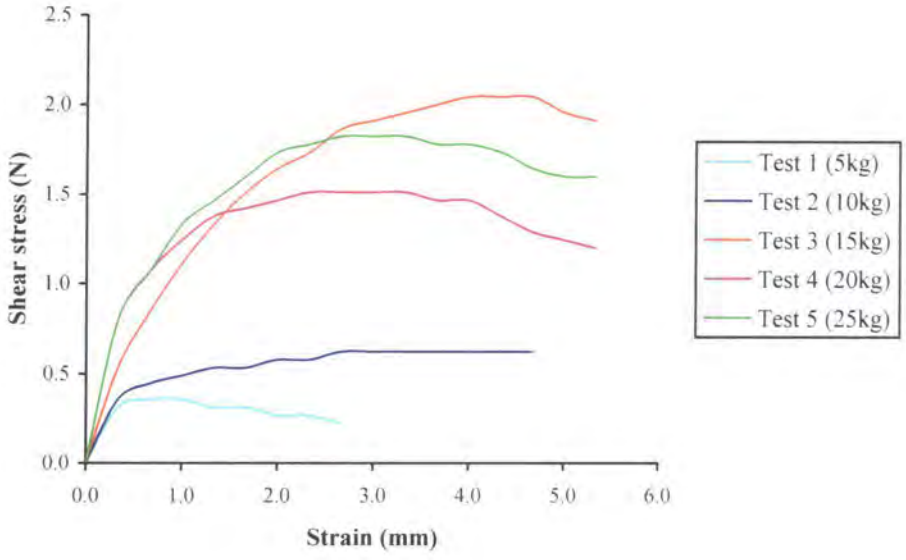


**Figure 4.11: Stress - strain plots for Ghajn Tuffieha Bay**

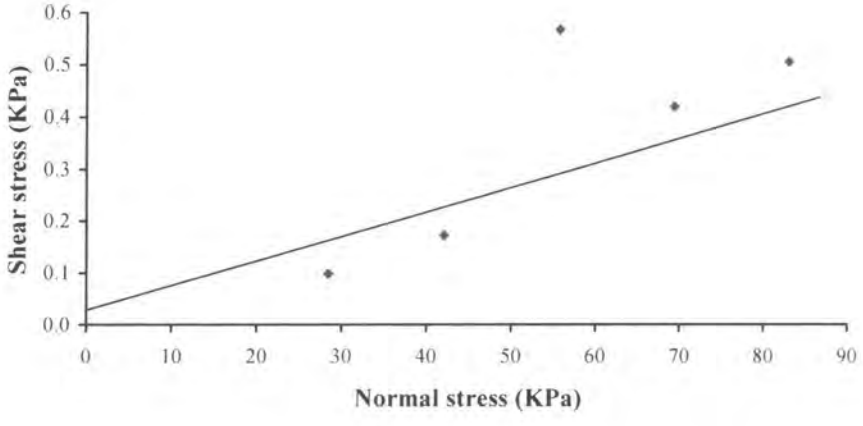


**Figure 4.12: Shear stress - normal stress plot for Ghajn Tuffieha Bay**

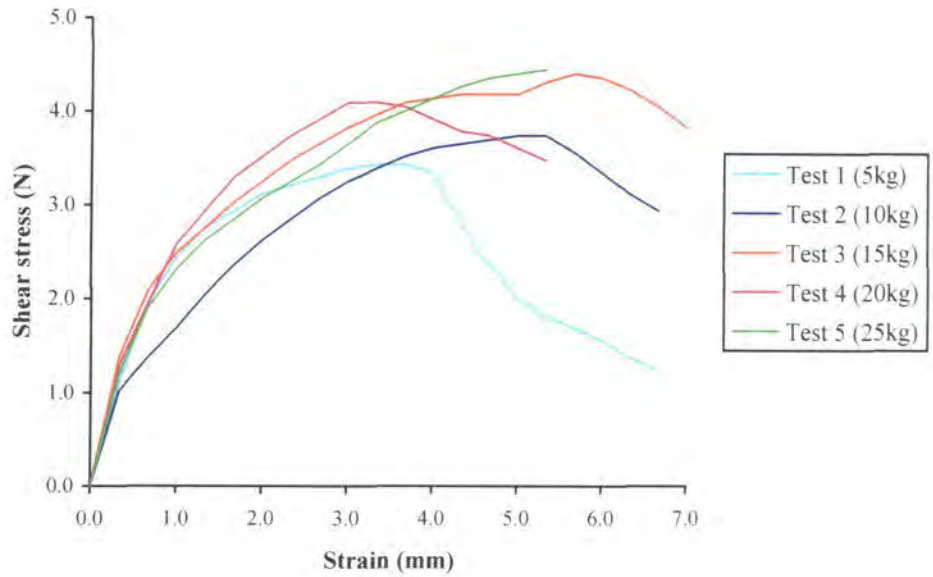


**Figure 4.13: Stress - strain plots for Rdum id-Delli**

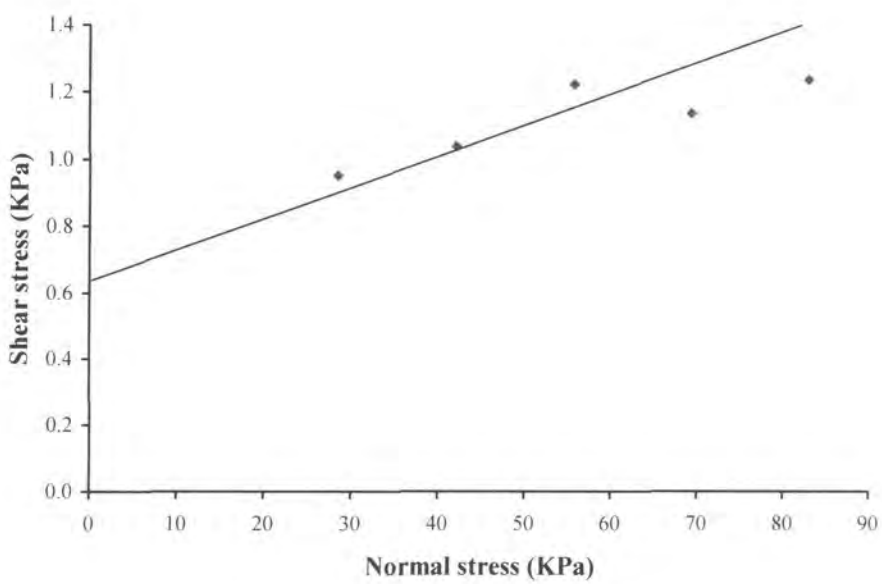


**Figure 4.14: Shear stress - normal stress plot for Rdum id-Delli**

Examination of the data presented in Table 4.7 and the graphical plots derived from geotechnical tests provide an indication of the strength of Blue Clay. It should be noted that the response of soil to stress is determined by its mechanical strength, defined as the ability of soil to resist deformation and fracture without significant failure (Summerfield, 1991). Strength is closely controlled by water content which influences the behaviour of fine-grained soils significantly. This is expressed by the Atterberg Limits. Positive pore water pressures decrease soil strength, thus saturated soil on a slope is weaker than a dry mass. As a result landslides usually take place during and after rainfall events which increase the moisture content of the soil (Selby, 1985).

The strength or load-supporting capacity of soils varies considerably. Different conditions of moisture and density lead to variations in the strength of any specific soil (Rahn, 1996). Low bulk densities usually exhibit high moisture contents, low strengths and high permeability (Allison, 1986). This is the case of Ghajn Tuffieha Bay where Blue Clay has a low bulk density, high moisture content and a low cohesion value, indicating low strength. The opposite situation applies for Gnejna Bay and Rdum id-Delli where a higher bulk density and lower moisture content contribute to a higher cohesion value, thus an increase in material strength.

The strength of soil is related to cohesion and the angle of internal friction, known as the strength parameters (Rahn, 1996). This relationship is described by the Coulomb equation.

Cohesion is the shearing strength of an unstressed soil which is very high in clay, but less significant in silt and sand. It is influenced by attraction of particles due to molecular forces and the presence of moisture. Thus the cohesive force in a particular soil varies with its moisture content. Dry clay has low cohesion which increases as moisture content increases until clay reaches the Plastic Limit. All of the three investigation sites exhibit low values of cohesion. This is due to the fact that soil is dry at each site since the moisture content is lower than the Plastic Limit values. However it should be noted that although Ghajn Tuffieha Bay has moisture content and Plastic Limit values which are very similar it exhibits the lowest cohesion value. A further increase in moisture beyond this limit reduces cohesion (Rahn, 1996),

especially when soil reaches the Liquid Limit. At this point cohesion would be largely overcome due to a high moisture content. Skempton and Northey (1953) and Wood and Wroth (1978) (*in* Head, 1980) indicate that at the Plastic Limit, shear strength may be more than one hundred times greater than at the Liquid Limit. This is also confirmed by Selby (1985) who maintains that for most soils shear strength at the Plastic Limit is about 110 KN/m$^2$ and at the Liquid Limit this is about 1.6 KN/m$^2$.

In cohesive, non-granular materials the shear strength is equal to cohesion (Pitty, 1979). Thus values of cohesion give an indication of the strength of the soil. Ghajn Tuffieha Bay has the lowest cohesion value of the three sites. Consideration should be given to the fact that Blue Clay at this site is mainly composed of silt which is less cohesive than clay, contributing to a decrease in material strength. Where Blue Clay has a high clay content, such as at Rdum id-Delli, cohesion is more significant and the material stronger. At Gnejna Bay, Blue Clay has equal fractions of silt and clay and the value for cohesion lies between that for the other two sites. The silt fraction contributes to a lower cohesion than at Rdum id-Delli but the clay content increases the cohesion above that of Ghajn Tuffieha Bay.

The basic control on the strength of soil and of most rocks is the frictional resistance to sliding between mineral particles in contact. Frictional strength is directly proportional to the normal stress (Selby, 1993) and increases with sand and gravel content. Clay has low internal friction that varies with the moisture content. In dry clay internal friction is much higher than in saturated clay, since grains can slide more easily once lubricated with water (Rahn, 1996). The internal friction of a material is expressed by the angle of internal friction or angle of shearing resistance. The value of the friction angle decreases with increasing plasticity and water content (Selby, 1993). Rdum id-Delli which has the highest Plasticity Index exhibits the lowest angle of internal friction and highest cohesion value, indicating a high percentage of clay content within the soil. Gnejna Bay and Ghajn Tuffieha Bay have higher friction angles and lower cohesion values due to a larger proportion of silt and sand found within the material. Ghajn Tuffieha Bay has a lower friction angle than Gnejna Bay.

An inverse relationship exists between the Liquid Limit and angle of internal friction (Watry and Ellis, 1995 *in* Rahn, 1996). Nelson (1992 *in* Rahn, 1996) found that an

angle of internal friction of 30° compares with Liquid Limit values around 40, whereas an angle of 6° compares with Liquid Limit values around 80. It can be assumed that an increased clay content lowers the angle of internal friction, and therefore the strength of the soil, and increases the Liquid Limit. This can apply for Rdum id-Delli, where Blue Clay has the highest clay content, lowest friction angle and highest Liquid Limit value. At all three sites both the Liquid Limit and friction angle values are high, implying that besides moisture content, other factors such as particle size distribution should be considered. High values for friction angles are explained by the fact that Blue Clay is a dry soil.

Shear strength of a material can also be determined by studying the relationship between stress and strain which help in predicting the behaviour of soils. In general soil is treated as an elastoplastic material (Selby, 1993). A perfectly elastoplastic material, also known as St.Venant material, is perfectly elastic for stresses less than the yield stress and perfectly plastic for stresses equal to the yield stress (Selby, 1993). Vyalov (1986 *in* Selby, 1993) claims that most soils are viscoelastic-plastic materials with non-linear behaviour, that is soils exhibit all forms of behaviour - elasticity, plasticity and viscosity. Soils composed of clay and silt will change their behaviour with changing water content. Soil behaves as an elastic solid and fails by brittle fracture at very low water contents. At the Plastic Limit it will deform plastically and at the Liquid Limit it will behave as a viscous fluid (Selby, 1985) due to a high water content.

Blue Clay is a normally-consolidated material which has low cohesion values and can be classified as soft clay (Table 4.2). Normally-consolidated material has undergone deposition only and has never been overloaded by additional burden. The stress-strain plots (Figures 4.9, 4.11 and 4.13) do not exhibit pronounced peak strength curves as in the case of over-consolidated material. The stress-strain curves for Blue Clay samples correspond best to rheological models applicable to elastoplastic materials. When stress is applied the material initially undergoes a phase of elastic behaviour. During this phase the entire strain is recoverable once the load is removed. As the load becomes sufficiently large, irreversible sliding of particles against each other occurs (Selby, 1993). When the stress is removed deformation will be permanent and the material experiences plastic behaviour. This is characterised by a

steady decrease in the gradient of the stress-strain curve. When the stress becomes great, bonds in the material will break and a shear surface will develop as a result of strain weakening resulting in a decrease in strength (Petley and Allison, 1997). The loss of strength with increasing strain is mainly due to particle reorientation and a breakdown of the soil fabric. Once the peak strength has been overcome and a shear surface is fully developed, the strength will settle to a residual value. The residual strength can only be achieved when a shear surface has been developed and has the nature of pure friction (Taylor and Cripps, 1987). The residual value is important when assessing shear surfaces produced by landslides. The shear strength along such surfaces is less than the strength of the surrounding undisturbed soils. This strength needs to be determined when assessing the stability of existing landslides (Coduto, 1999).

Most normally-consolidated clays are slightly ductile, and have residual strengths that are slightly less than the peak strength. This is noted in the case of Blue Clay. At low stresses, the stress-strain curves for Gnejna Bay and Ghajn Tuffieha Bay indicate a ductile behaviour (Figure 4.15a). At peak strength samples do not undergo weakening but retain a constant strength for a considerable further accumulation of strain (Petley and Allison, 1997). At higher stresses, the strain-stress curves display a brittle behaviour (Figure 4.15b) where a peak and a residual strength can be identified (Coduto, 1999). Only in the case of Rdum id-Delli do the curves exhibit brittle behaviour for all stresses applied, indicating a competent material.

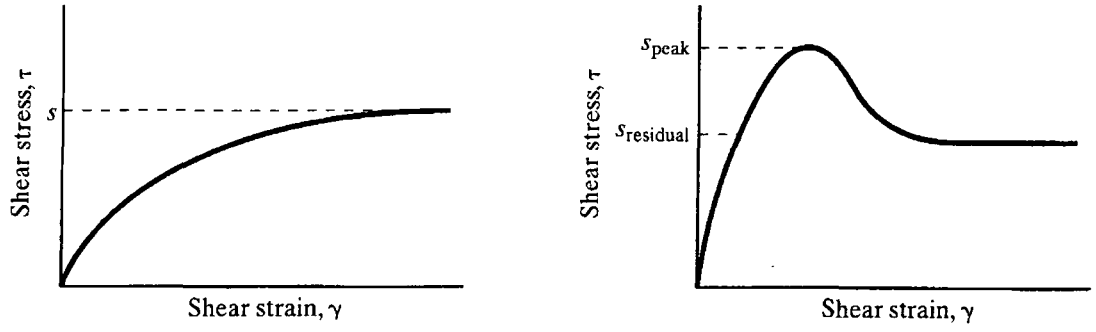


**(a) Ductile behaviour** **(b) Brittle behaviour**

**Figure 4.15: Stress - strain curves for ductile and brittle behaviour in soils**
Source: Coduto, 1999

Examination of Blue Clay samples after mechanical testing provides additional information on the behaviour of soil. Ductile behaviour is indicated by samples which were permanently deformed but do not show any fracturing. Alternatively brittle behaviour is clearly indicated by samples which developed a single shear plane. The latter results in a decrease in material strength at the base of the landslide. This explains the sudden failure in deep-seated landslides (Petley and Allison, 1997).

## 4.5 Conclusion

Knowledge of material properties provides useful information regarding the processes involved in the formation of geomorphological features. In the case of Blue Clay analysis of results derived from laboratory testing provides links between the physical properties and geotechnical properties which give an indication of the way soil behaves. Various similarities and differences can be distinguished between the three field investigation sites.

Ghajn Tuffieha Bay exhibits a low bulk density, low cohesion value, high moisture content, greater percolation and high water retention capacities. This leads to an increased mudslide activity. Gnejna Bay and Rdum id-Delli exhibit similar properties. Both sites have lower moisture contents, higher bulk densities and higher cohesion values, resulting in an increase in material strength. Three main conclusions regarding the stability of the three field sites can be drawn from physical and geotechnical laboratory data.

i. Rdum id-Delli is the most stable site.
ii. Gnejna Bay shows stability with a trend towards instability.
iii. Ghajn Tuffieha Bay is the site most prone to instability.

The above information derived from laboratory testing can be used to explain geomorphological processes and landforms. Field observations at all three sites highlight the presence of mass movement processes, although these were not operating at the time of geomorphological mapping and sample collection. There is an

indication of instability especially at Rdum id-Delli, where mudslides are inactive. Reactivation may initiate when rainfall starts increasing water content and pore water pressure and leading to unstable conditions. Geomorphological mapping has showed that mudslides develop where Blue Clay outcrops at the base of an Upper Coralline Limestone plateau. They are distinct individual features some having a vegetation cover, whereas others have bare surfaces. Curved back scars and slip surfaces at Rdum id-Delli indicate the presence of deep-seated rotational slides, typical of argillaceous material (Enriquez-Reyes *et al.*, 1990).

Outcrops of Blue Clay are prone to erosion by water during high intensity storms when moisture content increases and the material starts losing strength. Long duration rainfall events saturate bare ground surfaces, resulting in overland flow and runoff. Water running on exposed clay erodes the ground surface, leading to the formation of gullies. The presence of desiccation cracks especially at Gnejna Bay and Rdum id-Delli indicates dry conditions, slower rates of movement and more stable conditions.

Blue Clay is a normally-consolidated clay which has low cohesion values and can be classified as a soft clay. From geotechnical testing it has been observed that a low clay content contributes to a decrease in material strength. Ghajn Tuffieha Bay has the lowest clay content and lowest cohesion value, whereas Rdum id-Delli has the highest percentage of clay and the highest cohesion value. Gnejna Bay and Ghajn Tuffieha Bay have higher friction angles due to a larger proportion of silt and sand.

Stress and strain curves for Blue Clay correspond best to rheological models which display an elastoplastic behaviour. At low stresses, the stress-strain curves for Gnejna Bay and Ghajn Tuffieha Bay display a ductile behaviour. At higher stresses the behaviour becomes brittle and a shear plane develops. At Rdum id-Delli the stress-strain curves exhibit brittle behaviour for all stresses indicating a competent material. Development of the shear surface leads to a decrease in material strength at the base of the landslide resulting in a sudden failure.

An understanding of shear strength is fundamental to the behaviour of a soil mass and is of major importance for slope stability (Barnes, 1995). Strength determines the ultimate force required to cause failure and is closely controlled by water content.

Landslides usually take place during and after rainfall events when there is an increase in moisture content. Values of shear strength and shear stress permit the determination of the Factor of Safety, expressed as the ratio between the two variables (Summerfield, 1991).

Slope stability analysis is performed in the following chapter (chapter 5), which deals with the modelling of coastal slope instability for north-west Malta. Quantitative data derived from laboratory testing and data available from the surveyed slopes at each field site, are used to perform a modelling exercise utilising XSTABL software. From the input data, Factor of Safety values corresponding to the most critical surfaces along which failure can occur, are calculated using the Bishop Method of analysis.

# *Chapter 5*

# *Stability analysis of coastal Blue Clay slopes*

## 5.1 Introduction

Issues of slope stability, instability and related mass movements represent research interests where there is often interaction between geotechnical engineers and geomorphologists. Engineers are usually concerned with site specific projects. Geomorphologists are interested in longer term slope stability and slope evolution. The main distinction between geomorphologists and engineers lies in the objectives not the methodology of analysis of slope stability. Collaboration between the two professions should be encouraged as this yield benefits (Anderson and Richards, 1987).

In recent years there has been an increasing effort to quantify the stability of natural slopes (Sidle *et al.*, 1985). This is clearly important when a judgement is needed about whether the slope is stable or not and decisions are to be made as a consequence (Nash, 1987). Consequently principles and techniques developed in engineering rock mechanics and soil mechanics (for example Terzaghi and Peck, 1967; Lambe and Whitman, 1979) have played a major role (Sidle *et al.*, 1985). The techniques have been adopted by geomorphologists as a quantitative technique, allowing the detailed assessment of landforms (Allison, 1986).

The stability analysis of landslides forms a major branch of soil mechanics (Goudie *et al.*, 1990) and is a long established method of providing a quantitative statement on the stability of a slope by considering its geometry and mechanical properties (Graham, 1984 *in* Allison, 1986). Most of the work regarding models of slope processes concentrates on soft sediments and soils (Allison and Kimber, 1998). The focus on soft earth materials which have experienced little or no lithification, partly reflects the availability of modelling techniques developed in parallel disciplines (Michalowski, 1995a, 1995b; Duncan, 1996 *in* Allison and Kimber, 1998) which can be applied to geomorphological problems. Modelling techniques which allow for modifications such as differences in pore water pressure are often the best analysis procedure (Michalowski, 1995b *in* Allison, 1996).

The accuracy of the analysis of a particular slope depends on precise calculations of the slope geometry, the groundwater conditions and soil properties. It is also important that the analysis models the slope conditions precisely and that the method of analysis is reliable (Nash, 1987). A key element in the interpretation of slope stability is the rigorous incorporation of the hydrological element (Anderson and Richards, 1987). Having collected data on slope geometry, weight, pore water pressure and soil strength, an appropriate model of analysis can then be chosen (Goudie *et al.*, 1990).

There are several methods of stability analysis but the procedures are similar in concept. Nash (1987) gives a comprehensive review of Limit Equilibrium Methods of analysis which are presently used. The slope is modelled theoretically (Nash, 1987) utilising field and laboratory data from geomorphological and geotechnical investigations (Allison, 1986) and the stability of the slope is determined by means of a Factor of Safety. This is known as a deterministic analysis. Other analyses express stability as a probability of failure, referred to as a probabilistic analysis (Coduto, 1999).

For the purpose of stability analysis, slip surfaces in homogeneous cohesive soils are assumed to have a circular failure surface which is a simplification of reality (Záruba and Mencl, 1969) (Figure 5.1a). Rotational failures are treated as a series of vertical slices (Selby, 1993) and are analysed by various circular arc methods, such as Bishop Method of Slices (1955) (Goudie *et al.*, 1990). Where non-homogeneous soil profiles exist, such as with layered strata, a non-circular slip surface may be appropriate (Barnes, 1995) (Figure 5.1b). The shape of non-circular curved failure planes is considered in several analytical methods such as Simplified Janbu Method and Spencer's Method (Selby, 1993).

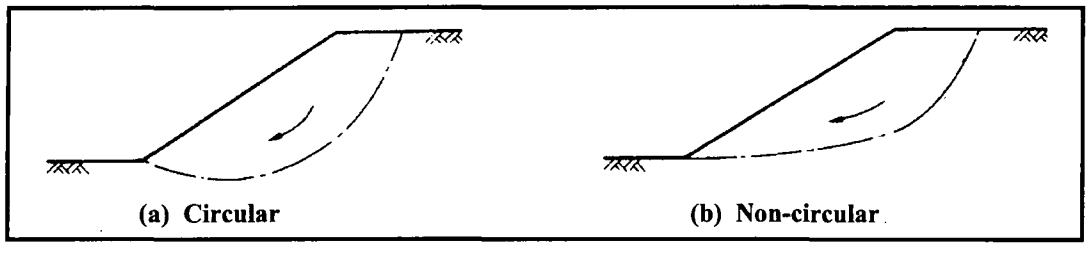


**Figure 5.1: Circular and non-circular rotational failures**
Source: Craig, 1978

The results of a stability analysis are usually expressed by a Factor of Safety, which is applied to the shear strength of the soil and can be used to predict instability. Alternatively, the analysis can be adapted to give the slope angle at which failure will occur, the highest groundwater level or the ultimate surface loading that generates instability. In general different failure surfaces are examined and the one yielding the smallest Factor of Safety determined (Nash, 1987).

Slope stability analysis has wide application. It may be used for the analysis of slopes with complicated geometry, non-homogeneous soil conditions, seepage and for circular or non-circular failure surfaces. With the advent of computers the use of stability analysis has become routine (Nash, 1987) and more complex analysis can be performed (Selby, 1993). Microcomputer availability has increased the use of models such as the Finite Element Method and an improved representation of soil stress-strain states (Duncan, 1996 *in* Allison, 1996). However despite their wide use, all stability analysis have limitations (Allison, 1986) since they are dependent on theoretical models adopted for the slope and the soil. Measured values may not be entirely representative of overall mean site conditions (Allison, 1986).

## 5.2 Factor of Safety

The stability of a slope is usually expressed in terms of a Factor of Safety (Fs) (Selby, 1993), defined by the relationship between forces tending to resist driving stresses and forces tending to disturb the slope material causing it to move (Cooke and Doornkamp, 1990). In simpler terms it is the ratio between shear strength and shear stress. When the Factor of Safety is equal to unity, forces promoting stability are exactly equal to the forces promoting instability. When the Factor of Safety is smaller than unity, the slope is in a condition of failure. When the Factor of Safety is larger than unity, the slope is likely to be stable (Selby, 1993). Most natural slopes on which landslides occur have Factor of Safety values between 1 and 1.3. Earthquakes, undercutting and high pore water pressures reduce this value and trigger landsliding (Selby, 1985).

The calculation of the Factor of Safety depends upon measurement of the geotechnical properties of the slope materials (Petley, 1984 *in* Cooke and Doornkamp, 1990). The Factor of Safety can only be calculated when there is an appropriate method of analysis. In an analysis, the Factor of Safety is evaluated for the most critical surface or circle which yields the lowest Factor of Safety value (Terzaghi and Peck, 1967; Lambe and Whitman, 1979; Barnes, 1995 and Coduto, 1999). The Factor of Safety of a slope decreases as the pore pressure increases, and the most critical condition will occur when pore pressures are greatest (Barnes, 1995).

Although the Factor of Safety approach provides a good understanding of the parameters which promote movement, it has limited applicability to some situations. This is because both cohesion and pore water pressure are highly variable on most natural slopes, even over short distances and brief periods of time (Summerfield, 1991). Another reason is that the Factor of Safety is determined using geotechnical data which may fail to consider external factors that are likely to influence slope stability. Geomorphological studies consider these external influences and help to identify sites that are likely to fail.

## 5.3 Slope stability models

The analysis of slopes has its origin in the work of Coulomb in 1776, when he introduced the concept that shear resistance of a soil is the sum of cohesive and frictional components (Heyman, 1972 *in* Nash, 1987). During the first half of the nineteenth century, field observations were made of slides in cuttings and embankments, mainly associated with construction of the railways and canals. Gregory and Colthurst (1840s) reported failures in Britain and Collin (1846) studied a number of failures in clays in France and concluded that slip surfaces are generally curved (Nash, 1987).

In the early part of the last century the more modern methods of stability analysis were developed in Sweden (Petterson, 1955; Bjerrum and Flodin, 1960 *in* Nash, 1987). During the construction of Gothenberg harbour there were several failures of

quay walls and in 1910 Fellenius developed the wedge analysis. This analysis assumed frictional behaviour of the soil and it was followed by the friction circle method presented by Hultin and Peterson in 1916. The discovery of the principle of effective stress by Terzaghi in the early 1920s led to its incorporation into stability analysis with pore pressure specified as an independent variable (Nash, 1987). In 1955 Bishop presented his Method of Slices for circular arc analysis, a method which is still widely used today. Similar methods were developed for the analysis of slips on non-circular slip surfaces (for example Janbu *et al.*, 1956). The above methods are considered as Limit Equilibrium Methods of analysis (Nash, 1987).

Limit Equilibrium Methods form a major framework for analysis of slope stability (Craig, 1978; Atkinson, 1981; Sidle *et al.*, 1985; Anderson and Richards, 1987 and Coduto, 1999). Atkinson (1981) lists several advantages that make the Limit Equilibrium Method the most widely used method for examining the stability of soil structures. Limit Equilibrium analyses first define a potential failure surface, which is where shearing would occur if the slope were to fail (Coduto, 1999). The analyses aim to compute an average Factor of Safety that defines the ratio of the stresses resisting failure to the stresses required to bring a slope into a state of limiting equilibrium along a given failure surface (Sidle *et al.*, 1985). Most Limit Equilibrium analyses are two-dimensional (Craig, 1978; Coduto, 1999) and are applicable to the analysis of slopes in static equilibrium. They are not well suited to the analysis of dynamic stability of slopes, such as debris flows, avalanches and slopes under earthquake loading (Nash, 1987).

Limit Equilibrium analysis make use of the Method of Slices. In this method, a circular arc slip surface is presumed and the soil segment is divided into a number of approximately equal vertical slices for convenience of analysis (Figure 5.2). The forces acting on each slice are computed and summed for the whole mass (Atkinson, 1981; Goudie *et al.*, 1990). The basis of the Method of Slices lies in the fact that the normal stress acting at a point of the failure arc should be influenced mainly by the weight of soil lying above that point (Lambe and Whitman, 1979).

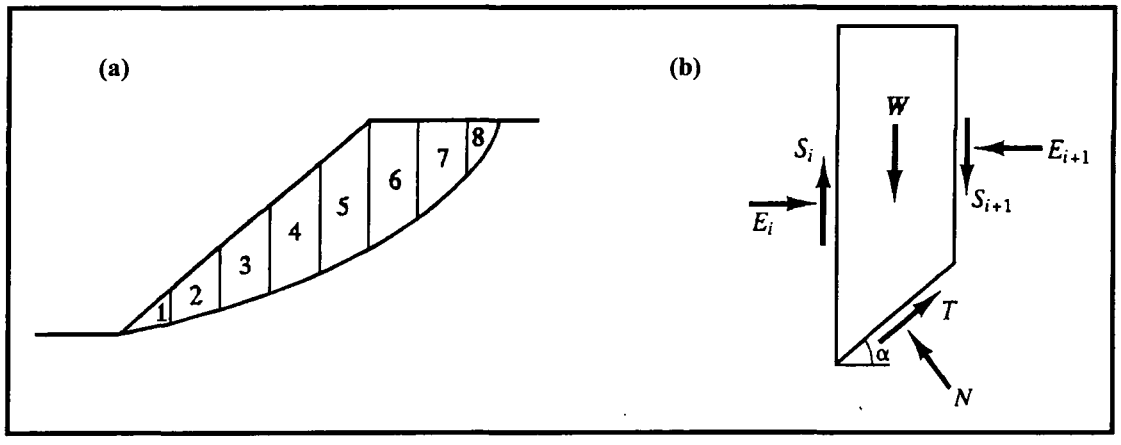


**Figure 5.2: (a) Division of failure mass into vertical slices**
**(b) Summary of forces acting on each slice**
Source: Coduto, 1999

The method of analysis by slices was first proposed by Fellenius (1936 *in* Selby, 1993). Despite errors in determining the Factor of Safety, Fellenius Method (also known as the Ordinary or Swedish Method of Slices) is widely used because of its simplicity and because it is possible to do hand calculations. The method has now been programmed for computers (Lambe and Whitman, 1979). The Fellenius Method treats each slice as though it were nearly rectangular and assumes that the forces acting upon the sides of any slice have zero resultant in the direction normal to the failure arc for that slice (Lambe and Whitman, 1979; Coduto, 1999). For a slice with a curved base and an upper surface which is not parallel to the failure plane corrections have to be made. An alternative method was proposed by Bishop (1955) to take slip surface curvature into account. It was simplified by Janbu *et al.* (1956).

Bishop (1955) originally presented his method for analysis of circular slip surfaces but it can be applied to non-circular slip surfaces by adopting a fictional centre of rotation. In this method it is assumed that the interslice shear forces may be neglected. The total normal force is assumed to act at the centre of the base of each slice, and is determined by resolving the forces on each slice vertically. By taking moments about the centre of the circle the overall stability is examined and a value of the Factor of Safety is obtained (Nash, 1987). The Simplified Bishop Method over-determines the problem and values of the Factor of Safety are not exact. However it was shown by several examples that the method gives values for the Factor of Safety

which fall within the range of more rigorous methods and is recommended for general practice. Hand calculations are possible and computer programs are available (Lambe and Whitman, 1979). The Bishop Method is the recommended method for circular failure surfaces (Coduto, 1999).

Janbu *et al.* (1956), following Bishop's work, published one of the first routine methods for the analysis of non-circular slip surfaces. In this method the assumption is made that the interslice shear forces are zero and thus the expression obtained for the total normal force on the base of each slice is the same as that obtained by Bishop. By examining overall horizontal force equilibrium a value of the Factor of Safety is obtained. This method of analysis over-specifies the problem. In general, overall moment equilibrium is not satisfied. Like the Bishop Method it is amenable to hand calculation and so is useful in practice (Nash, 1987).

## 5.4 Slope stability analysis of the three field sites

Slope stability analysis is important to this research as it enables a quantitative assessment of the stability of Blue Clay slopes for the north-west coast of Malta and instability can be predicted. This was not possible during geomorphological and geotechnical analysis. Stability analysis thus provides a link with the other main aspects of this study, namely geology, geomorphology and geotechnical investigations. The analysis should be regarded as complementary to this study rather than be considered as the main objective of the research.

Techniques used in this thesis involve a two-dimensional analysis of three-dimensional problems, using the Limit Equilibrium Method of analysis. Geomorphological mapping proves to be useful since critical parameters not included in geotechnical investigation can be identified. Although there are several slope stability models, it is very rare to find more than one model relevant to any specific study. Consequently it is very important to identify the most suitable model (Allison, 1986).

Since effective stress is a better indicator of soil strength, an effective stress analysis was performed for the purpose of this research. In this type of analysis the effective strength parameters are evaluated using appropriate laboratory tests, computing the effective normal stress along the failure surface and computing the shear strength using Mohr-Coulomb equation (Coduto, 1999). The pore pressure is specified as an independent variable (Nash, 1987). In practice this is achieved if the failure mass of soil is divided into a number of slices, such as with the Bishop Method of Slices.

### 5.4.1 Choice of model

Initially slope stability analysis for this research was performed using both the Bishop and Janbu methods. However Bishop's Method (1955) was chosen to perform slope stability analysis on Blue Clay slopes as the Factor of Safety for circular failure surfaces calculated by Bishop's Method is greater than the value from Janbu's formulation. The Bishop's Factor of Safety value is generally within 5% of the Factor of Safety values that are calculated by more rigorous methods such as the General Limit Equilibrium method. For this reason, the Simplified Bishop Method is generally used for the analysis of circular failure surfaces. Janbu's Method is more flexible as the formulation can be applied to calculate the Factor of Safety for circular and non-circular surfaces. The Simplified Bishop Method has been formulated for circular surfaces only and cannot be used for non-circular surfaces.

Another reason for selecting Bishop's Method (1955) for the analysis of Blue Clay slopes is because all the required parameters can be measured in the field and in the laboratory at each field site. Slope geometry and material geotechnical properties have been determined in previous investigations and used for the stability analysis. In this method all input variables can be kept constant. Alternatively an individual parameter can be changed to examine how this influences overall stability. In this case the pore pressure ratio ($r_u$) was changed to study its effect on the stability of Blue Clay slopes by identifying the critical phreatic conditions at which the slopes fail.

A computer program was utilised to perform the analysis of slopes for the three coastal sites where previous geomorphological and geotechnical investigations have

been undertaken. The computer program utilised for slope stability analysis is XSTABL. This is a fully integrated slope stability analysis program which permits the development of slope geometry. XSTABL consists of two interactive but separate parts: a data preparation interface and a slope stability analysis. The program uses the Method of Slices to perform a two-dimensional Limit Equilibrium analysis to compute the Factor of Safety for a slope according to General Limit Equilibrium (GLE) Method, Janbu's Generalized Procedure of Slices (GPS), Simplified Bishop and Simplified Janbu.

The Simplified Bishop and Janbu Methods of analysis are used by the program for all search analyses which are used to identify the most critical surface with the lowest Factor of Safety. The use of the computer program in performing the stability analysis offers a number of advantages.

i. Once the basic input data have been entered, the program allows for other data to be varied.
ii. The most critical slip surface along which failure is likely to occur can be determined.
iii. Current state of stability of the monitored slopes can be assessed by utilising measured parameters and predicted data.
iv. Calculations are computed quickly enabling a large number of analyses to be carried out over a short period of time.

Despite the advantages it should be noted that stability models are simplifications of reality and can exclude important data. A model simulates the effect of an actual or hypothetical set of processes, and forecasts one or more possible outcomes. Models can never fully represent the real world, but can only be analogies or analogues which have some features and behaviours in common with it (Kirkby *et al.*, 1993). Selby (1982 *in* Allison, 1986) suggests that an error factor of $\pm$ 10% in modelling can be supplemented by mapping which can improve the knowledge of local conditions. The geomorphological mapping exercise discussed in chapter 3 provides additional information, such as the presence and location of mass movement processes and landforms, on the north-west coast of Malta with special reference to the three study sites.

### 5.4.2 Input data

At the start of a stability analysis, it is necessary to know the geometry of the slide mass which is bounded by the shear plane and ground surface. The other parameters necessary to complete stability analysis can be understood from Coulomb's failure law (Nash, 1987; Goudie *et al.*, 1990). Coulomb's law indicates that the weight of the slide mass (unit weight), pore water pressure and strength parameters need to be known in order to calculate all the relevant forces in a stability analysis. Stability is also dependent upon overall slope height and angle (Goudie *et al.*, 1990). A good appreciation of the geology and hydrogeology is essential, and often it is useful to classify the instability mechanism. In general a two-dimensional analysis will be made, and the geometry must be simplified so that representative cross-sections may be drawn (Nash, 1987).

The greatest uncertainties in stability problems arise in the selection of the pore pressure and strength parameters (Lambe and Whitman, 1979). The distribution of pore pressures within the slope is required if an effective stress analysis is being carried out. Where possible this is obtained from instrumentation in the field. However often a model of groundwater is needed as a basis to interpret observations and for interpolation (Nash, 1987).

The data required for the stability analysis has been collected during geomorphological and geotechnical investigations and discussed in chapters 3 and 4. It includes data on the slope geometry and material strength which includes cohesion, angle of internal friction, and bulk unit weight. Data for the slope profile was entered in terms of x and y coordinates corresponding to horizontal distance and vertical height above sea-level respectively. Data for the slope geometry was collected during surveying whereas the strength parameters were measured during laboratory testing. The user is also required to specify the number of soil units, that is if the slope is composed of soil materials with different properties. In this case there was only one soil unit, since the investigated slopes are all composed of Blue Clay. The default is set for isotropic conventional strength, using the Mohr-Coulomb equation.

Since the strength parameters were determined and an effective stress analysis was performed, the pore pressure is specified as an independent variable. Pore pressure ratio ($r_u$) value was used in this analysis since pore water pressure was not measured in the field due to lack of instrumentation and because the precise distribution of pore pressures is unknown. The pore pressure ratio value is the ratio between the pore pressure and the total vertical stress at the same depth and can be used to represent overall or local pore pressure conditions in a slope (Barnes, 1995). Typically pore pressure ratio values are usually less than or equal to about 0.5. Larger values are likely to give numerical problems when using XSTABL. In this program the pore pressure ratio permits a search for the most critical surface. However it is usually reserved for estimating the Factor of Safety value from slope stability charts or for assessing the stability of a single surface.

The pore pressure ratio represents overall pore pressure conditions in Blue Clay slopes and is the only variable parameter for the whole analysis. For the first analysis at each site the pore pressure ratio is set at 0.0. This ratio increases by a factor of 0.05 each time a new analysis is performed until the ratio generates a calculated Factor of Safety which is less than unity, indicating a state of instability. At this point other analyses were not performed, since the transition between stability and instability is established. Differences can be observed between the three sites where instability is reached at different pore pressure ratio values.

The computer program generates an input file which contains all the required data to perform the analysis. XSTABL offers a selection of five different analyses. For the purpose of this study the Circular Surface Search is chosen. The user is required to select either the Bishop Method or the Janbu Method for calculating the Factor of Safety. In this type of analysis the user is required to establish the number of failure surfaces to be generated (in this case this is set at ten), the number of surfaces to be generated from each failure surface (this is set as 1) and the initiation and termination points in terms of the x-coordinates where the surfaces should be generated along the slope profile.

XSTABL changes the input file into an output file, which permits the actual slope stability analysis to be performed on the basis of the input data. A plot of the geometry of the slope profile is generated first. This is followed by another plot which generates all the failure surfaces previously requested. The final plot displays the ten most critical surfaces. The surface with the lowest Factor of Safety is considered as the most critical surface along which failure is likely to occur. This surface is clearly distinguished on the plot. The plots are displayed for each of the three sites in Figures 5.3, 5.4 and 5.5. In the output file the stability analysis generates the x and y coordinate points for the most critical circular failure surface analysed by the Simplified Bishop Method and a summary of the ten most critical surfaces for the whole analysis. For each surface the Factor of Safety, circle centre x and y coordinates, radius of the circles used during the analysis as failure surfaces, initial and terminal x coordinates and resisting moment are given. Results of the output files for all the three investigated sites are presented in the Appendix.

### 5.4.3 Stability analysis

Slope stability analysis was conducted on coastal slopes previously identified for geomorphological and geotechnical investigations at Gnejna Bay, Ghajn Tuffieha Bay and Rdum id-Delli. The geometry of slope profiles and Factor of Safety results for each of the three sites are presented in sections 5.4.3.1 and 5.4.3.2 respectively. A discussion on the interpretation of results as related to the key issue of slope stability follows in section 5.4.3.3.

#### 5.4.3.1 Slope geometry

The slope profile at Gnejna Bay (Figure 3.17, Table 3.1) shows a remarkably steep gradient at the rear of the slope (mean gradient 35.49°); whereas the main part (mean slope angle is 23.50°) and the toe slope area (mean slope angle is 25.20°) are gentler. The mean gradient for the entire slope is 26.31° (Table 5.1). The profile extends along the entire slope from the toe lobe to the rear part at the base of the Upper Coralline Limestone plateau. It covers a horizontal distance of 132.77 m and reaches a maximum height of 71.68 m above sea-level. The toe is situated at an elevated height of 9.28 m resting above a Globigerina Limestone cliff. The profile is divided into 14 segments.

## Table 5.1: Mean gradient characteristics of surveyed slopes

| *Gnejna Bay* | | *Ghajn Tuffieha Bay* | | *Rdum id-Delli* | |
|---|---|---|---|---|---|
| ***Slope sections*** | ***Mean gradient (°)*** | ***Slope sections*** | ***Mean gradient (°)*** | ***Slope sections*** | ***Mean gradient (°)*** |
| Toe area | 25.20 | Toe area | Bulge - 31.20<br>Flat top - 10.89 | Toe area | 16.38 |
| Main section | 23.50 | Main section | 19.34 | Main section | 22.32 |
| Rear part | 35.49 | Rear part | 23.04 | Rear part | 27.78 |
| Entire slope | 26.31 | Entire slope | 19.22 | Entire slope | 22.20 |
| **Angle of internal friction** | **30.00** | **Angle of internal friction** | **25.00** | **Angle of internal friction** | **22.50** |

At Ghajn Tuffieha Bay, the slope profile (Figure 3.19 and Table 3.2) extends from the base of the Upper Coralline Limestone plateau to sea-level. The toe of the slope is marked by a steep gradient (31.20°) which bulges on the beach. The main part of the slope stretches over a horizontal distance of 125.94 m and has a mean slope angle of 19.34°. The rear part of the slope steepens again and reaches a mean gradient of 23.04°. The mean gradient for the entire slope excluding the beach is 19.22° (Table 5.1). The slope is divided into 22 segments. It stretches over a horizontal distance of 226.77 m and reaches a maximum height above sea-level of 74.31 m.

The slope profile at Rdum id-Delli (Figure 3.21 and Table 3.3) is characterised by a flattened area at the lower part of the slope (mean slope gradient is 16.38°), a gentle main slope section (mean slope gradient is 22.32°) and a steeper rear slope (mean slope gradient 27.78°). The mean gradient for the entire slope is 22.20° (Table 5.1). The slope stretches over a horizontal distance of 118.35 m and reaches a maximum height of 44.81 m above sea-level. This profile is shorter than the profiles at Gnejna Bay and Ghajn Tuffieha Bay. The surveyed slope stretches from the base of the small cliff below the Upper Coralline Limestone plateau towards the Globigerina Limestone cliff where this is interrupted by boulder scree at sea-level. The slope geometry consists of 12 segments.

The data presented in this section and in chapter 3, together with field observations indicate that the steepest slope profile is that at Gnejna Bay, whereas Ghajn Tuffieha Bay has the lowest mean slope angle. The gradient at Rdum id-Delli lies between those of the other two sites. In all three cases the rear part of the slope tends to be steeper when compared with the rest of the slope (Table 5.1). The main slope section has usually the most gentle gradient which is similar to the mean gradient for the entire slope. The toe area is steeper than the main section. At Ghajn Tuffieha Bay, the toe area is characterised by two distinct parts: a top flat area and a steep slope bulging onto the sandy beach below. The bulge is the steepest part of the entire slope. At Rdum id-Delli the toe of the slope is identified by a flat area. In this case the gradient is gentler than that of the main section (Table 5.1).

### 5.4.3.2 Factor of Safety values

XSTABL accepted all input data for the three sites. Thus it is assumed that the measured slope geometries and strength parameters are indicative of site conditions. The measured parameters used as initial input data were used in the analysis to calculate Factors of Safety, which determine quantitatively the stability conditions of the investigated slopes at each of the three coastal sites. Computations of the Factor of Safety and a summary of the ten most critical failure surfaces generated by the Simplified Bishop Method for each analysis for the three sites are presented in the Appendix.

Various values for the Factor of Safety are presented for each investigated slope (Table 5.2) since several analyses were performed for each site to determine the critical conditions under which failure occurs. A range of results is more relevant especially when considering the geotechnical aspect of this study. The latter involves measurement of parameters which can vary through time and space, influencing the overall stability conditions. Ultimately when interpreting results Factor of Safety values can be linked with laboratory data to assess slope stability.

At Gnejna Bay, eight stability analyses were performed using the Simplified Bishop Method, generating eight Factor of Safety values (Table 5.2). Plots generated by the stability analyses are shown in Figure 5.3. All parameters were kept constant except for the pore pressure ratio. This was changed each time an analysis was carried out until an unstable condition was reached. Assuming the pore pressure ratio to be zero, the calculated Factor of Safety is very high (1.554) indicating stable conditions. As the pore pressure ratio starts to increase, the Factor of Safety value decreases leading to instability. It is noted that as the pore pressure ratio increases by a factor of 0.05 each time a new analysis is performed, the Factor of Safety decreases by a factor of around 0.089. The slope remains stable until the pore pressure ratio is 0.30 and the corresponding Factor of Safety is close to unity (1.020). The transition between stability and instability is reached when the pore pressure ratio is increased to 0.35. The value of the Factor of Safety in this case is below unity (0.932) indicating instability (Table 5.2).

**Table 5.2: Calculated Factor of Safety values using the Simplified Bishop Method**

| *Gnejna Bay* | | *Ghajn Tuffieha Bay* | | *Rdum id-Delli* | |
|---|---|---|---|---|---|
| *Pore pressure ratio* | *Factor of Safety* | *Pore pressure ratio* | *Factor of Safety* | *Pore pressure ratio* | *Factor of Safety* |
| 0.00 | 1.554 | 0.00 | 1.391 | 0.00 | 1.181 |
| 0.05 | 1.465 | 0.05 | 1.314 | 0.05 | 1.115 |
| 0.10 | 1.376 | 0.10 | 1.236 | 0.10 | 1.049 |
| 0.15 | 1.286 | 0.15 | 1.158 | 0.15 | 0.984 |
| 0.20 | 1.197 | 0.20 | 1.080 | | |
| 0.25 | 1.109 | 0.25 | 1.003 | | |
| 0.30 | 1.020 | 0.30 | 0.925 | | |
| 0.35 | 0.932 | | | | |

**Figure 5.3: Slope stability plots for Gnejna Bay generated by the Simplified Bishop Method**

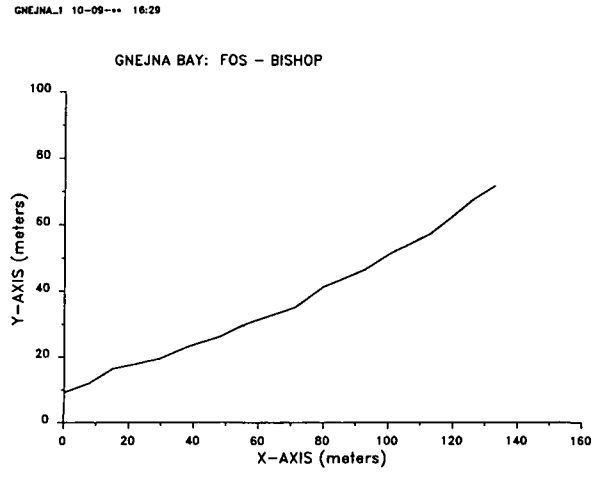


**(a) Slope profile**

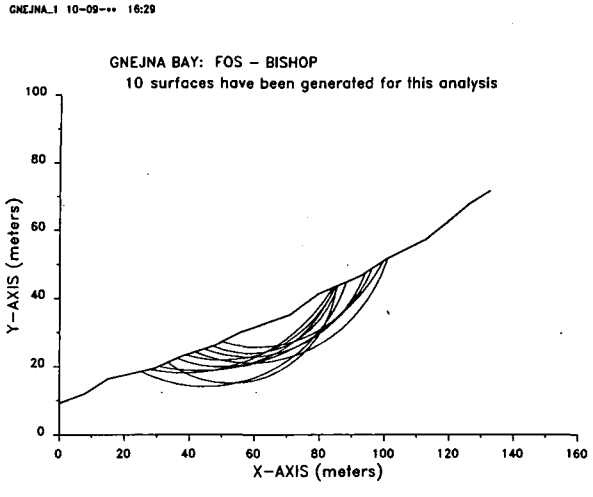


**(b) Generated failure surfaces**

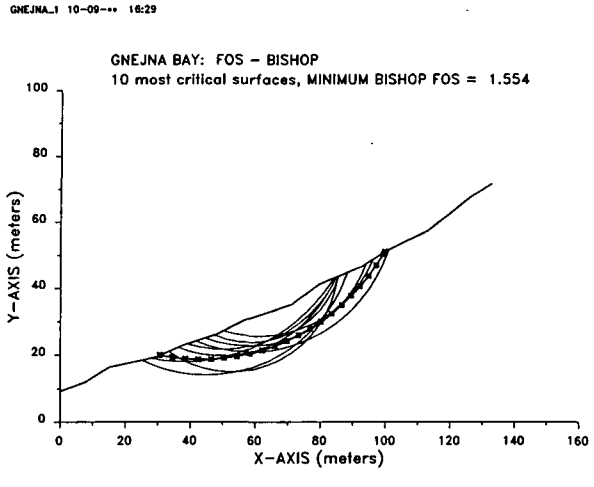


**(c) Critical failure surfaces**

At Ghajn Tuffieha Bay, seven stability analyses were carried out using the Simplified Bishop Method. Seven Factor of Safety values are produced (Table 5.2). Plots generated by the stability analyses are shown in Figure 5.4. The pore pressure ratio is the only variable that kept changing during the different analyses to identify the critical phreatic conditions when the slope fails. When it was assumed that the pore pressure ratio was zero, the slope was at its maximum stable condition, yielding a Factor of Safety of 1.391. The subsequent analyses show a decrease in the Factor of Safety by a factor of around 0.078 as the pore pressure ratio increased by a factor of 0.05. The slope remains in a stable state until the pore pressure ratio is 0.25 producing a Factor of Safety of 1.003. Instability is reached when the pore pressure ratio is increased to 0.30, yielding a Factor of Safety below unity (0.925) (Table 5.2).

At Rdum id-Delli only four stability analyses were carried out using the Simplified Bishop Method. Thus four Factor of Safety values were calculated (Table 5.2). Plots generated by the stability analyses are shown in Figure 5.5. The pore pressure ratio was varied for each analysis to determine the critical phreatic conditions at which the investigated slope fails. When the pore pressure ratio is assumed to be zero, the Factor of Safety is 1.181. The Factor of Safety decreased by a factor of around 0.066 as the pore pressure ratio increased by a factor of 0.05 (Table 5.2). The slope remains stable until the pore pressure ratio is 0.10 yielding a Factor of Safety which is slightly higher than unity (1.049). The transition between stability and instability is reached when the pore pressure ratio is 0.15 yielding a Factor of Safety of 0.984 (Table 5.2).

**Figure 5.4: Slope stability plots for Ghajn Tuffieha Bay generated by the Simplified *Bishop Method***

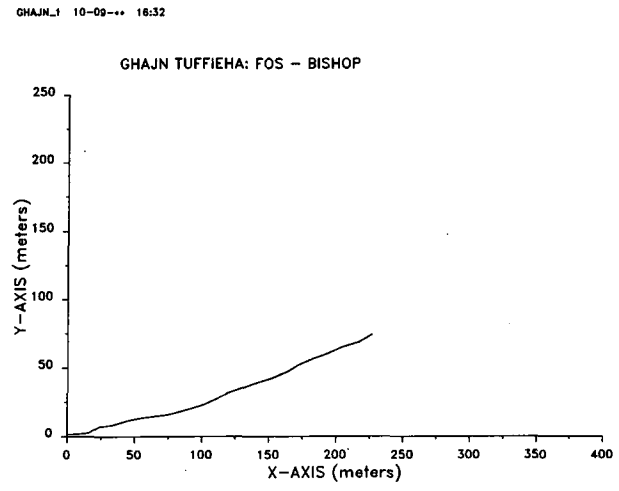


**(a) Slope profile**

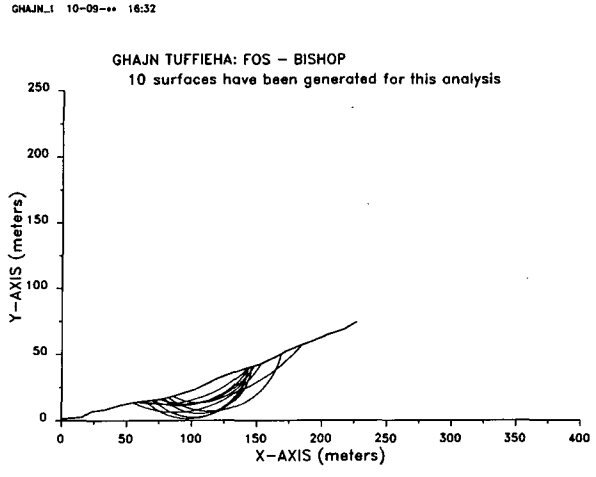


**(b) Generated failure surfaces**

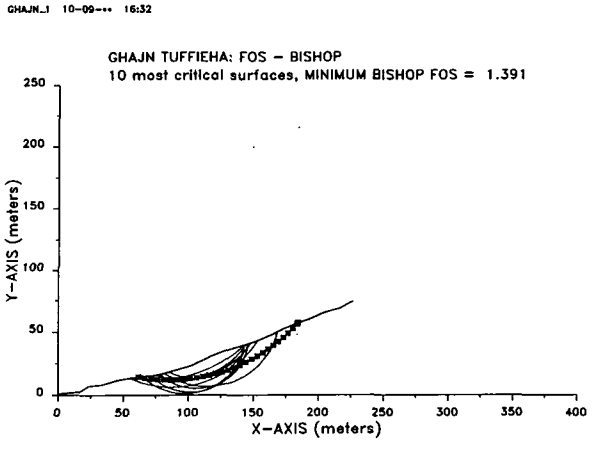


**(c) Critical failure surfaces**

**Figure 5.5: Slope stability plots for Rdum id-Delli generated by the Simplified Bishop Method**

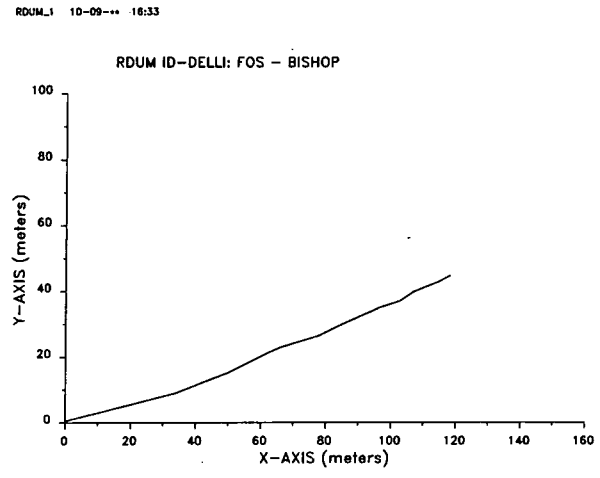


**(a) Slope profile**

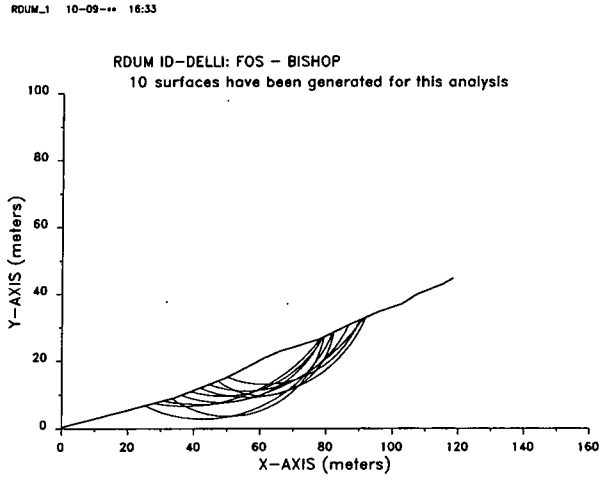


**(b) Generated failure surfaces**

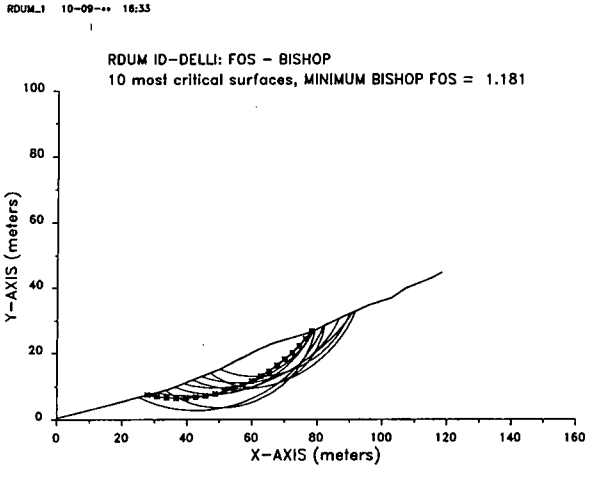


**(c) Critical failure surfaces**

### 5.4.3.3 Discussion and interpretation of results

The maximum slope at which the material is stable is referred to as the angle of repose. The angle of repose is fundamentally related to the peak friction angle (Lambe and Whitman, 1979). If the angle of internal friction is equal to the slope angle, the Factor of Safety is equal to unity. If the angle of internal friction is larger than the slope angle, the Factor of Safety is greater than unity yielding a stable slope. Instability and sliding will occur when the angle of internal friction is less than the slope angle (West, 1995). Gradient characteristics of the selected slopes can therefore provide a significant assessment of slope stability when compared with the angles of internal friction measured in the laboratory. The difference between slope angle and friction angle is that slope angle refers to the gradient of the slope measured in the field whereas friction angle refers to the angle of internal friction determined from geotechnical tests on the material carried out in the laboratory.

In the case of Gnejna Bay, the mean gradient for the entire slope is smaller than the angle of internal friction, indicating stable conditions (Table 5.1). This is also confirmed through geomorphological and geotechnical investigations. The average gradient is greater than the angle of internal friction only at the rear part of the slope. This indicates that this is the most unstable part of the slope where perhaps the highest pore water pressures are found. The main section and toe area seem to be in a stable condition as their gradients are lower than the angle of internal friction.

At Ghajn Tuffieha Bay the mean slope gradient for the entire slope is less than the angle of internal friction. The rear part, main section and upper toe area seem to be stable and have a mean gradient smaller than the angle of internal friction. There is an indication of instability at the lower bulge of the toe area which extends on the beach. The gradient in this part is steep (31.20°) and greater than the angle of internal friction (Table 5.1). It should also be noted that Ghajn Tuffieha Bay which is the site most prone to instability has the lowest mean slope angle of all three sites. This indicates that other factors besides the gradient influence slope stability.

Interpretations regarding the comparison of the mean gradient characteristics with the angle of internal friction at Rdum id-Delli are similar to Gnejna Bay. The mean

gradient for the entire slope is lower than but almost equal to the angle of internal friction (Table 5.1). As in the case of Gnejna Bay, the rear part seems to be unstable and its gradient is greater than the angle of internal friction. It can be assumed that pore water pressures are high on this part of the slope. This assumption can only be confirmed if the pore water pressure distribution for this slope is measured on site by means of appropriate instrumentation, such as piezometers.

Additional to and more important than the relationship between the slope gradient and angle of internal friction, stability for Blue Clay slopes has been determined by modelling the slopes under study. The information used as input data to run the slope stability modelling was collected and measured in late winter and throughout spring. Consequently the stability analyses for this study simulate spring conditions characterised by a lower amount of rainfall and lack of moisture when compared with the rainy season. For this reason slopes were in a stable condition when measurements were recorded. This is also indicated by geotechnical testing, which has revealed that at the time of data collection, clay was dry and acting as a solid material. This factor explains the high Factor of Safety values calculated when performing the stability analyses. Collection of data during the winter months would have presented a different situation. A high amount of rainfall results in an increase in moisture content and pore water pressure leading to unstable conditions. During the winter months Factor of Safety values would be lower than the values presented in section 5.4.3.2, due to an increase in moisture content and a decrease in material strength.

The Factor of Safety values for Gnejna Bay are the highest for the three sites. The results presented in the previous section indicate stable conditions. Instability will take place when the pore water pressure is high, perhaps during an exceptional rainy season. This has also been confirmed during field observations and geomorphological mapping which indicate slope stability conditions with no apparent sliding taking place. Geomorphological mapping has established that Gnejna Bay is well drained by a system of stable gullies generally situated at the lateral sides of the clay slopes. Consequently water exhibits itself as overland flow, preventing the accumulation of high pore water pressures in the material. This fact can be explained by the texture of

Blue Clay at this site which has a clay content of 44%, resulting in a more permeable type of soil, with a low water retention capacity.

Stability of a slope is effected to a large extent by internal friction and cohesion (Rahn, 1996). The angle of internal friction for Gnejna Bay is the highest for all three sites and the cohesion value is lower than that at Rdum id-Delli but higher than that at Ghajn Tuffieha Bay. This reflects the soil texture which is composed of equal proportions of clay and silt and a lower amount of sand. Laboratory testing for Gnejna Bay indicates that Blue Clay has a low moisture content, a high bulk density and bulk unit weight. The load bearing capacity of the material which is relevant to slope stability is indicated by the bulk density. The Activity Index at Gnejna Bay falls under the inactive category. Laboratory testing and field observation confirm the accuracy of the modelling exercise suggesting that the studied slope at Gnejna Bay is stable.

Stability analyses for Ghajn Tuffieha Bay generate lower Factor of Safety values than at Gnejna Bay for a given pore pressure ratio (Table 5.2). Instability at this site will also take place when the pore pressure ratio is high but this will be reached before Gnejna Bay. During geomorphological investigation no landslides were observed and slopes seemed to be in a stable condition. This observation corresponds to the Factor of Safety values indicating that the studied slope was stable when data were collected and confirms the accuracy of the slope stability analyses. Geomorphological mapping has revealed a concentration of active and stable gullies especially found at the lateral sides of bulges which back the entire stretch of the sandy beach. This indicates that there is an established drainage pattern and that the phreatic surface is high at the lowermost parts of the slopes.

Laboratory tests have showed that Blue Clay at this site has a low bulk density and bulk unit weight, low Plasticity Index, high moisture content and high water retention capacities leading to unstable conditions. Cohesion is lowest for all three sites, leading to a decrease in material strength. This is related to the soil texture which is composed of a high silt content contributing to a dilatant material and a lower clay percentage. High water retention and percolation rates suggest that the material can absorb a high amount of water, whilst remaining in a stable state. This is supported by high Factor

of Safety values which predict that instability will only occur at an exceptional high pore water pressure which the material will no longer be able to sustain. The high silt content at Ghajn Tuffieha Bay results in a more permeable soil, whereas the clay minerals may have a high swell capacity accounting for the high moisture content.

Factor of Safety values at Rdum id-Delli are the lowest for the three sites (Table 5.2). These show a significant decrease on the Factor of Safety values calculated for the other two sites at the same pore pressure ratios. Thus it can be assumed that instability at Rdum id-Delli is reached when the pore water pressures are low, compared with the other two sites. This is also confirmed from field observations and geomorphological mapping. It is evident that sliding events have occurred at this site, although at the time of data collection these landforms were stable. Mudslides will reactivate once the pore water pressure is increased as a result of rainfall, most significant during the winter months.

Rdum id-Delli exhibits similar physical and mechanical properties as at Gnejna Bay: low moisture content, high bulk density and unit weight and higher cohesion values, resulting in an increase in material strength. The high Plasticity Index indicates that the material has a high water retention capacity and is less permeable than the material found at the other two sites. This can cause an accumulation of high pore water pressure within the soil. Blue Clay at this site exhibits the highest cohesion value and lowest angle of internal friction for all the three sites. This is related to the texture of Blue Clay at Rdum id-Delli which has the highest clay content and lowest sand proportion for the three sites. Due to the high clay content, the soil is capable of absorbing and retaining a significant amount of water. Geotechnical investigations have concluded that Rdum id-Delli is the most stable site.

Slope stability analyses and low Factor of Safety values predict that at Rdum id-Delli instability is reached before the other two sites. This hypothesis may be related to the fact that once the clay is fully saturated and the swell capacity of the clay minerals is at its maximum, additional water creates excessive pore water pressures which are too large to be sustained resulting in sliding and instability. In this case the slope stability analyses also seem to reflect the prevalent situation, indicating that such an exercise can assess the current situation and predict instability with a high degree of accuracy.

Differences between the stability results derived from the laboratory and discussed in chapter 4 and modelling analyses, discussed in this section, are evident, especially with regards to Ghajn Tuffieha Bay and Rdum id-Delli. Laboratory results have determined that Rdum id-Delli is the most stable site, Gnejna Bay shows stability with a trend towards instability and Ghajn Tuffieha Bay is the site most prone to instability. The slope stability analyses have generated different Factor of Safety values for each site and the transition between stability and instability is reached at different pore pressure ratios. This transition is first reached at Rdum id-Delli followed by Ghajn Tuffieha Bay and Gnejna Bay respectively. Thus the stability analyses give the indication that Rdum id-Delli reaches instability before the other two sites. Gnejna Bay is the most stable site yielding the highest Factor of Safety values. Instability at Ghajn Tuffieha Bay is reached almost at the same stage as at Gnejna Bay when the pore pressure ratio is quite high, indicating that this is also a stable site.

Disparity in the stability results may arise from the fact that the results were determined using different techniques and data collected during geotechnical and geomorphological investigations. Stability results derived from the laboratory are based on analysis of samples tested in the laboratory. Results derived from the modelling analyses are based on a combination of lab data and other information related to slope surveying which could have influenced the overall stability assessment for Blue Clay slopes.

## 5.5 Conclusion

Stability analysis is important to this research as it provides additional details and information on issues relating to coastal slope stability for the north-west coast of Malta. By linking the results obtained from the stability analysis with laboratory tests and geomorphological mapping, significant interpretations and conclusions can be made. Both geomorphological mapping and geotechnical investigation suggest that the slopes at Gnejna Bay, Ghajn Tuffieha Bay and Rdum id-Delli are stable for most of the year. For example, from laboratory tests it was found that at all three sites,

Blue Clay behaves as a solid material since the moisture content is lower than the Plastic Limit. Also the presence of desiccation cracks especially at Gnejna Bay and Rdum id-Delli indicate loss of moisture as a result of dry conditions. Only during the winter months Blue Clay slopes are likely to experience instability as a result of high pore water pressures from rainfall.

Due to a high Plasticity Index, Blue Clay has a high swell capacity, lower permeability, is more compressible and consolidates over a longer period of time under load. This indicates that Blue Clay can absorb a significant amount of water before soil reaches a liquid state and instability occurs at high pore water pressure. This is also confirmed by Factor of Safety values calculated from the stability analyses. At Gnejna Bay and Ghajn Tuffieha Bay instability is reached when the pore pressure ratio is high, resulting from a fully saturated soil. Rdum id-Delli produces the lowest Factor of Safety values and the transition between stability and instability is reached before the other two sites. Gnejna Bay generates the highest Factor of Safety values for all three sites. Ghajn Tuffieha Bay also produces high Factor of Safety values, although they are significantly less than those at Gnejna Bay (Table 5.2).

The low cohesion values typical of the three sites result from Blue Clay being a dry soil with moisture contents below the Plastic Limit. It is interesting to note that Rdum id-Delli which has the highest cohesion value, indicating an increase in material strength, produces the lowest Factor of Safety values. It can be concluded that although the material is competent it becomes unstable more quickly than expected. In fact landslide activity was observed only at this site, indicating that mass movement processes are present although inactive during dry periods. Factor of Safety values and geotechnical data suggest an inverse situation for Ghajn Tuffieha Bay. Although the material at this site shows a decrease in strength, it remains stable even under saturated conditions. Instability is reached when the pore water pressure is exceptionally high to be sustained by the material.

Stability depends on a variety of parameters, such as cohesion, angle of internal friction, gradient, bulk unit weight and pore water pressure. It can be concluded from stability analyses that the investigated slopes are very sensitive to changes in the

phreatic surface and groundwater conditions simulated by changes in the pore pressure ratio. In all cases as the pore pressure ratio increases the Factor of Safety decreases leading to instability. High pore water pressures can be produced from rainfall, resulting in a decrease in shear resistance and consequently slope failure (Cooke and Doornkamp, 1990).

Various results of the Factor of Safety are presented for each site in Table 5.2 since several analyses were performed. This is more significant when analysing and interpreting slope conditions and relating results to other elements of the study. Additional detail is provided and previously measured parameters can be used and applied with more knowledge. Factor of Safety values show significant differences between the three sites. The transition between stability and instability is reached at different pore pressure ratios. The slope at Gnejna Bay remains the most stable slope at a high pore pressure ratio. This is followed by Ghajn Tuffieha Bay and Rdum id-Delli. Factor of Safety values decrease in this order. The modelling exercise proved to be useful as it determines the prevalent conditions at each of the three sites and predicts instability rigorously.

While recognizing the limitations, slope stability analyses have become a common analytical tool to assess the Factor of Safety for natural and man-made slopes (Fredlund, 1987) and overall failure conditions can be established with reasonable accuracy providing reliable results. The methods can offer solutions to stability problems and predict instability by identifying critical parameters which influence slope stability. This fact emphasizes the importance of undertaking slope stability analysis in major projects and research work of this type. The aim of a stability analysis is to provide a quantitative assessment of slope stability, supporting information and conclusions derived from other investigations. Consequently in the context of this research, this exercise should be regarded as providing a link to other elements of the study and should not be considered as a separate task independent from other investigations.

# *Chapter 6*

# *Conclusions*

## 6.1 Conclusions

This thesis presents an integrated study on mass movement processes along the northern coast of Malta. Particular attention is given to clay slopes. The aims of this study, listed in section 1.1, were to highlight the spatial distribution of coastal features, especially landslides; determine the mass movement processes; examine the relationship between geology and geomorphology; identify three key sites for detailed investigation; perform a geotechnical investigation to examine soil material; assess the current stability of Blue Clay slopes and determine the critical conditions resulting in slope failure.

The following work presented in the study makes an original contribution to knowledge.

A detailed geomorphological survey of coastal landforms north of the Great Fault was undertaken (chapter 3). This region was selected as it provides a challenging environment to conduct research. The structural setting (section 2.4.1) associated with the geological units exhibit a variety of landforms particularly at the coast. The region under study has always been included as part of integrated studies on the Maltese Islands and never dealt with separately.

Links between geology and geomorphology have been examined in section 3.5.1 and the spatial distribution of coastal landforms north of the Victoria Lines Fault has been described in section 3.5.2. Two geomorphological maps have been produced (Figures 3.5 and 3.6). Mass movement processes occurring along the northern coast are dealt in section 3.5.3. These fall under three main categories: slides, falls and creep. Slides and falls predominate the north-west coast and specific localities on the northern and north-east coasts. In Malta, rockfall can be considered as the most important mass movement process along the northern coast. This develops in the Upper Coralline Limestone Formation and varies in magnitude from debris to boulder scree and large blocks. Soil creep (section 3.5.3.5) is the least significant process identified at one locality - Rdum id-Delli, operating on soil within a Quaternary solution subsidence structure.

Slides are of three types: translational slides and rotational slides occurring in Upper Coralline Limestone and mudslides which develop in Blue Clay. The geological formations are described in chapter 2 (sections 2.3.2.3 and 2.3.2.5).

Translational slides (section 3.5.3.1) are found in several localities, but are more common on the north-west coast. Sometimes during movement slides can break up and become incorporated in mudslides or rockfall. Rotational slides (section 3.5.3.2) are usually situated below the *in situ* material from where they have been detached. Where multiple *en-echelon* failures occur, slides extend from the base of the Upper Coralline Limestone plateau to sea-level. Rotational slides are also common on the north-west coast. Both rotational and translational slides vary in magnitude. Rotational slides are usually smaller in length than translational slides. The latter can reach a length of 40 m, with an average range between 10 m to 15 m.

Mudslides (section 3.5.3.3) are evident where Blue Clay outcrops. Blue Clay is exposed in most of the localities on the north-west coast but it is also found in few localities on the northern and north-east coasts. Mudslides become active during the rainy season occurring in the autumn and winter months when moisture content and pore water pressure in the clay increases as a result of heavy and prolonged rainfall events.

Rockfall (section 3.5.3.4) is found extensively on the north-west coast and at specific localities on the north and north-east coasts. This process is related to different factors and occurs when blocks of rock are detached from the Upper Coralline Limestone plateau and either rest below or move away from *in situ* material. Rockfall can be classified under two categories: debris falls and boulder falls. Boulder falls extend from 10 m to 30 m in length. Debris falls result from the fragmentation of boulders and are very often found close to the larger blocks. Slab failure can be identified at several points where the Upper Coralline Limestone plateau exhibits faults or cracks parallel to the scarp face. Wedge and toppling failures are absent since failure of limestone blocks tends to occur along a set of discontinuities trending in the same direction and there is no indication of a forward rotational movement as the rock falls.

From the geomorphological survey three key sites have been identified for detailed investigation. The three sites, representative of the northern region, are Gnejna Bay, Ghajn Tuffieha Bay and Rdum id-Delli (section 3.6). A thorough description of the geology, geomorphological features and processes and hydrological pattern for each site can be found in sections 3.6.1, 3.6.2 and 3.6.3.

A slope transect was selected at each site to perform subsequent studies on material properties and stability analysis. A description of the selected slope transects can be found at the end of sections 3.6.1, 3.6.2 and 3.6.3 and in section 5.4.3.1. The steepest slope profile is that found at Gnejna Bay, whereas Ghajn Tuffieha Bay has the gentlest gradient. The rear part of the investigated slopes tends to be steeper when compared with the rest of the slope, whereas the main slope section has usually the most gentle gradient similar to the mean gradient for the entire slope. The toe area is steeper than the main section at Gnejna Bay and Ghajn Tuffieha Bay whereas it is gentler at Rdum id-Delli.

A detailed geotechnical investigation of Blue Clay has been conducted (chapter 4). This is the first time that this material has been subjected to detailed investigation. Previous geomorphological studies in Malta do not include information on material properties and behaviour which ultimately influences geomorphological processes and landform development. This new approach was introduced into geomorphological research fairly recently (for example Yatsu, 1966; Whalley, 1976 and Selby, 1982 *in* Hart, 1986) and it is now considered that geomorphological studies which lack information on material properties are incomplete (Goudie *et al.*, 1990).

Two types of tests were carried out on Blue Clay: physical properties tests (section 4.3) and geotechnical properties tests (section 4.4). The results are very important in assessing slope stability and understanding the mechanisms of mass movement processes operating on coasts. Physical and geotechnical properties tests indicate that Blue Clay shows variations at the three sites, although similarities are evident especially at Gnejna Bay and Rdum id-Delli. Ghajn Tuffieha Bay displays a low bulk density and high moisture content when compared with the other two sites (sections 4.3.1 and 4.3.2). This results in greater percolation and higher water retention capacities, increasing the chance for mudslide activity to take place. Gnejna Bay and

Rdum id-Delli have lower moisture content and higher bulk density (sections 4.3.1 and 4.3.2) indicating drier conditions and slower rates of movements especially evident with the widespread presence of desiccation cracks.

Particle size distribution tests (section 4.3.3) indicate that Blue Clay is composed of a high clay content, contributing to a cohesive material, a low sand proportion and silt content found in significant percentages especially at Ghajn Tuffieha Bay. These proportions of clay, silt and sand are found in different percentages for the three sites. However Gnejna Bay and Ghajn Tuffieha Bay exhibit a similar texture. Rdum id-Delli differs as the material is composed of a high percentage of clay which makes the soil less permeable. When the silt proportion is high, such as at Ghajn Tuffieha Bay, the soil is more permeable.

Atterberg Limits tests (section 4.3.4) and the related indices (especially the Liquidity Index and Consistency Index) have shown that Blue Clay at all three sites behaves as a solid material since the moisture content is lower than the Plastic Limit. This results in a stronger and competent material and more stable conditions. Due to a high Plasticity Index, Blue Clay experiences an increase in density under pressure and a decrease in specific volume. The Activity Index places Blue Clay within the inactive category for Gnejna Bay and Rdum id-Delli and within the normal category for Ghajn Tuffieha Bay. This is due to the variations in physical properties namely moisture content, bulk density and Plasticity Index.

Geotechnical tests (section 4.4) provide an indication of the strength of Blue Clay as controlled by cohesion and the angle of internal friction. Blue Clay at all three sites exhibits low cohesion values. Rdum id-Delli has the highest cohesion whereas Ghajn Tuffieha Bay has the lowest cohesion value. The angle of internal friction is high for all three sites. Rdum id-Delli has the lowest angle of internal friction, whereas the other two sites have higher friction angles.

Blue Clay can be classified as a soft clay. Stress-strain curves for Blue Clay (section 4.4) correspond best to rheological models applicable to elastoplastic materials, where initially the stress causes a recoverable strain but additional load causes permanent deformation. In the case of Gnejna Bay and Ghajn Tuffieha Bay, Blue Clay displays

a ductile behaviour at low stresses, whereas at higher stresses a brittle behaviour is noted. Rdum id-Delli displays brittle behaviour at all stresses, resulting in a more competent material than at the other two sites.

Interpretation of results derived from both the physical tests and geotechnical tests have reached three main conclusions. Rdum id-Delli is the most stable site; Gnejna Bay shows stability with a trend towards instability; Ghajn Tuffieha Bay is the site most prone to instability.

Slope stability analysis has been conducted (chapter 5) on previously surveyed Blue Clay slopes at each of the three sites to determine the current stability situation and the critical phreatic conditions which ultimately cause failure. The input data utilised in the stability analysis remained constant except for the pore pressure ratio which was the only variable parameter. Results have shown that the investigated slopes are very sensitive to changes in the phreatic surface and groundwater conditions simulated by changes in pore pressure ratio. In all cases as the pore pressure ratio increases the Factor of Safety decreases leading to instability.

The Simplified Bishop Method was utilised to perform the slope stability analyses and calculate Factor of Safety values for each of the three sites. Various Factor of Safety values are presented for each investigated slope since several analyses were performed at each site. Factor of Safety values indicate that the transition between stability and instability is reached at different pore pressure ratios for the three sites (section 5.4.3.2). Stability analyses for this study simulate spring conditions because input data used in the modelling exercise was collected and measured in late winter and throughout spring. Spring is characterised by a lower amount of rainfall and lack of moisture when compared with the rainy season. This factor explains the stable condition of slopes when measurements were recorded and the high Factor of Safety values calculated from the stability analyses (section 5.4.3.2).

A detailed discussion on the interpretation of Factor of Safety results as related to the issue of slope stability is found in section 5.4.3.3. Factor of Safety values are highest for Gnejna Bay, indicating stable conditions confirmed from geomorphological mapping and laboratory testing. Instability will occur when the pore water pressure is

very high. Ghajn Tuffieha Bay has generated lower Factor of Safety values than Gnejna Bay. Therefore instability is reached before Gnejna Bay but will still take place when the pore water pressure is high. During geomorphological mapping no active landslides were observed and slopes appeared to be in a stable condition. Rdum id-Delli exhibits the lowest Factor of Safety values for the three sites with a significant decrease on the other two sites. It can be assumed that instability is reached before the other two sites at low pore water pressures. Sliding events were observed during geomorphological mapping although at the time of the survey these were inactive. The results can be related to soil texture composed of a high clay content resulting in a less permeable soil with a high water retention capacity. High pore water pressure is accumulated and this will be too large to be sustained by the soil resulting in sliding. Slope stability analyses provide a very useful exercise in assessing the current situation and predicting instability with a high degree of accuracy. In all three cases the analyses reflect the prevalent situation as confirmed from geomorphological mapping and geotechnical investigation.

An indication of slope stability is also given when comparing gradient characteristics of the selected slopes with angles of internal friction measured in the laboratory (section 5.4.3.3). Such a comparison indicates stable conditions when the mean gradient of the entire slope is considered at all three sites. In the case of Gnejna Bay and Rdum id-Delli only the rear part appears to be unstable. Ghajn Tuffieha Bay shows instability at the lower bulge of the toe area which extends on the beach.

## *6.2 Update on previous studies*

The research presented in this thesis updates existing studies in a number of ways.

The research has contributed to new knowledge in terms of coastal mass movement processes in Malta, which lack or are very limited in other significant studies dealing with coastal geomorphology (for example Guilcher and Paskoff, 1975; Paskoff and Sanlaville, 1978; Ellenberg, 1983 and Paskoff, 1985). Previous studies are limited to the description of coastal landforms and related processes but do not deal with mass

movement processes and slope instability as main issues. Alexander (1988) includes some information on mass movements but this is very general and extremely limited offering only a sparse picture.

As already noted in chapter 1 (section 1.3) the interest in the geology of the Maltese Islands is supported by a significant amount of publications presented by various contributors dating back from the mid-19$^{th}$ century. For some reason, interest in the geomorphology of the islands has been less with few key studies (for example House *et al.*, 1961; Vossmerbäumer, 1972 and Alexander, 1988). Information on the physical and geotechnical properties of limestone and Blue Clay is inadequate and limited to some Civil Engineering and Architecture undergraduate dissertations. However the majority focus on limestone and lack information on clay material.

## *6.3 Recommendations for further research*

Recommendations can be made for further research.

i. Further studies on Blue Clay slopes will provide additional knowledge on mechanisms of mass movement processes operating on slopes. This study was limited to three sites. A larger number of sites would give a more realistic picture.

ii. Monitoring of mudslides using appropriate instrumentation to record the movement of specific mudslides over a period of time would be an advantage. The use of piezometers to measure pore water pressures and records of climatic data can give more accurate results regarding the triggering factors of slope failure but a number of years is required to collect a satisfactory set of data.

iii. A more extensive geotechnical investigation covering several sites will yield a greater amount of information. The physical and mechanical properties of Blue Clay could be determined in greater detail and spatial similarities and contrasts could be detected between sites.

iv. Clay mineralogy may have an influence on landslides, controlling properties such as moisture content, Atterberg Limits and other related indices especially Plasticity Index and Activity Index. X-Ray diffraction analysis would be useful in this context.

v. The coastal zone was examined in this study. Similar work can be applied to inland slopes where Blue Clay outcrops.

This thesis makes an important contribution in understanding mass movement processes on Blue Clay slopes for the northern coast in Malta. The multidisciplinary approach adopted for this study presents information on the study area and provides additional knowledge to geomorphological studies in general. The conclusions derived from this work should serve as a basis for further research, extending issues already dealt with in previous studies and contributing new information on coastal slope instability in Malta.

# *Appendix*

*Factor of Safety values calculated for Gnejna Bay*

Factors of Safety for Gnejna Bay have been calculated by the SIMPLIFIED BISHOP METHOD, when pore pressure ratio is **0.00**.

The most critical circular failure surface is specified by 22 coordinate points

| Point No. | x-surf (m) | y-surf (m) |
|---|---|---|
| 1 | 30.56 | 20.03 |
| 2 | 34.50 | 19.36 |
| 3 | 38.48 | 18.93 |
| 4 | 42.47 | 18.74 |
| 5 | 46.47 | 18.81 |
| 6 | 50.46 | 19.11 |
| 7 | 54.42 | 19.66 |
| 8 | 58.34 | 20.46 |
| 9 | 62.21 | 21.49 |
| 10 | 66.00 | 22.75 |
| 11 | 69.71 | 24.25 |
| 12 | 73.32 | 25.97 |
| 13 | 76.82 | 27.91 |
| 14 | 80.19 | 30.06 |
| 15 | 83.43 | 32.41 |
| 16 | 86.51 | 34.96 |
| 17 | 89.44 | 37.69 |
| 18 | 92.19 | 40.59 |
| 19 | 94.76 | 43.66 |
| 20 | 97.13 | 46.88 |
| 21 | 99.30 | 50.24 |
| 22 | 99.71 | 50.96 |

**Simplified BISHOP FOS = 1.554**

The following is a summary of the TEN most critical surfaces

| | FOS BISHOP | Circle Centre x-coord (m) | Circle Centre y-coord (m) | Radius (m) | Initial x-coord (m) | Terminal x-coord (m) | Resisting Moment (kN-m) |
|---|---|---|---|---|---|---|---|
| 1 | 1.554 | 43.46 | 83.99 | 65.25 | 30.56 | 99.71 | 3.49E+05 |
| 2 | 1.580 | 61.01 | 63.98 | 38.38 | 50.00 | 96.26 | 1.22E+05 |
| 3 | 1.642 | 38.53 | 72.17 | 54.08 | 27.78 | 84.08 | 1.81E+05 |
| 4 | 1.655 | 50.14 | 60.64 | 38.89 | 38.89 | 84.97 | 1.08E+05 |
| 5 | 1.668 | 57.95 | 61.45 | 38.75 | 44.44 | 94.07 | 1.55E+05 |
| 6 | 1.687 | 58.56 | 65.49 | 44.54 | 41.67 | 100.87 | 2.63E+05 |
| 7 | 1.760 | 58.36 | 52.29 | 28.56 | 47.22 | 85.55 | 7.52E+04 |
| 8 | 1.772 | 49.70 | 57.43 | 37.62 | 36.11 | 84.49 | 1.33E+05 |
| 9 | 1.884 | 44.87 | 60.18 | 46.10 | 25.00 | 88.28 | 3.13E+05 |
| 10 | 2.191 | 52.57 | 48.06 | 33.05 | 33.33 | 85.31 | 2.14E+05 |

Factors of Safety for Gnejna Bay have been calculated by the SIMPLIFIED BISHOP METHOD, when pore pressure ratio is **0.05**.

The most critical circular failure surface is specified by 22 coordinate points

| Point No. | x-surf (m) | y-surf (m) |
|---|---|---|
| 1 | 30.56 | 20.03 |
| 2 | 34.50 | 19.36 |
| 3 | 38.48 | 18.93 |
| 4 | 42.47 | 18.74 |
| 5 | 46.47 | 18.81 |
| 6 | 50.46 | 19.11 |
| 7 | 54.42 | 19.66 |
| 8 | 58.34 | 20.46 |
| 9 | 62.21 | 21.49 |
| 10 | 66.00 | 22.75 |
| 11 | 69.71 | 24.25 |
| 12 | 73.32 | 25.97 |
| 13 | 76.82 | 27.91 |
| 14 | 80.19 | 30.06 |
| 15 | 83.43 | 32.41 |
| 16 | 86.51 | 34.96 |
| 17 | 89.44 | 37.69 |
| 18 | 92.19 | 40.59 |
| 19 | 94.76 | 43.66 |
| 20 | 97.13 | 46.88 |
| 21 | 99.30 | 50.24 |
| 22 | 99.71 | 50.96 |

**Simplified BISHOP FOS = 1.465**

The following is a summary of the TEN most critical surfaces

| | FOS BISHOP | Circle Centre x-coord (m) | Circle Centre y-coord (m) | Radius (m) | Initial x-coord (m) | Terminal x-coord (m) | Resisting Moment (kN-m) |
|---|---|---|---|---|---|---|---|
| 1 | 1.465 | 43.46 | 83.99 | 65.25 | 30.56 | 99.71 | 3.29E+05 |
| 2 | 1.489 | 61.01 | 63.98 | 38.38 | 50.00 | 96.26 | 1.15E+05 |
| 3 | 1.549 | 38.53 | 72.17 | 54.08 | 27.78 | 84.08 | 1.71E+05 |
| 4 | 1.561 | 50.14 | 60.64 | 38.89 | 38.89 | 84.97 | 1.02E+05 |
| 5 | 1.573 | 57.95 | 61.45 | 38.75 | 44.44 | 94.07 | 1.46E+05 |
| 6 | 1.591 | 58.56 | 65.49 | 44.54 | 41.67 | 100.87 | 2.48E+05 |
| 7 | 1.660 | 58.36 | 52.29 | 28.56 | 47.22 | 85.55 | 7.10E+04 |
| 8 | 1.672 | 49.70 | 57.43 | 37.62 | 36.11 | 84.49 | 1.26E+05 |
| 9 | 1.779 | 44.87 | 60.18 | 46.10 | 25.00 | 88.28 | 2.95E+05 |
| 10 | 2.071 | 52.57 | 48.06 | 33.05 | 33.33 | 85.31 | 2.02E+05 |

Factors of Safety for Gnejna Bay have been calculated by the SIMPLIFIED BISHOP METHOD, when pore pressure ratio is **0.10**.

The most critical circular failure surface is specified by 22 coordinate points

| Point No. | x-surf (m) | y-surf (m) |
|---|---|---|
| 1 | 30.56 | 20.03 |
| 2 | 34.50 | 19.36 |
| 3 | 38.48 | 18.93 |
| 4 | 42.47 | 18.74 |
| 5 | 46.47 | 18.81 |
| 6 | 50.46 | 19.11 |
| 7 | 54.42 | 19.66 |
| 8 | 58.34 | 20.46 |
| 9 | 62.21 | 21.49 |
| 10 | 66.00 | 22.75 |
| 11 | 69.71 | 24.25 |
| 12 | 73.32 | 25.97 |
| 13 | 76.82 | 27.91 |
| 14 | 80.19 | 30.06 |
| 15 | 83.43 | 32.41 |
| 16 | 86.51 | 34.96 |
| 17 | 89.44 | 37.69 |
| 18 | 92.19 | 40.59 |
| 19 | 94.76 | 43.66 |
| 20 | 97.13 | 46.88 |
| 21 | 99.30 | 50.24 |
| 22 | 99.71 | 50.96 |

**Simplified BISHOP FOS = 1.376**

The following is a summary of the TEN most critical surfaces

| | FOS BISHOP | Circle Centre x-coord (m) | Circle Centre y-coord (m) | Radius (m) | Initial x-coord (m) | Terminal x-coord (m) | Resisting Moment (kN-m) |
|---|---|---|---|---|---|---|---|
| 1 | 1.376 | 43.46 | 83.99 | 65.25 | 30.56 | 99.71 | 3.09E+05 |
| 2 | 1.399 | 61.01 | 63.98 | 38.38 | 50.00 | 96.26 | 1.08E+05 |
| 3 | 1.456 | 38.53 | 72.17 | 54.08 | 27.78 | 84.08 | 1.60E+05 |
| 4 | 1.467 | 50.14 | 60.64 | 38.89 | 38.89 | 84.97 | 9.54E+04 |
| 5 | 1.478 | 57.95 | 61.45 | 38.75 | 44.44 | 94.07 | 1.37E+05 |
| 6 | 1.495 | 58.56 | 65.49 | 44.54 | 41.67 | 100.87 | 2.33E+05 |
| 7 | 1.561 | 58.36 | 52.29 | 28.56 | 47.22 | 85.55 | 6.67E+04 |
| 8 | 1.573 | 49.70 | 57.43 | 37.62 | 36.11 | 84.49 | 1.18E+05 |
| 9 | 1.674 | 44.87 | 60.18 | 46.10 | 25.00 | 88.28 | 2.78E+05 |
| 10 | 1.951 | 52.57 | 48.06 | 33.05 | 33.33 | 85.31 | 1.90E+05 |

Factors of Safety for Gnejna Bay have been calculated by the SIMPLIFIED BISHOP METHOD, when pore pressure ratio is **0.15**.

The most critical circular failure surface is specified by 22 coordinate points

| Point No. | x-surf (m) | y-surf (m) |
|---|---|---|
| 1 | 30.56 | 20.03 |
| 2 | 34.50 | 19.36 |
| 3 | 38.48 | 18.93 |
| 4 | 42.47 | 18.74 |
| 5 | 46.47 | 18.81 |
| 6 | 50.46 | 19.11 |
| 7 | 54.42 | 19.66 |
| 8 | 58.34 | 20.46 |
| 9 | 62.21 | 21.49 |
| 10 | 66.00 | 22.75 |
| 11 | 69.71 | 24.25 |
| 12 | 73.32 | 25.97 |
| 13 | 76.82 | 27.91 |
| 14 | 80.19 | 30.06 |
| 15 | 83.43 | 32.41 |
| 16 | 86.51 | 34.96 |
| 17 | 89.44 | 37.69 |
| 18 | 92.19 | 40.59 |
| 19 | 94.76 | 43.66 |
| 20 | 97.13 | 46.88 |
| 21 | 99.30 | 50.24 |
| 22 | 99.71 | 50.96 |

**Simplified BISHOP FOS = 1.286**

The following is a summary of the TEN most critical surfaces

| | FOS BISHOP | Circle Centre x-coord (m) | Circle Centre y-coord (m) | Radius (m) | Initial x-coord (m) | Terminal x-coord (m) | Resisting Moment (kN-m) |
|---|---|---|---|---|---|---|---|
| 1 | 1.286 | 43.46 | 83.99 | 65.25 | 30.56 | 99.71 | 2.89E+05 |
| 2 | 1.308 | 61.01 | 63.98 | 38.38 | 50.00 | 96.26 | 1.01E+05 |
| 3 | 1.363 | 38.53 | 72.17 | 54.08 | 27.78 | 84.08 | 1.50E+05 |
| 4 | 1.373 | 50.14 | 60.64 | 38.89 | 38.89 | 84.97 | 8.93E+04 |
| 5 | 1.383 | 57.95 | 61.45 | 38.75 | 44.44 | 94.07 | 1.29E+05 |
| 6 | 1.399 | 58.56 | 65.49 | 44.54 | 41.67 | 100.87 | 2.18E+05 |
| 7 | 1.462 | 58.36 | 52.29 | 28.56 | 47.22 | 85.55 | 6.25E+04 |
| 8 | 1.474 | 49.70 | 57.43 | 37.62 | 36.11 | 84.49 | 1.11E+05 |
| 9 | 1.569 | 44.87 | 60.18 | 46.10 | 25.00 | 88.28 | 2.60E+05 |
| 10 | 1.831 | 52.57 | 48.06 | 33.05 | 33.33 | 85.31 | 1.79E+05 |

Factors of Safety for Gnejna Bay have been calculated by the SIMPLIFIED BISHOP METHOD, when pore pressure ratio is **0.20**.

The most critical circular failure surface is specified by 22 coordinate points

| Point No. | x-surf (m) | y-surf (m) |
|---|---|---|
| 1 | 30.56 | 20.03 |
| 2 | 34.50 | 19.36 |
| 3 | 38.48 | 18.93 |
| 4 | 42.47 | 18.74 |
| 5 | 46.47 | 18.81 |
| 6 | 50.46 | 19.11 |
| 7 | 54.42 | 19.66 |
| 8 | 58.34 | 20.46 |
| 9 | 62.21 | 21.49 |
| 10 | 66.00 | 22.75 |
| 11 | 69.71 | 24.25 |
| 12 | 73.32 | 25.97 |
| 13 | 76.82 | 27.91 |
| 14 | 80.19 | 30.06 |
| 15 | 83.43 | 32.41 |
| 16 | 86.51 | 34.96 |
| 17 | 89.44 | 37.69 |
| 18 | 92.19 | 40.59 |
| 19 | 94.76 | 43.66 |
| 20 | 97.13 | 46.88 |
| 21 | 99.30 | 50.24 |
| 22 | 99.71 | 50.96 |

**Simplified BISHOP FOS = 1.197**

The following is a summary of the TEN most critical surfaces

| | FOS BISHOP | Circle Centre x-coord (m) | Circle Centre y-coord (m) | Radius (m) | Initial x-coord (m) | Terminal x-coord (m) | Resisting Moment (kN-m) |
|---|---|---|---|---|---|---|---|
| 1 | 1.197 | 43.46 | 83.99 | 65.25 | 30.56 | 99.71 | 2.69E+05 |
| 2 | 1.218 | 61.01 | 63.98 | 38.38 | 50.00 | 96.26 | 9.43E+04 |
| 3 | 1.271 | 38.53 | 72.17 | 54.08 | 27.78 | 84.08 | 1.40E+05 |
| 4 | 1.280 | 50.14 | 60.64 | 38.89 | 38.89 | 84.97 | 8.32E+04 |
| 5 | 1.289 | 57.95 | 61.45 | 38.75 | 44.44 | 94.07 | 1.20E+05 |
| 6 | 1.304 | 58.56 | 65.49 | 44.54 | 41.67 | 100.87 | 2.03E+05 |
| 7 | 1.363 | 58.36 | 52.29 | 28.56 | 47.22 | 85.55 | 5.83E+04 |
| 8 | 1.375 | 49.70 | 57.43 | 37.62 | 36.11 | 84.49 | 1.04E+05 |
| 9 | 1.465 | 44.87 | 60.18 | 46.10 | 25.00 | 88.28 | 2.43E+05 |
| 10 | 1.712 | 52.57 | 48.06 | 33.05 | 33.33 | 85.31 | 1.67E+05 |

Factors of Safety for Gnejna Bay have been calculated by the SIMPLIFIED BISHOP METHOD, when pore pressure ratio is **0.25**.

The most critical circular failure surface is specified by 22 coordinate points

| Point No. | x-surf (m) | y-surf (m) |
|---|---|---|
| 1 | 30.56 | 20.03 |
| 2 | 34.50 | 19.36 |
| 3 | 38.48 | 18.93 |
| 4 | 42.47 | 18.74 |
| 5 | 46.47 | 18.81 |
| 6 | 50.46 | 19.11 |
| 7 | 54.42 | 19.66 |
| 8 | 58.34 | 20.46 |
| 9 | 62.21 | 21.49 |
| 10 | 66.00 | 22.75 |
| 11 | 69.71 | 24.25 |
| 12 | 73.32 | 25.97 |
| 13 | 76.82 | 27.91 |
| 14 | 80.19 | 30.06 |
| 15 | 83.43 | 32.41 |
| 16 | 86.51 | 34.96 |
| 17 | 89.44 | 37.69 |
| 18 | 92.19 | 40.59 |
| 19 | 94.76 | 43.66 |
| 20 | 97.13 | 46.88 |
| 21 | 99.30 | 50.24 |
| 22 | 99.71 | 50.96 |

**Simplified BISHOP FOS = 1.109**

The following is a summary of the TEN most critical surfaces

| | FOS BISHOP | Circle Centre x-coord (m) | Circle Centre y-coord (m) | Radius (m) | Initial x-coord (m) | Terminal x-coord (m) | Resisting Moment (kN-m) |
|---|---|---|---|---|---|---|---|
| 1 | 1.109 | 43.46 | 83.99 | 65.25 | 30.56 | 99.71 | 2.49E+05 |
| 2 | 1.128 | 61.01 | 63.98 | 38.38 | 50.00 | 96.26 | 8.73E+04 |
| 3 | 1.178 | 38.53 | 72.17 | 54.08 | 27.78 | 84.08 | 1.30E+05 |
| 4 | 1.186 | 50.14 | 60.64 | 38.89 | 38.89 | 84.97 | 7.72E+04 |
| 5 | 1.195 | 57.95 | 61.45 | 38.75 | 44.44 | 94.07 | 1.11E+05 |
| 6 | 1.209 | 58.56 | 65.49 | 44.54 | 41.67 | 100.87 | 1.88E+05 |
| 7 | 1.265 | 58.36 | 52.29 | 28.56 | 47.22 | 85.55 | 5.41E+04 |
| 8 | 1.276 | 49.70 | 57.43 | 37.62 | 36.11 | 84.49 | 9.61E+04 |
| 9 | 1.361 | 44.87 | 60.18 | 46.10 | 25.00 | 88.28 | 2.26E+05 |
| 10 | 1.593 | 52.57 | 48.06 | 33.05 | 33.33 | 85.31 | 1.55E+05 |

Factors of Safety for Gnejna Bay have been calculated by the SIMPLIFIED BISHOP METHOD, when pore pressure ratio is **0.30**.

The most critical circular failure surface is specified by 22 coordinate points

| Point No. | x-surf (m) | y-surf (m) |
|---|---|---|
| 1 | 30.56 | 20.03 |
| 2 | 34.50 | 19.36 |
| 3 | 38.48 | 18.93 |
| 4 | 42.47 | 18.74 |
| 5 | 46.47 | 18.81 |
| 6 | 50.46 | 19.11 |
| 7 | 54.42 | 19.66 |
| 8 | 58.34 | 20.46 |
| 9 | 62.21 | 21.49 |
| 10 | 66.00 | 22.75 |
| 11 | 69.71 | 24.25 |
| 12 | 73.32 | 25.97 |
| 13 | 76.82 | 27.91 |
| 14 | 80.19 | 30.06 |
| 15 | 83.43 | 32.41 |
| 16 | 86.51 | 34.96 |
| 17 | 89.44 | 37.69 |
| 18 | 92.19 | 40.59 |
| 19 | 94.76 | 43.66 |
| 20 | 97.13 | 46.88 |
| 21 | 99.30 | 50.24 |
| 22 | 99.71 | 50.96 |

**Simplified BISHOP FOS = 1.020**

The following is a summary of the TEN most critical surfaces

| | FOS BISHOP | Circle Centre x-coord (m) | Circle Centre y-coord (m) | Radius (m) | Initial x-coord (m) | Terminal x-coord (m) | Resisting Moment (kN-m) |
|---|---|---|---|---|---|---|---|
| 1 | 1.020 | 43.46 | 83.99 | 65.25 | 30.56 | 99.71 | 2.29E+05 |
| 2 | 1.038 | 61.01 | 63.98 | 38.38 | 50.00 | 96.26 | 8.03E+04 |
| 3 | 1.086 | 38.53 | 72.17 | 54.08 | 27.78 | 84.08 | 1.20E+05 |
| 4 | 1.093 | 50.14 | 60.64 | 38.89 | 38.89 | 84.97 | 7.11E+04 |
| 5 | 1.101 | 57.95 | 61.45 | 38.75 | 44.44 | 94.07 | 1.02E+05 |
| 6 | 1.114 | 58.56 | 65.49 | 44.54 | 41.67 | 100.87 | 1.74E+05 |
| 7 | 1.167 | 58.36 | 52.29 | 28.56 | 47.22 | 85.55 | 4.99E+04 |
| 8 | 1.178 | 49.70 | 57.43 | 37.62 | 36.11 | 84.49 | 8.87E+04 |
| 9 | 1.258 | 44.87 | 60.18 | 46.10 | 25.00 | 88.28 | 2.09E+05 |
| 10 | 1.475 | 52.57 | 48.06 | 33.05 | 33.33 | 85.31 | 1.44E+05 |

Factors of Safety for Gnejna Bay have been calculated by the SIMPLIFIED BISHOP METHOD, when pore pressure ratio is **0.35**.

The most critical circular failure surface is specified by 22 coordinate points

| Point No. | x-surf (m) | y-surf (m) |
|---|---|---|
| 1 | 30.56 | 20.03 |
| 2 | 34.50 | 19.36 |
| 3 | 38.48 | 18.93 |
| 4 | 42.47 | 18.74 |
| 5 | 46.47 | 18.81 |
| 6 | 50.46 | 19.11 |
| 7 | 54.42 | 19.66 |
| 8 | 58.34 | 20.46 |
| 9 | 62.21 | 21.49 |
| 10 | 66.00 | 22.75 |
| 11 | 69.71 | 24.25 |
| 12 | 73.32 | 25.97 |
| 13 | 76.82 | 27.91 |
| 14 | 80.19 | 30.06 |
| 15 | 83.43 | 32.41 |
| 16 | 86.51 | 34.96 |
| 17 | 89.44 | 37.69 |
| 18 | 92.19 | 40.59 |
| 19 | 94.76 | 43.66 |
| 20 | 97.13 | 46.88 |
| 21 | 99.30 | 50.24 |
| 22 | 99.71 | 50.96 |

**Simplified BISHOP FOS = 0.932**

The following is a summary of the TEN most critical surfaces

| | FOS BISHOP | Circle Centre x-coord (m) | Circle Centre y-coord (m) | Radius (m) | Initial x-coord (m) | Terminal x-coord (m) | Resisting Moment (kN-m) |
|---|---|---|---|---|---|---|---|
| 1 | 0.932 | 43.46 | 83.99 | 65.25 | 30.56 | 99.71 | 2.09E+05 |
| 2 | 0.949 | 61.01 | 63.98 | 38.38 | 50.00 | 96.26 | 7.34E+04 |
| 3 | 0.994 | 38.53 | 72.17 | 54.08 | 27.78 | 84.08 | 1.10E+05 |
| 4 | 1.001 | 50.14 | 60.64 | 38.89 | 38.89 | 84.97 | 6.51E+04 |
| 5 | 1.008 | 57.95 | 61.45 | 38.75 | 44.44 | 94.07 | 9.37E+04 |
| 6 | 1.020 | 58.56 | 65.49 | 44.54 | 41.67 | 100.87 | 1.59E+05 |
| 7 | 1.069 | 58.36 | 52.29 | 28.56 | 47.22 | 85.55 | 4.57E+04 |
| 8 | 1.080 | 49.70 | 57.43 | 37.62 | 36.11 | 84.49 | 8.13E+04 |
| 9 | 1.155 | 44.87 | 60.18 | 46.10 | 25.00 | 88.28 | 1.92E+05 |
| 10 | 1.358 | 52.57 | 48.06 | 33.05 | 33.33 | 85.31 | 1.32E+05 |

*Factor of Safety values calculated for Ghajn Tuffieha Bay*

Factors of Safety for Ghajn Tuffieha Bay have been calculated by the SIMPLIFIED BISHOP METHOD, when pore pressure ratio is **0.00**.

The most critical circular failure surface is specified by 29 coordinate points

| Point No. | x-surf (m) | y-surf (m) | Point No. | x-surf (m) | y-surf (m) |
|---|---|---|---|---|---|
| 1 | 61.67 | 14.48 | 16 | 135.27 | 21.86 |
| 2 | 66.60 | 13.64 | 17 | 139.86 | 23.84 |
| 3 | 71.55 | 12.99 | 18 | 144.38 | 25.99 |
| 4 | 76.53 | 12.54 | 19 | 148.80 | 28.32 |
| 5 | 81.53 | 12.27 | 20 | 153.14 | 30.81 |
| 6 | 86.52 | 12.19 | 21 | 157.38 | 33.47 |
| 7 | 91.52 | 12.31 | 22 | 161.51 | 36.28 |
| 8 | 96.51 | 12.62 | 23 | 165.53 | 39.25 |
| 9 | 101.49 | 13.12 | 24 | 169.43 | 42.38 |
| 10 | 106.44 | 13.81 | 25 | 173.21 | 45.65 |
| 11 | 111.36 | 14.68 | 26 | 176.86 | 49.07 |
| 12 | 116.25 | 15.75 | 27 | 180.38 | 52.62 |
| 13 | 121.09 | 17.00 | 28 | 183.76 | 56.30 |
| 14 | 125.88 | 18.44 | 29 | 184.64 | 57.34 |
| 15 | 130.61 | 20.06 | | | |

**Simplified BISHOP FOS = 1.391**

The following is a summary of the TEN most critical surfaces

| | FOS BISHOP | Circle Centre x-coord (m) | Circle Centre y-coord (m) | Radius (m) | Initial x-coord (m) | Terminal x-coord (m) | Resisting Moment (kN-m) |
|---|---|---|---|---|---|---|---|
| 1 | 1.391 | 85.99 | 142.61 | 130.42 | 61.67 | 184.64 | 1.16E+06 |
| 2 | 1.472 | 76.36 | 108.26 | 95.85 | 58.33 | 143.72 | 3.49E+05 |
| 3 | 1.512 | 95.61 | 74.56 | 62.13 | 75.00 | 148.10 | 3.27E+05 |
| 4 | 1.538 | 90.70 | 75.48 | 64.29 | 68.33 | 144.49 | 3.35E+05 |
| 5 | 1.637 | 105.63 | 57.49 | 44.15 | 85.00 | 146.50 | 2.31E+05 |
| 6 | 1.728 | 87.86 | 82.79 | 76.55 | 55.00 | 153.23 | 7.13E+05 |
| 7 | 1.893 | 114.29 | 62.88 | 55.90 | 81.67 | 168.74 | 7.24E+05 |
| 8 | 2.131 | 106.35 | 45.40 | 40.09 | 78.33 | 146.15 | 3.87E+05 |
| 9 | 2.193 | 97.61 | 47.38 | 46.07 | 65.00 | 143.02 | 5.27E+05 |
| 10 | 2.241 | 102.03 | 43.80 | 41.46 | 71.67 | 143.30 | 4.52E+05 |

Factors of Safety for Ghajn Tuffieha Bay have been calculated by the SIMPLIFIED BISHOP METHOD, when pore pressure ratio is **0.05**.

The most critical circular failure surface is specified by 29 coordinate points

| Point No. | x-surf (m) | y-surf (m) | Point No. | x-surf (m) | y-surf (m) |
|---|---|---|---|---|---|
| 1 | 61.67 | 14.48 | 16 | 135.27 | 21.86 |
| 2 | 66.60 | 13.64 | 17 | 139.86 | 23.84 |
| 3 | 71.55 | 12.99 | 18 | 144.38 | 25.99 |
| 4 | 76.53 | 12.54 | 19 | 148.80 | 28.32 |
| 5 | 81.53 | 12.27 | 20 | 153.14 | 30.81 |
| 6 | 86.52 | 12.19 | 21 | 157.38 | 33.47 |
| 7 | 91.52 | 12.31 | 22 | 161.51 | 36.28 |
| 8 | 96.51 | 12.62 | 23 | 165.53 | 39.25 |
| 9 | 101.49 | 13.12 | 24 | 169.43 | 42.38 |
| 10 | 106.44 | 13.81 | 25 | 173.21 | 45.65 |
| 11 | 111.36 | 14.68 | 26 | 176.86 | 49.07 |
| 12 | 116.25 | 15.75 | 27 | 180.38 | 52.62 |
| 13 | 121.09 | 17.00 | 28 | 183.76 | 56.30 |
| 14 | 125.88 | 18.44 | 29 | 184.64 | 57.34 |
| 15 | 130.61 | 20.06 | | | |

**Simplified BISHOP FOS = 1.314**

The following is a summary of the TEN most critical surfaces

| | FOS BISHOP | Circle,Centre x-coord (m) | y-coord (m) | Radius (m) | Initial x-coord (m) | Terminal x-coord (m) | Resisting Moment (kN-m) |
|---|---|---|---|---|---|---|---|
| 1 | 1.314 | 85.99 | 142.61 | 130.42 | 61.67 | 184.64 | 1.10E+06 |
| 2 | 1.391 | 76.36 | 108.26 | 95.85 | 58.33 | 143.72 | 3.30E+05 |
| 3 | 1.428 | 95.61 | 74.56 | 62.13 | 75.00 | 148.10 | 3.09E+05 |
| 4 | 1.454 | 90.70 | 75.48 | 64.29 | 68.33 | 144.49 | 3.17E+05 |
| 5 | 1.547 | 105.63 | 57.49 | 44.15 | 85.00 | 146.50 | 2.19E+05 |
| 6 | 1.634 | 87.86 | 82.79 | 76.55 | 55.00 | 153.23 | 6.74E+05 |
| 7 | 1.790 | 114.29 | 62.88 | 55.90 | 81.67 | 168.74 | 6.85E+05 |
| 8 | 2.017 | 106.35 | 45.40 | 40.09 | 78.33 | 146.15 | 3.67E+05 |
| 9 | 2.077 | 97.61 | 47.38 | 46.07 | 65.00 | 143.02 | 4.99E+05 |
| 10 | 2.122 | 102.03 | 43.80 | 41.46 | 71.67 | 143.30 | 4.28E+05 |

Factors of Safety for Ghajn Tuffieha Bay have been calculated by the SIMPLIFIED BISHOP METHOD, when pore pressure ratio is **0.10**.

The most critical circular failure surface is specified by 29 coordinate points

| Point No. | x-surf (m) | y-surf (m) | Point No. | x-surf (m) | y-surf (m) |
|---|---|---|---|---|---|
| 1 | 61.67 | 14.48 | 16 | 135.27 | 21.86 |
| 2 | 66.60 | 13.64 | 17 | 139.86 | 23.84 |
| 3 | 71.55 | 12.99 | 18 | 144.38 | 25.99 |
| 4 | 76.53 | 12.54 | 19 | 148.80 | 28.32 |
| 5 | 81.53 | 12.27 | 20 | 153.14 | 30.81 |
| 6 | 86.52 | 12.19 | 21 | 157.38 | 33.47 |
| 7 | 91.52 | 12.31 | 22 | 161.51 | 36.28 |
| 8 | 96.51 | 12.62 | 23 | 165.53 | 39.25 |
| 9 | 101.49 | 13.12 | 24 | 169.43 | 42.38 |
| 10 | 106.44 | 13.81 | 25 | 173.21 | 45.65 |
| 11 | 111.36 | 14.68 | 26 | 176.86 | 49.07 |
| 12 | 116.25 | 15.75 | 27 | 180.38 | 52.62 |
| 13 | 121.09 | 17.00 | 28 | 183.76 | 56.30 |
| 14 | 125.88 | 18.44 | 29 | 184.64 | 57.34 |
| 15 | 130.61 | 20.06 | | | |

**Simplified BISHOP FOS = 1.236**

The following is a summary of the TEN most critical surfaces

| | FOS BISHOP | Circle Centre x-coord (m) | Circle Centre y-coord (m) | Radius (m) | Initial x-coord (m) | Terminal x-coord (m) | Resisting Moment (kN-m) |
|---|---|---|---|---|---|---|---|
| 1 | 1.236 | 85.99 | 142.61 | 130.42 | 61.67 | 184.64 | 1.03E+06 |
| 2 | 1.309 | 76.36 | 108.26 | 95.85 | 58.33 | 143.72 | 3.10E+05 |
| 3 | 1.345 | 95.61 | 74.56 | 62.13 | 75.00 | 148.10 | 2.91E+05 |
| 4 | 1.369 | 90.70 | 75.48 | 64.29 | 68.33 | 144.49 | 2.98E+05 |
| 5 | 1.457 | 105.63 | 57.49 | 44.15 | 85.00 | 146.50 | 2.06E+05 |
| 6 | 1.541 | 87.86 | 82.79 | 76.55 | 55.00 | 153.23 | 6.35E+05 |
| 7 | 1.688 | 114.29 | 62.88 | 55.90 | 81.67 | 168.74 | 6.46E+05 |
| 8 | 1.903 | 106.35 | 45.40 | 40.09 | 78.33 | 146.15 | 3.46E+05 |
| 9 | 1.960 | 97.61 | 47.38 | 46.07 | 65.00 | 143.02 | 4.71E+05 |
| 10 | 2.002 | 102.03 | 43.80 | 41.46 | 71.67 | 143.30 | 4.04E+05 |

Factors of Safety for Ghajn Tuffieha Bay have been calculated by the SIMPLIFIED BISHOP METHOD, when pore pressure ratio is **0.15**.

The most critical circular failure surface is specified by 29 coordinate points

| Point No. | x-surf (m) | y-surf (m) | Point No. | x-surf (m) | y-surf (m) |
|---|---|---|---|---|---|
| 1 | 61.67 | 14.48 | 16 | 135.27 | 21.86 |
| 2 | 66.60 | 13.64 | 17 | 139.86 | 23.84 |
| 3 | 71.55 | 12.99 | 18 | 144.38 | 25.99 |
| 4 | 76.53 | 12.54 | 19 | 148.80 | 28.32 |
| 5 | 81.53 | 12.27 | 20 | 153.14 | 30.81 |
| 6 | 86.52 | 12.19 | 21 | 157.38 | 33.47 |
| 7 | 91.52 | 12.31 | 22 | 161.51 | 36.28 |
| 8 | 96.51 | 12.62 | 23 | 165.53 | 39.25 |
| 9 | 101.49 | 13.12 | 24 | 169.43 | 42.38 |
| 10 | 106.44 | 13.81 | 25 | 173.21 | 45.65 |
| 11 | 111.36 | 14.68 | 26 | 176.86 | 49.07 |
| 12 | 116.25 | 15.75 | 27 | 180.38 | 52.62 |
| 13 | 121.09 | 17.00 | 28 | 183.76 | 56.30 |
| 14 | 125.88 | 18.44 | 29 | 184.64 | 57.34 |
| 15 | 130.61 | 20.06 | | | |

**Simplified BISHOP FOS = 1.158**

The following is a summary of the TEN most critical surfaces

| | FOS BISHOP | Circle Centre x-coord (m) | Circle Centre y-coord (m) | Radius (m) | Initial x-coord (m) | Terminal x-coord (m) | Resisting Moment (kN-m) |
|---|---|---|---|---|---|---|---|
| 1 | 1.158 | 85.99 | 142.61 | 130.42 | 61.67 | 184.64 | 9.66E+05 |
| 2 | 1.228 | 76.36 | 108.26 | 95.85 | 58.33 | 143.72 | 2.91E+05 |
| 3 | 1.261 | 95.61 | 74.56 | 62.13 | 75.00 | 148.10 | 2.73E+05 |
| 4 | 1.284 | 90.70 | 75.48 | 64.29 | 68.33 | 144.49 | 2.80E+05 |
| 5 | 1.368 | 105.63 | 57.49 | 44.15 | 85.00 | 146.50 | 1.93E+05 |
| 6 | 1.447 | 87.86 | 82.79 | 76.55 | 55.00 | 153.23 | 5.97E+05 |
| 7 | 1.586 | 114.29 | 62.88 | 55.90 | 81.67 | 168.74 | 6.07E+05 |
| 8 | 1.789 | 106.35 | 45.40 | 40.09 | 78.33 | 146.15 | 3.25E+05 |
| 9 | 1.844 | 97.61 | 47.38 | 46.07 | 65.00 | 143.02 | 4.43E+05 |
| 10 | 1.883 | 102.03 | 43.80 | 41.46 | 71.67 | 143.30 | 3.80E+05 |

Factors of Safety for Ghajn Tuffieha Bay have been calculated by the SIMPLIFIED BISHOP METHOD, when pore pressure ratio is **0.20**.

The most critical circular failure surface is specified by 29 coordinate points

| Point No. | x-surf (m) | y-surf (m) | Point No. | x-surf (m) | y-surf (m) |
|---|---|---|---|---|---|
| 1 | 61.67 | 14.48 | 16 | 135.27 | 21.86 |
| 2 | 66.60 | 13.64 | 17 | 139.86 | 23.84 |
| 3 | 71.55 | 12.99 | 18 | 144.38 | 25.99 |
| 4 | 76.53 | 12.54 | 19 | 148.80 | 28.32 |
| 5 | 81.53 | 12.27 | 20 | 153.14 | 30.81 |
| 6 | 86.52 | 12.19 | 21 | 157.38 | 33.47 |
| 7 | 91.52 | 12.31 | 22 | 161.51 | 36.28 |
| 8 | 96.51 | 12.62 | 23 | 165.53 | 39.25 |
| 9 | 101.49 | 13.12 | 24 | 169.43 | 42.38 |
| 10 | 106.44 | 13.81 | 25 | 173.21 | 45.65 |
| 11 | 111.36 | 14.68 | 26 | 176.86 | 49.07 |
| 12 | 116.25 | 15.75 | 27 | 180.38 | 52.62 |
| 13 | 121.09 | 17.00 | 28 | 183.76 | 56.30 |
| 14 | 125.88 | 18.44 | 29 | 184.64 | 57.34 |
| 15 | 130.61 | 20.06 | | | |

**Simplified BISHOP FOS = 1.080**

The following is a summary of the TEN most critical surfaces

| | FOS BISHOP | Circle Centre x-coord (m) | Circle Centre y-coord (m) | Radius (m) | Initial x-coord (m) | Terminal x-coord (m) | Resisting Moment (kN-m) |
|---|---|---|---|---|---|---|---|
| 1 | 1.080 | 85.99 | 142.61 | 130.42 | 61.67 | 184.64 | 9.01E+05 |
| 2 | 1.147 | 76.36 | 108.26 | 95.85 | 58.33 | 143.72 | 2.72E+05 |
| 3 | 1.178 | 95.61 | 74.56 | 62.13 | 75.00 | 148.10 | 2.55E+05 |
| 4 | 1.200 | 90.70 | 75.48 | 64.29 | 68.33 | 144.49 | 2.61E+05 |
| 5 | 1.278 | 105.63 | 57.49 | 44.15 | 85.00 | 146.50 | 1.81E+05 |
| 6 | 1.354 | 87.86 | 82.79 | 76.55 | 55.00 | 153.23 | 5.59E+05 |
| 7 | 1.485 | 114.29 | 62.88 | 55.90 | 81.67 | 168.74 | 5.68E+05 |
| 8 | 1.676 | 106.35 | 45.40 | 40.09 | 78.33 | 146.15 | 3.05E+05 |
| 9 | 1.727 | 97.61 | 47.38 | 46.07 | 65.00 | 143.02 | 4.15E+05 |
| 10 | 1.765 | 102.03 | 43.80 | 41.46 | 71.67 | 143.30 | 3.56E+05 |

Factors of Safety for Ghajn Tuffieha Bay have been calculated by the SIMPLIFIED BISHOP METHOD, when pore pressure ratio is **0.25**.

The most critical circular failure surface is specified by 29 coordinate points

| Point No. | x-surf (m) | y-surf (m) | Point No. | x-surf (m) | y-surf (m) |
|---|---|---|---|---|---|
| 1 | 61.67 | 14.48 | 16 | 135.27 | 21.86 |
| 2 | 66.60 | 13.64 | 17 | 139.86 | 23.84 |
| 3 | 71.55 | 12.99 | 18 | 144.38 | 25.99 |
| 4 | 76.53 | 12.54 | 19 | 148.80 | 28.32 |
| 5 | 81.53 | 12.27 | 20 | 153.14 | 30.81 |
| 6 | 86.52 | 12.19 | 21 | 157.38 | 33.47 |
| 7 | 91.52 | 12.31 | 22 | 161.51 | 36.28 |
| 8 | 96.51 | 12.62 | 23 | 165.53 | 39.25 |
| 9 | 101.49 | 13.12 | 24 | 169.43 | 42.38 |
| 10 | 106.44 | 13.81 | 25 | 173.21 | 45.65 |
| 11 | 111.36 | 14.68 | 26 | 176.86 | 49.07 |
| 12 | 116.25 | 15.75 | 27 | 180.38 | 52.62 |
| 13 | 121.09 | 17.00 | 28 | 183.76 | 56.30 |
| 14 | 125.88 | 18.44 | 29 | 184.64 | 57.34 |
| 15 | 130.61 | 20.06 | | | |

**Simplified BISHOP FOS = 1.003**

The following is a summary of the TEN most critical surfaces

| | FOS BISHOP | Circle Centre x-coord (m) | Circle Centre y-coord (m) | Radius (m) | Initial x-coord (m) | Terminal x-coord (m) | Resisting Moment (kN-m) |
|---|---|---|---|---|---|---|---|
| 1 | 1.003 | 85.99 | 142.61 | 130.42 | 61.67 | 184.64 | 8.36E+05 |
| 2 | 1.066 | 76.36 | 108.26 | 95.85 | 58.33 | 143.72 | 2.53E+05 |
| 3 | 1.095 | 95.61 | 74.56 | 62.13 | 75.00 | 148.10 | 2.37E+05 |
| 4 | 1.116 | 90.70 | 75.48 | 64.29 | 68.33 | 144.49 | 2.43E+05 |
| 5 | 1.189 | 105.63 | 57.49 | 44.15 | 85.00 | 146.50 | 1.68E+05 |
| 6 | 1.261 | 87.86 | 82.79 | 76.55 | 55.00 | 153.23 | 5.20E+05 |
| 7 | 1.383 | 114.29 | 62.88 | 55.90 | 81.67 | 168.74 | 5.29E+05 |
| 8 | 1.563 | 106.35 | 45.40 | 40.09 | 78.33 | 146.15 | 2.84E+05 |
| 9 | 1.612 | 97.61 | 47.38 | 46.07 | 65.00 | 143.02 | 3.87E+05 |
| 10 | 1.646 | 102.03 | 43.80 | 41.46 | 71.67 | 143.30 | 3.32E+05 |

Factors of Safety for Ghajn Tuffieha Bay have been calculated by the SIMPLIFIED BISHOP METHOD, when pore pressure ratio is **0.30**.

The most critical circular failure surface is specified by 29 coordinate points

| Point No. | x-surf (m) | y-surf (m) | Point No. | x-surf (m) | y-surf (m) |
|---|---|---|---|---|---|
| 1 | 61.67 | 14.48 | 16 | 135.27 | 21.86 |
| 2 | 66.60 | 13.64 | 17 | 139.86 | 23.84 |
| 3 | 71.55 | 12.99 | 18 | 144.38 | 25.99 |
| 4 | 76.53 | 12.54 | 19 | 148.80 | 28.32 |
| 5 | 81.53 | 12.27 | 20 | 153.14 | 30.81 |
| 6 | 86.52 | 12.19 | 21 | 157.38 | 33.47 |
| 7 | 91.52 | 12.31 | 22 | 161.51 | 36.28 |
| 8 | 96.51 | 12.62 | 23 | 165.53 | 39.25 |
| 9 | 101.49 | 13.12 | 24 | 169.43 | 42.38 |
| 10 | 106.44 | 13.81 | 25 | 173.21 | 45.65 |
| 11 | 111.36 | 14.68 | 26 | 176.86 | 49.07 |
| 12 | 116.25 | 15.75 | 27 | 180.38 | 52.62 |
| 13 | 121.09 | 17.00 | 28 | 183.76 | 56.30 |
| 14 | 125.88 | 18.44 | 29 | 184.64 | 57.34 |
| 15 | 130.61 | 20.06 | | | |

**Simplified BISHOP FOS = 0.925**

The following is a summary of the TEN most critical surfaces

| | FOS BISHOP | Circle Centre x-coord (m) | Circle Centre y-coord (m) | Radius (m) | Initial x-coord (m) | Terminal x-coord (m) | Resisting Moment (kN-m) |
|---|---|---|---|---|---|---|---|
| 1 | 0.925 | 85.99 | 142.61 | 130.42 | 61.67 | 184.64 | 7.72E+05 |
| 2 | 0.985 | 76.36 | 108.26 | 95.85 | 58.33 | 143.72 | 2.34E+05 |
| 3 | 1.012 | 95.61 | 74.56 | 62.13 | 75.00 | 148.10 | 2.19E+05 |
| 4 | 1.031 | 90.70 | 75.48 | 64.29 | 68.33 | 144.49 | 2.25E+05 |
| 5 | 1.100 | 105.63 | 57.49 | 44.15 | 85.00 | 146.50 | 1.56E+05 |
| 6 | 1.168 | 87.86 | 82.79 | 76.55 | 55.00 | 153.23 | 4.82E+05 |
| 7 | 1.282 | 114.29 | 62.88 | 55.90 | 81.67 | 168.74 | 4.90E+05 |
| 8 | 1.451 | 106.35 | 45.40 | 40.09 | 78.33 | 146.15 | 2.64E+05 |
| 9 | 1.497 | 97.61 | 47.38 | 46.07 | 65.00 | 143.02 | 3.59E+05 |
| 10 | 1.529 | 102.03 | 43.80 | 41.46 | 71.67 | 143.30 | 3.09E+05 |

***Factor of Safety values calculated for Rdum id-Delli***

Factors of Safety for Rdum id-Delli have been calculated by the SIMPLIFIED BISHOP METHOD, when pore pressure ratio is **0.00**.

The most critical circular failure surface is specified by 20 coordinate points

| Point No. | x-surf (m) | y-surf (m) |
|---|---|---|
| 1 | 27.78 | 7.48 |
| 2 | 30.74 | 6.99 |
| 3 | 33.72 | 6.68 |
| 4 | 36.72 | 6.54 |
| 5 | 39.72 | 6.58 |
| 6 | 42.71 | 6.80 |
| 7 | 45.69 | 7.19 |
| 8 | 48.63 | 7.75 |
| 9 | 51.54 | 8.49 |
| 10 | 54.40 | 9.39 |
| 11 | 57.20 | 10.46 |
| 12 | 59.94 | 11.69 |
| 13 | 62.60 | 13.08 |
| 14 | 65.17 | 14.63 |
| 15 | 67.64 | 16.32 |
| 16 | 70.02 | 18.16 |
| 17 | 72.28 | 20.13 |
| 18 | 74.42 | 22.23 |
| 19 | 76.44 | 24.45 |
| 20 | 78.27 | 26.72 |

**Simplified BISHOP FOS = 1.181**

The following is a summary of the TEN most critical surfaces

| | FOS BISHOP | Circle Centre x-coord (m) | Circle Centre y-coord (m) | Radius (m) | Initial x-coord (m) | Terminal x-coord (m) | Resisting Moment (kN-m) |
|---|---|---|---|---|---|---|---|
| 1 | 1.181 | 37.56 | 57.67 | 51.14 | 27.78 | 78.27 | 1.01E+05 |
| 2 | 1.187 | 42.03 | 66.75 | 59.67 | 30.56 | 90.98 | 1.74E+05 |
| 3 | 1.245 | 48.73 | 44.53 | 35.01 | 38.89 | 79.06 | 6.00E+04 |
| 4 | 1.301 | 48.09 | 41.64 | 33.95 | 36.11 | 78.66 | 7.34E+04 |
| 5 | 1.331 | 55.99 | 44.81 | 33.79 | 44.44 | 86.70 | 7.19E+04 |
| 6 | 1.346 | 56.11 | 47.86 | 38.67 | 41.67 | 91.79 | 1.20E+05 |
| 7 | 1.382 | 42.97 | 45.18 | 42.41 | 25.00 | 81.93 | 1.64E+05 |
| 8 | 1.395 | 61.42 | 43.96 | 30.95 | 50.00 | 90.04 | 6.40E+04 |
| 9 | 1.583 | 50.33 | 33.15 | 29.61 | 33.33 | 79.31 | 1.09E+05 |
| 10 | 1.726 | 60.48 | 31.49 | 21.86 | 47.22 | 82.11 | 5.25E+04 |

Factors of Safety for Rdum id-Delli have been calculated by the SIMPLIFIED BISHOP METHOD, when pore pressure ratio is **0.05**.

The most critical circular failure surface is specified by 20 coordinate points

| Point No. | x-surf (m) | y-surf (m) |
|---|---|---|
| 1 | 27.78 | 7.48 |
| 2 | 30.74 | 6.99 |
| 3 | 33.72 | 6.68 |
| 4 | 36.72 | 6.54 |
| 5 | 39.72 | 6.58 |
| 6 | 42.71 | 6.80 |
| 7 | 45.69 | 7.19 |
| 8 | 48.63 | 7.75 |
| 9 | 51.54 | 8.49 |
| 10 | 54.40 | 9.39 |
| 11 | 57.20 | 10.46 |
| 12 | 59.94 | 11.69 |
| 13 | 62.60 | 13.08 |
| 14 | 65.17 | 14.63 |
| 15 | 67.64 | 16.32 |
| 16 | 70.02 | 18.16 |
| 17 | 72.28 | 20.13 |
| 18 | 74.42 | 22.23 |
| 19 | 76.44 | 24.45 |
| 20 | 78.27 | 26.72 |

**Simplified BISHOP FOS = 1.115**

The following is a summary of the TEN most critical surfaces

| | FOS BISHOP | Circle Centre x-coord (m) | Circle Centre y-coord (m) | Radius (m) | Initial x-coord (m) | Terminal x-coord (m) | Resisting Moment (kN-m) |
|---|---|---|---|---|---|---|---|
| 1 | 1.115 | 37.56 | 57.67 | 51.14 | 27.78 | 78.27 | 9.52E+04 |
| 2 | 1.121 | 42.03 | 66.75 | 59.67 | 30.56 | 90.98 | 1.64E+05 |
| 3 | 1.176 | 48.73 | 44.53 | 35.01 | 38.89 | 79.06 | 5.67E+04 |
| 4 | 1.230 | 48.09 | 41.64 | 33.95 | 36.11 | 78.66 | 6.94E+04 |
| 5 | 1.257 | 55.99 | 44.81 | 33.79 | 44.44 | 86.70 | 6.80E+04 |
| 6 | 1.272 | 56.11 | 47.86 | 38.67 | 41.67 | 91.79 | 1.14E+05 |
| 7 | 1.307 | 42.97 | 45.18 | 42.41 | 25.00 | 81.93 | 1.55E+05 |
| 8 | 1.319 | 61.42 | 43.96 | 30.95 | 50.00 | 90.04 | 6.05E+04 |
| 9 | 1.497 | 50.33 | 33.15 | 29.61 | 33.33 | 79.31 | 1.03E+05 |
| 10 | 1.634 | 60.48 | 31.49 | 21.86 | 47.22 | 82.11 | 4.97E+04 |

Factors of Safety for Rdum id-Delli have been calculated by the SIMPLIFIED BISHOP METHOD, when pore pressure ratio is **0.10**.

The most critical circular failure surface is specified by 20 coordinate points

| Point No. | x-surf (m) | y-surf (m) |
|---|---|---|
| 1 | 27.78 | 7.48 |
| 2 | 30.74 | 6.99 |
| 3 | 33.72 | 6.68 |
| 4 | 36.72 | 6.54 |
| 5 | 39.72 | 6.58 |
| 6 | 42.71 | 6.80 |
| 7 | 45.69 | 7.19 |
| 8 | 48.63 | 7.75 |
| 9 | 51.54 | 8.49 |
| 10 | 54.40 | 9.39 |
| 11 | 57.20 | 10.46 |
| 12 | 59.94 | 11.69 |
| 13 | 62.60 | 13.08 |
| 14 | 65.17 | 14.63 |
| 15 | 67.64 | 16.32 |
| 16 | 70.02 | 18.16 |
| 17 | 72.28 | 20.13 |
| 18 | 74.42 | 22.23 |
| 19 | 76.44 | 24.45 |
| 20 | 78.27 | 26.72 |

**Simplified BISHOP FOS = 1.049**

The following is a summary of the TEN most critical surfaces

| | FOS BISHOP | Circle Centre x-coord (m) | Circle Centre y-coord (m) | Radius (m) | Initial x-coord (m) | Terminal x-coord (m) | Resisting Moment (kN-m) |
|---|---|---|---|---|---|---|---|
| 1 | 1.049 | 37.56 | 57.67 | 51.14 | 27.78 | 78.27 | 8.96E+04 |
| 2 | 1.055 | 42.03 | 66.75 | 59.67 | 30.56 | 90.98 | 1.55E+05 |
| 3 | 1.107 | 48.73 | 44.53 | 35.01 | 38.89 | 79.06 | 5.34E+04 |
| 4 | 1.158 | 48.09 | 41.64 | 33.95 | 36.11 | 78.66 | 6.53E+04 |
| 5 | 1.185 | 55.99 | 44.81 | 33.79 | 44.44 | 86.70 | 6.40E+04 |
| 6 | 1.198 | 56.11 | 47.86 | 38.67 | 41.67 | 91.79 | 1.07E+05 |
| 7 | 1.231 | 42.97 | 45.18 | 42.41 | 25.00 | 81.93 | 1.46E+05 |
| 8 | 1.243 | 61.42 | 43.96 | 30.95 | 50.00 | 90.04 | 5.70E+04 |
| 9 | 1.412 | 50.33 | 33.15 | 29.61 | 33.33 | 79.31 | 9.74E+04 |
| 10 | 1.542 | 60.48 | 31.49 | 21.86 | 47.22 | 82.11 | 4.69E+04 |

Factors of Safety for Rdum id-Delli have been calculated by the SIMPLIFIED BISHOP METHOD, when pore pressure ratio is **0.15**.

The most critical circular failure surface is specified by 20 coordinate points

| Point No. | x-surf (m) | y-surf (m) |
|---|---|---|
| 1 | 27.78 | 7.48 |
| 2 | 30.74 | 6.99 |
| 3 | 33.72 | 6.68 |
| 4 | 36.72 | 6.54 |
| 5 | 39.72 | 6.58 |
| 6 | 42.71 | 6.80 |
| 7 | 45.69 | 7.19 |
| 8 | 48.63 | 7.75 |
| 9 | 51.54 | 8.49 |
| 10 | 54.40 | 9.39 |
| 11 | 57.20 | 10.46 |
| 12 | 59.94 | 11.69 |
| 13 | 62.60 | 13.08 |
| 14 | 65.17 | 14.63 |
| 15 | 67.64 | 16.32 |
| 16 | 70.02 | 18.16 |
| 17 | 72.28 | 20.13 |
| 18 | 74.42 | 22.23 |
| 19 | 76.44 | 24.45 |
| 20 | 78.27 | 26.72 |

**Simplified BISHOP FOS = 0.984**

The following is a summary of the TEN most critical surfaces

| | FOS BISHOP | Circle x-coord (m) | Center y-coord (m) | Radius (m) | Initial x-coord (m) | Terminal x-coord (m) | Resisting Moment (kN-m) |
|---|---|---|---|---|---|---|---|
| 1 | 0.984 | 37.56 | 57.67 | 51.14 | 27.78 | 78.27 | 8.40E+04 |
| 2 | 0.988 | 42.03 | 66.75 | 59.67 | 30.56 | 90.98 | 1.45E+05 |
| 3 | 1.038 | 48.73 | 44.53 | 35.01 | 38.89 | 79.06 | 5.00E+04 |
| 4 | 1.086 | 48.09 | 41.64 | 33.95 | 36.11 | 78.66 | 6.13E+04 |
| 5 | 1.112 | 55.99 | 44.81 | 33.79 | 44.44 | 86.70 | 6.01E+04 |
| 6 | 1.124 | 56.11 | 47.86 | 38.67 | 41.67 | 91.79 | 1.01E+05 |
| 7 | 1.156 | 42.97 | 45.18 | 42.41 | 25.00 | 81.93 | 1.37E+05 |
| 8 | 1.167 | 61.42 | 43.96 | 30.95 | 50.00 | 90.04 | 5.36E+04 |
| 9 | 1.326 | 50.33 | 33.15 | 29.61 | 33.33 | 79.31 | 9.15E+04 |
| 10 | 1.450 | 60.48 | 31.49 | 21.86 | 47.22 | 82.11 | 4.41E+04 |

# *References*

Adams, A.L. 1864. 'Outline of the geology of the Maltese Islands', *Annual Magazine of Natural History*, **14**, 1-11.

Adams, A.L. 1870. *Notes of a Naturalist in the Nile Valley and Malta*, Edmonston and Douglas, Edinburgh.

Adams, A.L. 1879. 'On remains of Mastodon and other Vertebrata of the Miocene Beds of the Maltese Islands', *Quarterly Journal of the Geological Society of London*, **35**, 517-531.

Alexander, D. 1988. 'A review of the physical geography of Malta and its significance for tectonic geomorphology', *Quaternary Science Reviews*, **7**, 41-53.

Allaby, A. and Allaby, M. 1990. *Oxford Concise Dictionary of Earth Sciences*, Oxford University Press, Oxford.

Allison, R.J. 1986. *Mass movements and coastal cliff development of the Isle of Purbeck, Dorset*, Unpublished PhD thesis, University of London.

Allison, R.J. 1992. 'Landslide types and processes', in Allison, R.J. (Ed.), *The Coastal Landforms of West Dorset*, The Geologists' Association, London, 35-49.

Allison, R.J. 1996. 'Slopes and slope processes', *Progress in Physical Geography*, **20**, 453-465.

Allison, R.J. and Brunsden, D. 1990. 'Some mudslide movement patterns', *Earth Surface Processes and Landforms*, **15**, 297-311.

Allison, R.J. and Kimber, O.G. 1998. 'Modelling failure mechanisms to explain rock slope change along the Isle of Purbeck coast, UK', *Earth Surface Processes and Landforms*, **23**, 731-750.

Anderson, M.G. and Richards, K.S. 1987. 'Modelling slope stability: the complimentary nature of geotechnical and geomorphological approaches', in Anderson, M.G. and Richards, K.S. (Eds), *Slope Stability: Geotechnical Engineering and Geomorphology*, John Wiley & Sons, New York, 1-9.

Atkinson, J.H. 1981. *Foundations and Slopes: An Introduction to Applications of Critical State Soil Mechanics*, McGraw-Hill, London.

Barnes, G.E. 1995. *Soil Mechanics: Principles and Practice*, Macmillan, London.

Bishop, A.W. 1955. 'The use of the slip circle in the stability analysis of slopes', *Géotechnique*, **5**, 7-17.

Bonello, S. 1988. *Engineering properties of rocks and soils of the Maltese Islands*, Unpublished BE&A dissertation, University of Malta.

British Standards Institution 1377. 1990. *British Standard Methods of Test for Soils for Civil Engineering Purposes. Part 2: Classification Tests*, British Standards Institution, London.

British Standards Institution 1377. 1990. *British Standard Methods of Test for Soils for Civil Engineering Purposes. Part 7: Shear Strength Tests*, British Standards Institution, London.

Carson, M.A. and Kirkby, M.J. 1972. *Hillslope Form and Process*, Cambridge University Press, Cambridge.

Central Office of Statistics. 1997. *Census of Population and Housing Malta 1995. Vol.1: Population, Age, Gender and Citizenship*, Central Office of Statistics, Malta.

Chadwick, O. 1884. *Report on the Water Supply of Malta*, Government Printing Office, Malta.

Chetcuti, D. 1988. *The climate of the Maltese Islands*, Unpublished B.Ed.(Hons.) dissertation, University of Malta.

Chetcuti, D., Buhagiar, A., Schembri, P.J. and Ventura, F. 1992. *The Climate of the Maltese Islands: A Review*, University of Malta, Malta.

Coduto, D.P. 1999. *Geotechnical Engineering: Principles and Practices*, Prentice Hall, New Jersey.

Cooke, J.H. 1893. 'The marls and clays of the Maltese Islands', *Quarterly Journal of the Geological Society of London*, **49**, 117-128.

Cooke, J.H. 1896. 'Notes on the Globigerina Limestone of the Maltese Islands', *Geological Magazine*, **33**, 502-511.

Cooke, R.U. and Doornkamp, J.C. 1990. *Geomorphology in Environmental Management, 2nd edition*, Oxford University Press, Oxford.

Craig, R.F. 1978. *Soil Mechanics, 2nd edition*, Van Nostrand Reinhold Company, London.

Ellenberg, L. 1983. 'Die küsten von Gozo', *Essener Geographische Arbeiten*, **6**, 129-160.

Enriquez-Reyes, M.P., Allison, R.J. and Jones, M.E. 1990. 'Slope instability in scaley clay terrains', in Cripps, J.C. and Moon, C.F. (Eds), *The Engineering Geology of Weak Rock*, Geological Society Engineering Group, London, 423-432.

Fan, C.H., Allison, R.J. and Jones, M.E. 1994. 'The effects of tropical weathering on the characteristics of argillaceous rocks', in Robinson, D.A. and Williams, R.B.G. (Eds), *Rock Weathering and Landform Evolution*, John Wiley & Sons, New York, 339-354.

Farrugia, P. 1993. *Porosity and related properties of local building stone*, Unpublished BE&A dissertation, University of Malta.

Felix, R. 1973. 'Oligo-Miocene stratigraphy of Malta and Gozo', *Mededeelingen Landbouwhogeschule Wageningen Nederlands*, **73**, 1-103.

Fredlund, D.G. 1987. 'Slope stability analysis incorporating the effect of soil suction', in Anderson, M.G. and Richards, K.S. (Eds), *Slope Stability: Geotechnical Engineering and Geomorphology*, John Wiley & Sons, New York, 113-144.

Gardiner, V. and Dackombe, R. 1983. *Geomorphological Field Manual*, George Allen & Unwin, London.

Gauci, V. 1993. 'Supply of irrigation water in a semi-arid area', in Options Méditerranéennes, *Malta: Food, Agriculture, Fisheries and the Environment*, CIHEAM, Montpellier, **7**, 83-91.

Goudie, A., Anderson, M., Burt, T., Lewin, J., Richards, K., Whalley, B. and Worsley, P. 1990. *Geomorphological Techniques, 2nd edition*, Routledge, London.

Guilcher, A. and Paskoff, R. 1975. 'Remarques sur la géomorphologie littorale de l'archipel Maltais', *Bulettin de l'Association de Géographes Français*, **427**, 225-231.

Hart, M.G. 1986. *Geomorphology: Pure and Applied*, George Allen & Unwin, London.

Head, K.H. 1980. *Manual of Soil Laboratory Testing. Vol.1: Soil Classification and Compaction Tests*, Pentech Press, London.

House, M.R., Dunham, K.C. and Wigglesworth, J.C. 1961. 'Geology and structure of the Maltese Islands', in Bowen-Jones, H., Dewdney, J.C. and Fisher, W.B. (Eds), *Malta: Background for Development*, University of Durham.

House, M.R., Dunham, K.C. and Wigglesworth, J.C. 1961. 'Relief and landforms', in Bowen-Jones, H., Dewdney, J.C. and Fisher, W.B. (Eds), *Malta: Background for Development*, University of Durham.

Hutchinson, J.N. 1988. 'General report: morphological and geotechnical parameters of landslides in relation to geology and hydrogeology', *Proceedings of the 5th International Symposium on Landslides*, Balkema, Rotterdam, **1**, 3-35.

Hyde, H.P.T. 1955. *The Geology of the Maltese Islands*, Lux Press, Malta.

Illies, J.H. 1980. 'Form and formation of graben structures: the Maltese Islands', in Closs, H., Gehlen, K.V., Illies, J.H., Kuntz, E., Neumann, J. and Seibold, E. (Eds), *Mobile Earth*, Harald Boldt Verlag, Bonn, 161-184.

Illies, J.H. 1981. 'Graben formation – the Maltese Islands – a case history', *Tectonophysics*, **73**, 151-168.

Janbu, N., Bjerrum, L. and Kjaernsli, B. 1956. 'Soil mechanics applied to some engineering problems' [in Norwegian with English summary], *Norwegian Geotechnical Institute Publication*, **16**, 30-32.

Kirkby, M.J., Naden, P.S., Burt, T.P. and Butcher, D.P. 1993. *Computer Simulation in Physical Geography, 2nd edition*, John Wiley & Sons, New York.

Lambe, T.W. and Whitman, R.V. 1979. *Soil Mechanics, SI Version*, John Wiley & Sons, New York.

Lanfranco, E. 1996. 'Vascular plants', in Sultana, J. and Falzon, V. (Eds), *Wildlife of the Maltese Islands*, Environment Protection Department, Malta, 41-85.

Morris, T.O. 1952. *The Water Supply Resources of Malta*, Government Printing Office, Malta.

Murray, J. 1890. 'The Maltese Islands with special reference to their geological structure', *Scottish Geographical Magazine*, **6**, 449-488.

Nash, D. 1987. 'A comparative review of limit equilibrium methods of stability analysis', in Anderson, M.G. and Richards, K.S. (Eds), *Slope Stability: Geotechnical Engineering and Geomorphology*, John Wiley & Sons, New York, 11-75.

Newbery, J. 1963. *Geological factors controlling water supply in the Upper Coralline areas of the Maltese Islands*, Unpublished PhD thesis, University of London.

Newbery, J. 1968. 'The perched water table in the Upper Limestone aquifer of Malta', *Journal of the Institution of Water Engineers*, **22**, 551-570.

Paskoff, R. 1985. 'Malta', in Bird, E.C. and Schwartz, M.L. (Eds), *The World's Coastlines*, Van Nostrand Reinhold Company, New York.

Paskoff, R. and Sanlaville, P. 1978. 'Observations géomorphologiques sur les côtes de l'archipel Maltais', *Zeitschrift für Geomorphologie*, **22**, 310-328.

Pedley, H.M. 1975. *The Oligo-Miocene sediments of the Maltese Islands*, Unpublished PhD thesis, University of Hull.

Pedley, H.M. 1976. 'A palaeoecological study of the Upper Coralline Limestone, Terebratula-Aphelesia Bed (Miocene, Malta) based on Bryozoan growth-form studies and Brachiopod distributions', *Palaeogeography, Palaeoclimatology, Palaeoecology*, **20**, 209-234.

Pedley, H.M. 1978. 'A new lithostratigraphical and palaeoenvironmental interpretation for the Coralline Limestone Formations (Miocene) of the Maltese Islands', *Overseas Geology and Mineral Resources*, **54**, 1-17.

Pedley, H.M., House, M.R. and Waugh, B. 1976. 'The geology of Malta and Gozo', *Proceedings of the Geologists' Association*, **87**, 325-341.

Pedley, H.M., House, M.R. and Waugh, B. 1978. 'The geology of the Pelagian Block: the Maltese Islands', in Nairn, A.E.M., Kanes, W.H. and Stehli, F.G. (Eds), *The Ocean Basins and Margins. Vol.4B: The Western Mediterranean*, Plenum Press, London, 417-433.

Petley, D.N. and Allison, R.J. 1997. 'The mechanics of deep-seated landslides', *Earth Surface Processes and Landforms*, **22**, 747-758.

Pitty, A.F. 1979. *Geography and Soil Properties*, Methuen, London.

Planning Authority. 1992. *Development Planning Act 1992, Section 46*, Planning Authority, Malta.

Psaila, I. 1995. *A methodology for the classification of limestone with particular reference to the Gozitan formation*, Unpublished BE&A (Hons.) dissertation, University of Malta.

Rahn, P.H. 1996. *Engineering Geology, 2nd edition*, Prentice Hall, New Jersey.

Ransley, N. and Azzopardi, A. 1988. *A Geography of the Maltese Islands, 4th edition*, St.Aloysius' College, Malta.

Reed, F.R.C. 1949. *The Geology of the British Empire*, Arnold, London.

Reuther, C.D. 1984. 'Tectonics of the Maltese Islands', *Centro*, **1**, 1-20.

Rizzo, C. 1914. 'Geologia dell'arcipelago di Malta', *Bollettino della Reale Società Geografica*, **10**, 1059-1075.

Rizzo, C. 1932. *Report on the Geology of the Maltese Islands*, Government Printing Office, Malta.

Rosenak, S. 1963. *Soil Mechanics*, Batsford, London.

Saliba, J. 1990. *The shear strength of the Globigerina Limestone*, Unpublished BE&A dissertation, University of Malta.

Savigear, R.A.G. 1965. 'A technique of morphological mapping', *Annals of the Association of American Geographers*, **55**, 514-539.

Schembri, P.J. 1990. 'The Maltese coastal environment and its protection', in Atti dell'Ottavo Convegno Internazionale: Mare e Territorio, *La Protezione dell'Ambiente Mediterraneo ed il Piano della Commissione delle Comunità Europee*, Università degli Studi di Palermo, Palermo, 107-112.

Schembri, P.J. 1993. 'Physical geography and ecology of the Maltese Islands: a brief overview', in Options Méditerranéennes, *Malta: Food, Agriculture, Fisheries and the Environment*, CIHEAM, Montpellier, **7**, 27-39.

Selby, M.J. 1985. *Earth's Changing Surface*, Clarendon Press, Oxford.

Selby, M.J. 1993. *Hillslope Materials and Processes, 2nd edition*, Oxford University Press, Oxford.

Sharpe, C.F.S. 1938. *Landslides and Related Phenomena*, Columbia University Press, New York.

Sidle, R.C., Pearce, A.J. and O'Loughlin, C.L. 1985. *Hillslope Stability and Land Use*, American Geophysical Union, Washington DC.

Spratt, T.A.B. 1843. 'On the geology of the Maltese Islands', *Proceedings of the Geological Society of London*, **4**, 1-8.

Spratt, T.A.B. 1852. *On the Geology of Malta and Gozo*, Valletta, Malta.

Spratt, T.A.B. 1867. 'On the bone caves near Qrendi, Zebbug and Mellieha in the island of Malta', *Quarterly Journal of the Geological Society of London*, **23**, 283-297.

Summerfield, M.A. 1991. *Global Geomorphology*, Longman, Essex.

Taylor, R.K. and Cripps, J.C. 1987. 'Weathering effects: slopes in mudrocks and over-consolidated clays', in Anderson, M.G. and Richards, K.S. (Eds), *Slope Stability: Geotechnical Engineering and Geomorphology*, John Wiley & Sons, New York, 405-445.

Terzaghi, K. and Peck, R.B. 1967. *Soil Mechanics in Engineering Practice, 2nd edition*, John Wiley & Sons, New York.

Trechmann, C.T. 1938. 'Quaternary conditions in Malta', *Geological Magazine*, **75**, 1-26.

Trenhaile, A.S. 1997. *Coastal Dynamics and Landforms*, Clarendon Press, Oxford.

Varnes, D.J. 1958. 'Landslide types and processes', in Eckel, E.B. (Ed.), *Landslides and Engineering Practice*, Highway Research Board Special Report, Washington DC, **29**, 20-47.

Varnes, D.J. 1978. 'Slope movement types and processes', in Schuster, R.L. and Krizek, R.J. (Eds), *Landslides: Analysis and Control*, Transportation Research Board Special Report, Washington DC, **176**, 11-33.

Vickers, B. 1978. *Laboratory Work in Civil Engineering: Soil Mechanics*, Granada, London.

Vossmerbäumer, H. 1972. 'Malta, ein beitrag zur geologie und geomorphologie des Zentral-mediterranean raumes', *Würzburger Geographische Arbeiten*, **38**, 1-213.

Water Services Corporation. 1998. *Annual Report 1997/98*, Water Services Corporation, Malta.

West, T.R. 1995. *Geology Applied to Engineering*, Prentice Hall, New Jersey.

Wigglesworth, J.C. 1964. *The tertiary stratigraphy and Echinoid palaeontology of Gozo, Malta*, Unpublished PhD thesis, University of Durham.

Zammit, T. 1931. *The Water Supply of the Maltese Islands*, Government Printing Office, Malta.

Zammit-Maempel, G. 1977. *An Outline of Maltese Geology*, Malta.

Záruba, Q. and Mencl, V. 1969. *Landslides and Their Control*, Elsevier, Amsterdam.

Zezza, F. 1971. 'Aspetti idrogeologici delle formazioni terziarie di Malta', *Geologia Applicata e Idrogeologia*, **6**, 113-135.

Aħrax Point
Rdum l-Aħmar
Ramla tat-Torri
Armier Bay
Rdum tal-Madonna
Daħlet ix-Xilep
Il-Marbat
Rdum il-Ħmar
Il-Parsott
Ta' l-Imgħarrqa
Għar Baqrat
Ramla tal-Qortin
Ramla tal-Bir
Marfa Point
Ċirkewwa
Paradise Bay
Ta' Qassisu
Rdum il-Qawwi
Qammieħ Point
Rdum il-Qammieħ
Iċ-Ċumnija
Ras in-Niexfa
Il-Prajjet
Rdum id-Delli
Rdum Majesa
Ras il-Waħx
Ir-Ramla tal-Mixquqa
Għajn Tuffieħa Bay
Il-Qarraba
Ġnejna Bay
Ras il-Pellegrin
Fomm ir-Riħ Bay
Ras ir-Raħeb

Cliff Face
Translational Slide
Rotational Slide
Mudslide / Clay Slope
Rockfall
Soil Creep
Rocky Shoreline
Rock Shore Platform
Sand / Shingle
A Agriculture In Use
(A) Abandoned Agriculture

0 200m
N

Cliff Face

Translational Slide

Rotational Slide

Mudslide / Clay Slope

Rockfall

Rocky Shoreline

Rock Shore Platform

Sand / Shingle

(A) Abandoned Agriculture

N

0 200m

Ras l-Irqieqa

Il-Blata l-Bajda

Bahar iċ-Caghaq Bay

Qrejten Point

Qalet Marku

Ghallis Rocks

Ghallis Point

Salina Bay

Qawra

Qawra Point

Buġibba

Rdum l-Abjad

St.Paul's Bay

St.Paul's Islands

Rdum il-Bies

Ras il-Mignuna

Mistra Bay

Rdum Rxawn

Rxawn Point

Xemxija

Ta l-Għażżelin

Il-Mahruq

Ghajn Rasul

Pwales Beach

Blata l-Bajda

Mġiebaħ

Ras il-Griebeġ

Ghajn Żejtuna

Mellieħa Bay